UNIFIED DESIGN OF EXTENDED END-PLATE MOMENT CONNECTIONS SUBJECT TO CYCLIC LOADING

by

Emmett A. Sumner, III

Dissertation submitted to the Faculty of the Virginia Polytechnic Institute and State University in partial fulfillment of the requirements for the degree of

DOCTOR OF PHILOSOPHY

IN

CIVIL ENGINEERING

Approved:

_____
Thomas M. Murray, Chair

_____	_____
Finley A. Charney	W. Samuel Easterling
_____	_____
Siegfried M. Holzer	Mahendra P. Singh

June 17, 2003
Blacksburg, Virginia

Keywords: End-plate, Steel, Connection, Bolted, Seismic, Cyclic

UNIFIED DESIGN OF EXTENDED END-PLATE MOMENT CONNECTIONS SUBJECT TO CYCLIC LOADING

by

Emmett A. Sumner, III

(ABSTRACT)

Experimental and analytical research has been conducted to develop unified design procedures for eight extended end-plate moment connection configurations subject to cyclic/seismic loading. In addition the suitability of extended end-plate moment connections for use in seismic force resisting moment frames was investigated. Eleven full-scale cyclic and nine monotonic extended end-plate moment connection tests were conducted. Design procedures for determining the required bolt diameter and grade, end-plate thickness, and column flange thickness were developed. The proposed design procedure utilizes a strong column, strong connection, and weak beam design philosophy. This forces the connecting beam to provide the required inelastic deformations through formation of a plastic hinge adjacent to the connection region. The proposed design procedure was used to make comparisons with ninety experimental tests conducted over the past twenty-six years. A limited finite element study was conducted to investigate the behavior of the column flange.

The experimental results demonstrate that extended end-plate moment connections can be detailed and designed to be suitable for use in seismic force resisting moment frames. The proposed design procedure strength predictions correlated well with the results from ninety experimental tests. The limited finite element modeling conducted as a part of this study, correlated well with the strength predictions produced by the proposed design procedure.

ACKNOWLEDGMENTS

Partial funding for this research was provided by the Federal Emergency Management Agency through the SAC Joint Venture. SAC is a partnership of the Structural Engineers Association of California, the Applied Technology Council, and California Universities for Research in Earthquake Engineering. Partial funding for this research was also provided by the Metal Building Manufacturers Association through the 2001 MBMA Graduate Fellowship program. Sincere appreciation is extended to MBMA for their gracious support of this research and the fellowship program. Appreciation is extended to FEI Limited, Cives Steel Company, PSI, Inc., Nucor-Yamato Steel Company, The Lincoln Electric Company, and Star Building Systems, Inc. for the generous donation of test materials and fabrication services.

I would like to express my sincere gratitude to Thomas M. Murray for his guidance and encouragement during the course of this research and over the past ten years. His generosity and support will not be forgotten. Thanks also to Dr. W. Samuel Easterling, Dr. Siegfried M. Holzer, Dr. Finley A. Charney, and Dr. Mahendra P. Singh for serving on my graduate committee. A great deal of thanks is extended to Brett Farmer and Dennis Huffman for their help in the laboratory with the many hours of experimental testing.

Finally, I wish to thank my wife and family for their endless love, support, and encouragement over the past five years. Their encouragement provided the often needed motivation to push through the hard times.

TABLE OF CONTENTS

LIST OF FIGURES

LIST OF TABLES

UNIFIED DESIGN OF EXTENDED END-PLATE MOMENT CONNECTIONS SUBJECT TO CYCLIC LOADING

Chapter 1 – INTRODUCTION

1.1 General

A great deal of research on the behavior and design of steel seismic load resisting moment frames has been conducted over the past several years. The research was initiated by the unexpected failure of numerous fully-welded beam-to-column connections during the 1994 Northridge, California earthquake. A significant amount of the research was funded by the Federal Emergency Management Agency through the SAC Joint Venture. This research, commonly know as the *SAC Steel Project*, was divided into two phases. The initial phase focused on determining the cause of the fully-welded connection failures. The second phase focused on finding alternative connections for use in seismic force resisting steel moment frames. The extended end-plate moment connection is one alternative that has been investigated during the second phase of research. The investigation included experimental testing and analytical modeling to determine the suitability of end-plate moment connections for use in seismic force resisting moment frames. This dissertation presents the results of the experimental and analytical study. The results include unified design procedures for eight end-plate moment connection configurations.

1.2 End-Plate Moment Connections

End-plate moment connections consist of a plate that is shop-welded to the end of a beam that is then field bolted to the connecting member using rows of high strength bolts. The connections are primarily used to connect a beam to a column or to splice two beams together. The typical uses of end-plate moment connections are illustrated in Figure 1.1. There are two major types of end-plate connections: flush, as shown in Figure 1.2 and extended, as shown in Figure 1.3.

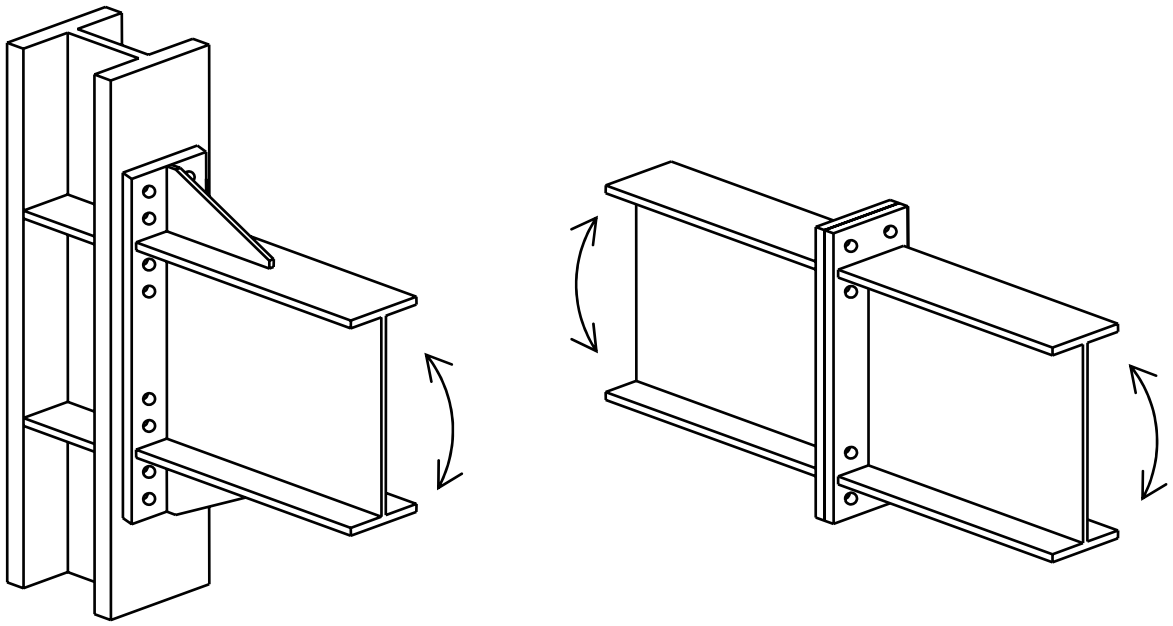

a) Beam-to-Column Connection b) Beam Splice Connection

FIGURE 1.1: TYPICAL USES FOR END-PLATE MOMENT CONNECTIONS

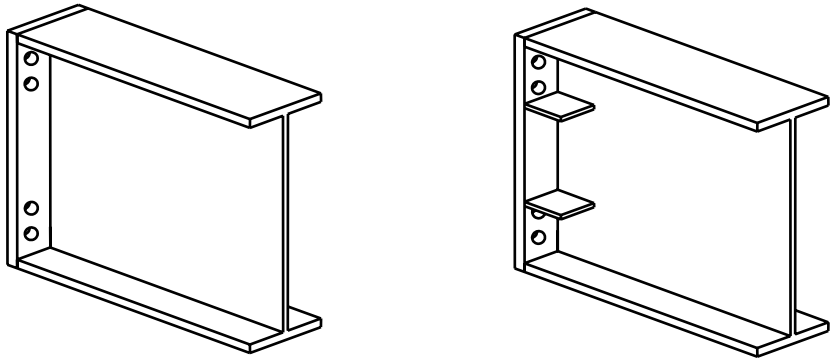

(a) Unstiffened (b) Stiffened

FIGURE 1.2: EXAMPLES OF FLUSH END-PLATE CONNECTIONS

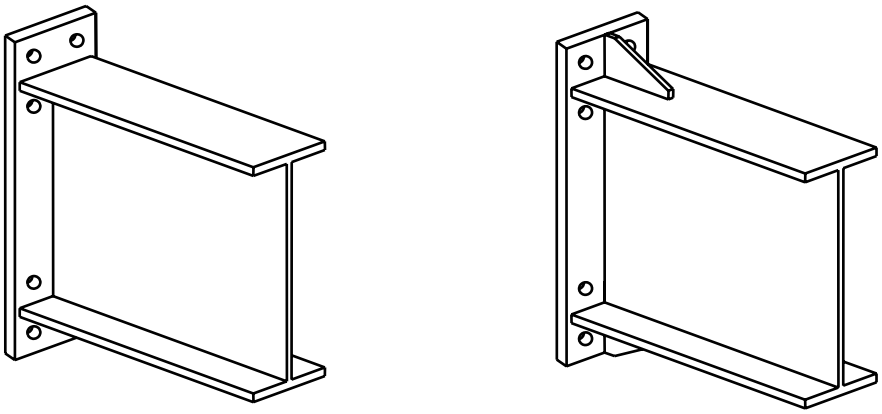

(a) Unstiffened (b) Stiffened

FIGURE 1.3: EXAMPLES OF EXTENDED END-PLATE CONNECTIONS

A flush end-plate connection has an end-plate that does not extend beyond the outside of the connecting beam flanges and all of the bolt rows are positioned inside the flanges. Flush end-plate connections can be stiffened or unstiffened. The stiffened configurations have gusset plates (stiffeners) welded to the beam web and to the end-plate on both sides of the web, as shown in Figure 1.2(b). The stiffeners can be positioned between the bolt rows or outside the bolt rows.

An extended end-plate connection has an end-plate that extends beyond the outside of the connecting beam flanges and at least one row of bolts is positioned outside the flanges on the extended part of the end-plate. Extended end-plate connections can be stiffened or unstiffened. The stiffened configurations have a gusset plate (stiffener) welded to the outside of the beam flange and to the end-plate, as shown in Figure 1.3(b). The stiffener is aligned with the web of the connecting beam to strengthen the extended portion of the end-plate. Extended end-plate moment connections are the focus of this research and will be the only type of end-plate connection discussed hereafter.

Moment end-plate connections are further described by the number of bolts at the tension flange and the configuration of the bolt rows. For gravity and/or wind load applications, the end-plate connection is often designed to carry tension only at one flange. For seismic/cyclic

loading, where the connection may experience load reversals, the end-plate is designed to carry tension at both flanges.

The primary advantage of moment end-plate connections is that they do not require field welding, which can be very time consuming and costly. They are easy to erect and cost approximately the same as other moment connections. The primary disadvantages are that they require precise beam length and bolt hole location tolerances. This problem has been greatly reduced with the increased use of computer controlled fabrication equipment.

1.3 Classification of End-Plate Connections

Moment end-plate connections can be classified as fully restrained, FR, or partially restrained, PR, depending on the type, configuration, and end-plate stiffness. Fully restrained construction is defined as "rigid frame" by AISC (1999a), and it is assumed that the connections have sufficient rigidity to maintain the angles between the intersecting members. The extended moment end-plate connection configurations provide sufficient stiffness for fully restrained construction.

1.4 Seismic Design Requirements

The seismic design requirements for steel moment resisting frames have significantly changed since the Northridge earthquake in 1994. The initial recommendations based on the preliminary results from the SAC Steel Project were published as the SAC Interim Guidelines (FEMA 1995, 1996). The final guidelines, developed from the results of the SAC Steel Project, are published as a series of FEMA documents (FEMA 2000a, 2000b, 2000c, 2000d). The provisions presented in the FEMA documents have been incorporated into the Seismic Provisions for Structural Steel Buildings (AISC 1997, 1999b, 2000b, 2002).

The revised specification provisions require that beam-to-column moment connections be designed with sufficient strength to force development of the plastic hinge away from the column face to a predetermined location within the beam span. In addition, all elements of the connection are required to have adequate strength to develop the forces resulting from the formation of the plastic hinge together with forces resulting from gravity loads. This results in a strong column, strong connection, and weak beam design philosophy.

The beam-to-column connections must be prequalified by laboratory testing, to show that they can provide adequate strength, stiffness and ductility. In particular, the connection assemblies used in regions of high seismicity must be capable of sustaining 0.04 radians of interstory drift rotation for at least one complete loading cycle. Lower inelastic rotation requirements have been established for areas of low-to-moderate seismicity.

1.5 Research Objectives

The purpose of the research included in this study was to develop unified procedures for the design of eight extended end-plate moment connections subject to cyclic/seismic forces. The five basic extended end-plate moment configurations considered are shown in Figure 1.4: (a) four bolt unstiffened, 4E, (b) four bolt stiffened, 4ES, (c) eight bolt stiffened, 8ES, (d) eight bolt unstiffened, four bolts wide unstiffened, 8E-4W, and (e) eight bolt unstiffened, four bolts wide stiffened, 8ES-4W. The three multiple row extended (MRE) end-plate moment connection configurations considered are shown in Figure 1.5: (a) MRE 1/2 unstiffened (one bolt row outside and two rows inside the flanges), (b) MRE 1/3 unstiffened (one bolt row outside and two rows inside the flanges), and (c) MRE 1/3 stiffened (one bolt row outside and two rows inside the flanges).

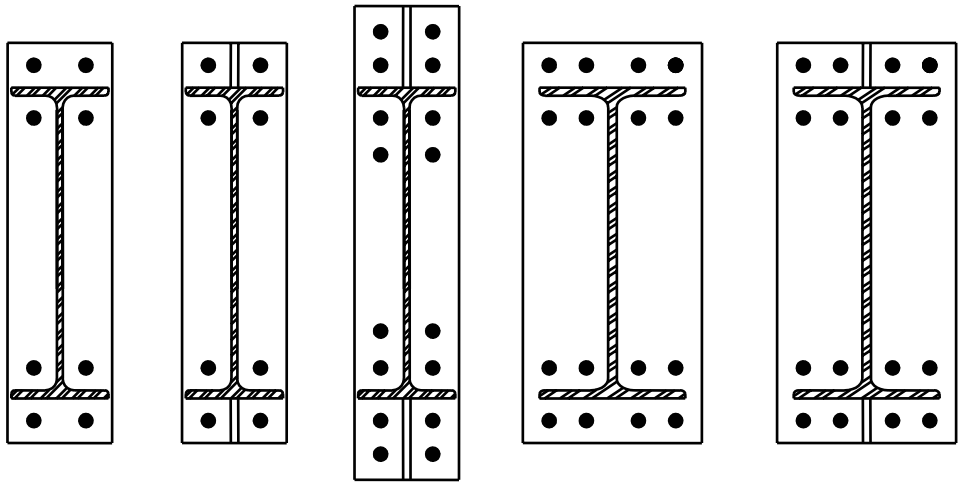

(a) 4E (b) 4ES (c) 8ES (d) 8E-4W (e) 8ES-4W

FIGURE 1.4: EXTENDED END-PLATE CONFIGURATIONS

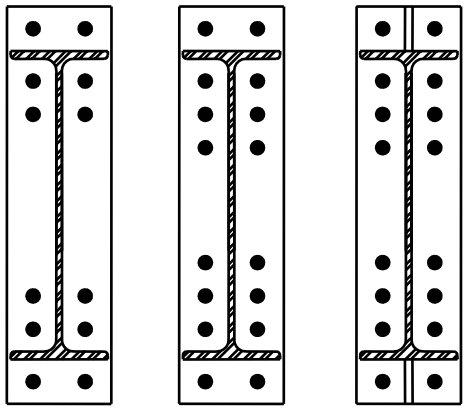

(a)MRE 1/2 (b) MRE 1/3 (c) MRES 1/3

FIGURE 1.5: MULTIPLE ROW EXTENDED END-PLATE CONFIGURATIONS

To properly develop the unified design procedure, five research objectives were identified:

Objective I: Suitability of End-Plate Connections for Seismic Regions. The first research objective was to determine the suitability of extended end-plate connections for use in seismic force resisting moment frames. The *AISC Seismic Provisions* (AISC 1997, 1999b, 2000b, 2002) require that a moment connection be prequalified before it can be used in a seismic force resisting moment frame. The prequalification procedure requires experimental testing of the connections to show that the connection can provide adequate strength, stiffness, and ductility. The testing must be conduced in accordance with the procedures specified in the *Protocol for Fabrication, Inspection, Testing and Documentation of Beam-Column Connection Tests and Other Experimental Specimens* (SAC 1997). The protocol specifies the minimum instrumentation and documentation requirements, as well as the loading procedure. Experimental testing to prequalify each of the eight end-plate configurations would be an enormous task. However, limited testing of three different end-plate moment connection configurations to determine their suitability and identify possible deficiencies of the design procedures has been performed. The testing details and results are presented in Chapter 3.

Objective II: End-Plate and Connection Bolt Design Procedure. The second objective was to develop unified design procedures for determining the strength of the end-plate and the

connection bolts when subject to cyclic/seismic loads. The proposed procedure, presented in Chapter 4, uses yield line analysis to predict the strength of the end-plate and a simplified bolt analysis procedure, which is based on the split-tee analogy, to predict the bolt forces.

Objective III: Column Flange Bending Design Procedures. The third objective was to develop unified design procedure for the evaluation of the column side limit state of column flange bending. The proposed procedure, presented in Chapter 4, uses yield line analysis to predict the strength of the column flange and a simplified bolt analysis procedure, which is based on the split-tee analogy, to predict the bolt forces. Both stiffened and unstiffened column flange configurations are considered.

Objective IV: Comparisons with Other Methods. The fourth objective was to compare the results of the proposed design method with the available experimental test data and limited finite element analysis results. Comparisons of the experimental data with the results from the proposed design procedure are presented in Chapter 5. Details and results from the finite element analysis conducted as a part of this study are presented in Chapter 6. Observations and conclusions from the comparisons are also presented.

Objective V: Detailing and Fabrication Practices. The fifth objective was to identify and develop the appropriate detailing and fabrication practices for extended end-plate moment connections subject to seismic/cyclic loading. Detailed recommendations for the connection geometry and stiffener design requirements are presented in Chapter 7. An experimentally tested welding procedure for the beam-to-end-plate welds is also presented.

1.6 Summary of Research Focus

The focus of this research is to develop unified procedures for the design of five extended and three multiple row extended end-plate moment connection configurations. Five specific research objectives needed to complete the development of the design procedure were identified. Prior to the completion of the five objectives, an extensive literature review was conducted. A summary of the available literature is presented in Chapter 2 along with the identification of needed research.

Chapter 2 – BACKGROUND

2.1 General

There is a great deal of literature available on the analysis and design of end-plate moment connections. In an effort to provide an organized view of the background literature, this literature review is separated into five sections: end-plate design, bolt design, column side design, cyclic testing of end-plate moment connections, and finite element analysis of end-plate moment connections. A brief overview of the major focus of each study is given and a summary of findings provided.

2.2 End-Plate Design

The first application of the end-plate moment connection was in the early 1960's. The concept of end-plate moment connections was developed from research on tee-stub moment connections in the late 1950's. End-plate moment connections offer several advantages over tee-stub moment connections: savings in material weight, smaller number of detail pieces to handle, cost savings in material cutting since in many cases the end-plates can be sheared, and because beam depth tolerances do not affect the alignment of the bolt holes (Disque, 1962).

An early study by Johnson et al. (1960) concluded that end-plate connections with high strength bolts can develop the full plastic capacity of the connected members. The formation of a plastic hinge in the beam provides inelastic rotation capacity within the member instead of within the connection.

Sherbourne (1961) conducted five end-plate connection tests and suggested that sufficient rotation capacity could be achieved through plastic deformation of the end-plate. The plastic deformation of the end-plate equalized the forces in the bolts and therefore increased the overall strength of the connection. He presented simple equations for the design of the connection components.

Beedle and Christopher (1964) concluded that a properly designed end-plate connection could develop the plastic capacity of the connected members which would provide inelastic deformations in the members instead of in the connection.

Douty and McGuire (1963, 1965) investigated the increase in bolt tension caused by prying effects in the end-plate and compared theoretical and experimental results. For the thinner end-plates, significant increases in bolt tension were reported. Semi-empirical equations were developed to predict the prying force ratio.

Bailey (1970) conducted 13 tests on specimens designed using Sherebourne's (1961) design method. Satisfactory agreement between theoretical and experimental results was obtained and the importance of stiffening the column web to prevent column failure was emphasized. An equation for the determination of slip resistance of the connection was presented.

Mann (1968) conducted six beam-to-column end-plate connection tests and developed equations to predict the strength of the end-plate.

Surtees and Mann (1970) refined the work by Mann (1968) and developed an alternate equation for determining the end-plate thickness, suggested the use of a 33 percent increase of the direct bolt tension force to account for prying forces, and concluded that the bolt pretension had little effect on the connection stiffness.

Zoetemeijer (1974) used yield line theory to develop a method for determining the strength of stiffened and unstiffened column flanges at the tension side of tee-stub and end-plate connections. The method considers column flange bending and bolt failure mechanisms. Results from a series of tests verified that the design method provides connections that satisfy the strength and serviceability limit states of the then current Dutch regulations for construction steel work.

Packer and Morris (1977) developed design equations for determining the end-plate thickness and the column flange strength. Yield line analysis, considering straight and curved yield lines, was used to predict the end-plate and column flange strengths. Good agreement with experimental results was achieved.

Mann and Morris (1979) considered the results of several research programs and proposed a design procedure for the extended end-plate connection. The procedure considered both strength and stiffness criteria. Yield line analysis was used to determine the strength of the end-plate and column flange. Prying forces were considered in the design of the bolts.

Krishnamurthy (1978) used finite element analysis to develop empirical relationships for determining the end-plate thickness. The relationships resulted in much thinner end-plates than previously obtained. The bolt prying forces were compared to a pressure bulb formed underneath the bolt head when the bolts are tightened. Krishnamurthy stated that the location of the pressure bulb shifts towards the edge of the end-plate as the flange force increases. At service load conditions, the flange forces are relatively small, and the pressure bulb is closer to the bolt head than the plate edge. This results in much smaller prying forces than predicted by previous studies. As a result, Krishnamurthy neglects prying forces and determines the bolt forces directly from the flange force.

Grundy et al. (1980) conducted two tests on extended end-plate connections with two rows of four bolts (eight total) at the tension flange. A procedure for the design of beam-to-column connections is presented in the paper. The bolt forces include a 20 percent increase to the direct force to account for prying action.

Tarpy and Cardinal (1981) used finite element analysis to develop equations for the design of unstiffened beam-to-column flange end-plate connections. The adequacy of the analytical model was shown through comparisons with experimental results.

Bahia et al. (1981) investigated the strength of tee-stubs and beam-to-column extended end-plate connections. The end-plate and column flange strengths were determined using yield line theory. The bolt forces including prying action were shown to depend on the areas of contact between the end-plate and column.

Zoetemeijer (1981) investigated the behavior of a flush end-plate and a stiffened column flange using an analytical model that utilizes an infinitely long plate bounded by two fixed edges and one free edge. Yield line analysis was used to generate design charts for determination of the end-plate and stiffened column flange strength

Graham (1981) conducted 21 beam to unstiffened column end-plate connection tests; bolt tension rupture was the predominant failure mode for the tests. It was shown that the unstiffened column flange greatly influenced the rotation capacity of the connections. Design equations that limit the connection deformation and predict the connection strength were developed.

Srouji et al. (1983a, 1983b) developed design methods for four different end-plate moment connection configurations; two bolt flush, four bolt flush, four bolt unstiffened extended, four bolt stiffened extended. The end-plate thickness was determined using yield line analysis. The bolt force predictions include the effects of prying, and were based on the tee-stub analogy design method developed by Kennedy et al. (1981) with a few modifications. Finite element analysis was used to establish stiffness criteria for the two and four bolt flush connections. The analytical procedure was verified with experimental testing, good correlation was observed. It was concluded that yield line analysis and the modified Kennedy method accurately predict the end-plate strength and bolt forces.

As a continuation of the work by Srouji, Hendrick et al. (1984) conducted tests on two four bolt flush end-plate moment connection configurations: one with a stiffener located between the two tension bolt rows, and one with the stiffener located below the two bolt rows. The end-plate thickness was determined using yield line analysis and the bolt force predictions were based on the Kennedy method with a few modifications. Good correlation between the experimental and analytical results was observed.

Unification of flush end-plate moment connection design procedures was presented by Hendrick et al. (1985). The unified procedure considered four flush connection configurations: two bolt flush, four bolt flush, four bolt flush stiffened between the bolt rows, and the four bolt flush stiffened below the bolt rows. The end-plate design was based on yield line theory and the bolt forces determined by the modified Kennedy method. An analysis of the connection stiffness resulted in the conclusion that the flush connections behaved as Type 1 or FR connections up to the point where eighty percent of the end-plate bending failure moment was obtained.

Morrison et al. (1985, 1986) continued the work of Srouji and Hendrick by extending the unified design method to the four bolt extended stiffened and the multiple row extended 1/3, one row extended three rows inside, end-plate moment connections. To account for uneven

distribution of the applied flange force to the inner and outer rows of bolts, additional modifications to the Kennedy method were made. The results of six tests were used to determine the appropriate flange force distribution factors. As with the other connection configurations, it was determined that the four bolt extended stiffened and the multiple row extended 1/3 connections could be classified as Type 1 or FR connections.

Bond and Murray (1989) presented the results of five tests of the six bolt flush end-plate moment connection. The objective of the study was to develop a design procedure and moment rotation relationship similar to the unified procedure presented by Hendrick et al. (1995). Yield-line analysis was used to determine the end-plate thickness and the Kennedy method, with specific modifications for this connection configuration, was used to determine the bolt forces. The correlation between the analytical and experimental results was reasonable.

The four bolt extended unstiffened connection configuration was studied by Abel and Murray (1992a). The analysis of the connections utilized yield line theory for determining the end-plate thickness and the modified Kennedy method for the calculation of bolt forces. Experimental tests were conducted, and good correlation with the analytical results was observed.

Testing of the multiple row extended 1/2, multiple row extended 1/3, and multiple row extended stiffened 1/3 was reported by SEI (1984), Abel and Murray (1992b), Rodkey and Murray (1993). Design equations based on yield line analysis and the modified Kennedy method were presented.

Kennedy and Hafez (1984) investigated the moment rotation characteristics of eight end-plate moment connections. An analytical model was developed and compared to experimental results. Good correlation of the results was observed.

Ahuja et al. (1982), Ghassemieh et al. (1983), and Murray and Kukreti (1985) investigated the behavior of the eight bolt extended stiffened end-plate connection. A series of experimental tests and extensive finite element analyses were conducted. Design procedures based on regression analysis of the finite element analysis results were developed. The

procedures include the effects of prying on the bolts and considers both strength and stiffness of the connection.

Murray and Kukreti (1988) continued their previous work on the eight bolt extended stiffened end-plate connection. The previously developed design procedures were modified to conform with the *Allowable Stress Design* and the *Load and Resistance Factor Design* methodologies. In addition, a simplified design procedure is presented.

Aggarwal and Coates (1987) conducted fifteen experimental tests on four bolt extended unstiffened end-plate moment connections. The specimens were tested under static and dynamic loads. It was shown that the Australian and British standards produced conservative end-plate and bolt strength predictions for the test loading. In addition, it was found that the margin of safety for the end-plate to beam flange welds dramatically decreased from the static tests to the dynamic tests.

Morris (1988) reviewed the connection design philosophies adopted in the United Kingdom and made practical recommendations and observations that are important for designers. The importance of proper design and detailing of extended and flush end-plate moment connections was emphasized.

Murray (1988) presented an overview of the past literature and design methods for both flush and extended end-plate configurations, including column side limit states. Design procedures, based on analytical and experimental research in the United States, were presented.

Murray (1990) presented design procedures for the four bolt unstiffened, four bolt wide unstiffened, and the eight bolt extended stiffened end-plate moment connections. The end-plate design procedures were based on works of Krishnamurthy (1978), Ghassemieh et al. (1983), and Murray and Kukreti (1988). The column side procedures were based on works by Curtis and Murray (1989), and Hendrick and Murray (1984).

Chasten et al. (1992) conducted seven tests on large extended unstiffened end-plate connections with eight bolts at the tension flange (four bolts wide). Both snug and fully tensioned bolts were used in the testing. End-plate shear fractures, bolt fractures, and weld fractures were the observed failure modes. Finite element modeling was used to predict the

distribution of the flange force to the tension bolts and to predict the magnitude and location of the prying force resultants. It was shown that the end-plate shear and bolt forces, including prying, can accurately be predicted using finite element analysis. In addition, simple design rules that complement the existing procedures are presented.

Graham (1993) reviewed the existing design methods and recommended a limit state design method for the design of rigid beam-to-unstiffened column extended end-plate connections.

Borgsmiller et al. (1995) conducted five tests on extended end-plate moment connections with large inner pitch distances, the distance from the inside of the flange to the first row of inside bolts. Results showing the end-plate, bolt, and connected beam behavior were presented.

Borgsmiller (1995) presented a simplified method for the design of four flush and five extended end-plate moment connection configurations. The bolt design procedure was a simplified version of the modified Kennedy method to predict the bolt strength including the effects of prying. The end-plate strength was determined using yield line analysis. Fifty-two end-plate connection tests were analyzed and it was concluded that the prying forces in the bolts become significant when ninety percent of the end-plate strength is achieved. This established a threshold for the point at which prying forces in the bolts can be neglected. If the applied load is less than ninety percent of the plate strength, the end-plate is considered to be 'thick' and no prying forces are considered; when the applied load is greater than ninety percent of the end plate strength, the end-plate is considered to be 'thin' and the prying forces are assumed to be at a maximum. This distinct threshold between 'thick' and 'thin' plate behavior greatly simplified the bolt force determination because only the case of no prying and maximum prying must be determined. Good correlation with past test results was obtained using the simplified design procedure.

Ober (1995) presented a simplified method for the design of five end-plate connection configurations. The end-plate strength is based on the tee-stub analogy and the concept of an effective number of bolts is used to calculate bolt strength. Comparisons with experimental results showed that the method produces conservative results.

Sumner and Murray (2001a) performed six multiple row extended 1/2 end-plate connection tests to investigate the validity of the current design procedures for gravity, wind and low seismic loading. In addition, the tests investigated the effects of standard and large inner pitch distances and the connections utilized both A325 and A490 bolts. Good correlation between the experimental and analytical results was observed.

Sumner and Murray (2001b) investigated extended end-plate connections with four high strength bolts per row instead of the traditional 2 bolts per row. The eight bolt extended, four bolts wide and the multiple row extended 1/2, four bolts wide end-plate moment connections were investigated. Seven end-plate connection tests were performed and a modified design procedure, similar to the procedure presented by Borgsmiller (1995), was presented. It was concluded that the modified design procedure conservatively predicts the strength of the two connection configurations.

Murray and Shoemaker (2002) presented a guide for the design and analysis of flush and extended end-plate moment connections. The guide includes provisions for the design of four flush and five extended end-plate connection configurations. The design provisions are limited to connections subject to gravity, wind and low-seismic forces; moderate and high seismic applications are not included. A unified design procedure, based on the simplified method presented by Borgsmiller (1995) was employed. It is based on yield line analysis for the determination of the end-plate thickness and the modified Kennedy method for determination of the bolt forces. A stiffness criterion for flush end-plate moment connections was also included in the procedure.

2.3 Bolt Design

Numerous studies have been conducted to investigate the behavior of the bolts utilized within end-plate moment connections. The primary focus of the studies has been to measure and predict the possible prying forces within end-plate connections. The majority of the bolt force prediction methods were developed using an analogy between the end-plate connection and an equivalent tee-stub in tension.

Douty and McGuire (1963, 1965), Kato and McGuire (1973), Nair et al. (1974), and Agerskov (1976, 1977) conducted early studies on tee-stubs to evaluate the bolt forces including

the effects of prying. All assumed the location of the prying force to be at or near the edge of the end-plate. For connections with a large degree of prying action, this results in large bolt diameters and thick end-plates. Fisher and Struik (1974) present a comprehensive review of the previously cited design methods.

Kennedy et al. (1981) developed a design procedure for tee stub connections. The procedure identifies three stages of tee stub flange plate behavior. The first stage of plate behavior occurs at low load levels and is identified by purely elastic behavior. The flange plate is said to be 'thick', and it is assumed that there are no prying forces. As the load increases and a plastic hinge forms in the flange plate at the base of the tee stem, a second stage of behavior exists. The plate is said to be of intermediate thickness, and prying forces are present. The third stage of plate behavior occurs as a subsequent plastic hinge forms at the bolt line. The plate is classified as thin, and prying forces are at a maximum. The analytical method correlated well with the two tee-stub tests conducted as a part of this study.

Srouji et al. (1983a, 1983b), Hendrick et al. (1984, 1985), Morrison et al. (1985, 1986), and Borgsmiller (1995) use a modified Kennedy approach to predict the bolt forces in flush, extended, stiffened, and unstiffened end-plate moment connection configurations. The primary modification to the Kennedy method is an adjustment to the location of prying force and modification of the distribution of the flange force to the particular bolt rows.

Ahuja et al. (1982) and Ghassemieh et al. (1983) used regression analysis of finite element studies to predict the bolt forces of the eight bolt extended stiffened end-plate moment connection configuration.

Fleischman et al. (1991) studied the strength and stiffness characteristics of large capacity end-plate connections with snug-tight bolts. They showed that the initial stiffness is slightly reduced in the snug tight connections but the ultimate strength is the same.

Kline et al. (1989), as also reported in Murray et al. (1992), investigated the behavior of end-plate moment connections with snug-tight bolts subject to cyclic wind loading. Eleven tests representing six different connection configurations were tested. The results were excellent and consistent with the analytical predictions. It was concluded that end-plate moment connections

with snug-tight bolts provide slightly reduced stiffness when compared to fully-tightened end-plate connections.

2.4 Column Side Design

There is a relatively small amount of literature on the column side design of end-plate moment connections. Numerous papers make observations about the behavior of the column during testing but no specific design criteria are discussed. The few papers that are available, outline recommendations for three failure modes: column web yielding, column web buckling, and column flange bending.

2.4.1 Web Yielding

Mann and Morris (1979) investigated the column web strength at end-plate moment connections. An evaluation of results from several research projects was conducted. It was recommended that the connecting beam flange force be distributed at a slope of 1:1 through the end-plate and then on a 2.5:1 slope through the column flange and web.

Hendrick and Murray (1983, 1984) conducted a series of tests and an analytical study to determine the column web compression yielding strength at end-plate moment connections. A design equation was developed and good correlation with the finite element and experimental results observed. It was recommended that the connecting beam flange force be distributed through the end-plate at a slope of 1:1 and then on a slope of 3:1 though the column.

2.4.2 Web Buckling

Newlin and Chen (1971) conducted numerous tests on welded beam-to-column connections to investigate the compressive strength of column webs. They recommended an interaction equation to check combined web yielding and web buckling. A simple check for web buckling alone was also recommended. The simple equation for web buckling was adopted by AISC in 1978.

Witteveen et al. (1982) conducted simulated compression tests on unstiffened flanges for welded flange and bolted end-plate connections. Witteveen et al. recommended a lower bound solution for the failure load. The solution was similar to the web yielding strength presented by

Mann and Morris (1979) and considered buckling, crippling and yielding of the web in compression.

2.4.3 Flange Bending

Fisher and Struik (1974) recommend column flange strength criteria for welded and bolted connections based on European standards. They suggest that column flange stiffeners be designed for the excess forces that the column web and flanges are not able to withstand.

Mann and Morris (1979) conducted an extensive study on the design of end-plate moment connections. Included in their study was the development of column side design provisions. The column side provisions were primarily based on the work of Packer and Morris (1977). They describe three possible modes of column flange failure and provide equations to predict the strength of each. For relatively thin column flanges, the effects of prying forces are accounted for by limiting the bolt tensile capacity.

Witteveen et al. (1982) studied welded flange and bolted end-plate connections and identified three possible column flange failure modes similar to the findings of Mann and Morris (1979). Design equations to predict the three modes and comparisons with experimental testing were presented.

Tarpy and Cardinal (1981) conducted an experimental and analytical study of the behavior of unstiffened beam-to-column end-plate connections. The experimental tests were conducted with axial load applied to the columns. The analytical study included the development of finite element models which were used to develop regression equations for predicting the end-plate and column flange strength.

Hendrick et al. (1983) evaluated the existing methods for predicting the column flange bending strength. They conducted limited experimental testing and concluded that the method presented by Mann and Morris (1979) was most suitable for the design of the tension region of the four bolt extended unstiffened end-plate moment connections. In addition, they modified the end-plate design procedure presented by Krishnamurthy (1978) by substituting the end-plate width with an effective column flange width. This procedure was calibrated to provide the same results as the Mann and Morris (1979) equations.

Curtis and Murray (1989) investigated the column flange strength at the tension region of the four bolt extended stiffened and eight bolt extended stiffened end-plate connections. Their design procedure is based on the Ghassemieh et al. (1983) end-plate design procedure with an effective column flange length substituted for the end-plate width.

Murray (1990) presented column side design procedures for the four bolt unstiffened, four bolt wide unstiffened, and the eight bolt extended stiffened end-plate moment connections. The column side procedures were based on works by Hendrick and Murray (1984), and Curtis and Murray (1989).

2.5 Cyclic Testing of End-Plate Moment Connections

Early investigations into the cyclic performance of end-plate moment connections were limited to small beam sections with unstiffened end-plates. Subsequent studies have investigated connections between larger sections. One of the primary distinctions between the different studies is the source of inelastic behavior. Some researchers have investigated the inelastic response of the end-plate and others the inelastic response of the connecting beam.

Four cruciform beam-to-column end-plate connection tests were conducted by Johnstone and Walpole (1981). The four-bolt extended unstiffened connections were designed to study the previously developed recommendations for monotonic loading together with the design rules in the New Zealand design standards. The results show that end-plate connections can transmit the necessary forces to force most of the inelastic deformations to occur in the beam. However, connections designed for less than the capacity of the beam may not provide the required ductility.

Popov and Tsai (1989) investigated cyclic loading of several different types of moment connections. The objective was to investigate realistic member size and the extent of cyclic ductility. Their results indicated that end-plate moment connections are a viable alternative to fully-welded connections in seismic moment-resisting frames. Continuing their research on end-plate connections, Tsai and Popov (1990) investigated the four bolt extended stiffened and unstiffened end-plate connection configurations. The results from their experimental and finite element studies showed the design procedures for monotonic loading need to be modified for seismic loading.

Research by Ghobarah et al. (1990) investigated the cyclic behavior of extended stiffened and unstiffened end-plate connections. Five specimens were tested, some with axial load applied to the column, to compare the performance of stiffened and unstiffened end-plates, stiffened and unstiffened column flanges, and to isolate the individual behavior of the beam, column flange, stiffeners, bolts and end-plate. They concluded that proper proportioning of the end-plate connections could provide sufficient energy dissipation capability without substantial loss of strength. They recommended that for unstiffened connections, the bolts and end-plate be designed for 1.3 times the plastic moment capacity of the beam to limit the bolt degradation and compensate for prying forces. It was also recommended that for stiffened connections, the end-plate and bolts be designed for the plastic moment capacity of the beam.

As an extension of the work by Ghobarah et al. (1990), Korol et al. (1990) conducted seven extended end-plate moment connection tests. Design equations that consider the strength, stiffness and energy dissipation requirements of extended end-plate connections were presented. They concluded that proper design and detailing of end-plate connections will produce end-plate connections that provide sufficient energy dissipation without substantial loss of strength or stiffness.

Ghobarah et al. (1992) continued their research on end-plate connections by testing four additional connections. The specimens were subjected to cyclic loading and axial load was applied to the column. They found that column panel zone yielding can dissipate large amounts of energy and that the end-plate helps to control the inelastic deformation of the panel zone. They recommended that panel zone yielding be used to increase the energy dissipating capacity of the end-plate moment connections.

Fleischman et al. (1990) conducted five cyclic beam-to-column tests utilizing four bolt wide extended unstiffened end-plate moment connections. The effect of snug versus fully-tightened bolts was investigated. The connections were designed weaker than the connecting beam and column so that the inelastic behavior of the end-plate could be investigated. It was observed that the connection stiffness gradually decreased in successive inelastic cycles, the energy absorption capacity increased as the end-plate thickness decreased, the bolt forces were

increased up to thirty percent because of prying action, and the snug-tightened connections exhibited higher energy absorption capacity.

Astaneh-Asl (1995) conducted two cyclic tests on the four bolt extended unstiffened end-plate moment connection. The specimens were designed using the existing AISC recommendations, which were not intended for seismic applications. The first test exhibited ductile behavior and resulted in local buckling of the connecting beam flange. The second test utilized an I-shaped shim between the end-plate and the column. The performance of the specimen was excellent until the shim began to yield in compression. The author concluded that the concept was sound but that a stronger shim was needed.

Adey et al (1997, 1998, 2000) investigated the effect of beam size, bolt layout, end-plate thickness, and extended end-plate stiffeners on the energy absorption ability of the end-plate. Fifteen end-plate connections subject to cyclic loading were conducted. Twelve of the fifteen connections were designed weaker than the connecting beams and columns to isolate the yielding in the end-plate. The other three tests were designed to develop the nominal plastic moment strength of the connected beam. It was concluded that the end-plate energy absorption capability decreases as the beam size increases and that extended end-plate stiffeners increase the end-plate absorption capability. In addition, a design procedure for the four bolt extended unstiffened and stiffened end-plate moment connections was presented. The design procedure utilizes yield line theory for the determination of the end-plate thickness. The connection bolts design procedure assumes a twenty percent increase in the bolt forces to account for the possible presence of prying forces.

Meng and Murray (1997) conducted a series of cyclic tests on the four bolt extended unstiffened end-plate moment connections. The test specimens were designed with the connections stronger than the connecting beam and column. The end-plate thickness was determined using yield line analysis and the bolt forces predicted by the modified Kennedy method. The testing identified a problem with the use of weld access holes in making the beam flange to end-plate welds. In all of the specimens with weld access holes, the flanges fractured after the first few inelastic cycles. In the specimens without weld access holes, a robust inelastic response and a large energy dissipation capacity were observed. Results from a subsequent finite

element analysis study indicated that the presence of the weld access hole greatly increases the flange strain in the region of the access hole. Based on the results of their study, they recommended that weld access holes not be used in end-plate moment connections. They concluded that properly designed end-plate connections are a viable connection for seismic moment frame construction.

Meng (1996) and Meng and Murray (1996) investigated the four bolt extended stiffened, four bolt wide extended stiffened, four bolt wide extended unstiffened, and shimmed end-plate moment connections. Design procedures for the connections are presented and comparisons with the experimental tests shown.

An overview of the previous research on bolted and rived connections subject to seismic loads is presented Leon (1995). He discusses the fundamentals of bolted and riveted connection design and identifies possible extensions of the monotonic design methods to the cyclic loading case. He concludes that properly designed bolted connections can provide equal or superior seismic performance to that of fully welded ones. In addition, a new, more fundamental and comprehensive approach is needed in current codes so that bolted connections can be properly designed in areas of moderate and high seismicity.

Castellani et al. (1998) presents preliminary results of ongoing European research on the cyclic behavior of beam-to-column connections. The extended unstiffened end-plate moment connection tests resulted in very regular hysteresis loops with no slippage and a progressive reduction in the energy absorption. A plastic hinge formed in the connecting beams and large deformations at the plastic hinge induced cracking in the beam flange, ultimately resulting in complete failure of the section.

Coons (1999) investigated the use of end-plate and tee-stub connections for use in seismic moment resisting frames. A database of previously published experimental data was created and analytical models developed to predict maximum moment capacity, failure mode, and maximum inelastic rotation. It was observed that the plastic moment strength of the connecting beams was twenty-two percent higher than predicted by the nominal plastic moment strength ($M_p = F_y Z_x$.) He recommended that the increased beam strength be considered for the

connection design, end-plate thickness be determined using yield line analysis, and the bolt forces be determined without including the effects of prying.

Boorse (1999) and Ryan (1999) investigated the inelastic rotation capability of flush and extended end-plate moment connections subject to cyclic loading. The specimens were beam-to-column connections between built-up members as used in the metal building industry. The specimens were designed with the end-plate connections weaker than the connecting members to investigate the inelastic behavior of the end-plate. The end-plate thickness and bolt forces were determined using yield line analysis and the modified Kennedy method respectively. The experimental results were compared with the analytical results with reasonable correlation. It was concluded that the flush end-plates could be designed to provide adequate inelastic rotation but the extended end-plates should be designed to force the inelastic behavior into the connecting beam.

2.6 Finite Element Analysis of End-Plate Moment Connections

Early finite element studies focused on correlation of results from 2-D models to 3-D models. This was important because of the substantially higher cost of creating and running 3-D models as compared to 2-D models. With the advances in PC computer technology, the use of 3-D models has become more common. More recent studies have focused on the suitability of finite element method to accurately predict the inelastic behavior of end-plate moment connections.

Krishnamurthy and Graddy (1976) conducted one of the earliest studies to investigate the behavior of bolted end-plate moment connections using finite element analysis. Thirteen connections were analyzed by 2-D and 3-D programs, so that their correlation characteristics could be applied for prediction of other 3-D values from corresponding 2-D results. The analysis programs utilized a 2-D constant strain triangle and a 3-D eight-node brick element. The connections were analyzed under bolt pretension, half service load, and full service load. Correlation factors were generated and used to predict the behavior of a 3-D model using results from the 2-D models.

Ahuja et al. (1982) investigated the elastic behavior of the eight bolt extended stiffened end-plate moment connection using finite element analysis. Ghassemieh et al. (1983) continued the work of Ahuja and included inelastic behavior.

Abolmaali et al. (1984) used finite element analysis to develop a design methodology for the two bolt flush end-plate moment connection configuration. Both 2-D and 3-D analyses were conducted to generate correlation coefficients. Finite element 2-D analysis was used to generate regression equations for the design of the connections. The results were adjusted by the correlation coefficients to more closely match the experimental results.

Kukreti et al. (1990) used finite element modeling to conduct parametric studies to predict the bolt forces and the end-plate stiffness of the eight bolt extended stiffened end-plate moment connection. Regression analysis of the parametric study data resulted in equations for predicting the end-plate strength, end-plate stiffness, and bolt forces. The predictions were compared to experimental results with reasonable correlation.

Gebbeken et al. (1994) investigated the behavior of the four bolt unstiffened end-plate connection using finite element analysis. The study emphasized modeling of the non-linear material behavior and the contact between the end-plate and the column flange or the adjacent end-plate. Comparisons between the finite element analysis and experimental test results were made.

Bahaari and Sherbourne (1994) used ANSYS, a commercially available finite element code, to analyze 3-D finite element models to successfully predict the behavior of the four bolt extended unstiffened end-plate moment connection. The models used plate, brick, and truss elements with non-linear material properties. They recommended that the three-dimensional models be used to generate analytical formulations to predict the behavior and strength of the connection components.

Bahaari and Sherbourne (1996a, 1996b) continued their investigation of the four bolt extended unstiffened end-plate connection by considering the effects of connecting the end-plate to a stiffened and an unstiffened column flange. 3-D finite element models of the end-plate and the column flange were developed using ANSYS. The finite element results were compared

with experimental results with good correlation. Once again, it is concluded that 3-D finite element analysis can predict the behavior of end-plate connections.

Choi and Chung (1996) investigated the most efficient techniques of modeling four bolt extended unstiffened end-plate connections using the finite element method.

Bose et al. (1997) used the finite element method to analyze flush unstiffened end-plate connections. The two and four bolt flush end-plate configurations were included in the study. Comparisons with experimental results were made with good correlation.

Bursi and Jaspart (1998) provided an overview of current developments for estimating the moment-rotation behavior of bolted moment resisting connections. In addition, a methodology for finite element analysis of end-plate connections was presented.

Meng (1996) used shell elements to model the cyclic behavior of the four bolt extended unstiffened end-plate connection. The primary purpose of the study was to investigate the effects of weld access holes on the beam flange strength. The finite element results correlated well with the experimental results.

Mays (2000) used finite element analysis to develop a design procedure for an unstiffened column flange and for the sixteen bolt extended stiffened end-plate moment connection. In addition, finite element models were developed and comparisons with experimental results for the four bolt extended unstiffened, eight bolt extended stiffened, and the four bolt wide unstiffened end-plate moment connections were made. Good correlation with experimental results was obtained.

2.7 Need for Further Research

Many articles are available concerning the design of end-plate connections. However, only a small percentage of the studies consider the design of end-plate connections for seismic or cyclic loading. The literature that is available generally discusses the behavior and does not present practical design procedures. The need for a design procedure that utilizes a unified approach for all of the different connection configurations is apparent.

Even a smaller number of articles are available on the design of the column side of end-plate connections. Further analysis of the column side limit states and a unified design procedure that addresses all of the different connection configurations is needed.

Recent finite element analysis studies have show that 3-D modeling can accurately predict the behavior of end-plate connections. The use of finite element analysis to conduct parametric studies of end-plate connections provides an efficient tool for researchers to expand the knowledge base on end-plate moment connections. Utilization of the finite element method and limited experimental testing should be used to investigate the cyclic behavior and column side design of end-plate moment connections. Details of the experimental test program and limited finite element analysis results conducted as a part of this study are presented in subsequent chapters.

Chapter 3 - EXPERIMENTAL INVESTIGATION

3.1 Overview

The need for additional experimental investigation into the behavior of end-plate moment connections has been identified by the background literature. The twenty extended end-plate moment connection tests performed as a part of this study will expand the database of available test data. Eleven tests were beam-to-column connections subjected to cyclic loading and nine of the tests were beam splice connections subject to monotonic loading. The purpose of the cyclic tests was to investigate the strength and inelastic rotation capacity of the connection assemblies and to determine if extended end-plate moment connections were suitable for use in seismic force resisting moment frames. The purpose of the monotonic tests was to investigate the strength and behavior of the end-plate and the connection bolts.

Details of the experimental testing programs are presented in this chapter. A description of the test specimens, test setup, testing procedure, and test results are provided for the cyclic and the monotonic testing programs. Additional information about the testing programs, not included in this chapter, is found in Sumner et al. (2000), and Sumner and Murray (2001a, 2001b).

3.2 Cyclic Testing Program

3.2.1 Test Specimens

The eleven cyclic beam-to-column connection tests, performed as a part of this study, were part of the *SAC Steel Project* sponsored by the Federal Emergency Management Agency through the SAC Joint Venture. Ten of the test specimens were exterior sub-assemblages consisting of a single beam connected to the flange of a single column. One of the test specimens was an interior sub-assemblage consisting of two beams connected to opposite flanges of a single column with a composite slab cast onto the top flanges of the connecting beams. In both cases, the beam-to-column connections were extended end-plate moment connections. Four different beam and column combinations were used: W24x68 beam with W14x120 column, two W24x68 beams with W14x257 column, W30x99 beam with W14x193 column, and W36x150

beam with W14x257 column. All connections were made with 1 ¼ in. diameter ASTM A325 or ASTM A490 strength bolts.

For each single beam test configuration, two connection tests were performed. One test utilized a "strong plate" connection and the other utilized a "weak plate" connection. The strong plate connection was designed for 110% of the nominal plastic moment strength of the connecting beam. This was done to assure that the connection would fully develop the strength of the beam resulting in a ductile beam failure mode, e.g. local flange and web buckling. The weak plate connection was designed to develop 80% of the nominal plastic moment strength of the connecting beam. This was done to investigate the behavior of the connections in the event that an over strength beam, that is, one with a higher than specified yield stress, was fabricated with an under strength connection, that is, one with lower than specified end-plate yield stress or under strength connection bolts were utilized.

The test matrix is shown in Table 3.1. The naming convention is a combination of the connection type, bolt diameter, end-plate thickness, and nominal beam depth. The three connection configurations are designated as follows: 4E for the four bolt extended unstiffened connection (Figure 1.4a), 8ES for the eight bolt extended stiffened connection (Figure 1.4c), 8E-4W for the eight bolt extended, four bolts wide connection (Figure 1.4d). In example, a test designation of 4E-1.25-1.5-24 indicates a four bolt extended unstiffened connection with 1 ¼ in. diameter bolts, a 1 ½ in. thick end-plate, and a nominal beam depth of 24 in.

The test specimen beams were ASTM A572 Grade 50 steel, and the test specimen columns were ASTM A572 Grade 50 steel, except for the composite slab test column which was ASTM A36 steel. The end-plates, end-plate stiffeners, continuity plates, and doubler plates were ASTM A36 steel. The steel deck used in the composite slab test was 2 in. Vulcraft 2VLI, 20 gage, zinc coated steel deck. The composite slab concrete was normal weight concrete (145 pcf) with a specified 28 day compressive strength of 4000 psi. The #4 bars used as reinforcement in the composite slab were ASTM A615.

TABLE 3.1: TEST MATRIX

Specimen ID	Beam(s)	Column	Number of Bolts (Grade)	Bolt Diameter (in.)	End-Plate Thickness (in.)
4E – 1.25 – 1.5 – 24 (Strong Plate)	W24X68	W14X120	8 (A490)	1 1/4	1 1/2
4E - 1.25 – 1.125 – 24 (Weak Plate)	W24X68	W14X120	8 (A325)	1 1/4	1 1/8
4E - 1.25 – 1.375 – 24 (Strong Plate)	W24X68(2)	W14X257	8 (A490)	1 1/4	1 3/8
8ES - 1.25 – 1.75 - 30 (Strong Plate)	W30X99	W14X193	16 (A490)	1 1/4	1 3/4
8ES - 1.25 - 1 – 30 (Weak Plate)	W30X99	W14X193	16 (A325)	1 1/4	1
8ES - 1.25 – 2.5 – 36 (Strong Plate)	W36X150	W14X257	16 (A490)	1 1/4	2 1/2
8ES - 1.25 – 1.25 - 36 (Weak Plate)	W36X150	W14X257	16 (A325)	1 1/4	1 1/4
8E-4W - 1.25 – 1.125 - 30 (Strong Plate)	W30X99	W14X193	16 (A490)	1 1/4	1 1/8
8E-4W – 1.25 - 1 – 30 (Weak Plate)	W30X99	W14X193	16 (A325)	1 1/4	1
8E-4W - 1.25 – 1.375 – 36 (Strong Plate)	W36X150	W14X257	16 (A490)	1 1/4	1 3/8
8E-4W - 1.25 – 1.25 – 36 (Weak Plate)	W36X150	W14X257	16 (A325)	1 1/4	1 1/4

The test specimens were fabricated by a combination of university laboratory personnel and commercial fabricators. The beam to end-plate welds were made using American Welding Society (AWS) certified welders employed by commercial fabricators. The beam to end-plate welds were inspected by an independent AWS certified inspector. Any defects were corrected in accordance with the AWS specification (AWS, 1998).

The end-plate to beam connection was made using complete joint penetration groove welds for the flanges and fillet welds for the web. All welds were made in accordance with the *AWS Structural Welding Code* (AWS, 1998) using the Flux Cored Arc Welding (FCAW) process and E71T-1 welding electrodes. The flange welds were similar to AWS TC-U4b-GF utilizing a full depth 45-degree bevel and a minimal root opening, backed by a 3/8 in. fillet on the underside of the flanges. Past research by Meng (1996) on end-plate connections subject to cyclic loading indicated a number of problems with the use of weld access holes. In accordance with the recommendations outlined by Meng, weld access holes were not used. The beam web to end-plate connection consisted of 5/16 in. fillet welds on both sides of the web. For the eight bolt extended stiffened connections, the stiffener to end-plate and stiffener to beam flange welds were complete joint penetration groove welds.

3.2.2 Test Setups

The ten bare steel specimens were exterior sub-assemblages consisting of a single beam connected to the flange of a single column. The assemblies were tested in a horizontal position to allow use of available reaction floor supports and for safety during testing. A typical test setup is shown in Figure 3.1. The test column ends were bolted to the support beams, which were bolted to the reaction floor. The boundary conditions for the column ends were considered partially restrained. The loading was applied to the beam tip using an Enerpac RR30036 double acting hydraulic ram. A roller was used to support the free end of the test beam. The purpose of the roller was to eliminate any bending moments caused by gravity forces perpendicular to the plane of loading. Beam lateral supports were provided at intervals close enough to prevent lateral torsional buckling prior to development of the beam nominal plastic moment strength. Each of the test beams was used for two tests because a different end-plate was attached to each end of the beam. The connection on one end was tested and then the beam was rotated for the second test. A beam web stiffener was used at the point of load application. The stiffeners and load points were a distance of at least one and a half times the nominal depth of the beam from the end of the beam. This clear distance was important to avoid any interaction between the load point stiffeners for one test and the beam hinge region for the other test.

The composite slab specimen was an interior sub-assemblage consisting of a single W14x257 column with W24x68 girders attached to each flange and a 5 in. composite slab. The

test setup is shown in Figure 3.2. The W14x22 filler beams, cantilevered perpendicular to the girders, were attached to the web of the column and girders. The 5 in. thick, 7 ft. wide by 21 ft. long composite slab consisted of 3 in. of normal weight concrete cover over 2 in. steel deck. The slab was reinforced with #4 bars at 12 in. on center both ways. The slab was made partially composite with the test beams and girders using ¾ in. diameter welded shear studs welded to the top flanges of the beam at approximately 12 in. on center.

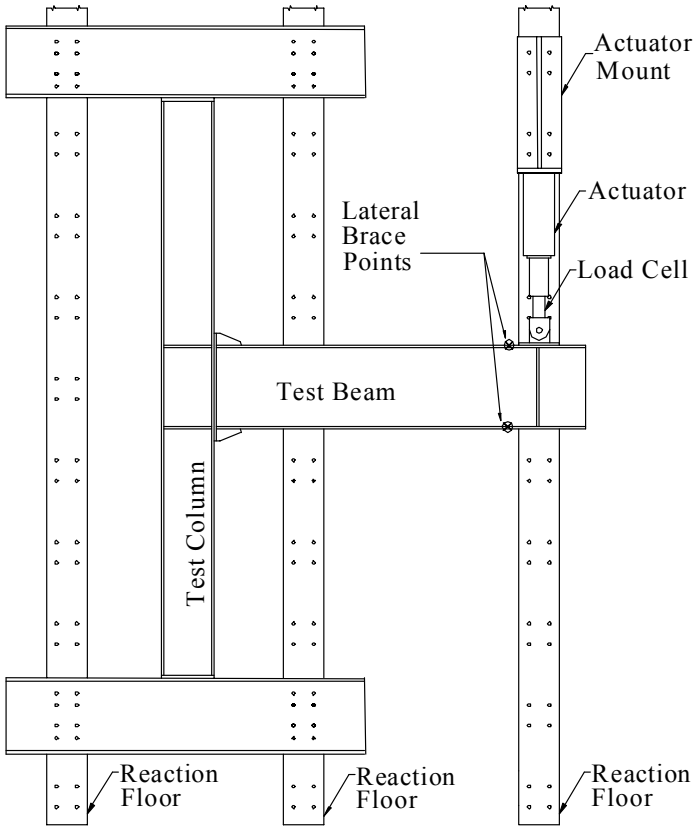

FIGURE 3.1: PLAN VIEW OF TYPICAL TEST SETUP

This assembly was tested with the column standing vertical and the beams, girders and slab horizontal. The test column was supported at its base by a clevis pin connection that provided restraint against translation but not rotation. The beam tips were supported by rigid links consisting of double acting hydraulic rams with clevis pin connections at both ends. The rigid links allowed translation of the beam tips in the horizontal direction but did not allow for any vertical translation. The use of hydraulic rams as rigid links allowed for final adjustment and leveling of the test specimen. The loading was applied to the column tip using an Enerpac

RR30036 double acting hydraulic ram. The base of the hydraulic ram was attached to a horizontal reaction frame. Lateral braces were provided at the ends of the test girders and at the top of the column just below the point of load application.

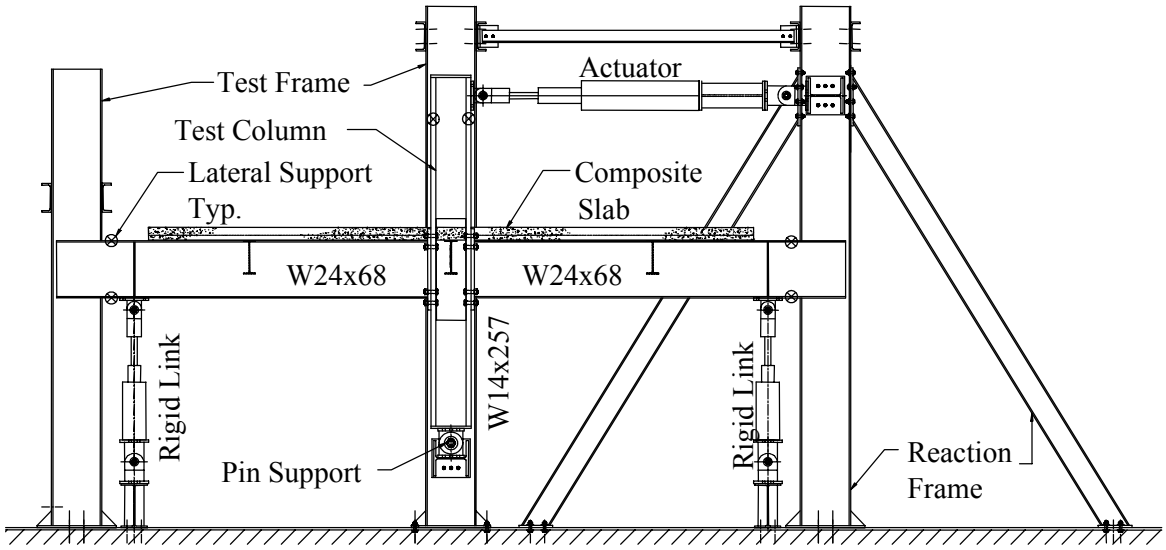

FIGURE 3.2: ELEVATION OF SLAB TEST SETUP

Instrumentation for the bare steel specimens was installed to measure the applied beam tip load, beam tip displacement, column rotation, panel zone rotation, rigid body rotation of the assembly, beam flange strains, column flange strains, panel zone shear strains, bolt strains, and end-plate separations. A plan view of the instrumentation layout is shown in Figure 3.3.

The instrumentation for the composite slab test specimen was installed to record the applied column tip load, beam tip loads, column tip displacement, column rotation, panel zone rotation, rigid body rotation of the assembly, slip of the concrete slab relative to the beam flanges, beam flange strains, panel zone shear strains, bolt strains, and end-plate separation. The typical layout of the displacement measurements is shown in Figure 3.4. The instrumentation was calibrated prior to testing and connected to the data acquisition system. All test data was recorded using a PC-based data acquisition system.

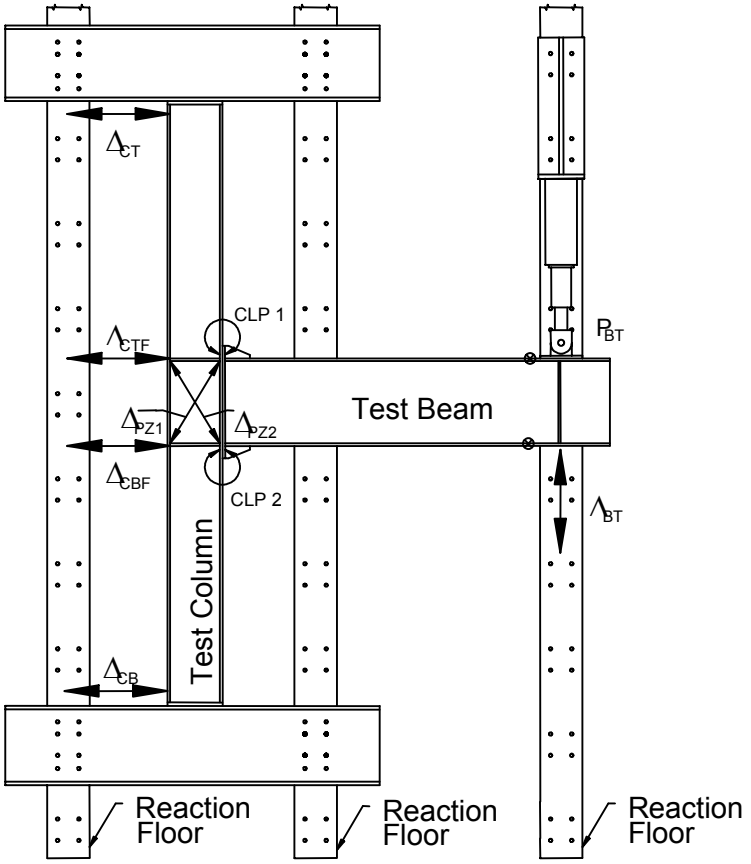

FIGURE 3.3: PLAN VIEW SHOWING TYPICAL INSTRUMENTATION

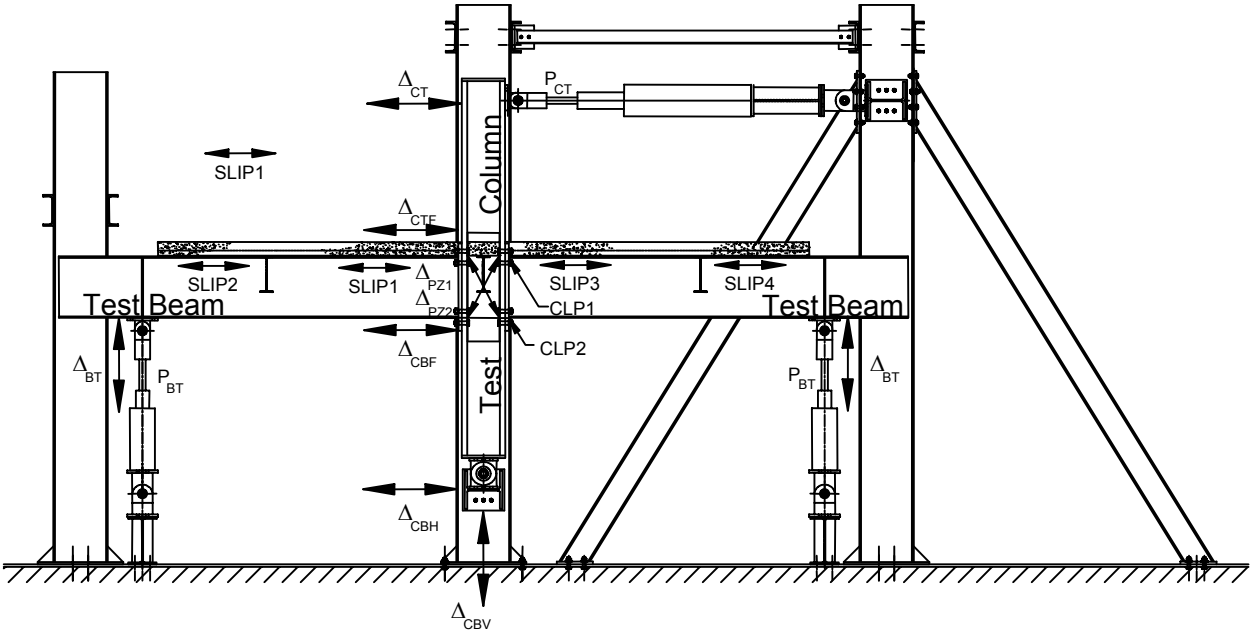

FIGURE 3.4: ELEVATION SHOWING INSTRUMENTATION

3.2.3 Testing Procedure

The same testing procedure was used for the bare steel specimens and the composite slab specimen. Once the specimens were erected in the test reaction frame, the instrumented connection bolts were installed. The instrumented bolts were connected to the PC based data acquisition system and the system zeroed. A bees wax based lubricant was liberally applied to the threads of the connection bolts and a hardened washer placed under the nut (the turned element). The bolts were then tightened, using an air impact wrench or a hydraulic impact wrench. The bolts were tightened until the minimum pretension specified by the *AISC LRFD Specification* (AISC, 1999a) was reached. The bolt tension was monitored using the data acquisition system and the load-strain relationship established by the bolt calibration. No specific tightening sequence was used. The general sequence was to tighten the most rigid part of the connection first and the least rigid portions last. Typically, two complete cycles of tightening were required to pull the plies of the connection together and to maintain the minimum bolt pretension. For the composite slab test, the composite slab was placed once the bolts were tightened.

The specimen was then "white washed" to permit the observation of yielding within the connection region. The remaining instrumentation was then installed and connected to the data acquisition system and the system zeroed. The calibration of each displacement transducers was verified and recalibration performed as necessary. The instrumentation was then zeroed and a preload cycle of approximately 0.0025 radians story drift applied. The initial stiffness of the specimen was then compared to the theoretical elastic stiffness and the behavior of the instrumentation closely observed. Any necessary adjustments to the instrumentation were made and the data acquisition system zeroed.

An initial zero reading was taken and the test was started. The loading sequence used was that prescribed by the SAC Protocol (SAC, 1997). The SAC Protocol specifies a series of load steps and the number of cycles for each as shown in Figure 3.5. Each load step corresponds to a total interstory drift angle. The load steps were executed and data points recorded at regular intervals. Observations were recoded and photographs taken at the end of each load step. The load steps were continued until the limit of the test frame was reached or until the specimen strength decreased to 40 percent of the maximum strength.

Tensile coupon tests were conducted on the major components of the test specimens. Two standard coupon test specimens were taken from the flanges and web of each beam and column, from the end-plate and from the doubler plate. The specimens were prepared in accordance with ASTM A370 "*Standard Test Methods and Definitions for Mechanical Testing of Steel Products*" and tested in accordance with Appendix D of the *SAC Protocol* (SAC, 1997). Summaries of the coupon test results are included in the Test Summary Reports located in the appendices.

Load Step Number	Interstory Drift Angle, θ (rad)	Number of Loading Cycles
1	0.00375	6
2	0.005	6
3	0.0075	6
4	0.01	4
5	0.015	2
6	0.02	2
7	0.03	2
Continue with increments in θ of 0.01, and perform two cycles at each step		

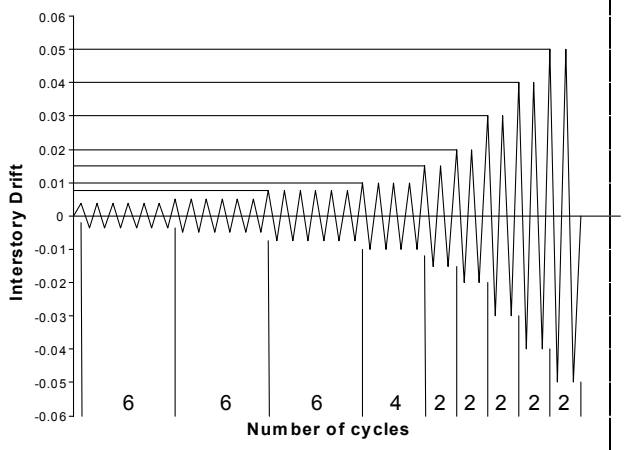

FIGURE 3.5: SAC LOADING PROTOCOL

3.2.4 Test Results

Summary sheets for each of the tests are found in Appendix A. The summary sheets include the most pertinent information about each component of the test specimens and the observed experimental behavior. Detailed connection summary reports are found in the appendices of Sumner et al. (2000). The summary reports include a detailed description of the specimen performance at each load step, summary of peak values observed, photographs before and after testing, various graphs showing the specimen response, and fabrication drawings.

Beam failure, as characterized by a combination of flange and web local buckling, was the expected failure mode for the strong plate connection specimens. The beam failure mode is a desirable failure mode that can be reliably predicted and it provides a great deal of ductility and energy dissipating characteristics. The weak plate connections were expected to fail in a brittle manner. The expected failure mode was end-plate yielding followed by bolt tension rupture. End-plate yielding can provide for a moderate amount of energy dissipation; however, it results in the formation of substantial prying forces in the bolts and ultimately results in bolt tension rupture, a brittle failure mode.

The critical specimen performance parameters used to evaluate the test results were the maximum applied moment, the maximum interstory drift angle, and the maximum inelastic interstory drift angle. The applied moment was calculated by multiplying the applied load by the distance from the beam tip to the face of the column. The total interstory drift angle, for a conventional moment frame, is determined by dividing the horizontal interstory displacement by the story height. For the test setup used in the bare steel connection tests, the interstory drift angle was determined by dividing the beam tip displacement by the distance from the centerline of the column to the beam tip, and subtracting any rigid body rotations of the column end supports. The inelastic, or plastic, interstory drift angle was determined by subtracting the elastic deformation component of the specimen response from the total deformation response. The elastic deformation component of the specimen response was calculated using an equation of the best-fit line of the elastic portion of the load deformation response plot.

3.2.4.1 Four Bolt Extended Connections

Two bare steel specimens and one composite slab specimen were tested with the four bolt extended unstiffened end-plate moment connection (Figure 1.4a). The bare steel specimens performed as expected. The strong plate connection test (4E-1.25-1.5-24) resulted in local flange and web buckling of the beam with no distress observed within the connection region. The connection displayed a great deal of ductility and energy dissipation capacity. Figure 3.6 shows graphs of the moment vs. total rotation and moment vs. plastic rotation response. As shown in Figures 3.7 and 3.8, the end-plates did not appear to yield but local beam flange and web buckling occurred. The bolt behavior was also as expected. The bolt strains remained constant, at the pretension strain, during most of the elastic cycles as shown in Figure 3.9. Then the strains gradually decreased towards zero as the load steps increased in magnitude. The bolt strains were not observed to increase substantially above the initial pretension strains.

The weak plate connection test (4E-1.25-1.125-24) resulted in end-plate yielding followed by bolt tension rupture. The yielding of the end-plate provided moderate energy dissipation capacity prior to failure. The bolts in the weak plate connection behaved similar to the bolts in strong plate connection during the lower load steps. However, as the load steps increased, a sharp increase in bolt strain was observed. This sharp increase was concurrent with the initial yielding of the end-plate. Yielding of the bolts prior to failure was indicated by permanent set of the bolt strains during the higher load steps. Typical plots of strong and weak plate bolt behavior are shown in Figures 3.9 and 3.10 respectively.

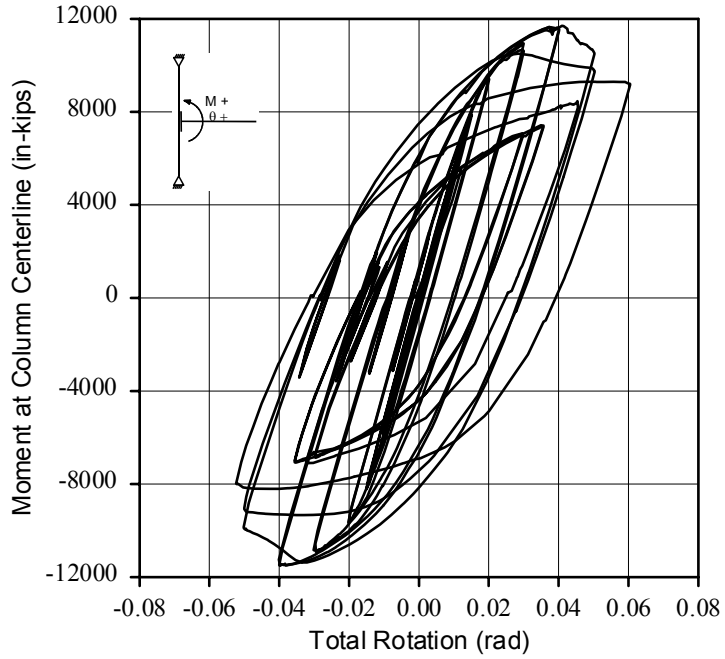

a) Moment vs. Total Rotation

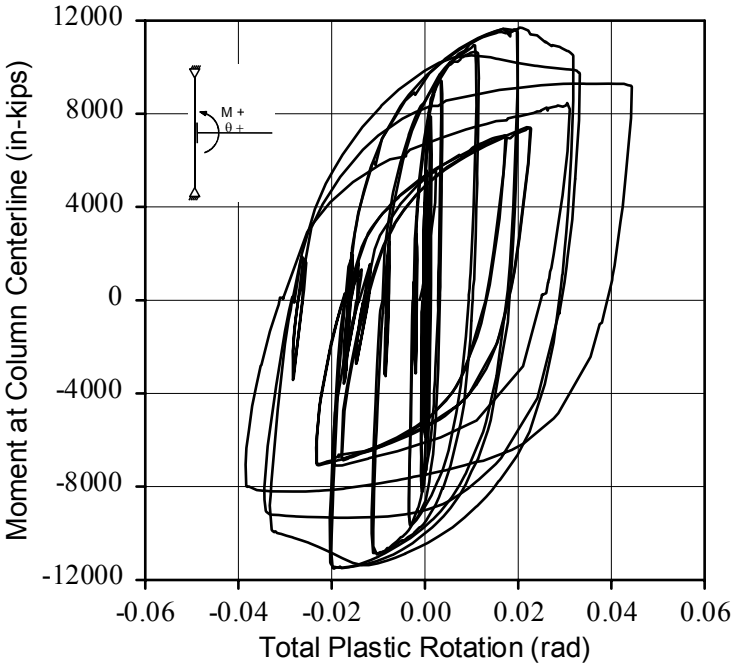

b) Moment vs. Plastic Rotation

FIGURE 3.6: FOUR BOLT EXTENDED UNSTIFFENED MOMENT ROTATION RESPONSE (4E-1.25-1.5-24)

FIGURE 3.7: FOUR BOLT EXTENDED UNSTIFFENED CONNECTION AFTER TESTING (4E-1.25-1.5-24)

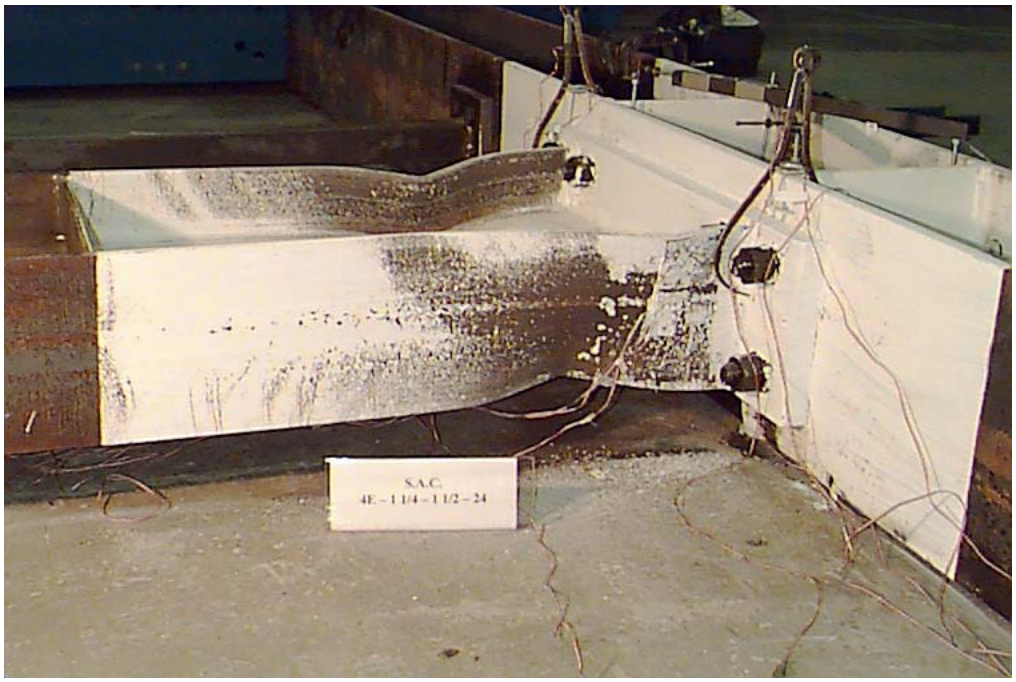

FIGURE 3.8: FOUR BOLT EXTENDED UNSTIFFENED CONNECTION AFTER TESTING SHOWING DETAIL OF BEAM FLANGE (4E-1.25-1.5-24)

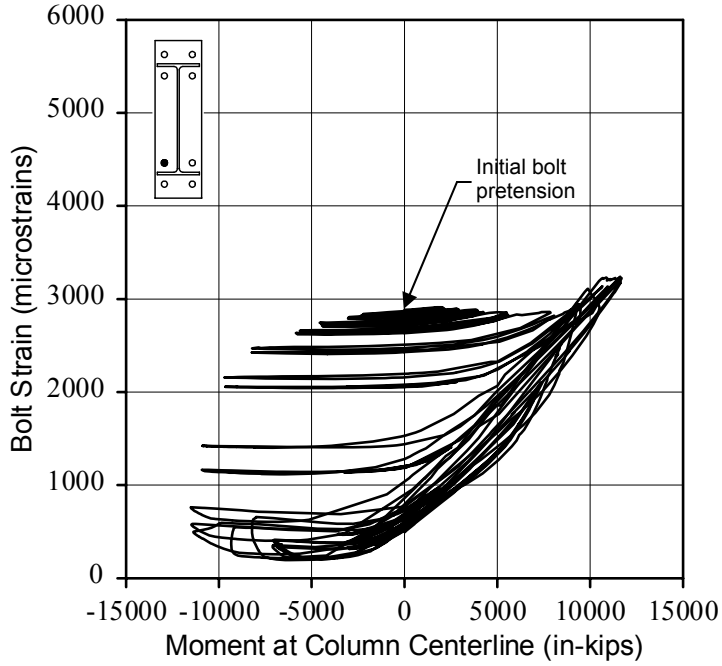

FIGURE 3.9: FOUR BOLT EXTENDED UNSTIFFENED STRONG PLATE BOLT RESPONSE (4E-1.25-1.5-24)

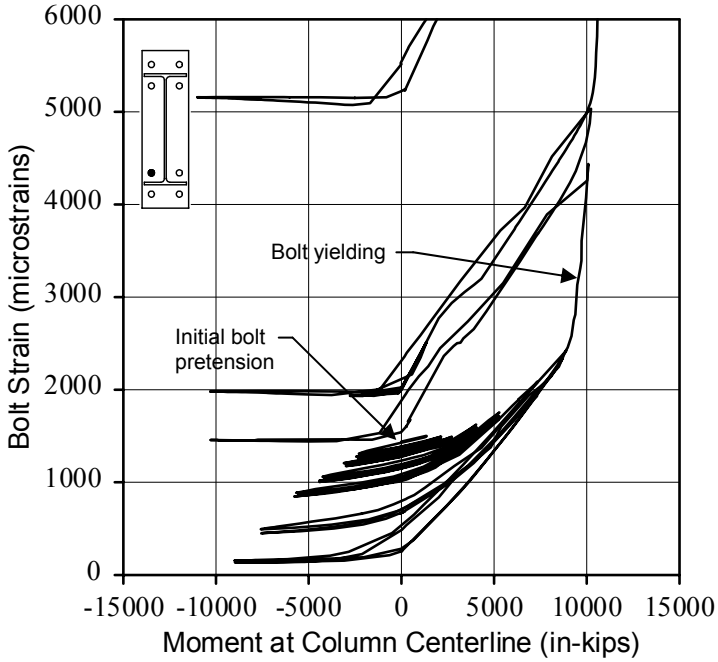

FIGURE 3.10: FOUR BOLT EXTENDED UNSTIFFENED WEAK PLATE BOLT RESPONSE (4E-1.25-1.5-24)

3.2.4.2 Eight Bolt Extended, Four Bolts Wide Connections

Four bare steel specimens were tested with the eight bolt extended, four bolts wide end-plate moment connection (Figure 1.4d). The specimens did not perform as expected. All of the specimens failed by bolt tension rupture and end-plate tearing. However, a considerable amount of energy dissipation capacity was observed prior to failure of the specimens. In many cases, the flanges of the connecting beam had completely yielded and local flange buckling appeared imminent. Figure 3.11 shows the typical moment vs. rotation response of the connections. Figure 3.12 shows a typical specimen after testing. The yielding of the specimen and tearing of the end-plate are clearly visible.

The bolts in the 30 in. beam specimens (4W-1.25-1.125-30 and 4W-1.25-1-30) behaved quite differently than the bolts in the 36 in. beam specimens (4W-1.25-1.375-36 and 4W-1.25-1.25-36). In the tests of the 30 in. specimens, the bolts closest to the centerline of the beam web (inside bolts) had much higher strains than the bolts farthest from the centerline of the beam web (outside bolts). This indicates an uneven distribution of the flange force between the inside and outside bolts. Figures 3.13 and 3.14 show typical bolt response plots for an inside and an outside bolt respectively. In the tests of the 36 in. specimens, the bolt strains in the inside and outside bolts did not vary as much as in the 30 in. specimen tests. This indicates a better distribution of the flange force to the inside and outside bolts. The inner and outer gages of the bolts for the 30 in. and 36 in. were the same. However, the 36 in. specimens had a wider flange than the 30 in. specimens and therefore the flange force was more effectively distributed to the outside bolts.

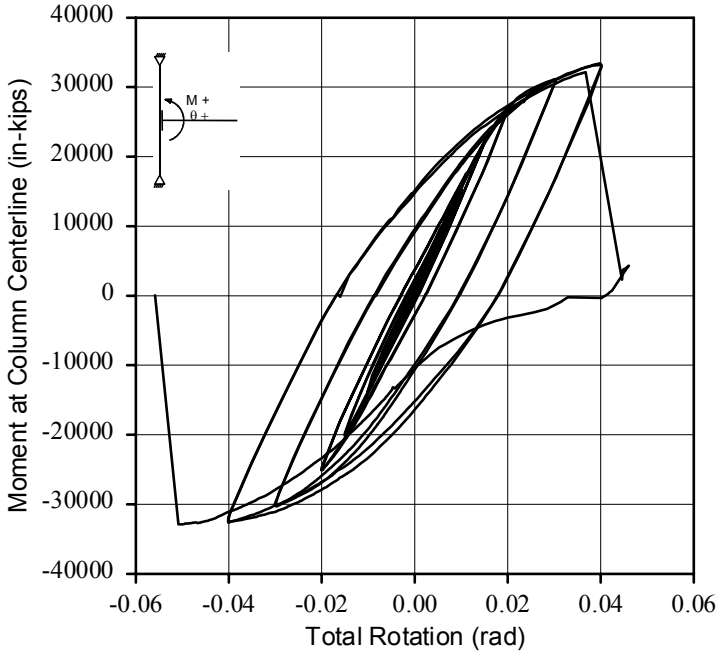

a) Moment vs. Total Rotation

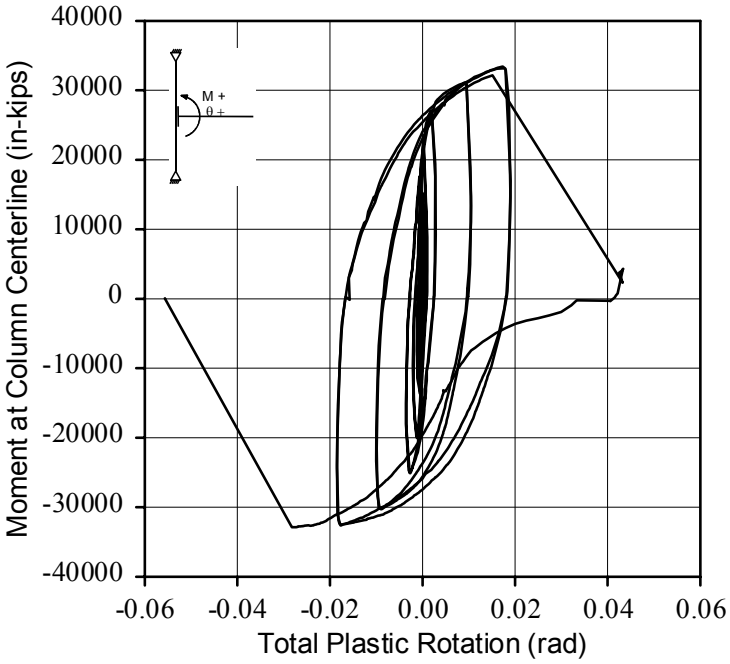

b) Moment vs. Plastic Rotation

FIGURE 3.11: EIGHT BOLT EXTENDED, FOUR BOLTS WIDE MOMENT VS. ROTATION RESPONSE (4W-1.25-1.25-36)

a) Back of End-Plate

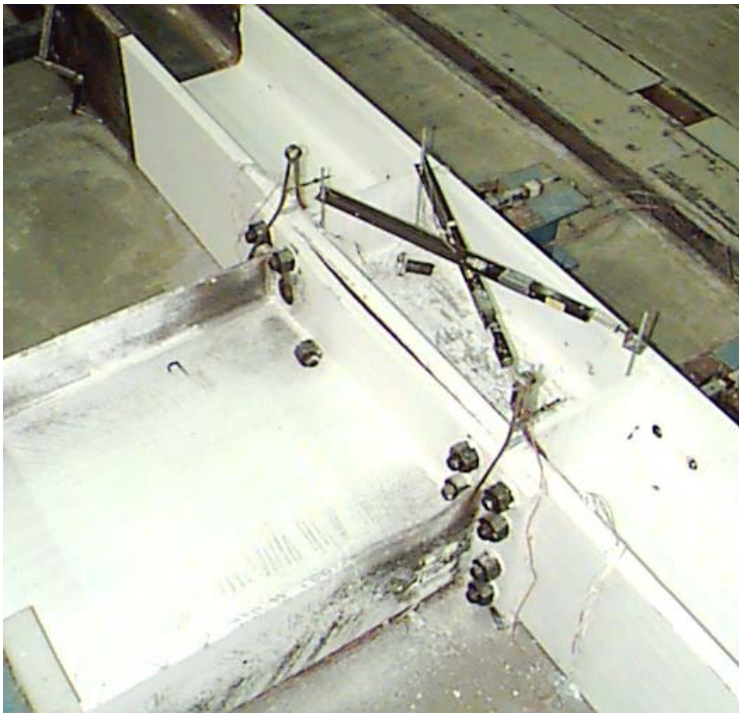

b) Overall View of Connection Region

FIGURE 3.12: EIGHT BOLT EXTENDED, FOUR BOLTS WIDE SPECIMEN AFTER TESTING (4W-1.25-1.125-30)

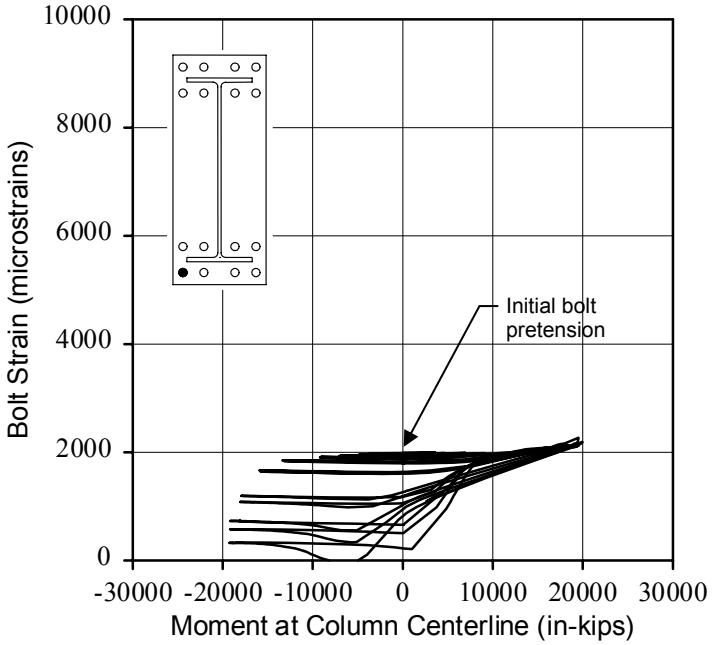

FIGURE 3.13: EIGHT BOLTS EXTENDED, FOUR BOLTS WIDE OUTSIDE BOLT RESPONSE (4W-1.25-1.125-30)

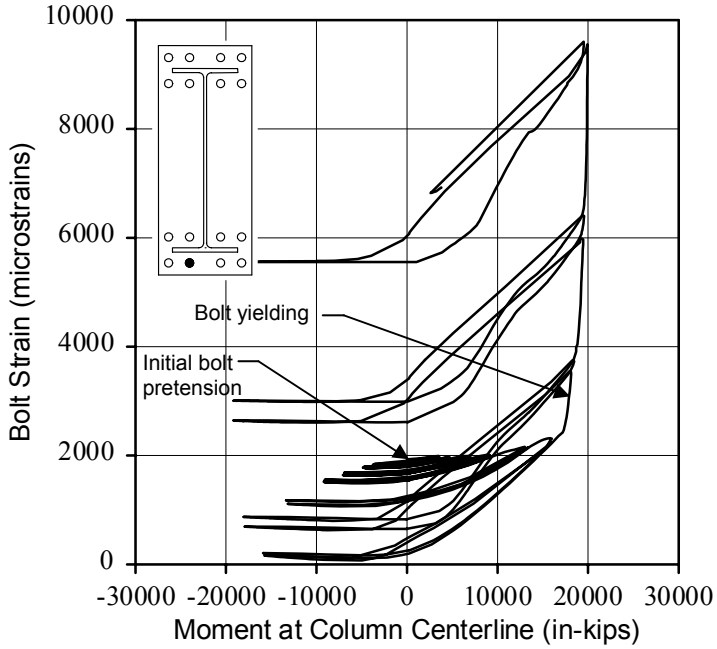

FIGURE 3.14: EIGHT BOLTS EXTENDED, FOUR BOLTS WIDE INSIDE BOLT RESPONSE (4W-1.25-1.125-30)

3.2.4.3 Composite Slab Test

Typically in the design of steel moment resisting frames, the effects of the composite slab are neglected. The assumption is that the concrete will crack or crush and will not contribute to the strength of the steel sections.

To investigate the behavior of end-plate connections with a composite slab, one four bolt extended unstiffened end-plate connection specimen was tested with a composite slab cast onto the top flange of the beams. The strong plate specimen did not behave as expected. The test initially resulted in flange local buckling of the bottom flanges of both test beams. However, as the inelastic loading cycles continued, the composite slab was still contributing to the strength of the specimen. This resulted in a higher than expected demand on the bottom flange connection bolts. Ultimately, the bolts failed in tension rupture prior to local buckling of the top flanges of the test beams. The failed specimen is shown in Figure 3.15. The substantial yielding of the beam section is apparent. The relatively small amount of yielding around the top flange area is noteworthy. In this case, the slab did crack and crush around the column, see Figure 3.15b, but the slab continued to contribute to the strength of the beam sections.

3.2.4.4 Summary of Cyclic Test Results

The performance of the eleven test specimens is summarized in Table 3.2. The ratio of the maximum applied moment at the centerline of the column to the expected plastic moment capacity of the beam is shown. The expected plastic moment capacity, $M_{p\ BEAM}$, is calculated using the following expression:

$$M_{p\ BEAM} = R_y\ [(F_y + F_u)/2\ ]Z_x \qquad (3.1)$$

where $R_y = 1.1$ for $F_y = 50$ ksi
F_y = Yield stress
F_u = Ultimate tensile stress
Z_x = Plastic section modulus of beam

Experimental tests have shown that the maximum plastic moment developed by a beam is more closely predicted using Equation 3.1 instead of the traditional nominal plastic moment strength, $M_p = F_y Z_x$, (Coons, 1999). Using the average of the yield stress and the tensile strength more closely represents the strength of the beam flanges during the inelastic cycles. The beam flanges initially yield and buckle, as the cycles are continued the beam flange undergo strain

(a) Connection Region

(b) View of Composite Slab Around Column

FIGURE 3.15: COMPOSITE SLAB TEST SPECIMEN AFTER TESTING (4E-1.25-1.375-24-SLAB)

TABLE 3.2: SUMMARY OF SPECIMEN PERFORMANCE

Test ID		$M_{max}/M_{n\ BEAM}$*	$\theta_{Total\ Sustained}$ (rad)	$\theta_{P\ Max\ Sustained}$ (rad)
4E-1 1/4-1 1/2-24 (Strong Plate)		1.00	0.052	0.038
4E-1 1/4-1 1/8-24 (Weak Plate)		0.95	0.040	0.021
4E-1 1/4-1 3/8-24 with 5" composite slab (Strong Plate)	North Beam	1.28	0.050	0.025
	South Beam	1.27	0.060	0.035
8ES-1 1/4-1 3/4-30 (Strong Plate)		1.00	0.050	0.036
8ES-1 1/4-1-30 (Weak Plate)		1.06	0.056	0.039
8ES-1 1/4-2 1/2-36 (Strong Plate)		1.06	0.050	0.028
8ES-1 1/4-1 1/4-36 (Weak Plate)		0.89	0.030	0.011
4W-1 1/4-1 1/8-30 (Strong Plate)		0.98	0.050	0.029
4W-1 1/4-1 –30 (Weak Plate)		0.91	0.040	0.021
4W-1 1/4-1 3/8-36 (Strong Plate)		0.89	0.040	0.019
4W-1 1/4-1 1/4-36 (Weak Plate)		0.88	0.040	0.019

* M_{max} = Maximum applied moment at the face of column
$M_{n\ BEAM} = R_y [(F_y + F_u)/2] Z_x = 1.1[(50+65)/2] Z_x$

hardening. This results in a higher effective strength of the beam section. Using the expected plastic moment capacity to calculate the moment ratio provides a more accurate comparison between the experimental and theoretical values.

In addition to the moment ratio, the maximum total story drift rotation angle, θ_{total}, and the maximum inelastic story drift rotation angle, θ_p, are shown in Table 3.2. It should be noted that the maximum total and inelastic story drift rotation angles were sustained for at least one complete loading cycle. For the strong plate tests, much larger story drift rotations could likely have been achieved, if the limits of the test setup had not been exceeded.

A comparison of the moment ratios shown for the composite slab test (4E-1.25-1.375-24) to the corresponding bare steel test (4E-1.25-1.5-24), indicates that the slab increased the moment capacity of the W24x68 section by approximately 27 percent at the time of failure. The total increase in strength can not be determined from this test because the bolts failed in tension prior to realization of the ultimate bending capacity of the composite section. This result is contrary to the traditional assumption that the composite slab will not contribute the strength of the beam during the large inelastic loading cycles.

3.3 Monotonic Testing

3.3.1 Test Specimens

Nine monotonic end-plate moment connection tests were also conducted as a part of this research. The tests were sponsored by Star Building Systems, Inc. and the Metal Building Manufacturers Association. The connection test specimens consisted of two built-up beam sections spliced together at midspan using either a multiple row extended 1/2 end-plate moment connection or an eight bolt extended, four bolts wide end-plate moment connection. The purpose of the testing was to investigate the strength of each individual connection component (end-plate and connection bolts) so that comparisons with analytical models could be made.

The test matrix is shown in Table 3.3. The nominal connection geometric parameters shown in the test matrix are defined in Figure 3.16. The test naming convention is the same as previously described.

The test specimen connections were designed weaker than the connecting beams to investigate thick plate (strong plate) and thin plate (weak plate) behavior. As previously described, thick plate behavior occurs when the end-plate is designed strong enough to cause a tension rupture failure of the connection bolts prior to the formation of substantial bolt prying forces. Thin plate behavior occurs when the bolts are designed to be stronger than the end-plate allowing the formation of bolt prying forces. The approach resulted in the design of two connections for each bolt layout pattern. ASTM A325 strength bolts were used for both the thick and thin plate connection tests. To investigate the behavior of ASTM A490 strength bolts, the thick plate tests were repeated using A490 strength bolts. The connection bolts were assumed to be "snug-tight." In accordance with the AISC/MBMA Design Guide (Murray and Shoemaker, 2002), the "snug-tight" condition is specified as a specific percentage of the LRFD (AISC, 1999a) minimum specified pretension force depending on the bolt diameter.

TABLE 3.3: MONOTONIC TEST MATRIX

Test Identification	Bolt Dia., d_b (in.)	Bolt Grade	End-Plate Thickness (in.)	Inner Pitch, p_{fi} (in.)	Outer Pitch, p_{fo} (in.)	Gage g, g_o (in.)	End-Plate Width, b_p (in.)	Flange Width, b_f (in.)	Beam Depth, d (in.)
Test A - 8E-4W-1-1/2-62	1	A325	1/2	1 3/8	1 3/8	3 1/2	14	12	61 1/2
Test C - 8E-4W-3/4-3/4-62	3/4	A325	3/4	1 3/8	1 3/8	3 1/2	14	12	61 1/2
Test F - 8E-4W-3/4-3/4-62	3/4	A490	3/4	1 3/8	1 3/8	3 1/2	14	12	61 1/2
Test A - MRE 1/2-3/4-3/8-30	3/4	A325	3/8	1 1/4	1 1/4	3	8	8	30
Test B - MRE 1/2-3/4-3/4-30	3/4	A325	3/4	1 1/4	1 1/4	3	8	8	30
Test B1 - MRE 1/2-3/4-3/4-30	3/4	A490	3/4	1 1/4	1 1/4	3	8	8	30
Test C - MRE 1/2-3/4-1/2-30	3/4	A325	1/2	5	1 1/4	3	8	8	30
Test D - MRE 1/2-3/4-3/4-30	3/4	A325	3/4	5	1 1/4	3	8	8	30
Test D1 - MRE 1/2-3/4-3/4-30	3/4	A490	3/4	5	1 1/4	3	8	8	30

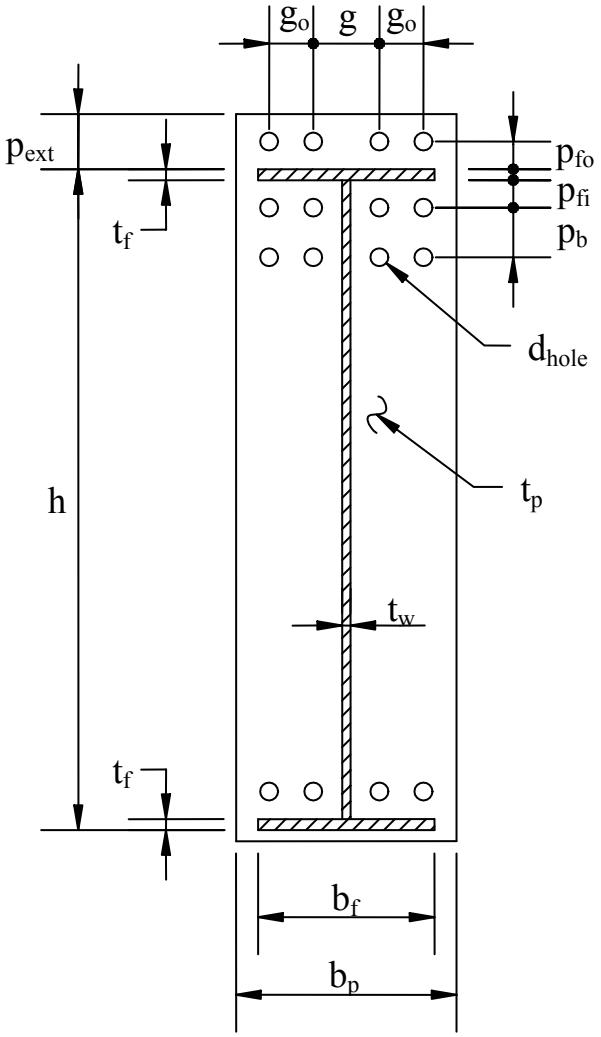

FIGURE 3.16: FOUR BOLTS WIDE END-PLATE CONNECTION GEOMETRY NOTATION

The test specimens were fabricated by Star Building Systems, Inc. The steel used for the end-plate and built-up beam section was ASTM A572 Grade 50 with a nominal yield strength of 50 ksi. ASTM A325 and A490 bolts were used along with ASTM A563 nuts, without washers. The welding of the specimens was performed in accordance with the current American Welding Society specifications (AWS, 1998). Detailed fabrication drawings are found in the appendices of Sumner and Murray (2001a, 2001b).

3.3.2 Test Setup

The connections were tested as a midspan beam splice connection loaded under pure moment. The test specimen was simply supported with rollers at each end. The ends were supported by stiffened support beams connected directly to the reaction floor. Symmetrical loading was applied using two hydraulic rams connected in parallel to a single hydraulic pump. The hydraulic rams were supported by vertical load frames bolted to the reaction floor. The specimens were braced laterally at intervals close enough to prevent lateral torsional buckling of the test beams. A typical test setup is shown in Figures 3.17 and 3.18.

The connection test specimens were instrumented to measure the applied load, specimen deflection, end-plate separation, and bolt forces. The instrumentation layout is shown in Figure 3.19. The instrumentation was calibrated prior to use and connected to a PC-based data acquisition system during testing.

3.3.3 Testing Procedure

Once the test specimen was erected in the reaction frame, the instrumented connection bolts were installed. The test bolts were connected to the PC-based data acquisition system and the system zeroed. The bolts were then tightened to the specified "snug tight" level as indicated by the bolt strain readings. The non-instrumented bolts were tightened to the same torque by "feel" with reference to the torque applied to the instrumented bolts. The tightening sequence was repeated until all bolts had achieved the same pretension level. The specimen was then white washed to allow the observation of yielding within the connection region.

The displacement transducers and calipers were setup and connected to the data acquisition system. The calibration of each transducer was then verified and recalibration performed as necessary. The instrumentation was then zeroed and a preload cycle of approximately 20 percent of the predicted failure load was applied. The initial stiffness of the specimen was compared to the theoretical elastic stiffness and the behavior of the instrumentation closely observed. Any necessary adjustments to the instrumentation were made and the data acquisition system zeroed.

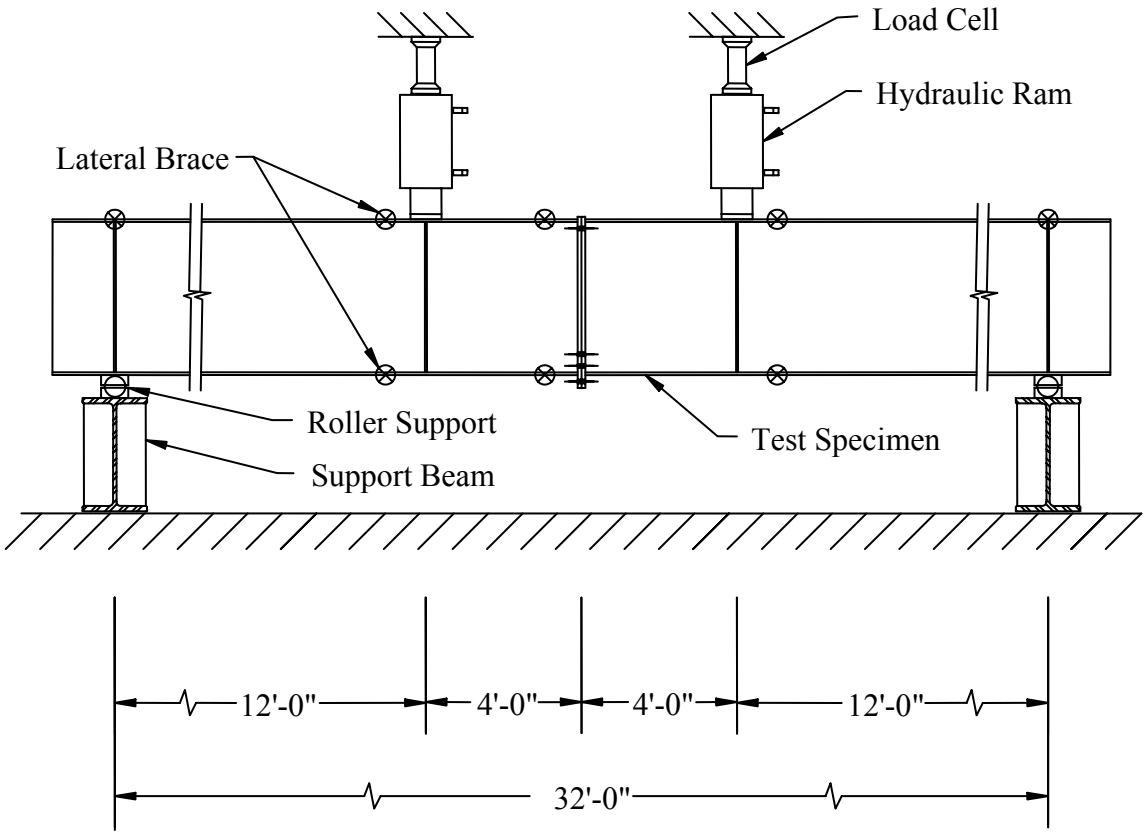

FIGURE 3.17: TYPICAL MONOTONIC TEST SETUP

FIGURE 3.18: PHOTOGRAPH OF A MONOTONIC TEST SETUP

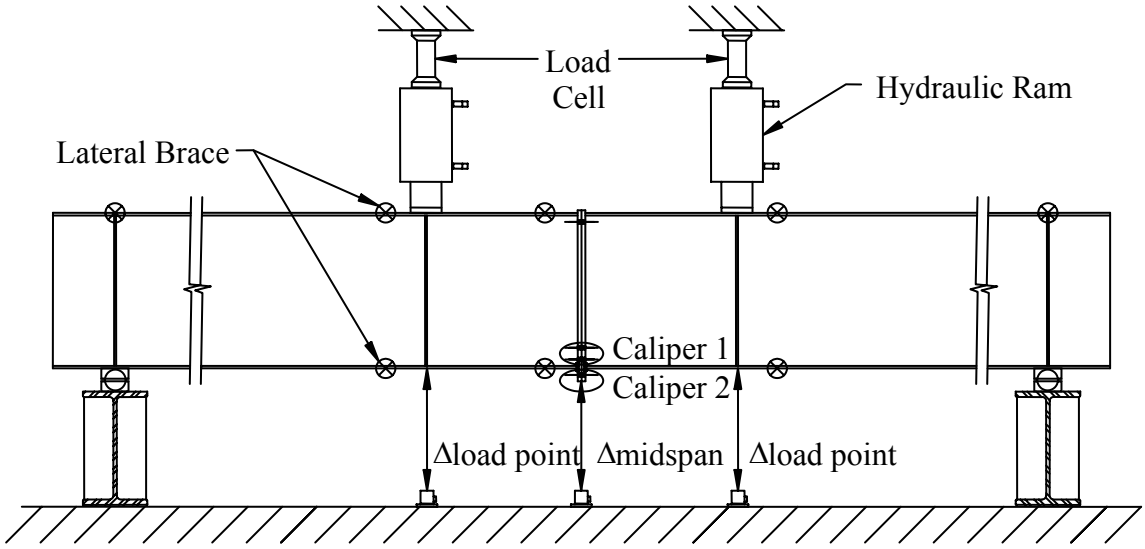

FIGURE 3.19: TYPICAL MONOTONIC TEST INSTRUMENTATION

An initial zero reading was recorded and the test was begun with loading applied in increments of approximately 10 percent of the predicted failure load. The specimen was allowed to "settle" at each load step. Data points were recorded and real-time plots of the test data monitored at each load step. As the specimen began to yield, indicated by flattening of the load-deflection plot, the load steps were applied based on a target deflection instead of a target load. The load steps were continued until failure of the connection.

Tensile coupon tests were conducted on the end-plate material used in the testing program. The standard tensile coupon specimens were prepared, measured and tested in accordance with ASTM A370 "*Standard Test Methods and Definitions for Mechanical Testing of Steel Products*". The yield strength was determined using a 0.2 percent offset of the recorded stress-strain relationship. The ultimate tensile strength and the total elongation were also determined.

3.3.4 Test Results

Summary sheets for each of the tests are found in Appendix B. The summary sheets include the most pertinent information about each component of the test specimens and the observed experimental behavior. Detailed connection test summaries are found in the

appendices of Sumner and Murray (2001a, 2001b). The test summaries include analyses calculations, graphs showing the specimen response, and photographs before and after testing.

Table 3.4 is a summary of the test results. The yield moment shown in Table 3.4 is determined using a bilinear curve fit of the end-plate separation data. The first line in the used in the curve fit represents the initial elastic stiffness of the end-plate and the second line represents the post yield stiffness. The intersection of the two lines is considered the yield moment. In a thin plate test, where the connection strength is controlled by the end-plate strength, the yield moment should correlate closely with the calculated moment strength of the end-plate, M_{pl}. In a thick plate test, where the strength is controlled by bolt tension rupture with no prying, the yield moment indicates the onset of bolt yielding.

TABLE 3.4: SUMMARY OF MONOTONIC CONNECTION TEST RESULTS

Test Identification	**Yield Moment M_y (k-ft)**	**Maximum Applied Moment, M_{max} (k-ft)**	**Failure Mode**
Test A - 8E-4W-1-1/2-62	1075	1539	EP Yielding
Test C - 8E-4W-3/4-3/4-62	1630	1825	Bolt Rupture
Test F - 8E-4W-3/4-3/4-62 (A490)	2110	2204	Bolt Rupture
Test A - MRE 1/2-3/4-3/8-30	330	462	EP Yielding / Bolt Rupt.
Test B - MRE 1/2-3/4-3/4-30	540	633	Bolt Tension Rupture
Test B1 - MRE 1/2-3/4-3/4-30	640	750	Bolt Tension Rupture
Test C - MRE 1/2-3/4-1/2-30	405	482	EP Yielding / Bolt Rupt.
Test D - MRE 1/2-3/4-3/4-30	500	559	Bolt Tension Rupture
Test D1 - MRE 1/2-3/4-3/4-30	450	623	Bolt Tension Rupture

Thin plate end-plate connections have two failure modes. One is end-plate failure which is characterized by yielding of the end-plate and non-linear (inelastic) end-plate separation. The other failure mode is bolt tension rupture due to a combination of direct bolt tension and prying forces. Thick plate end-plate connections have only one failure mode, bolt tension rupture without substantial prying forces. For the thick plate tests, the experimental yield moment only indicates the onset of yielding in the bolts and not end-plate failure.

3.3.4.1 Multiple Row Extended 1/2 Connections

Six multiple row extended 1/2 (MRE 1/2) end-plate moment connection tests were performed. Two primary types of connection behavior were observed, thick plate and thin plate. Two of the test specimens behaved as thin plate connections, resulting in end-plate yielding followed by bolt tension rupture. The results from these tests provide yield moments, M_y, that are used to validate end-plate yield-line mechanism design models. The load versus deflection and end-plate separation responses of a typical thin plate MRE 1/2 connection are shown in Figures 3.20 and 3.21, respectively. The inelastic load deflection response and the large end-plate separations prior to failure are noteworthy. Figure 3.22 is a typical bolt force response plot. The nominal bolt tensile strength, P_t, for the connection bolts is shown using a horizontal dashed line. The nominal bolt tensile strength, as defined by the *AISC LRFD Specification* (AISC, 1999), was calculated using the following:

$$P_t = F_t A_b \tag{3.2}$$

where: F_t = nominal tensile strength of bolt material, tabulated in Table J3.2 (AISC, 1999), (90 ksi for A325, 113 ksi for A490).
A_b = nominal unthreaded body area of bolt, in^2.

The sharp increase in bolt forces, indicating that the bolt is yielding and close to failure, as the applied moment becomes large is evident. Figure 3.23 shows a photograph of a typical thin plate specimen after testing. The extensive end-plate yielding, indicated by flaking of the whitewash, is apparent.

Four of the test specimens behaved as thick plate end-plate connections, resulting in bolt tension rupture prior to the onset of end-plate yielding. The thick plate connection test results provide ultimate strength moments, M_{max}, for the limit state of bolt tension rupture. These results are used to validate bolt force design models. The load versus deflection and end-plate separation responses of a typical MRE ½ connection are shown in Figures 3.24 and 3.25, respectively. Figure 3.25 shows a typical bolt response for a thick plate connection. The plot shows that each of the bolts reached their nominal proof load, P_t, prior to failure of the connection. This is an important observation for the validation of the bolt force design model. Figure 3.26 shows a photograph of a typical thick plate specimen after testing. The tension rupture failure of the bolts and the absence of end-plate yielding are apparent.

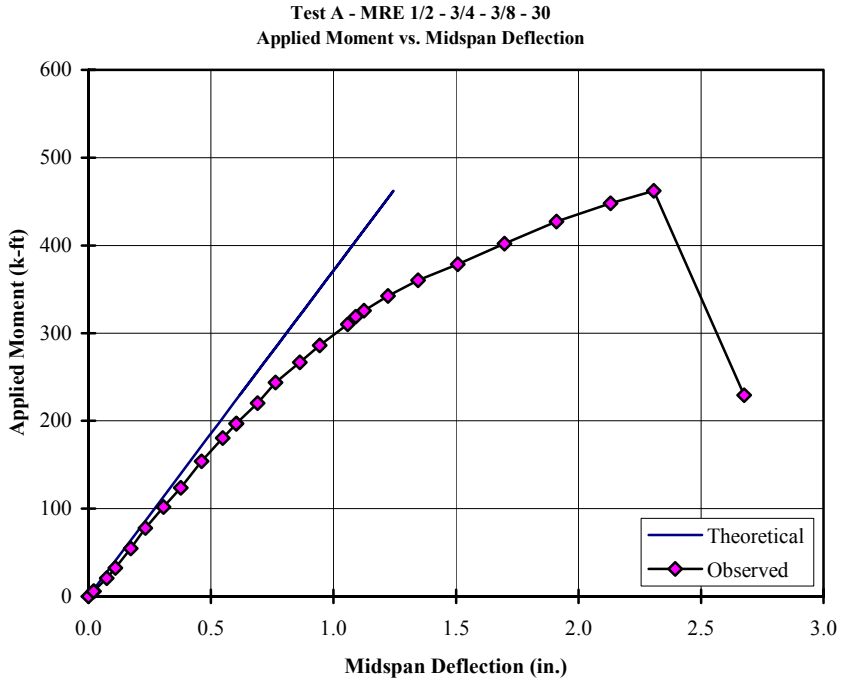

FIGURE 3.20: TYPICAL APPLIED MOMENT VS. MIDSPAN DEFLECTION RESPONSE FOR A THIN PLATE SPECIMEN (TEST A-MRE 1/2-3/4-3/8-30)

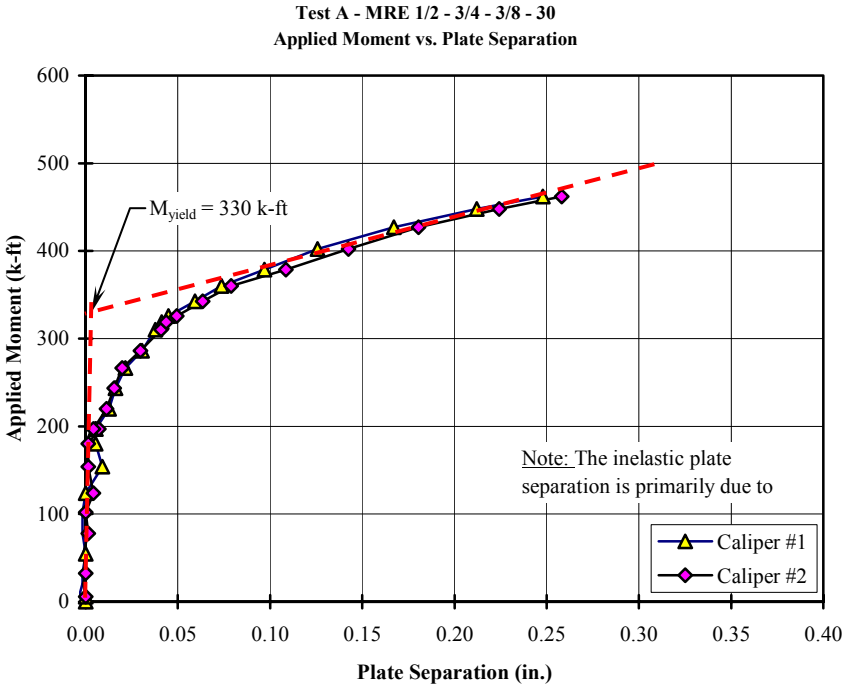

FIGURE 3.21: TYPICAL APPLIED MOMENT VS. END-PLATE SEPARATION RESPONSE FOR A THIN PLATE SPECIMEN (TEST A-MRE 1/2-3/4-3/8-30)

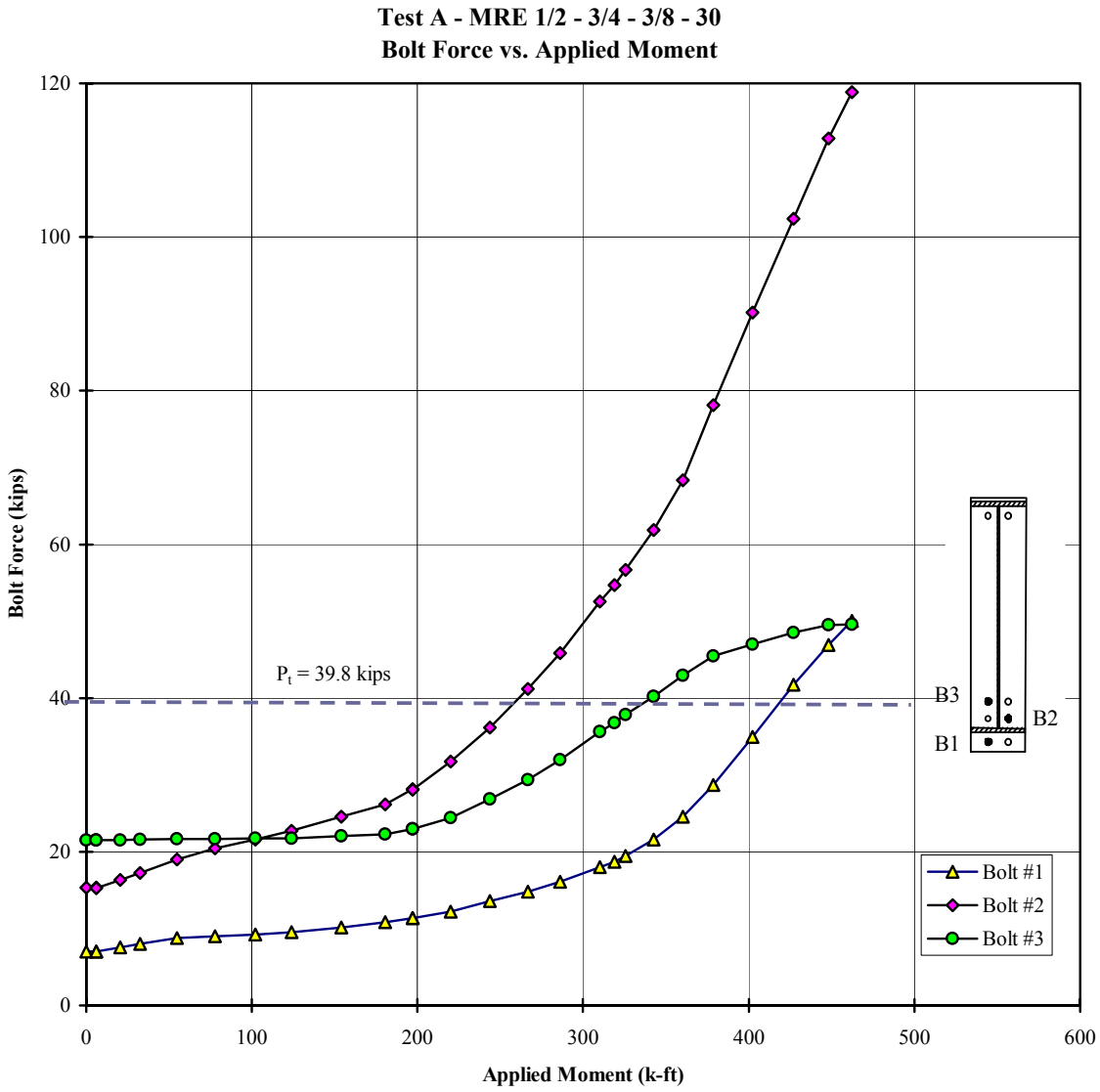

FIGURE 3.22: TYPICAL BOLT FORCE VS. APPLIED MOMENT RESPONSE FOR A THIN PLATE SPECIMEN (TEST A-MRE 1/2-3/4-3/8-30)

FIGURE 3.23: PHOTOGRAPH OF THIN PLATE FAILURE (TEST C-MRE 1/2-3/4-1/2-30)

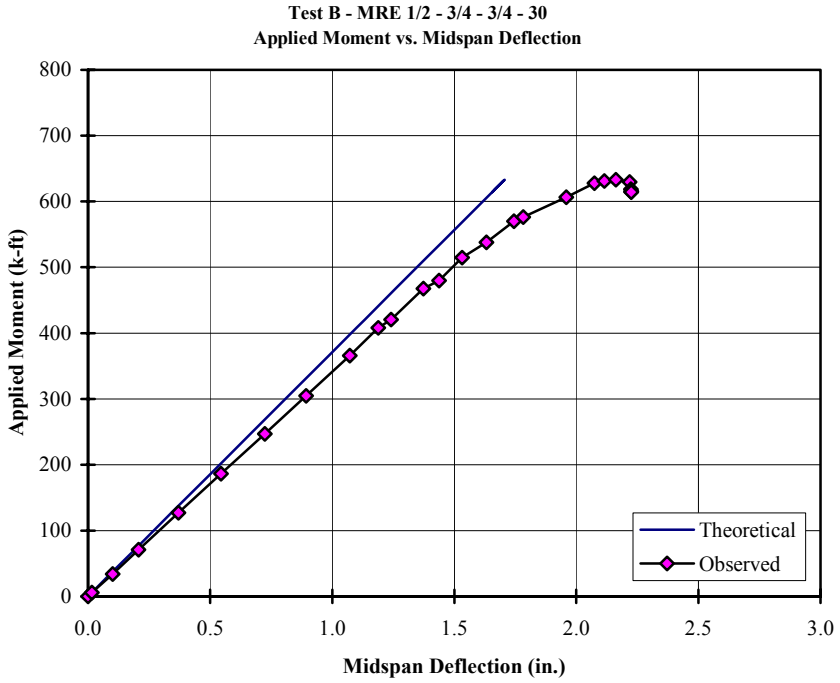

FIGURE 3.24: TYPICAL APPLIED MOMENT VS. MIDSPAN DEFLECTION RESPONSE FOR A THICK PLATE SPECIMEN (TEST B-MRE 1/2-3/4-3/4-30)

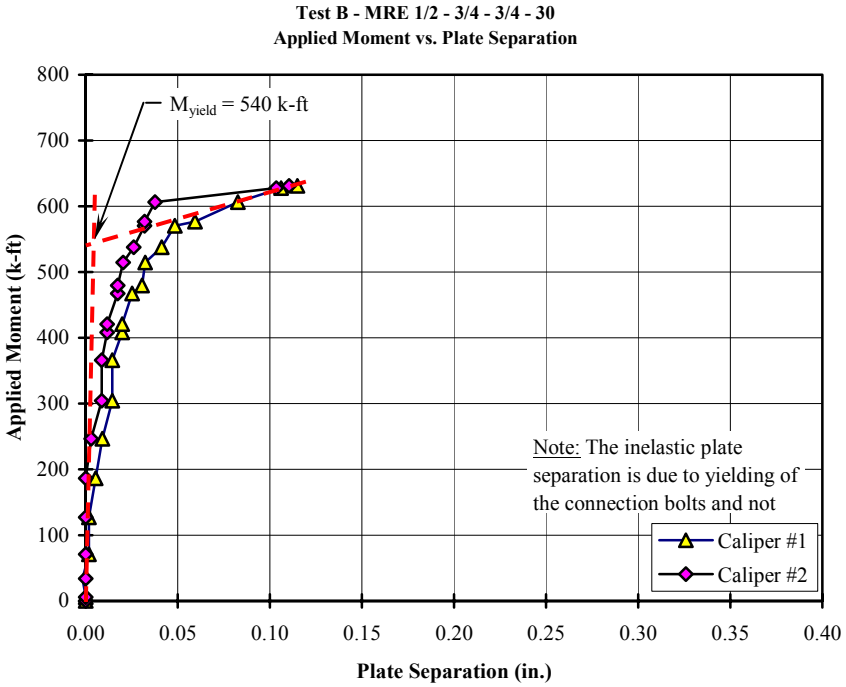

FIGURE 3.25: TYPICAL APPLIED MOMENT VS. END-PLATE SEPARATION RESPONSE FOR A THICK PLATE SPECIMEN (TEST B-MRE 1/2-3/4-3/4-30)

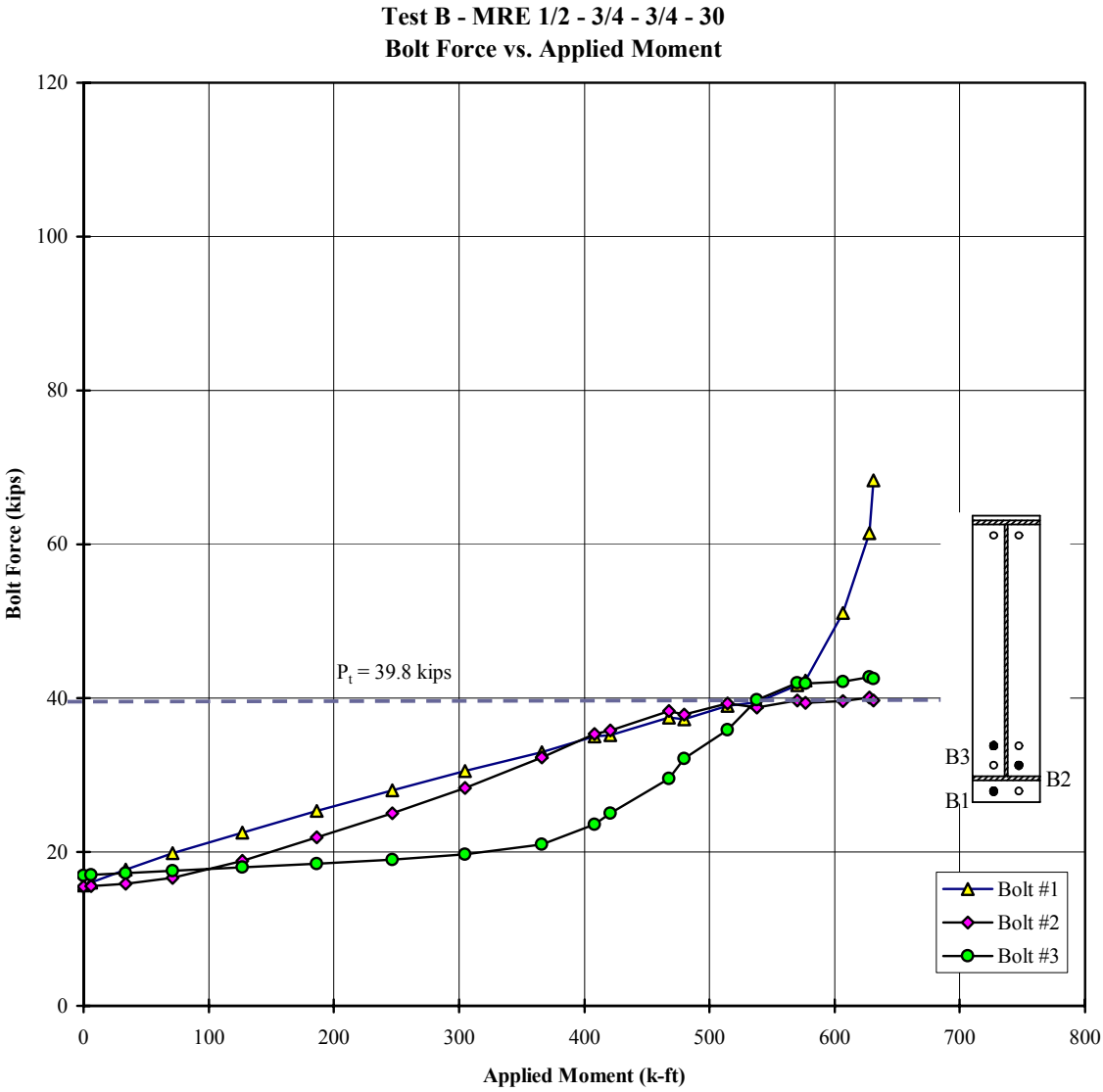

FIGURE 3.26: TYPICAL BOLT FORCE VS. APPLIED MOMENT RESPONSE FOR A THICK PLATE SPECIMEN (TEST B-MRE 1/2-3/4-3/4-30)

FIGURE 3.27: PHOTOGRAPH OF THICK PLATE FAILURE (TEST B - MRE 1/2-3/4-3/4-30)

3.3.4.2 Eight Bolt Extended, Four Bolts Wide Connections

Three eight bolt extended, four bolts wide end-plate moment connection tests were performed. One of the specimens behaved as thin plate end-plate connection, resulting in end-plate yielding followed by bolt tension rupture. The results from this test provide a yield moment, M_y, that is used to validate the end-plate yield-line mechanism design model. The load versus deflection and end-plate separation responses of the thin plate connection are shown in Figures 3.28 and 3.29, respectively. The inelastic load deflection response and the large end-plate separations prior to failure are evident. Figure 3.30 is a plot of the observed bolt response. The sharp increase in bolt force during the last few load steps can be seen. The test was stopped prior to tension rupture of the connection bolts. It is expected that bolts 1, 3, and 4 would exhibit similar behavior to bolt 2 before tension rupture would have occurred. Figure 3.31 shows a photograph of a thin plate specimen after testing. The large separation of the two end-plates is apparent.

Two of the test specimens behaved as thick plate end-plate connections, resulting in bolt tension rupture prior to the onset of end-plate yielding. The thick plate connection test results provide ultimate strength moments, M_{max}, for the limit state of bolt tension rupture. These results are used to validate bolt force design models. The load deflection and end-plate separation response of a typical 8E-4W connection are shown in Figures 3.32 and 3.33 respectively. Figure 3.34 is a plot of the observed bolt response. The small amount of inelastic response exhibited by this specimen is due to bolt yielding and not end-plate yielding, as determined by comparing the observed yield moment from the plate separation data with the bolt force response plot. The observed yield moment correlates closely with the point at which inelastic bolt behavior was observed. Figure 3.35 shows a photograph of a typical thick plate specimen after testing. The tension rupture failure of the bolts and the absence of end-plate yielding are apparent.

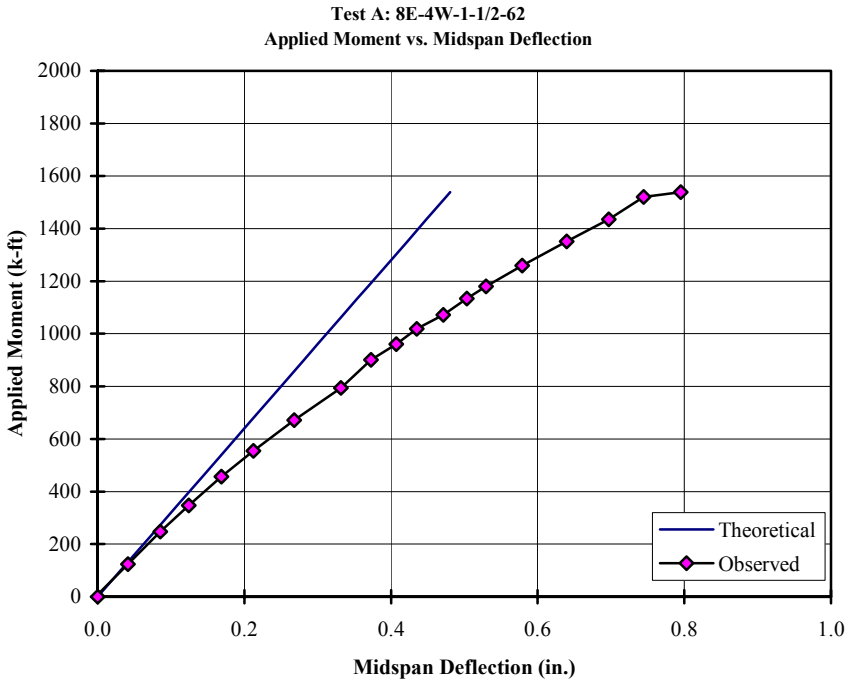

FIGURE 3.28: TYPICAL APPLIED MOMENT VS. MIDSPAN DEFLECTION RESPONSE FOR A THIN PLATE SPECIMEN (TEST A-8E-4W-1-1/2-62)

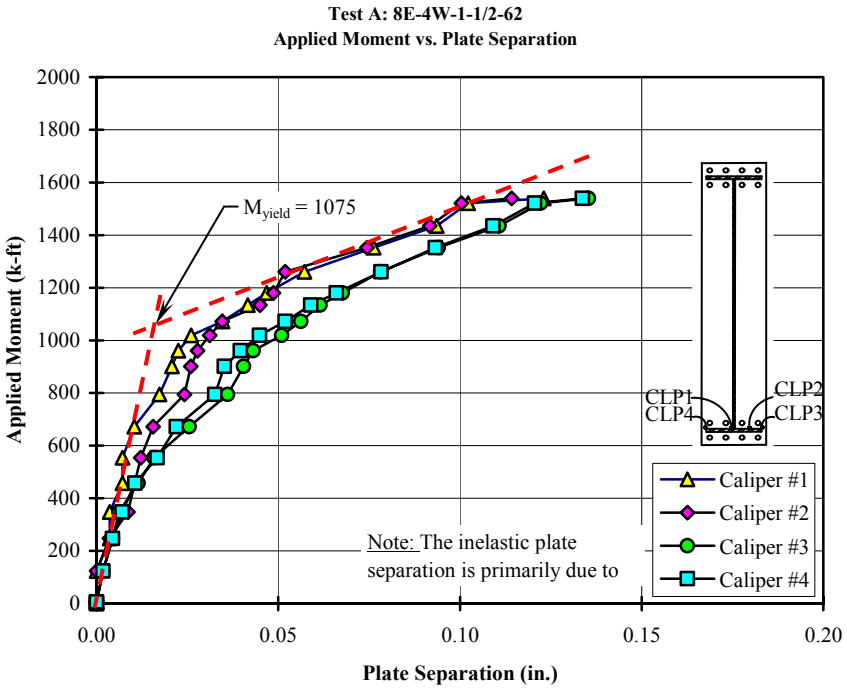

FIGURE 3.29: TYPICAL APPLIED MOMENT VS. END-PLATE SEPARATION RESPONSE FOR A THIN PLATE SPECIMEN (TEST A-8E-4W-1-1/2-62)

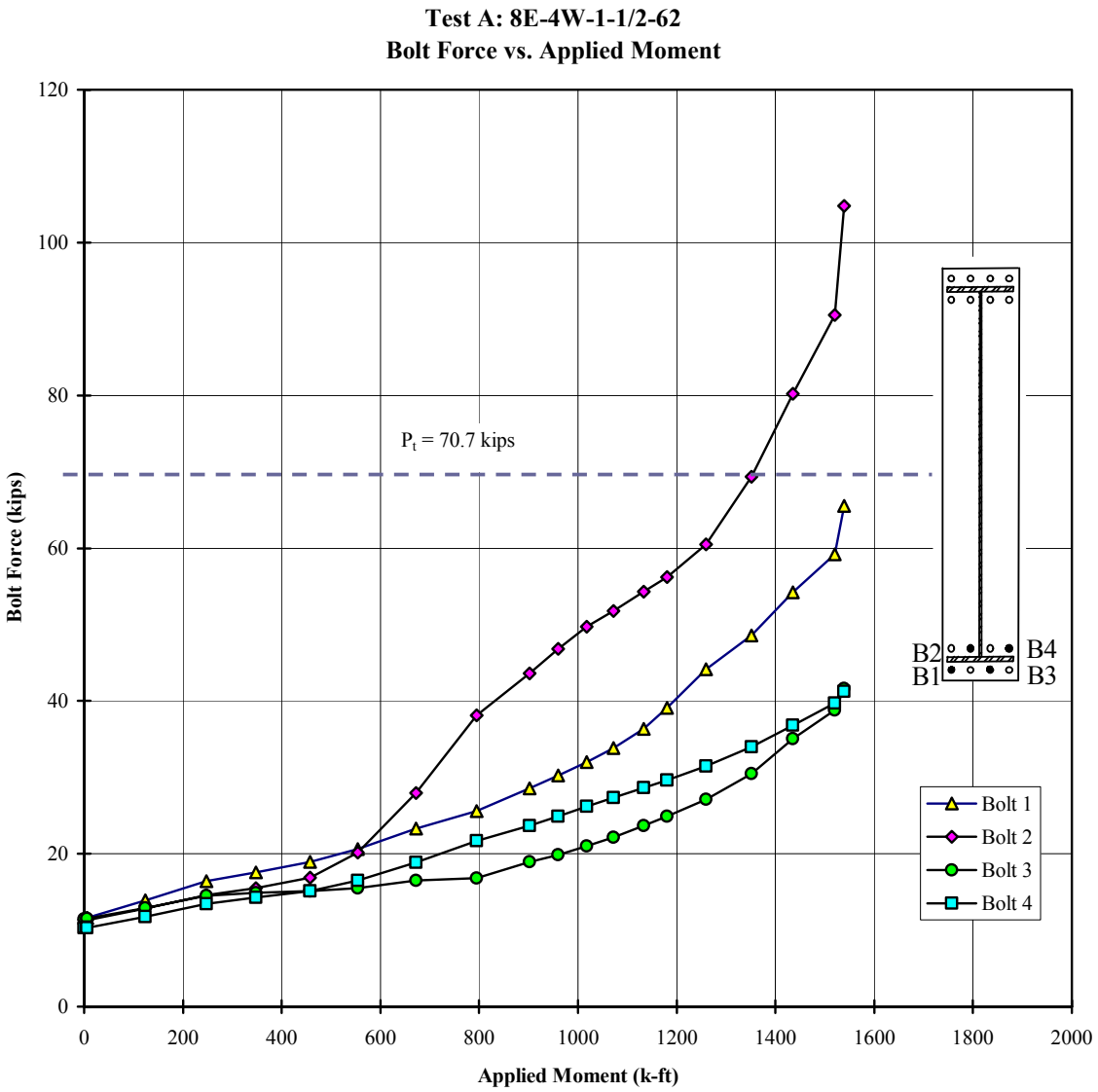

FIGURE 3.30: TYPICAL BOLT FORCE VS. APPLIED MOMENT RESPONSE FOR A THIN PLATE SPECIMEN (TEST A-8E-4W-1-1/2-62)

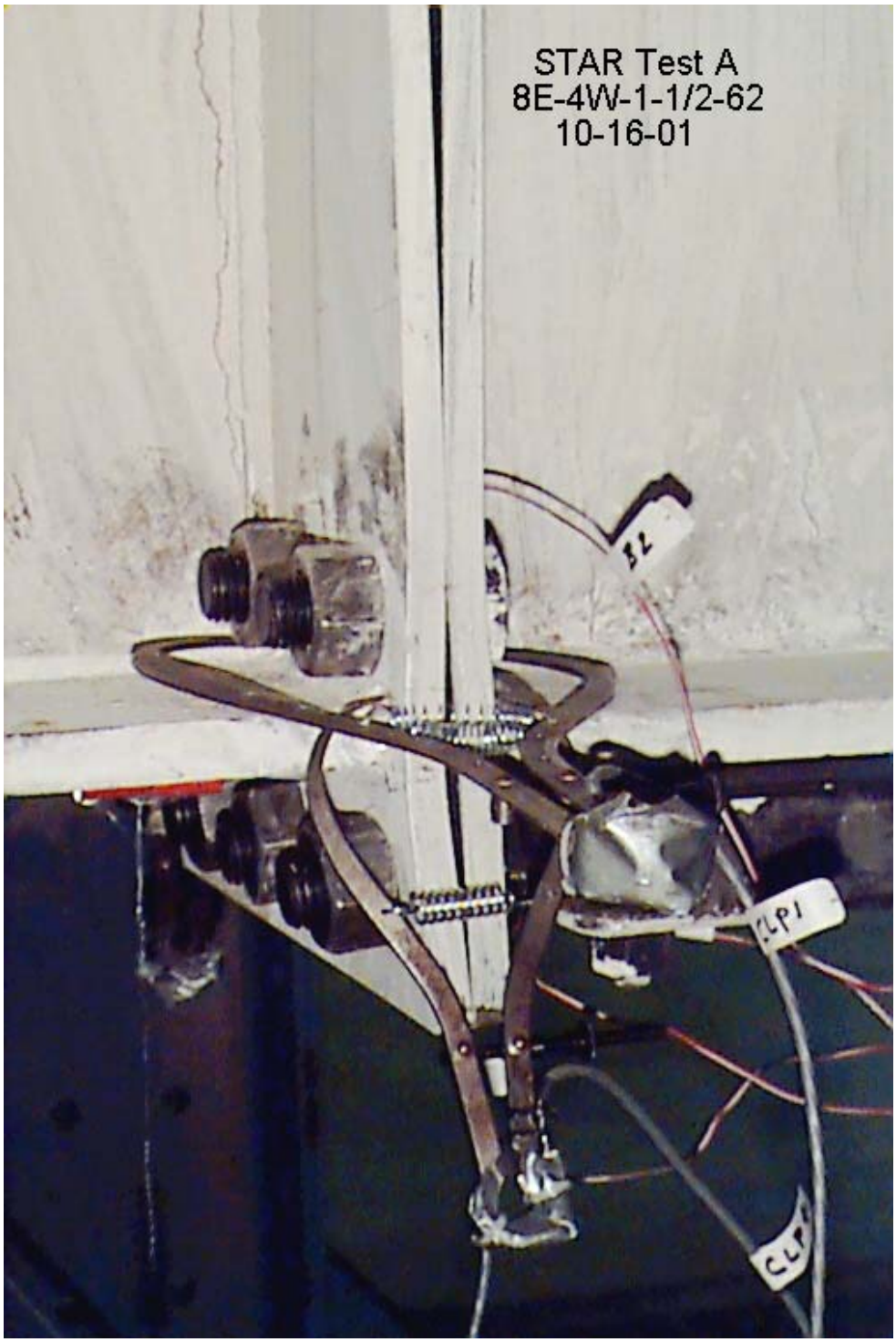

FIGURE 3.31: PHOTOGRAPH OF A THIN PLATE FAILURE (TEST A-8E-4W-1-1/2-62)

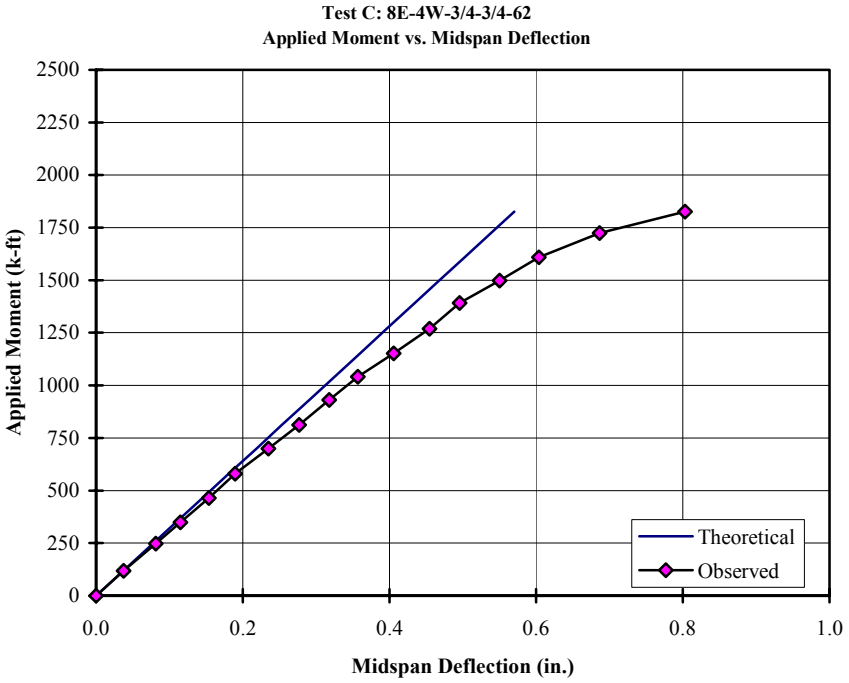

FIGURE 3.32: TYPICAL APPLIED MOMENT VS. MIDSPAN DEFLECTION RESPONSE FOR A THICK PLATE SPECIMEN (TEST C-8E-4W-3/4-3/4-62)

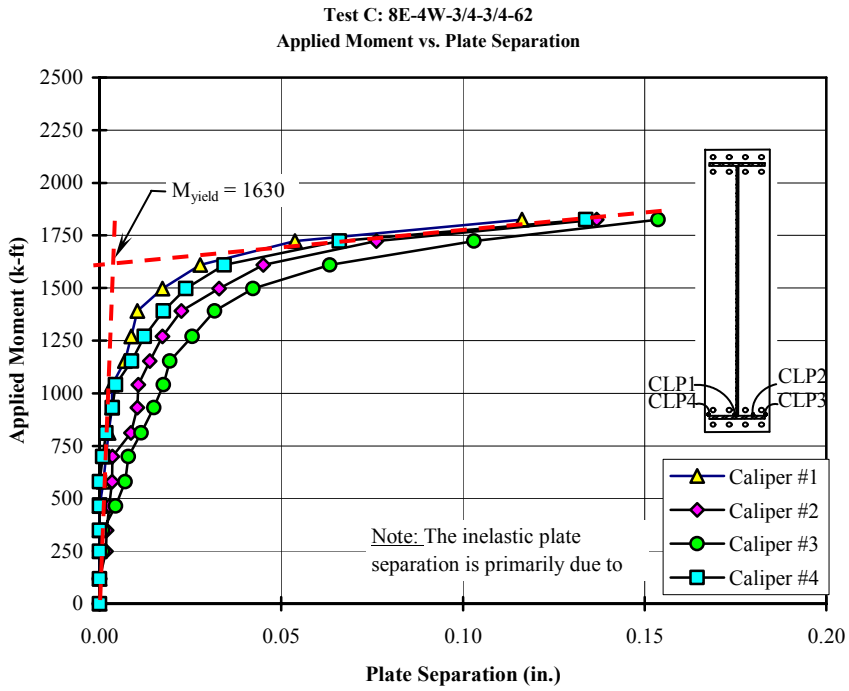

FIGURE 3.33: TYPICAL APPLIED MOMENT VS. END-PLATE SEPARATION RESPONSE FOR A THICK PLATE SPECIMEN (TEST C-8E-4W-3/4-3/4-62)

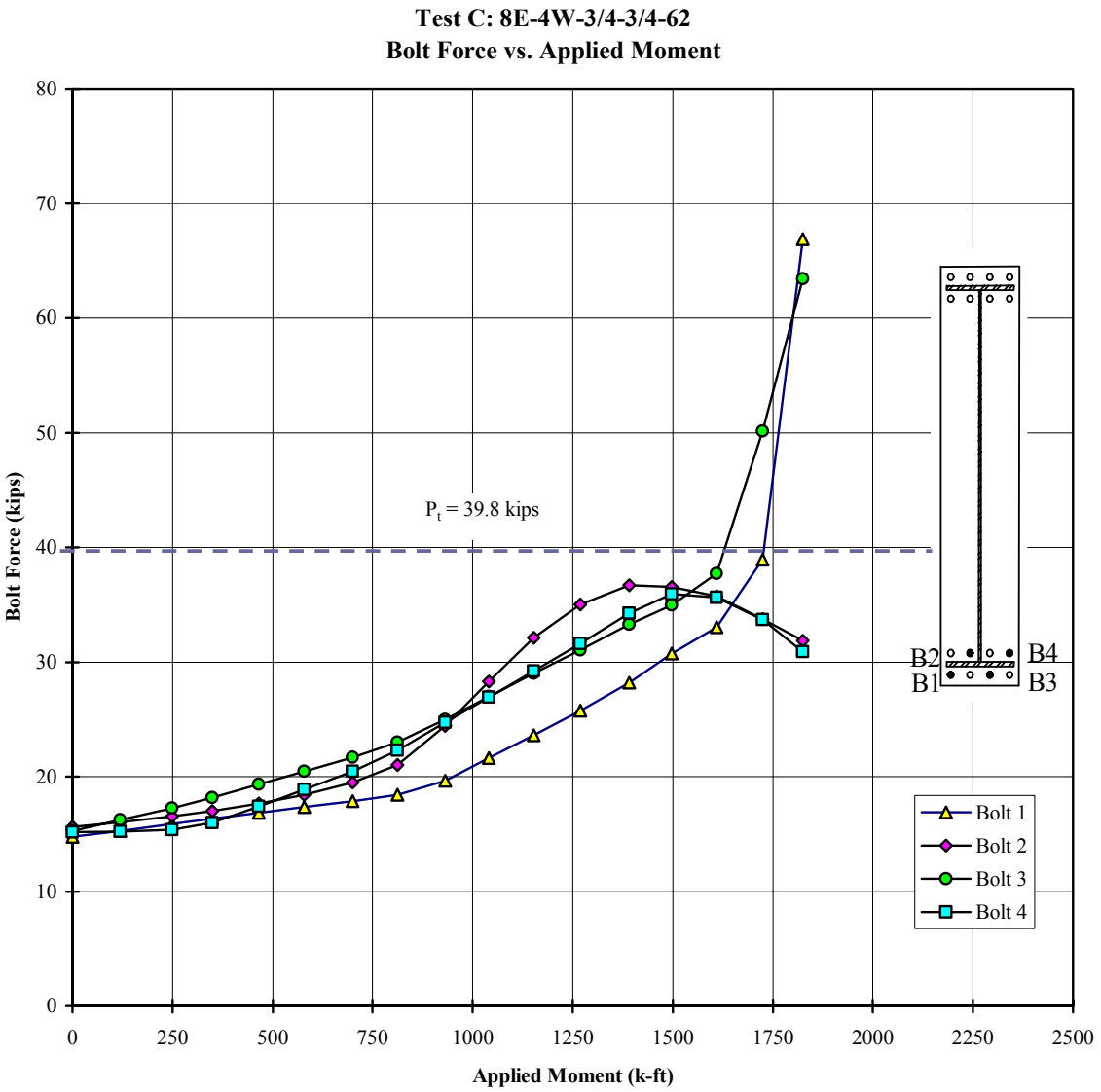

FIGURE 3.34: TYPICAL BOLT FORCE VS. APPLIED MOMENT RESPONSE FOR A THICK PLATE SPECIMEN (TEST C-8E-4W-3/4-3/4-62)

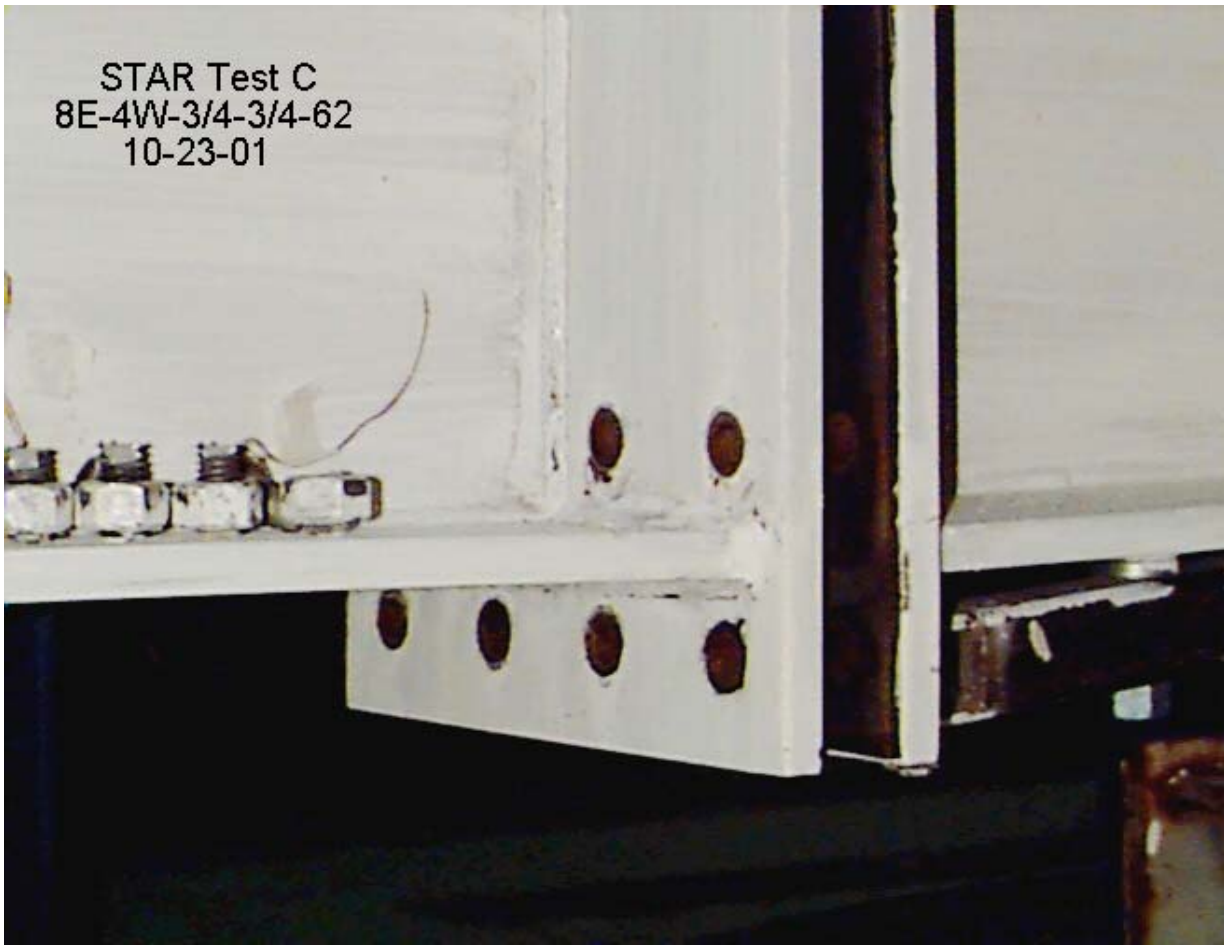

FIGURE 3.35: PHOTOGRAPH OF A THICK PLATE FAILURE (TEST C-8E-4W-3/4-3/4-62)

3.4 Summary

Eleven cyclic and nine monotonic extended end-plate moment connection tests were performed to determine the behavior and the strength characteristics of the connection components. The cyclic loaded connection tests resulted in performance data that will be used to evaluate the viability of the extended end-plate connection for use in seismic force resisting moment frames. The monotonic connection tests resulted in connection yield and ultimate moment strength data that will be used to validate the bolt force and end-plate yield line design models for the multiple row extended 1/2 and the eight bolt extended, four bolts wide end-plate moment connections.

Chapter 4 - DEVELOPMENT OF UNIFIED DESIGN PROCEDURE

4.1 Overview

The development of a unified design procedure for end-plate moment connections subject to cyclic loading requires careful consideration of four primary design parameters; the required connection design moment, end-plate strength, connection bolt strength, and column flange strength. Details of the background theory and design models used to develop the provisions for each design parameter are provided in this chapter.

4.2 Design Methodology

The current design methodology outlined in FEMA 350 (FEMA, 2000a) and adopted by the *AISC Seismic Provisions* (AISC, 1997, 1999b, 2000b, 2002) requires that the specified interstory drift of a steel moment frame be accommodated through a combination of elastic and inelastic frame deformations. The inelastic deformations are provided through development of plastic hinges at pre-determined locations within the frame. The plastic hinges are most commonly developed through inelastic flexural deformations in the connecting beams. This results in a strong column, strong connection and weak beam design philosophy.

The location of the plastic hinge formation within the connecting beams is dependant upon the type of beam-to-column connection used. For end-plate moment connections, the hinge location is different for unstiffened and stiffened configurations. For unstiffened end-plate moment connections, the plastic hinge forms at a distance equal to approximately one half the depth of the connecting beam from the face of the column. For stiffened end-plate moment connections, the plastic hinge forms at the base of the end-plate stiffeners. Figure 4.1 illustrates the locations of hinge formation for end-plate connections. The expected locations of the plastic hinges within the frame should be used to properly model the frame behavior, and to determine the strength demands at the critical sections within the connections.

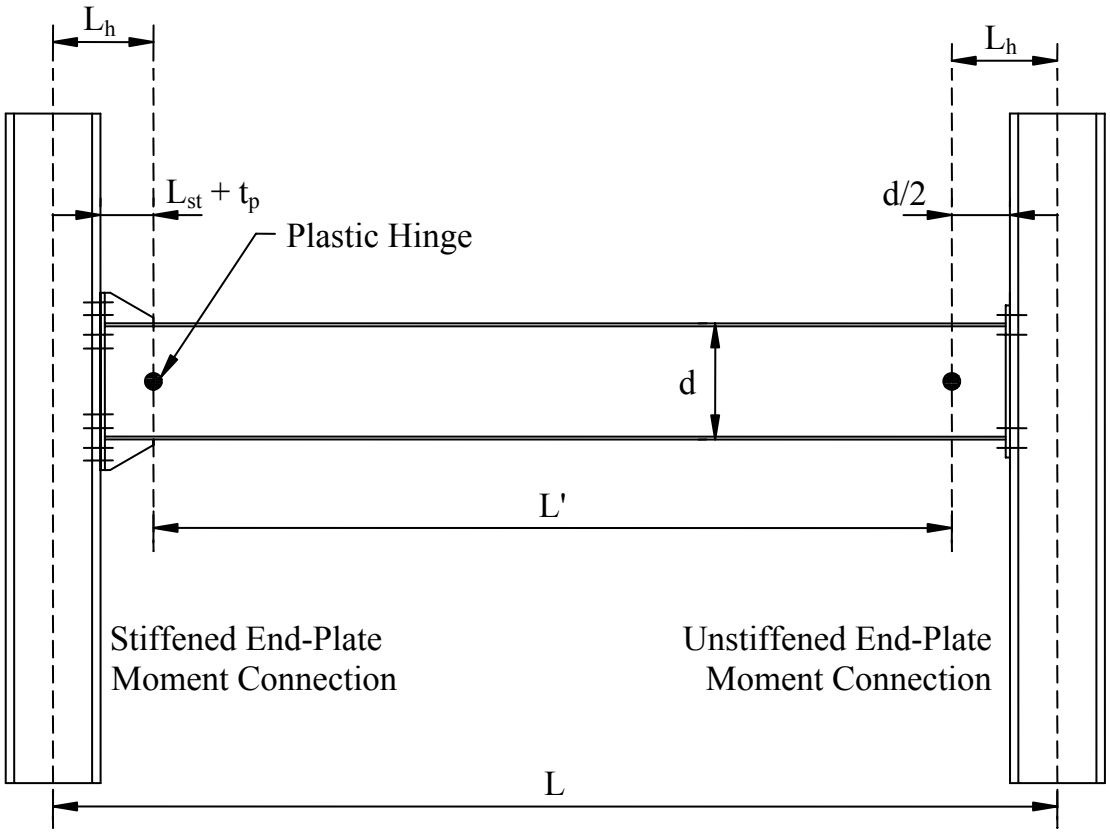

FIGURE 4.1: LOCATION OF PLASTIC HINGES

4.3 Connection Design Moment

The previously outlined design methodology requires that end-plate moment connections subject to cyclic loading be designed to develop the forces resulting from formation of plastic hinges within the connecting beam. Results from the extensive connection testing conducted as a part of the SAC Steel Project have shown that the expected plastic hinge moment, M_{pe}, developed in the connecting beam should be determined as follows (Coons, 1999, FEMA, 2000a):

$$M_{pe} = R_y \left(\frac{F_y + F_u}{2} \right) Z_x \tag{4.1}$$

Where: R_y is the ratio of the expected yield strength to the specified minimum yield strength, F_y is the specified minimum yield strength, F_u is the specified minimum tensile strength, and Z_x is the plastic section modulus of the connecting beam at the hinge location. The expected plastic

moment hinge strength accounts for the additional flexural strength developed by the connecting beam section through strain hardening of the beam flanges in the hinging region.

Using the expected moment at the plastic hinge, M_{pe}, and the location of the hinge, the flexural strength demands at each critical section can be determined. The critical section for the design of the column and the panel zone is different than the critical section for design of the beam-to-column connection components. The critical section for the design of end-plate moment connections is at the face of the column flange. The moment at the face of the column, M_{fc}, will be the sum of the expected moment at the plastic hinge, M_{pe}, and the additional moment caused by the eccentricity of the shear force present at the hinge location. Figure 4.2 illustrates this concept.

Applying the distances to the expected hinge locations for stiffened and unstiffened end-plate moment connections, results in the following expressions for the connection design moments.

$$M_{fc} = M_{pe} + V_p\left(\frac{d}{2}\right) \qquad \textit{for unstiffened connections} \tag{4.2}$$

$$M_{fc} = M_{pe} + V_p\left(L_{st} + t_p\right) \qquad \textit{for stiffened connections} \tag{4.3}$$

where V_p is the shear at the plastic hinge, d is the depth of the connecting beam, L_{st} is the length of the end-plate stiffener, and t_p is the thickness of the end-plate.

4.4 End-Plate and Column Flange Strength

4.4.1 Overview

The determination of the end-plate and column flange bending strength is an essential part of the design procedure. Both components of the connection must provide adequate strength to resist the critical design moment at the face of the column. The end-plate and column flange bending strength is determined using yield line analysis.

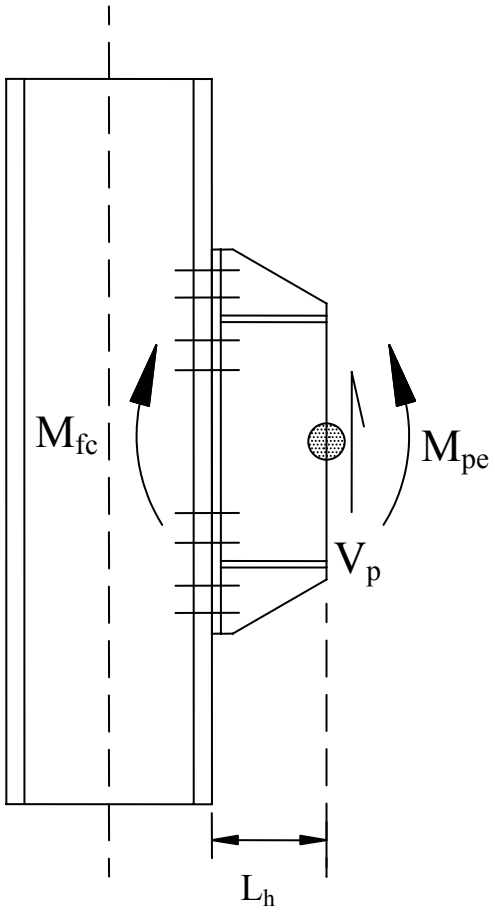

FIGURE 4.2: CALCULATION OF CONNECTION DESIGN MOMENT

4.4.2 Yield Line Analysis

Yield line theory was first introduced in the 1960's to analyze reinforced concrete slabs (Johansen, 1972). It is a powerful analysis method used to determine the flexural load at which a collapse mechanism will form in a flat plate structure. A yield line is the continuous formation of plastic hinges along a straight or curved line. As a plate structure is loaded in flexure, yield lines will form when the flexural yield strength of the plate is exceeded. Collapse of the plate structure occurs when the formation of the yield lines produces a collapse mechanism. This is similar to plastic design theory that has been used to design steel moment frames in the past. As in plastic design, the elastic deformations of the members are negligible compared to the plastic deformations at the locations of the plastic hinges or yield lines. This allows the assumption that the plate structure is divided by the yield lines into a series of rigid plate regions. The outline of the rigid plate regions is commonly called the yield line pattern.

Yield line analysis can be performed by two different methods; the virtual work or energy method, and the equilibrium method. The virtual work method is the preferred method for analysis of steel plates and will be used herein. In the virtual work method, a small arbitrary displacement (virtual displacement) is applied to the structure in the direction of the applied loads. The external work is generated as the load passes through the small displacement. The internal work of the plate is generated by the rotation of the plate along the yield lines of the assumed yield line pattern to accommodate the small displacement. To satisfy the conservation of energy principle, the internal work of the plate is set equal to the external work of the applied loads. The resulting equality can be solved to determine either the unknown failure load or the required plate flexural strength. This process of equating the internal and external work must be repeated for each assumed yield line pattern.

The virtual work method is an energy method that results in an upper bound solution for the plate strength. To determine the controlling yield line pattern for a plate, various yield line patterns must be considered. The pattern that produces the lowest failure load will control, and is considered the lowest upper bound solution.

The application of yield line theory to determine the strength of an end-plate requires three basic steps; assumption of a yield line pattern, generation of equations for internal and external work, and solution of internal and external work equality. These basic principles of yield line analysis are illustrated herein.

In determining an assumed yield line pattern within a steel plate, the following guidelines have been established by Srouji et al. (1983b):

- Axes of rotation generally lie along lines of support.
- Yield lines pass through the intersection of the axes of rotation of adjacent rigid plate segments.
- Along a yield line, the bending moment is assumed to be constant and equal to the plastic moment of the plate.

Utilizing these guidelines, an assumed yield line pattern is established. A unit virtual displacement is then applied by rotating the connecting beam through a virtual rotation about the centerline of the compression flange. Figure 4.3 illustrates the controlling yield line pattern and assumed virtual displacement for the four bolt extended unstiffened end-plate connections.

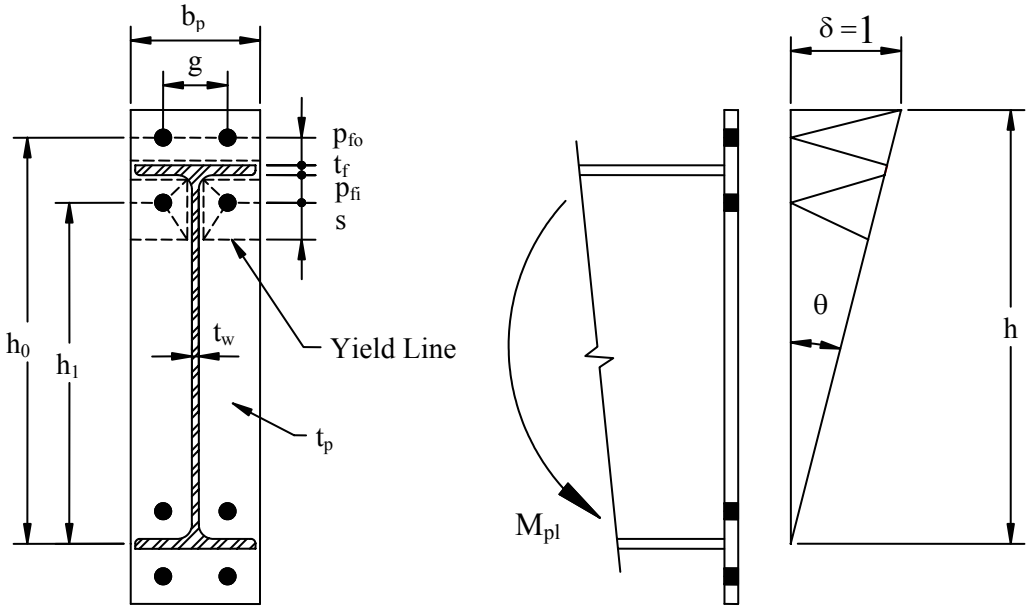

FIGURE 4.3: YIELD LINE PATTERN AND VIRTUAL DISPLACEMENT OF A FOUR BOLT EXTENDED UNSTIFFENED CONNECTION

The internal work stored within a yield line pattern is the sum of the internal work stored in each of the yield lines forming the mechanism. For the complex patterns observed in end-plate moment connections it is convenient to break the internal work components down into Cartesian (x- and y-) components. The general expression for internal work stored by the yield line pattern is (Srouji et al., 1983b)

$$W_i = \sum_{n=1}^{N} \left(m_p \theta_{nx} L_{nx} + m_p \theta_{ny} L_{ny} \right) \tag{4.4}$$

where θ_{nx} and θ_{ny} are the x- and y-components of the relative rotation of the rigid plate segments along the yield line, L_{nx} and L_{ny} are the x- and y- components of the yield line length, and m_p is the plastic moment strength of the plate per unit length,

$$m_p = F_{yp} Z = F_{yp} \left(\frac{(1)\ t_p^2}{4} \right) \tag{4.5}$$

The external work due to the unit virtual rotation is given by (Srouji et al., 1983b)

$$W_e = M_{fc}\ \theta = M_{fc} \left(\frac{1}{h} \right) \tag{4.6}$$

where M_{fc} is the applied moment at the face of the column, and θ is the applied virtual displacement. The applied virtual displacement is equal to 1/h, where h is the distance from the centerline of the compression flange to the tension side edge of the end-plate.

4.4.3 Simplifying Assumptions

To simplify the yield line equations, the following simplifications have been incorporated into the development of the yield line equations. No adjustment in end-plate or column flange strength is made to account for the plate material removed by bolt holes. The width of the beam or column web is considered to be zero in the yield line equations. The width of fillet welds along the flange or stiffeners and web are not considered in the yield line equations. Finally, the very small strength contribution from yield lines in the compression region of the connections is neglected.

4.4.4 End-Plate Strength

4.4.4.1 General

Past studies on end-plate moment connections have investigated numerous end-plate yield line patterns (Srouji et al. 1983b, SEI 1984, Borgsmiller 1995, Meng 1996, Murray and Shoemaker 2002). As a continuation of past studies, additional yield line patterns have been investigated as a part of this study and new patterns developed as appropriate for the eight end-plate moment connection configurations shown in Figures 1.4 and 1.5. Details of the yield line solutions for each connection configuration are presented in subsequent sections.

4.4.4.2 Four Bolt Extended

Srouji et al. (1983b) conducted a study on four bolt extended unstiffened end-plate moment connections. The following yield line solution is based upon that study with some minor modifications. Figure 4.4 shows the controlling yield line pattern and defines the geometric parameters. Equating the internal work, W_i, and the external work, W_e, results in the following expression for the strength of the end-plate M_{pl}.

$$M_{pl} = F_{yp}\, t_p^2 \left[\frac{b_p}{2} \left[h_1 \left(\frac{1}{p_{fi}} + \frac{1}{s} \right) + h_0 \left(\frac{1}{p_{fo}} \right) - \frac{1}{2} \right] + \frac{2}{g} \left[h_1 \left(p_{fi} + s \right) \right] \right] \tag{4.7}$$

Rearranging the expression for M_{pl} and solving for the thickness of plate, t_p, results in an expression for the required end-plate thickness to develop a desired moment M_{fc}.

$$t_p = \sqrt{\frac{M_{fc}}{F_{yp} \left[\frac{b_p}{2} \left[h_1 \left(\frac{1}{p_{fi}} + \frac{1}{s} \right) + h_0 \left(\frac{1}{p_{fo}} \right) - \frac{1}{2} \right] + \frac{2}{g} \left[h_1 \left(p_{fi} + s \right) \right] \right]}} \tag{4.8}$$

The unknown dimension, s, in Figure 4.4 and Equations 4.7 and 4.8 is found by differentiating the internal work expression with respect to s and setting the expression equal to zero. This process determines the dimension s that results in the minimum internal energy. The resulting expression is:

$$s = \frac{1}{2} \sqrt{b_p\, g} \tag{4.9}$$

In some situations, the end-plate connections may have an inner pitch distance, p_{fi}, greater than the dimension s. In these cases, the inner pitch distance, p_{fi}, should be set equal to s in the calculations. This modification accounts for the case where the horizontal yield lines do not form along the inside of the beam flange, but do form a distance s above the first inner bolt line.

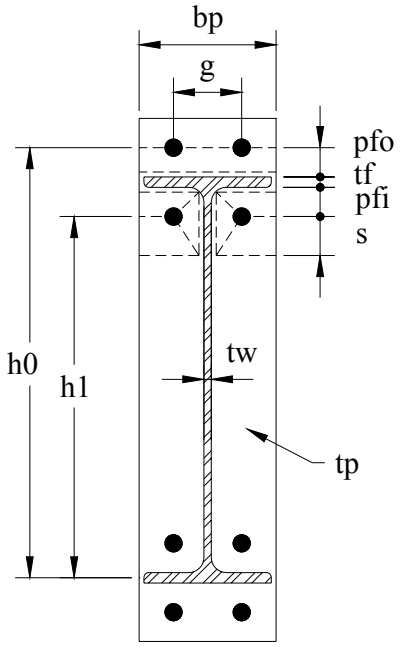

FIGURE 4.4: YIELD LINE PATTERN FOR FOUR BOLT EXTENDED UNSTIFFENED END-PLATE MOMENT CONNECTIONS

4.4.4.3 Four Bolt Extended Stiffened

Srouji et al. (1983b) conducted a study on four bolt extended stiffened end-plate moment connections. The following yield line solutions are based upon that study with some minor modifications. Figure 4.5 shows the two controlling yield line patterns and defines the geometric parameters. Two yield line patterns are required because of the possible formation of a horizontal yield line near the outer edge of the extended portion of the end-plate. The first pattern shown in Figure 4.5(a) does not have the yield line formed near the outer edge and is designated Case 1. The second pattern shown in Figure 4.5(b) does have the yield line near the outer edge of the end-plate and is designed Case 2. Case 1 applies when the distance from the outermost bolt row to the edge of the plate, d_e, is less than or equal to the dimension s. Case 2 applies when d_e is greater than the dimension s.

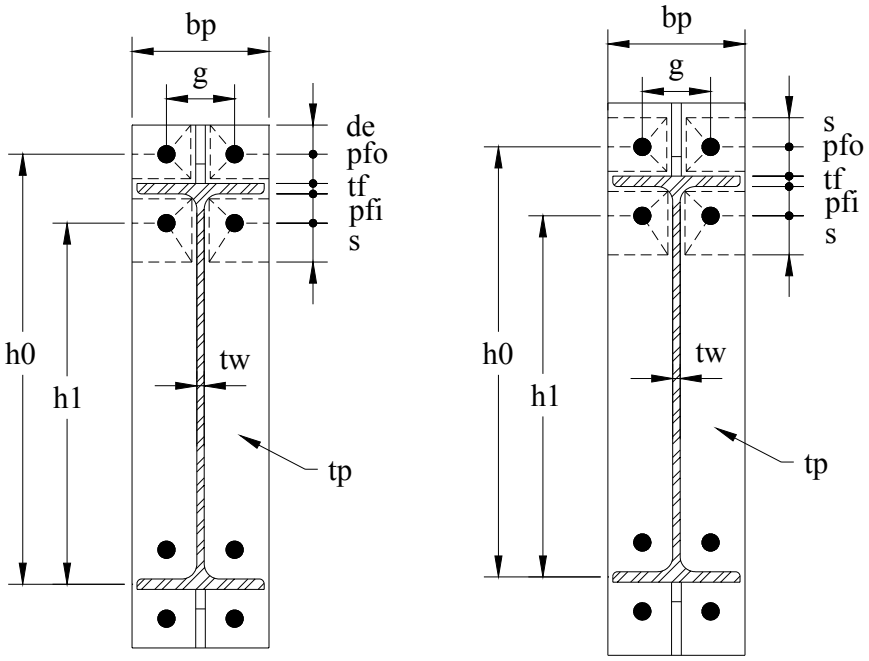

(a) Case 1($d_e \leq s$) (b) Case 2 ($d_e > s$)

FIGURE 4.5: YIELD LINE PATTERN FOR FOUR BOLT EXTENDED STIFFENED END-PLATE MOMENT CONNECTIONS

The expressions for the unknown dimension s, the strength of the end-plate, M_{pl}, and the thickness of end-plate required to develop the desired moment M_{fc} are found using the same procedure as discussed for the four bolt extended unstiffened configuration. The resulting expressions are:

$$s = \frac{1}{2}\sqrt{b_p\, g} \tag{4.10}$$

Case 1, (when $d_e \leq s$)

$$M_{pl} = F_{yp}\, t_p^2 \left[\frac{b_p}{2} \left[h_1 \left(\frac{1}{p_{fi}} + \frac{1}{s} \right) + h_0 \left(\frac{1}{s} + \frac{1}{p_{fo}} \right) \right] + \frac{2}{g} \left[h_1 \left(p_{fi} + s \right) + h_0 \left(s + p_{fo} \right) \right] \right] \tag{4.11}$$

$$t_p = \sqrt{\frac{M_{fc}}{F_{yp} \left[\frac{b_p}{2} \left[h_1 \left(\frac{1}{p_{fi}} + \frac{1}{s} \right) + h_0 \left(\frac{1}{s} + \frac{1}{p_{fo}} \right) \right] + \frac{2}{g} \left[h_1 \left(p_{fi} + s \right) + h_0 \left(s + p_{fo} \right) \right] \right]}} \tag{4.12}$$

Case 2, (when $d_e > s$)

$$M_{pl} = F_{yp}\, t_p^2 \left[\frac{b_p}{2} \left[h_1 \left(\frac{1}{p_{fi}} + \frac{1}{s} \right) + h_0 \left(\frac{1}{p_{fo}} + \frac{1}{2s} \right) \right] + \frac{2}{g} \left[h_1 (p_{fi} + s) + h_0 (d_e + p_{fo}) \right] \right] \tag{4.13}$$

$$t_p = \sqrt{\frac{M_{fc}}{F_{yp} \left[\frac{b_p}{2} \left[h_1 \left(\frac{1}{p_{fi}} + \frac{1}{s} \right) + h_0 \left(\frac{1}{p_{fo}} + \frac{1}{2s} \right) \right] + \frac{2}{g} \left[h_1 (p_{fi} + s) + h_0 (d_e + p_{fo}) \right] \right]}} \tag{4.14}$$

For connections with a large inner pitch distance ($p_{fi} > s$), the inner pitch distance, p_{fi}, is set equal to s in the calculations.

4.4.4.4 Eight Bolt Extended Stiffened

As a part of this research, a study was conducted to develop a yield line solution for the eight bolt extended stiffened end-plate moment connections. Several different yield line patterns were investigated to determine the controlling patterns. Figure 4.6 shows the two controlling yield line patterns and defines the geometric parameters. The expressions for the unknown dimension s, the strength of the end-plate, M_{pl}, and the thickness of end-plate required to develop the desired moment M_{fc} are found using the same procedure as discussed for the four bolt extended unstiffened configuration. The resulting expressions are:

$$s = \frac{1}{2} \sqrt{b_p\, g} \tag{4.15}$$

Case 1, (when $d_e \leq s$)

$$\begin{aligned} M_{pl} = F_{yp}\, t_p^2 \Bigg[& \frac{b_p}{2} \left[h_1 \left(\frac{1}{2d_e} \right) + h_2 \left(\frac{1}{p_{fo}} \right) + h_3 \left(\frac{1}{p_{fi}} \right) + h_4 \left(\frac{1}{s} \right) \right] + \\ & \frac{2}{g} \left[h_1 \left(d_e + \frac{p_b}{4} \right) + h_2 \left(p_{fo} + \frac{3p_b}{4} \right) + h_3 \left(p_{f,i} + \frac{p_b}{4} \right) + h_4 \left(s + \frac{3p_b}{4} \right) + p_b^2 \right] + g \Bigg] \end{aligned} \tag{4.16}$$

$$t_p = \sqrt{\frac{M_{fc}}{\begin{aligned} & F_{yp} \left[\frac{b_p}{2} \left[h_1 \left(\frac{1}{2d_e} \right) + h_2 \left(\frac{1}{p_{fo}} \right) + h_3 \left(\frac{1}{p_{fi}} \right) + h_4 \left(\frac{1}{s} \right) \right] + \right. \\ & \left. \frac{2}{g} \left[h_1 \left(d_e + \frac{p_b}{4} \right) + h_2 \left(p_{fo} + \frac{3p_b}{4} \right) + h_3 \left(p_{fi} + \frac{p_b}{4} \right) + h_4 \left(s + \frac{3p_b}{4} \right) + p_b^2 \right] + g \right] \end{aligned}}} \tag{4.17}$$

Case 2, (when $d_e > s$)

$$M_{pl} = F_{yp}\, t_p^2 \left[\frac{b_p}{2} \left[h_1 \left(\frac{1}{s} \right) + h_2 \left(\frac{1}{p_{fo}} \right) + h_3 \left(\frac{1}{p_{fi}} \right) + h_4 \left(\frac{1}{s} \right) \right] + \frac{2}{g} \left[h_1 \left(s + \frac{p_b}{4} \right) + h_2 \left(p_{fo} + \frac{3p_b}{4} \right) + h_3 \left(p_{fi} + \frac{p_b}{4} \right) + h_4 \left(s + \frac{3p_b}{4} \right) + p_b^2 \right] + g \right] \tag{4.18}$$

$$t_p = \sqrt{\frac{M_{fc}}{F_{yp} \left[\frac{b_p}{2} \left[h_1 \left(\frac{1}{s} \right) + h_2 \left(\frac{1}{p_{fo}} \right) + h_3 \left(\frac{1}{p_{fi}} \right) + h_4 \left(\frac{1}{s} \right) \right] + \frac{2}{g} \left[h_1 \left(s + \frac{p_b}{4} \right) + h_2 \left(p_{fo} + \frac{3p_b}{4} \right) + h_3 \left(p_{fi} + \frac{p_b}{4} \right) + h_4 \left(s + \frac{3p_b}{4} \right) + p_b^2 \right] + g \right]}} \tag{4.19}$$

For connections with a large inner pitch distance ($p_{fi} > s$), the inner pitch distance, p_{fi}, should be set equal to s in the calculations.

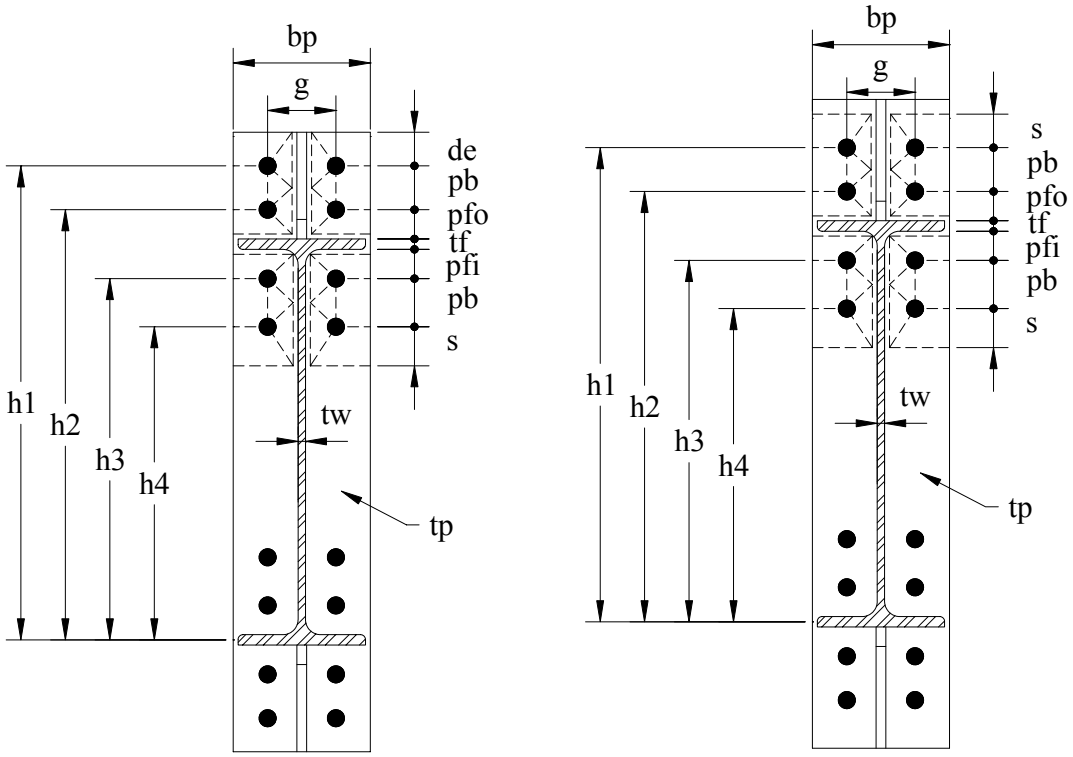

(a) Case 1($d_e \leq s$) (b) Case 2 ($d_e > s$)

FIGURE 4.6: YIELD LINE PATTERN FOR EIGHT BOLT EXTENDED STIFFENED END-PLATE MOMENT CONNECTIONS

4.4.4.5 Eight Bolt, Four Bolts Wide Extended

Meng (1996) conducted a study on eight bolt, four bolts wide extended unstiffened end-plate moment connections. The following yield line solution is based upon that study with some minor modifications. Figure 4.7 shows the controlling yield line pattern and defines the geometric parameters. The controlling yield line pattern is the same as the pattern for the four bolt extended unstiffened connections. The expressions for the strength of the end-plate, M_{pl}, the thickness of end-plate required to develop the desired moment M_{fc}, and the unknown dimension s, are:

$$M_{pl} = F_{yp}\, t_p^2 \left[\frac{b_p}{2} \left[h_1 \left(\frac{1}{p_{fi}} + \frac{1}{s} \right) + h_0 \left(\frac{1}{p_{fo}} \right) - \frac{1}{2} \right] + \frac{2}{g} \left[h_1 \left(p_{fi} + s \right) \right] \right] \tag{4.20}$$

$$t_p = \sqrt{\frac{M_{fc}}{F_{yp} \left[\frac{b_p}{2} \left[h_1 \left(\frac{1}{p_{fi}} + \frac{1}{s} \right) + h_0 \left(\frac{1}{p_{fo}} \right) - \frac{1}{2} \right] + \frac{2}{g} \left[h_1 \left(p_{fi} + s \right) \right] \right]}} \tag{4.21}$$

$$s = \frac{1}{2} \sqrt{b_p\, g} \tag{4.22}$$

For connections with a large inner pitch distance ($p_{fi} > s$), the inner pitch distance, p_{fi}, should be set equal to s in the calculations.

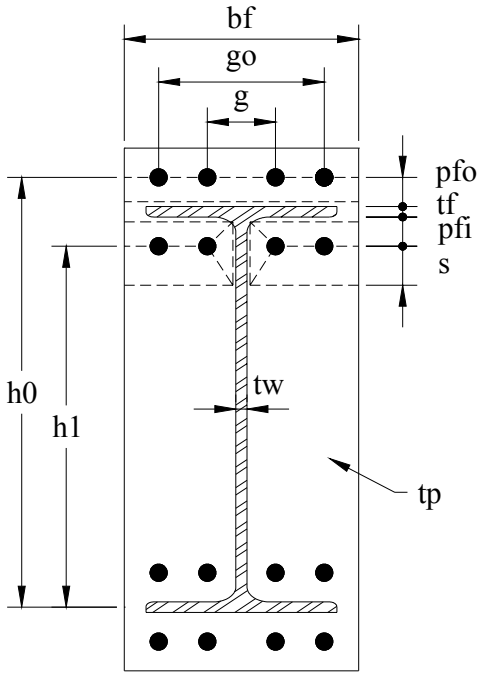

FIGURE 4.7: YIELD LINE PATTERN FOR EIGHT BOLT, FOUR BOLTS WIDE EXTENDED UNSTIFFENED END-PLATE MOMENT CONNECTIONS

4.4.4.6 Eight Bolt, Four Bolts Wide, Extended Stiffened

Meng (1996) conducted a study on eight bolt, four bolts wide extended stiffened end-plate moment connections. The following yield line solutions are based upon that study with some minor modifications. Figure 4.8 shows the two controlling yield line patterns and defines the geometric parameters. The controlling yield line patterns are the same as for the four bolt extended stiffened end-plate moment connections. The expressions for the unknown dimension s, the strength of the end-plate, M_{pl}, and the thickness of end-plate required to develop the desired moment M_{fc} are:

$$s = \frac{1}{2}\sqrt{b_p\, g} \tag{4.23}$$

Case 1, (when $d_e \leq s$)

$$M_{pl} = F_{yp}\, t_p^2 \left[\frac{b_p}{2} \left[h_1 \left(\frac{1}{p_{fi}} + \frac{1}{s} \right) + h_0 \left(\frac{1}{s} + \frac{1}{p_{fo}} \right) \right] + \frac{2}{g} \left[h_1 \left(p_{fi} + s \right) + h_0 \left(s + p_{fo} \right) \right] \right] \tag{4.24}$$

$$t_p = \sqrt{\frac{M_{fc}}{F_{yp}\left[\frac{b_p}{2}\left[h_1\left(\frac{1}{p_{fi}}+\frac{1}{s}\right)+h_0\left(\frac{1}{s}+\frac{1}{p_{fo}}\right)\right]+\frac{2}{g}\left[h_1\left(p_{fi}+s\right)+h_0\left(s+p_{fo}\right)\right]\right]}} \quad (4.25)$$

Case 2, (when $d_e > s$)

$$M_{pl} = F_{yp}\, t_p^2\left[\frac{b_p}{2}\left[h_1\left(\frac{1}{p_{fi}}+\frac{1}{s}\right)+h_0\left(\frac{1}{p_{fo}}+\frac{1}{2s}\right)\right]+\frac{2}{g}\left[h_1(p_{fi}+s)+h_0(d_e+p_{fo})\right]\right] \quad (4.26)$$

$$t_p = \sqrt{\frac{M_{fc}}{F_{yp}\left[\frac{b_p}{2}\left[h_1\left(\frac{1}{p_{fi}}+\frac{1}{s}\right)+h_0\left(\frac{1}{p_{fo}}+\frac{1}{2s}\right)\right]+\frac{2}{g}\left[h_1(p_{fi}+s)+h_0(d_e+p_{fo})\right]\right]}} \quad (4.27)$$

For connections with a large inner pitch distance ($p_{fi} > s$), the inner pitch distance, p_{fi}, is set equal to s in the calculations.

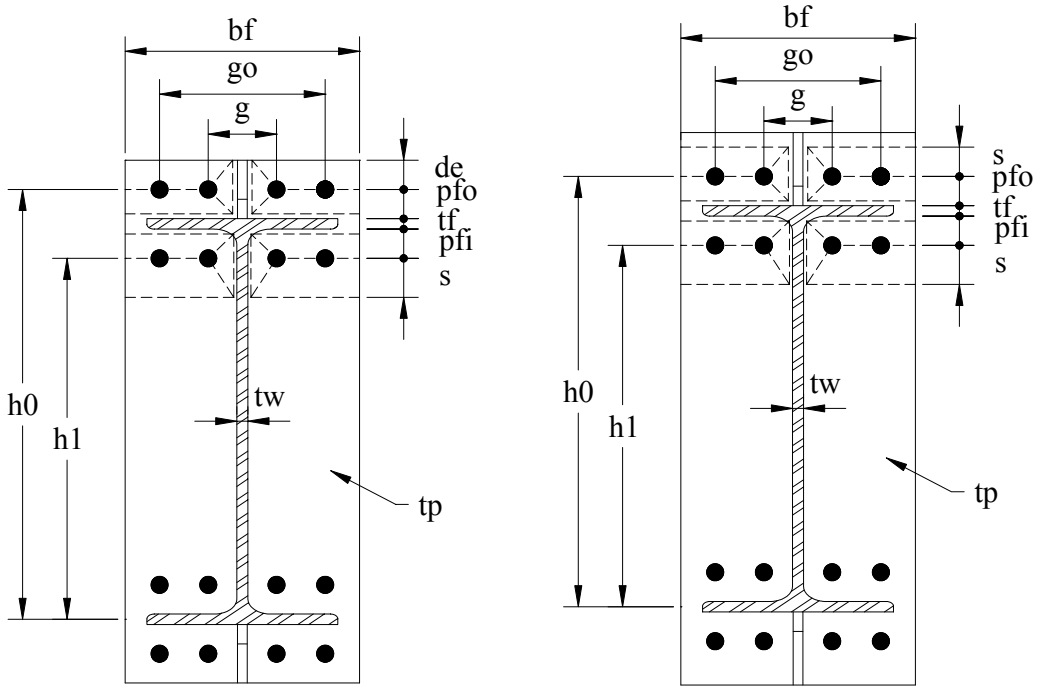

(a) Case 1($d_e \leq s$) (b) Case 2 ($d_e > s$)

FIGURE 4.8: YIELD LINE PATTERN FOR EIGHT BOLT, FOUR BOLTS WIDE EXTENDED STIFFENED END-PLATE MOMENT CONNECTIONS

4.4.4.7 Multiple Row Extended 1/2

As a part of this research, a study was conducted to validate a yield line solution for the multiple row extended 1/2 unstiffened end-plate moment connections. Several different yield line patterns were investigated to determine the controlling patterns. Figure 4.9 shows the controlling yield line pattern and defines the geometric parameters. The expressions for the strength of the end-plate, M_{pl}, the thickness of end-plate required to develop the desired moment M_{fc}, and the unknown dimension s are found using the same procedure as discussed for the four bolt extended unstiffened configuration. The resulting expressions are:

$$M_{pl} = F_{yp}\, t_p^2 \left[\frac{b_p}{2} \left[h_1 \left(\frac{1}{p_{fi}} \right) + h_2 \left(\frac{1}{s} \right) + h_0 \left(\frac{1}{p_{fo}} \right) - \frac{1}{2} \right] + \frac{2}{g} \left[h_1 \left(p_{fi} + \frac{3p_b}{4} \right) + h_2 \left(s + \frac{p_b}{4} \right) \right] + \frac{g}{2} \right] \tag{4.28}$$

$$t_p = \sqrt{\frac{M_{fc}}{F_{yp} \left[\frac{b_p}{2} \left[h_1 \left(\frac{1}{p_{fi}} \right) + h_2 \left(\frac{1}{s} \right) + h_0 \left(\frac{1}{p_{fo}} \right) - \frac{1}{2} \right] + \frac{2}{g} \left[h_1 \left(p_{fi} + \frac{3p_b}{4} \right) + h_2 \left(s + \frac{p_b}{4} \right) \right] + \frac{g}{2} \right]}} \tag{4.29}$$

$$s = \frac{1}{2} \sqrt{b_p\, g} \tag{4.30}$$

For connections with a large inner pitch distance ($p_{fi} > s$), the inner pitch distance, p_{fi}, is set equal to s in the calculations.

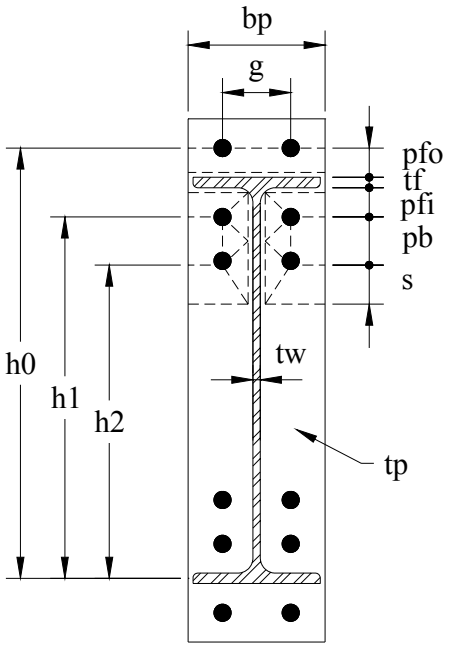

FIGURE 4.9: YIELD LINE PATTERN FOR MULTIPLE ROW EXTENDED 1/2 UNSTIFFENED END-PLATE MOMENT CONNECTIONS

4.4.4.8 Multiple Row Extended 1/3

As a part of this research, a study was conducted to validate a yield line solution for the multiple row extended 1/3 unstiffened end-plate moment connections. Several different yield line patterns were investigated to determine the controlling patterns. Figure 4.10 shows the controlling yield line pattern and defines the geometric parameters. The expressions for the strength of the end-plate, M_{pl}, the thickness of end-plate required to develop the desired moment M_{fc}, and the unknown dimension s are found using the same procedure as discussed for the four bolt extended unstiffened configuration. The resulting expressions are:

$$M_{pl} = F_{yp}\, t_p^2 \left[\frac{b_p}{2} \left[h_1 \left(\frac{1}{p_{fi}} \right) + h_3 \left(\frac{1}{s} \right) + h_0 \left(\frac{1}{p_{fo}} \right) - \frac{1}{2} \right] + \frac{2}{g} \left[h_1 \left(p_{fi} + \frac{3p_b}{2} \right) + h_3 \left(s + \frac{p_b}{2} \right) \right] + \frac{g}{2} \right] \tag{4.31}$$

$$t_p = \sqrt{\frac{M_{fc}}{F_{yp}\left[\frac{b_p}{2}\left[h_1\left(\frac{1}{p_{fi}}\right)+h_3\left(\frac{1}{s}\right)+h_0\left(\frac{1}{p_{fo}}\right)-\frac{1}{2}\right]+\frac{2}{g}\left[h_1\left(p_{fi}+\frac{3p_b}{2}\right)+h_3\left(s+\frac{p_b}{2}\right)\right]+\frac{g}{2}\right]}} \tag{4.32}$$

$$s = \frac{1}{2}\sqrt{b_p\, g} \tag{4.33}$$

For connections with a large inner pitch distance ($p_{fi} > s$), the inner pitch distance, p_{fi}, is set equal to s in the calculations.

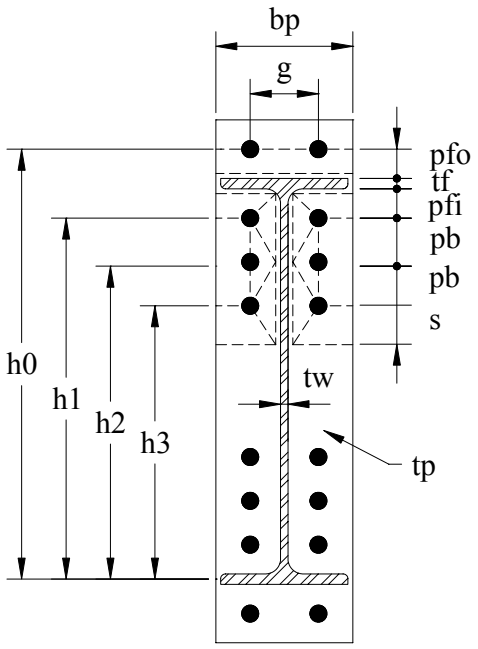

FIGURE 4.10: YIELD LINE PATTERN FOR MULTIPLE ROW EXTENDED 1/3 UNSTIFFENED END-PLATE MOMENT CONNECTIONS

4.4.4.9 Multiple Row Extended Stiffened 1/3

As a part of this research, a study was conducted to validate a yield line solution for the multiple row extended 1/3 stiffened end-plate moment connections. Several different yield line patterns were investigated to determine the controlling patterns. Figure 4.11 shows the two controlling yield line patterns and defines the geometric parameters. The expressions for the unknown dimension s, the strength of the end-plate, M_{pl}, and the thickness of end-plate required to develop the desired moment M_{fc} are found using the same procedure as discussed for the four bolt extended unstiffened configuration. The resulting expressions are:

$$s = \frac{1}{2}\sqrt{b_p\, g} \tag{4.34}$$

Case 1, (when $d_e \leq s$)

$$M_{pl} = F_{yp}\, t_p^2 \left[\frac{b_p}{2} \left[h_1 \left(\frac{1}{p_{fi}} \right) + h_3 \left(\frac{1}{s} \right) + h_0 \left(\frac{1}{p_{fo}} + \frac{1}{2s} \right) \right] + \frac{2}{g} \left[h_1 \left(p_{fi} + \frac{3p_b}{2} \right) + h_3 \left(s + \frac{p_b}{2} \right) + h_0 \left(d_e + p_{fo} \right) \right] + \frac{g}{2} \right] \tag{4.35}$$

$$t_p = \sqrt{\frac{M_{fc}}{F_{yp} \left[\frac{b_p}{2} \left[h_1 \left(\frac{1}{p_{fi}} \right) + h_3 \left(\frac{1}{s} \right) + h_0 \left(\frac{1}{p_{fo}} + \frac{1}{2s} \right) \right] + \frac{2}{g} \left[h_1 \left(p_{fi} + \frac{3p_b}{2} \right) + h_3 \left(s + \frac{p_b}{2} \right) + h_0 \left(d_e + p_{fo} \right) \right] + \frac{g}{2} \right]}} \tag{4.36}$$

Case 2, (when $d_e > s$)

$$M_{pl} = F_{yp}\, t_p^2 \left[\frac{b_p}{2} \left[h_1 \left(\frac{1}{p_{fi}} \right) + h_3 \left(\frac{1}{s} \right) + h_0 \left(\frac{1}{p_{fo}} + \frac{1}{s} \right) \right] + \frac{2}{g} \left[h_1 \left(p_{fi} + \frac{3p_b}{2} \right) + h_3 \left(s + \frac{p_b}{2} \right) + h_0 \left(s + p_{fo} \right) \right] + \frac{g}{2} \right] \tag{4.37}$$

$$t_p = \sqrt{\frac{M_{fc}}{F_{yp}\left[\frac{b_p}{2}\left[h_1\left(\frac{1}{p_{fi}}\right)+h_3\left(\frac{1}{s}\right)+h_0\left(\frac{1}{p_{fo}}+\frac{1}{s}\right)\right]+\frac{2}{g}\left[h_1\left(p_{fi}+\frac{3p_b}{2}\right)+h_3\left(s+\frac{p_b}{2}\right)+h_0\left(s+p_{fo}\right)\right]+\frac{g}{2}\right]}} \quad (4.38)$$

For connections with a large inner pitch distance ($p_{fi} > s$), the inner pitch distance, p_{fi}, is set equal to s in the calculations.

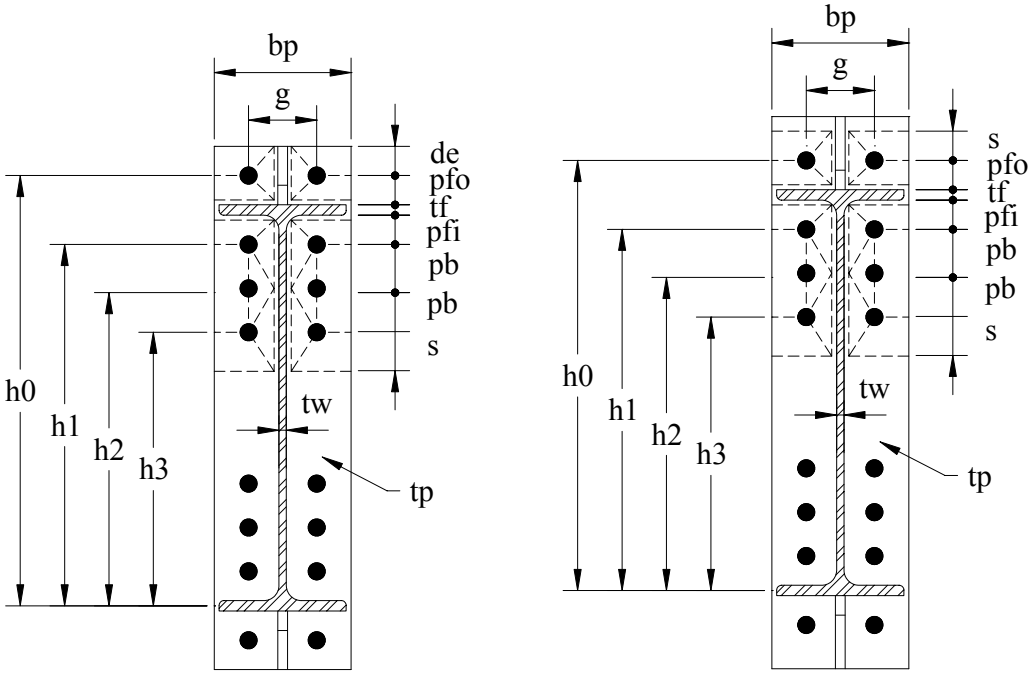

(a) Case 1($d_e \leq s$) (b) Case 2 ($d_e > s$)

FIGURE 4.11: YIELD LINE PATTERN FOR MULTIPLE ROW EXTENDED 1/3 STIFFENED END-PLATE MOMENT CONNECTIONS

4.4.5 Column Flange Strength

4.4.5.1 General

There have been relatively few studies conducted to determine the column flange strength in beam-to-column end-plate moment connections. In a beam-to-column end-plate moment connection, the beam flange tension forces are transmitted directly to the column flange by the connection bolts. The column flange must provide adequate strength to resist the applied bolt

tensile forces. The column flanges can be configured as stiffened or unstiffened. A stiffened column flange has flange stiffener plates, often called continuity plates, installed perpendicular to the column web and in-line with the connecting beam flanges. An unstiffened column flange does not have stiffener or continuity plates.

As a part of this research, yield line analysis has been used to develop solutions for the stiffened and unstiffened column flange configurations for the eight end-plate moment connection configurations shown in Figures 1.4 and 1.5. Details of the yield line solutions for each connection configuration are presented in subsequent sections.

4.4.5.2 Four Bolt Extended

Column flange strength equations for the four bolt extended unstiffened and stiffened end-plate moment connections were developed using yield line analysis. Yield line patterns for the stiffened and unstiffened column flange configurations have been developed. Figure 4.12 shows the controlling yield line patterns and defines the geometric parameters. The strength of the column flange, M_{cf}, is found by equating the internal work, W_i, and the external work, W_e for the yield line patterns. Rearranging the expressions for M_{cf} and solving for the column flange thickness, t_{cf}, results in expressions for the required column flange thickness to develop a desired moment M_{fc}. The resulting expressions for M_{cf} and t_{cf} are as follows:

Unstiffened Column Flange

$$M_{cf} = F_{yc} t_{cf}^2 \left[\frac{b_{cf}}{2} \left[h_1 \left(\frac{1}{s} \right) + h_0 \left(\frac{1}{s} \right) \right] + \frac{2}{g} \left[h_1 \left(s + \frac{3c}{4} \right) + h_0 \left(s + \frac{c}{4} \right) + \frac{c^2}{2} \right] + \frac{g}{2} \right] \tag{4.39}$$

$$t_{cf} = \sqrt{\frac{M_{fc}}{F_{yc} \left[\frac{b_{cf}}{2} \left[h_1 \left(\frac{1}{s} \right) + h_0 \left(\frac{1}{s} \right) \right] + \frac{2}{g} \left[h_1 \left(s + \frac{3c}{4} \right) + h_0 \left(s + \frac{c}{4} \right) + \frac{c^2}{2} \right] + \frac{g}{2} \right]}} \tag{4.40}$$

Stiffened Column Flange

$$M_{cf} = F_{yc} t_{cf}^2 \left[\frac{b_{cf}}{2} \left[h_1 \left(\frac{1}{s} + \frac{1}{p_{si}} \right) + h_0 \left(\frac{1}{s} + \frac{1}{p_{so}} \right) \right] + \frac{2}{g} \left[h_1 \left(s + p_{si} \right) + h_0 \left(s + p_{so} \right) \right] \right] \tag{4.41}$$

$$t_{cf} = \sqrt{\frac{M_{fc}}{F_{yc}\left[\frac{b_{cf}}{2}\left[h_1\left(\frac{1}{s}+\frac{1}{p_{si}}\right)+h_0\left(\frac{1}{s}+\frac{1}{p_{so}}\right)\right]+\frac{2}{g}\left[h_1\left(s+p_{si}\right)+h_0\left(s+p_{so}\right)\right]\right]}} \tag{4.42}$$

The unknown dimension, s, is determined as previous to be

$$s = \frac{1}{2}\sqrt{b_{cf}\ g} \tag{4.43}$$

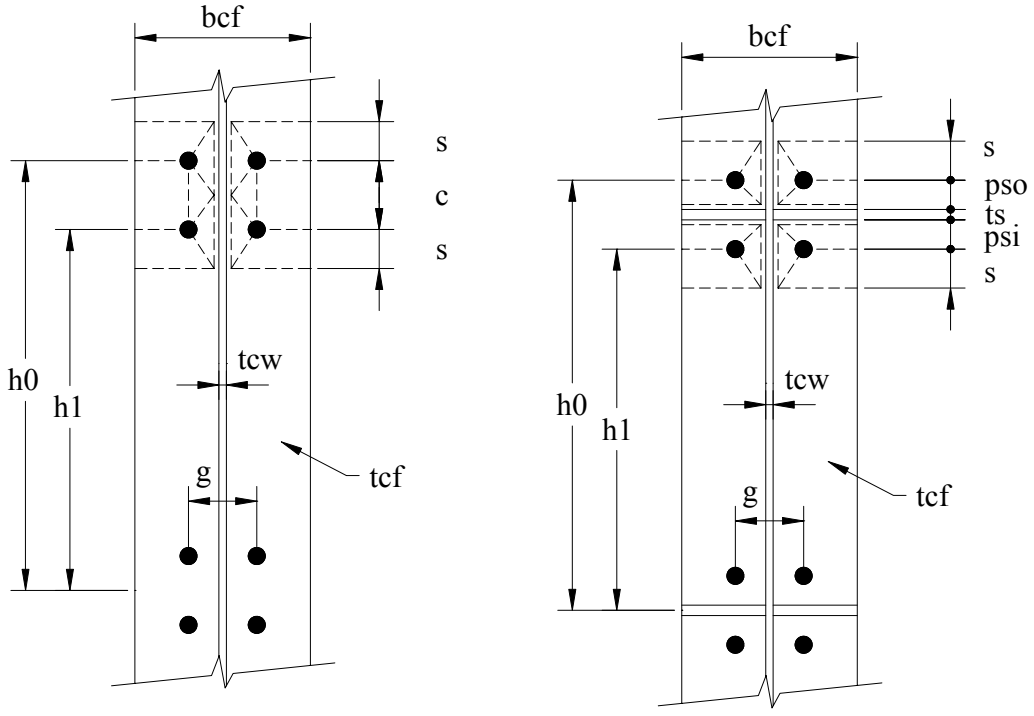

(a) Unstiffened Flange (b) Stiffened Flange

FIGURE 4.12: COLUMN FLANGE YIELD LINE PATTERN FOR FOUR BOLT EXTENDED END-PLATE MOMENT CONNECTIONS

4.4.5.3 Eight Bolt Extended Stiffened

Column flange strength equations for the eight bolt extended stiffened end-plate moment connection was developed using yield line analysis. Yield line patterns for the stiffened and unstiffened column flange configurations have been developed. Figure 4.13 shows the controlling yield line patterns and defines the geometric parameters. The expressions for

strength of the column flange, M_{cf}, thickness of the column flange to develop the desired moment, M_{fc}, and the unknown dimension s are found using the same procedures as for the four bolt extended connections. The resulting expressions are:

Unstiffened Column Flange

$$M_{cf} = F_{yc} t_{cf}^2 \left[\frac{b_{cf}}{2} \left[h_1 \left(\frac{1}{s} \right) + h_4 \left(\frac{1}{s} \right) \right] + \frac{2}{g} \left[h_1 \left(p_b + \frac{c}{2} + s \right) + h_2 \left(\frac{p_b}{2} + \frac{c}{4} \right) + h_3 \left(\frac{p_b}{2} + \frac{c}{2} \right) + h_4 (s) \right] + \frac{g}{2} \right] \tag{4.44}$$

$$t_{cf} = \sqrt{\frac{M_{fc}}{F_{yc} \left[\frac{b_{cf}}{2} \left[h_1 \left(\frac{1}{s} \right) + h_4 \left(\frac{1}{s} \right) \right] + \frac{2}{g} \left[h_1 \left(p_b + \frac{c}{2} + s \right) + h_2 \left(\frac{p_b}{2} + \frac{c}{4} \right) + h_3 \left(\frac{p_b}{2} + \frac{c}{2} \right) + h_4 (s) \right] + \frac{g}{2} \right]}} \tag{4.45}$$

Stiffened Column Flange

$$M_{cf} = F_{yp}\, t_{cf}^2 \left[\frac{b_{cf}}{2} \left[h_1 \left(\frac{1}{s} \right) + h_2 \left(\frac{1}{p_{so}} \right) + h_3 \left(\frac{1}{p_{si}} \right) + h_4 \left(\frac{1}{s} \right) \right] + \frac{2}{g} \left[h_1 \left(s + \frac{p_b}{4} \right) + h_2 \left(p_{so} + \frac{3p_b}{4} \right) + h_3 \left(p_{si} + \frac{p_b}{4} \right) + h_4 \left(s + \frac{3p_b}{4} \right) + p_b^2 \right] + g \right] \tag{4.46}$$

$$t_{cf} = \sqrt{\frac{M_{fc}}{F_{yc} \left[\frac{b_{cf}}{2} \left[h_1 \left(\frac{1}{s} \right) + h_2 \left(\frac{1}{p_{so}} \right) + h_3 \left(\frac{1}{p_{si}} \right) + h_4 \left(\frac{1}{s} \right) \right] + \frac{2}{g} \left[h_1 \left(s + \frac{p_b}{4} \right) + h_2 \left(p_{so} + \frac{3p_b}{4} \right) + h_3 \left(p_{si} + \frac{p_b}{4} \right) + h_4 \left(s + \frac{3p_b}{4} \right) + p_b^2 \right] + g \right]}} \tag{4.47}$$

$$s = \frac{1}{2} \sqrt{b_{cf}\, g} \tag{4.48}$$

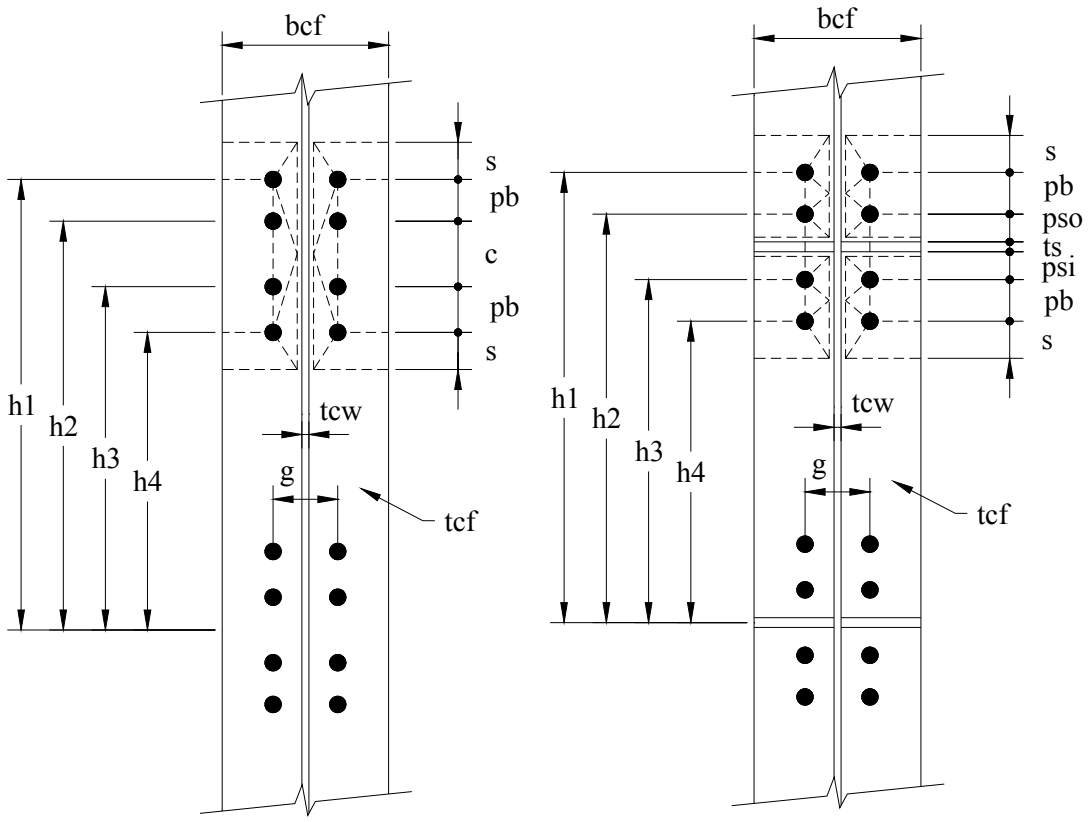

(a) Unstiffened Flange (b) Stiffened Flange

FIGURE 4.13: COLUMN FLANGE YIELD LINE PATTERN FOR EIGHT BOLT EXTENDED STIFFENED END-PLATE MOMENT CONNECTIONS

4.4.5.4 Eight Bolt, Four Bolts Wide Extended

Column flange strength equations for the eight bolt, four bolts wide extended unstiffened and stiffened end-plate moment connections were developed using yield line analysis. Yield line patterns for the stiffened and unstiffened column flange configurations have been developed. Figure 4.14 shows the controlling yield line patterns and defines the geometric parameters. The column flange yield line patterns and corresponding solutions are the same as the four bolt extended end-plate connections. The expressions for strength of the column flange, M_{cf}, thickness of the column flange to develop the desired moment, M_{fc}, and the unknown dimension s are:

Unstiffened Column Flange

$$M_{cf} = F_{yc} t_{cf}^2 \left[\frac{b_{cf}}{2} \left[h_1 \left(\frac{1}{s} \right) + h_0 \left(\frac{1}{s} \right) \right] + \frac{2}{g} \left[h_1 \left(s + \frac{3c}{4} \right) + h_0 \left(s + \frac{c}{4} \right) + \frac{c^2}{2} \right] + \frac{g}{2} \right] \tag{4.49}$$

$$t_{cf} = \sqrt{\frac{M_{fc}}{F_{yc} \left[\frac{b_{cf}}{2} \left[h_1 \left(\frac{1}{s} \right) + h_0 \left(\frac{1}{s} \right) \right] + \frac{2}{g} \left[h_1 \left(s + \frac{3c}{4} \right) + h_0 \left(s + \frac{c}{4} \right) + \frac{c^2}{2} \right] + \frac{g}{2} \right]}} \tag{4.50}$$

Stiffened Column Flange

$$M_{cf} = F_{yc} t_{cf}^2 \left[\frac{b_{cf}}{2} \left[h_1 \left(\frac{1}{s} + \frac{1}{p_{si}} \right) + h_0 \left(\frac{1}{s} + \frac{1}{p_{so}} \right) \right] + \frac{2}{g} \left[h_1 (s + p_{si}) + h_0 (s + p_{so}) \right] \right] \tag{4.51}$$

$$t_{cf} = \sqrt{\frac{M_{fc}}{F_{yc} \left[\frac{b_{cf}}{2} \left[h_1 \left(\frac{1}{s} + \frac{1}{p_{si}} \right) + h_0 \left(\frac{1}{s} + \frac{1}{p_{so}} \right) \right] + \frac{2}{g} \left[h_1 (s + p_{si}) + h_0 (s + p_{so}) \right] \right]}} \tag{4.52}$$

$$s = \frac{1}{2} \sqrt{b_{cf}\ g} \tag{4.53}$$

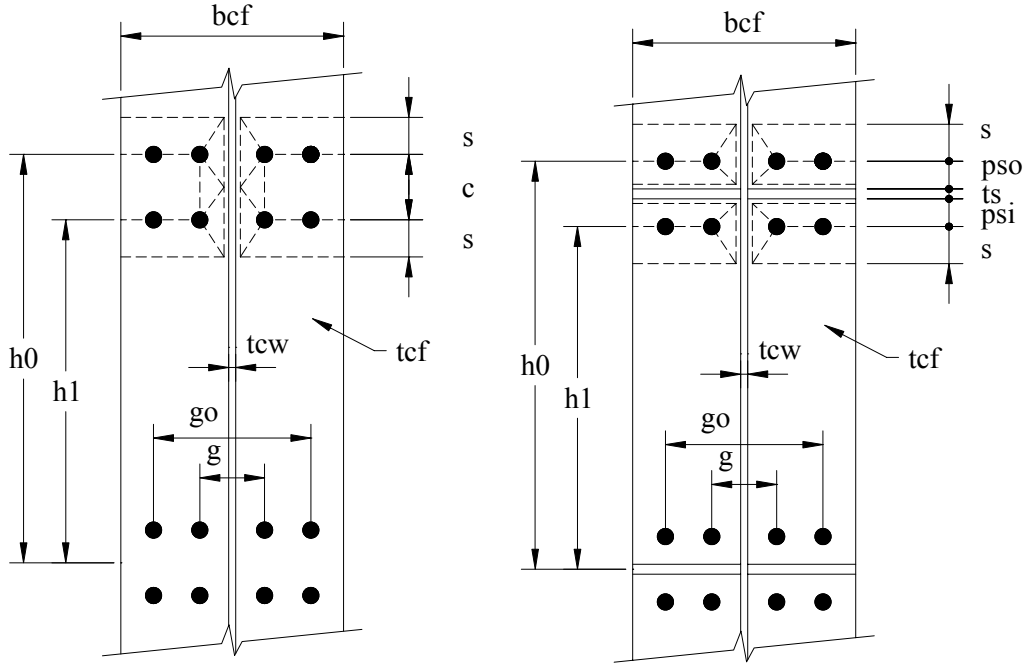

(a) Unstiffened Flange (b) Stiffened Flange

FIGURE 4.14: COLUMN FLANGE YIELD LINE PATTERNS FOR EIGHT BOLT, FOUR BOLTS WIDE EXTENDED END-PLATE MOMENT CONNECTIONS

4.4.5.5 Multiple Row Extended 1/2

Column flange strength equations for the multiple row extended 1/2 unstiffened end-plate moment connection was developed using yield line analysis. Yield line patterns for the stiffened and unstiffened column flange configurations have been developed. Figure 4.15 shows the controlling yield line patterns and defines the geometric parameters. The expressions for strength of the column flange, M_{cf}, thickness of the column flange to develop the desired moment, M_{fc}, and the unknown dimension s are found using the same procedures as for the four bolt extended connections. The resulting expressions are:

Unstiffened Column Flange

$$M_{cf} = F_{yc} t_{cf}^2 \left[\frac{b_{cf}}{2} \left[h_0 \left(\frac{1}{s} \right) + h_2 \left(\frac{1}{s} \right) \right] + \frac{2}{g} \left[h_0 (s + c) + h_1 (p_b) + h_2 (s) \right] + \frac{g}{2} \right] \tag{4.54}$$

$$t_{cf} = \sqrt{\frac{M_{fc}}{F_{yc} \left[\frac{b_{cf}}{2} \left[h_0 \left(\frac{1}{s} \right) + h_2 \left(\frac{1}{s} \right) \right] + \frac{2}{g} \left[h_0 (s + c) + h_1 (p_b) + h_2 (s) \right] + \frac{g}{2} \right]}} \tag{4.55}$$

Stiffened Column Flange

$$M_{cf} = F_{yc}\, t_{cf}^2 \left[\frac{b_{cf}}{2} \left[h_1 \left(\frac{1}{p_{si}} \right) + h_2 \left(\frac{1}{s} \right) + h_0 \left(\frac{1}{p_{so}} + \frac{1}{s} \right) \right] + \frac{2}{g} \left[h_1 \left(p_{si} + \frac{3p_b}{4} \right) + h_2 \left(s + \frac{p_b}{4} \right) + h_0 (s + p_{so}) \right] + \frac{g}{2} \right] \tag{4.56}$$

$$t_{cf} = \sqrt{\frac{M_{fc}}{F_{yc} \left[\frac{b_{cf}}{2} \left[h_1 \left(\frac{1}{p_{si}} \right) + h_2 \left(\frac{1}{s} \right) + h_0 \left(\frac{1}{p_{so}} + \frac{1}{s} \right) \right] + \frac{2}{g} \left[h_1 \left(p_{si} + \frac{3p_b}{4} \right) + h_2 \left(s + \frac{p_b}{4} \right) + h_0 (s + p_{so}) \right] + \frac{g}{2} \right]}} \tag{4.57}$$

$$s = \frac{1}{2} \sqrt{b_{cf}\, g} \tag{4.58}$$

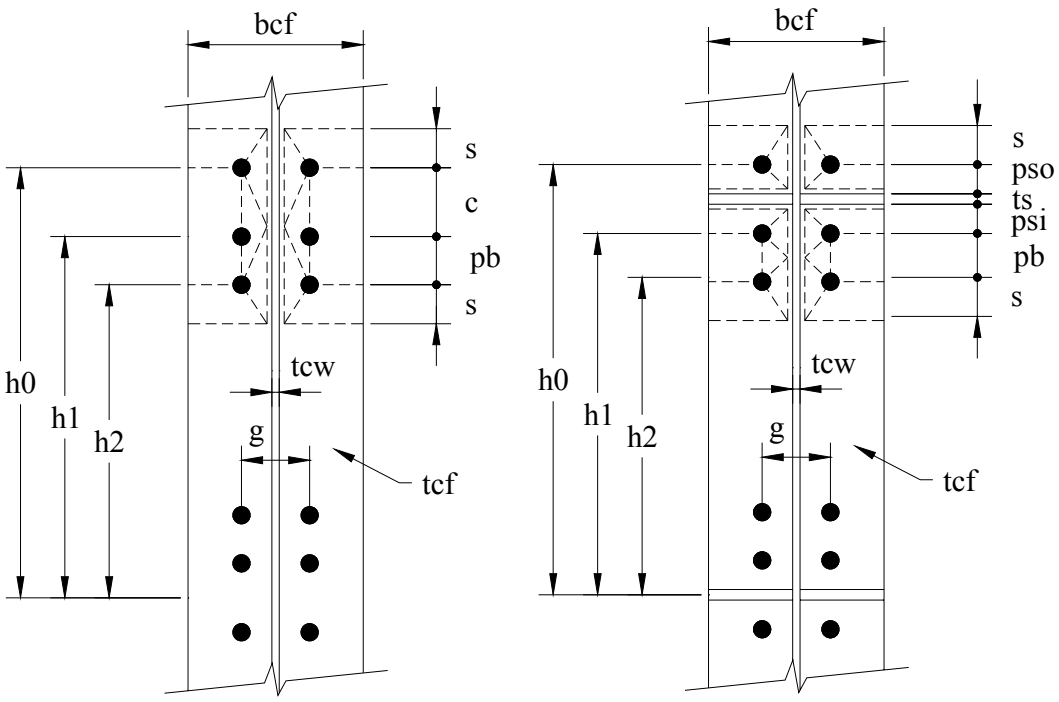

(a) Unstiffened Flange (b) Stiffened Flange

FIGURE 4.15: COLUMN FLANGE YIELD LINE PATTERN FOR MULTIPLE ROW EXTENDED 1/2 END-PLATE MOMENT CONNECTIONS

4.4.5.6 Multiple Row Extended 1/3

Column flange strength equations for the multiple row extended 1/3 unstiffened and stiffened end-plate moment connections were developed using yield line analysis. Yield line patterns for the stiffened and unstiffened column flange configurations have been developed. Figure 4.16 shows the controlling yield line patterns and defines the geometric parameters. The expressions for strength of the column flange, M_{cf}, thickness of the column flange to develop the desired moment, M_{fc}, and the unknown dimension s are found using the same procedures as for the four bolt extended connections. The resulting expressions are:

Unstiffened Column Flange

$$M_{cf} = F_{yc} t_{cf}^2 \left[\frac{b_{cf}}{2} \left[h_0 \left(\frac{1}{s} \right) + h_3 \left(\frac{1}{s} \right) \right] + \frac{2}{g} \left[h_0 \left(\frac{p_b}{2} + c + s \right) + h_1 \left(\frac{3p_b}{4} \right) + h_2 \left(\frac{3p_b}{4} \right) + h_3 (s) \right] + \frac{g}{2} \right] \tag{4.59}$$

$$t_{cf} = \sqrt{\frac{M_{fc}}{F_{yc} \left[\frac{b_{cf}}{2} \left[h_0 \left(\frac{1}{s} \right) + h_3 \left(\frac{1}{s} \right) \right] + \frac{2}{g} \left[h_0 \left(\frac{p_b}{2} + c + s \right) + h_1 \left(\frac{3p_b}{4} \right) + h_2 \left(\frac{3p_b}{4} \right) + h_3 (s) \right] + \frac{g}{2} \right]}} \tag{4.60}$$

Stiffened Column Flange

$$M_{cf} = F_{yc}\, t_{cf}^2 \left[\frac{b_{cf}}{2} \left[h_1 \left(\frac{1}{p_{si}} \right) + h_3 \left(\frac{1}{s} \right) + h_0 \left(\frac{1}{p_{so}} + \frac{1}{s} \right) \right] + \frac{2}{g} \left[h_1 \left(p_{si} + \frac{3p_b}{2} \right) + h_3 \left(s + \frac{p_b}{2} \right) + h_0 \left(s + p_{so} \right) \right] + \frac{g}{2} \right] \tag{4.61}$$

$$t_{cf} = \sqrt{\frac{M_{fc}}{F_{yc} \left[\frac{b_{cf}}{2} \left[h_1 \left(\frac{1}{p_{si}} \right) + h_3 \left(\frac{1}{s} \right) + h_0 \left(\frac{1}{p_{so}} + \frac{1}{s} \right) \right] + \frac{2}{g} \left[h_1 \left(p_{si} + \frac{3p_b}{2} \right) + h_3 \left(s + \frac{p_b}{2} \right) + h_0 \left(s + p_{so} \right) \right] + \frac{g}{2} \right]}} \tag{4.62}$$

$$s = \frac{1}{2} \sqrt{b_{cf}\ g} \tag{4.63}$$

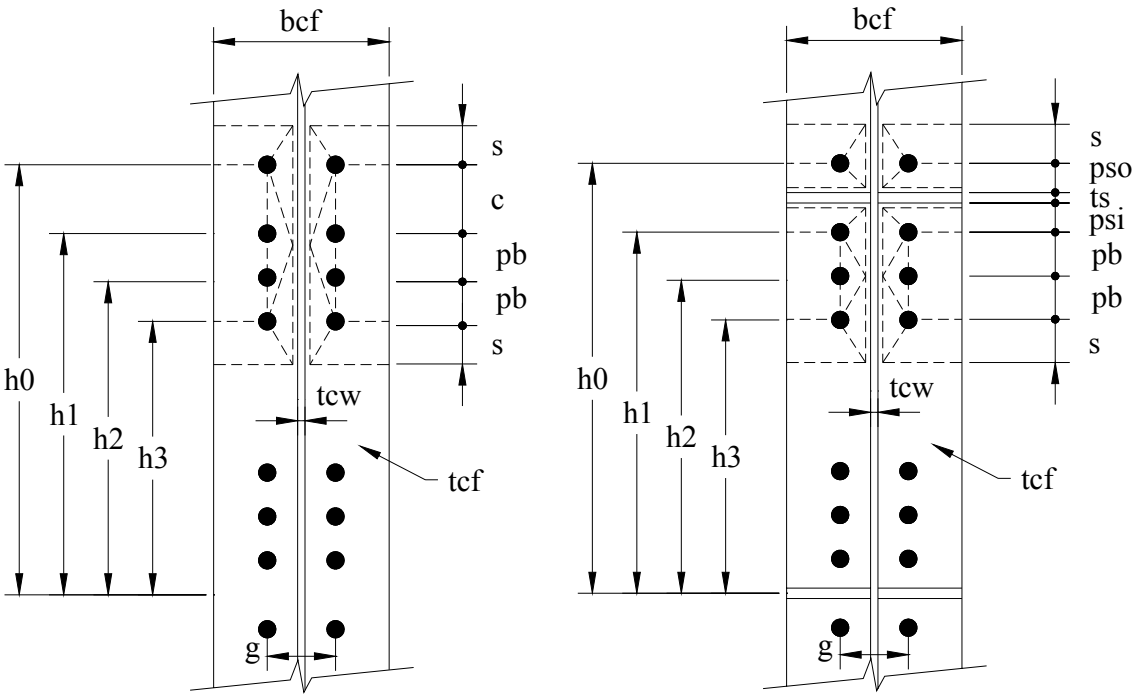

(a) Unstiffened Flange (b) Stiffened Flange

FIGURE 4.16: COLUMN FLANGE YIELD LINE PATTERN FOR MULTIPLE ROW EXTENDED 1/3 END-PLATE MOMENT CONNECTIONS

4.5 Bolt Force Model

4.5.1 General

Numerous studies have been conducted to investigate the behavior of the bolts in end-plate moment connections. The primary focus of the studies has been to measure and predict the possible prying forces within end-plate connections. The majority of the bolt force prediction methods were developed using an analogy between the end-plate connection and an equivalent tee-stub in tension. The design model developed by Kennedy et al. (1982) is the most commonly used procedure for determining the bolt forces in end-plate moment connections. Srouji et al. (1983a, 1983b), Hendrick et al. (1984, 1985), Morrison et al. (1985, 1986), and Borgsmiller (1995) all used a modified Kennedy approach to predict the bolt forces in flush, extended, stiffened, and unstiffened end-plate moment connection configurations. The primary modification to the Kennedy method is an adjustment to the location of prying force and modification of the distribution of the flange force to the particular bolt rows.

4.5.2 Kennedy Bolt Force Model

The Kennedy design procedure identifies three stages of tee stub flange plate behavior. The first stage of plate behavior occurs at low load levels and is identified by purely elastic behavior. The flange plate is said to be 'thick', and it is assumed that there are no prying forces. As the load increased and a plastic hinge forms in the flange plate at the base of the tee stem, a second stage of behavior exists. The plate is said to be of intermediate thickness, and prying forces are present. The third stage of plate behavior occurs as a subsequent plastic hinge forms at the bolt line. The plate is classified as thin, and prying forces are at a maximum. Figure 4.17 illustrates the three stages of plate behavior.

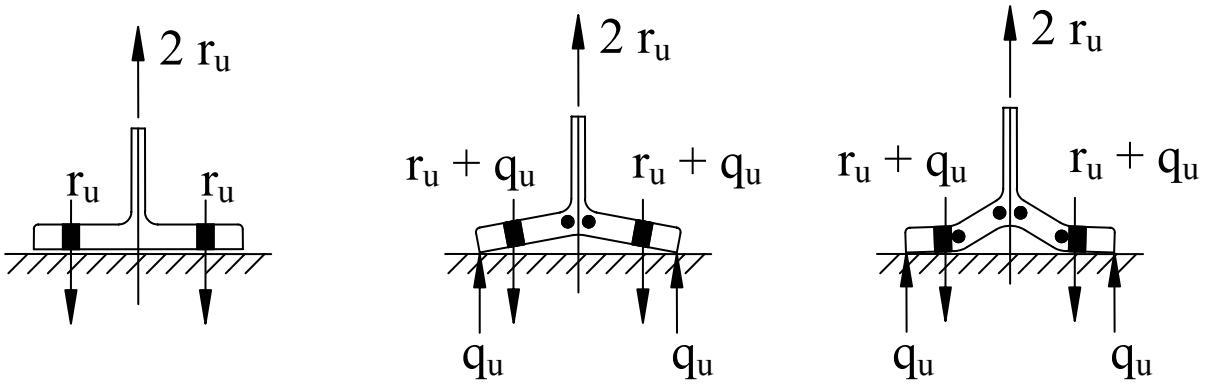

(a) Thick (b) Intermediate (c) Thin

FIGURE 4.17: THREE STAGES OF PLATE BEHAVIOR IN KENNEDY MODEL

4.5.3 Borgsmiller Simplified Procedure

The Kennedy model was modified by Srouji et al. (1983a, 1983b), Hendrick et al. (1984, 1985), Morrison et al. (1985, 1986) to adjust the location of the prying forces and to modify the distribution of the flange tension force to the various bolt rows. Borgsmiller (1995) presented a simplified version of the modified Kennedy method to predict the bolt strength including the effects of prying. The simplified method considers only two stages of plate behavior; thick plate behavior with no prying forces, and thin plate behavior with maximum prying forces. The intermediate plate behavior, as defined in the Kennedy model, is not considered. This simplification allows for direct solution of the bolt forces.

The threshold between thick and thin plate behavior was established to be at the point where the bolt prying forces are negligible. Based upon past experimental test results, Borgsmiller (1995) determined this threshold to be at the point where ninety percent of the end-plate strength is achieved. If the applied load is less than ninety percent of the plate strength, the end-plate is considered to be 'thick' and no prying forces are considered; when the applied load is greater than ninety percent of the end plate strength, the end-plate is considered to be 'thin' and the prying forces are assumed to be at a maximum.

4.5.4 Application to Unified Procedure

The modified Kennedy and the simplified Borgsmiller method were developed to predict the bolt forces in tee stub and end-plate moment connections subject to monotonic loading. The application of cyclic (seismic) loading to the end-plate connections requires careful consideration. The previously discussed design philosophy is to have a strong column, strong connection and a weak beam. This forces the inelastic behavior into the connecting beam and requires that the connection and column remain elastic. Applying this philosophy to the connection requires that the end-plate and column flange be designed to exhibit 'thick' plate behavior. This will ensure that the end-plate and column flange remain elastic and that the bolts are not subject to any significant prying forces.

For thick plate behavior, the bolt forces are determined by taking the static moment of the bolts about the centerline of the compression flange. The connection strength, based upon bolt tension rupture, then becomes the static moment of the bolt strengths about the centerline of the compression flange. Figure 4.18 illustrates this concept for the MRE 1/3 connection. The no-prying moment for the bolt strength, M_{np}, is expressed by:

$$M_{np} = nP_t \sum_{i=1}^{N} h_i \tag{4.64}$$

where n is the number of bolts in each row, N is the number of bolt rows, and h_i is the distance from the centerline of the compression flange to the centerline of the bolt row. P_t is the bolt tensile strength and is expressed as follows:

$$P_t = F_t A_b \tag{4.65}$$

where F_t is the specified tensile strength in the LRFD Specification (AISC 1999a) and A_b is the nominal area of the bolt.

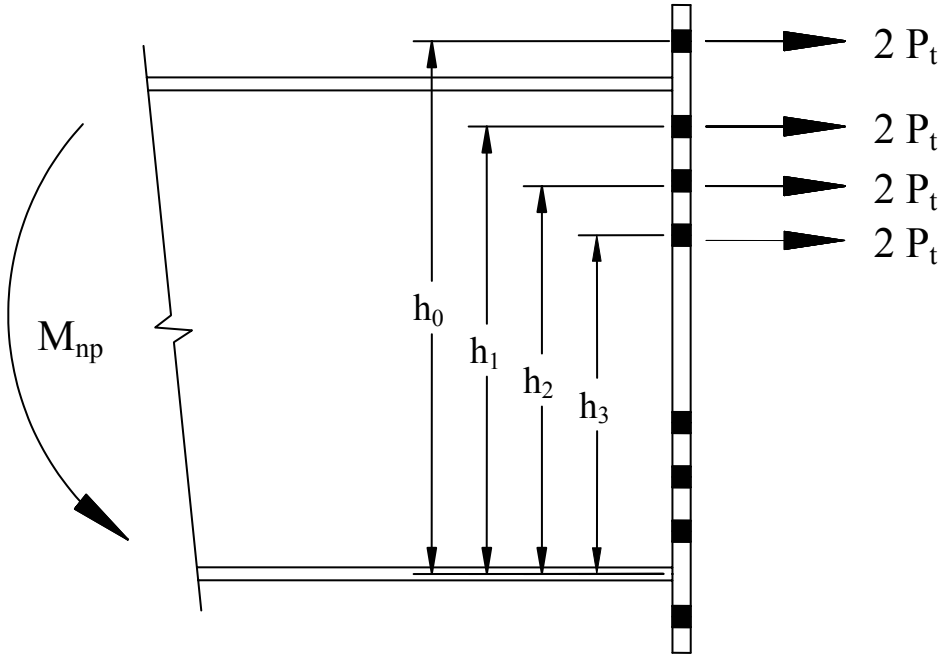

FIGURE 4.18: THICK PLATE BOLT FORCE DESIGN MODEL (MRE 1/3 SHOWN)

The no-prying bolt moment utilizes the full tensile strength of each bolt within the connection. A common assumption that plane sections remain plane indicates that the outermost bolts will reach their tensile strength first. The underlying assumption in the Borgsmiller model is that the outer bolts will yield and provide enough deformation to develop the full tensile force in each of the inner connection bolt rows. This assumption has been investigated in multiple row extended 1/2 connections by Sumner and Murray (2001a) and was determined to be valid.

The no prying bolt strength, calculated using Equation 4.64, implies that the end-plate and column flange will exhibit thick plate behavior. To ensure thick plate behavior, the no prying strength of the bolts must be less than or equal to ninety percent of the end-plate and column flange strength. Another way to state the same requirement is that the end-plate and column flange strength must be greater than or equal to one hundred and ten percent of the strength of the bolts. Equations 4.66 and 4.67 express the thick plate design requirements.

$$M_{np} \leq 0.9M_{pl} \quad \text{and} \quad M_{np} \leq 0.9M_{cf} \tag{4.66}$$

$$M_{pl} \geq 1.1M_{np} \quad \text{and} \quad M_{cf} \geq 1.1M_{np} \tag{4.67}$$

Where M_{np} is the no prying moment given in Equation 4.64, M_{pl} is the end-plate strength, and M_{cf} is the column flange strength.

4.6 Summary

The design methodology for the development of the unified design procedure and the required connection design moment has been presented. Details of the development of the strength equations for the design of the end-plate, column flange and connection bolts have also been presented. Comparisons of the strength models with experimental and finite element results will be presented in subsequent chapters.

Chapter 5 – COMPARISON WITH EXPERIMENTAL RESULTS

5.1 Introduction

5.1.1 Overview

The results of ninety extended end-plate moment connection tests have been identified from a combination of eighteen journal papers and research reports (Abel and Murray, 1992a, Abel and Murray, 1992b, Adey et al., 1997, Borgsmiller et al., 1995, Ghassemieh et al., 1983, Ghobarah, 1992, Ghobarah, 1990, Meng and Murray, 1996, Morrison et al., 1985, Morrison et al., 1986, Packer and Morris, 1977, Rodkey and Murray, 1993, Ryan and Murray, 1999, SEI, 1984, Sumner et al., 2000, Sumner and Murray, 2001a, Sumner and Murray, 2001b, Tsai and Popov, 1990). Each of the nine end-plate moment connection configurations shown in Figures 1.4 and 1.5 are in the ninety test set. In this chapter, comparisons between the experimental results and analytical results from the proposed design procedure are presented.

5.1.2 Experimental Testing

End-plate moment connections have been tested using numerous test setup configurations. As discussed in Chapter 3, end-plate connections are typically tested as beam splice connections or beam-to-column connections. A beam splice connection test setup utilizes two beam sections connected at mid-span using an end-plate moment connection (see Figure 3.17). The loading is usually applied at two locations, each an equal distance from the mid-span connection. A beam-to-column connection test setup utilizes a single column with one or two beams connected, using an end-plate moment connection, to the column flanges (see Figures 3.1 and 3.2). The loading can be applied at the end of the beam or at one end of the column. Monotonic and cyclic loading protocols are used in end-plate connection tests. Generally, monotonic loading is applied for beam splice connections and cyclic loading is applied for beam-to-column connections. The type of test setup and loading protocol used for each test is specified in the comparison tables.

5.2 Interpretation of Experimental Results

5.2.1 Limit States (Failure Modes)

End-plate moment connections have three primary limit states (failure modes) that are observed during experimental testing; end-plate bending, bolt tension rupture, and column flange bending. The connected beam(s) and column have three additional limit states (failure modes) that are commonly observed: beam flexure, panel zone yielding, and column flexure. The test results for each of the ninety end-plate connection tests have been carefully evaluated to identify the experimental values for each of the applicable limit states. In some cases, the experimental value cannot be determined because of inadequate documentation of the test specimen response.

5.2.1.1 End-plate and Column Flange Bending

The end-plate and column flange bending limit state was observed in many of the connection tests used in the comparisons presented in this chapter. These limit states are easily identified during the test because of the large connection deformations and yielding within the connection region. The end-plate and column flange strengths are yielding limits that are compared to the experimentally observed yield moment, M_y. The end-plate and column flange yield moment is one of the most difficult parameters to identify in older test reports. To properly identify the yield moment, the test specimen must be instrumented to measure the separation or deformation of the end-plate and column flange. The end-plate or column flange yield moment can then be determined by plotting the applied load versus the end-plate and column flange deformation. A bi-linear curve fit is then utilized to determine the experimental yield moment, M_y. Figure 5.1 illustrates this concept. The first line is fit to the initial portion of the experimental response curve and represents the elastic response of the end-plate or column flange. The second line is fit to the inelastic portion of the curve and represents the inelastic response of the end-plate or column flange. The intersection of the two lines is the end-plate or column flange yield moment, M_y. Because this is a yield limit state and not a rupture limit state, exceeding the yield moment results in inelastic connection deformations, but not immediate collapse of the connection. Many of the experimental tests continued well beyond the end-plate and column flange bending strength and ultimately failed in another mode, bolt tension rupture or beam flexure.

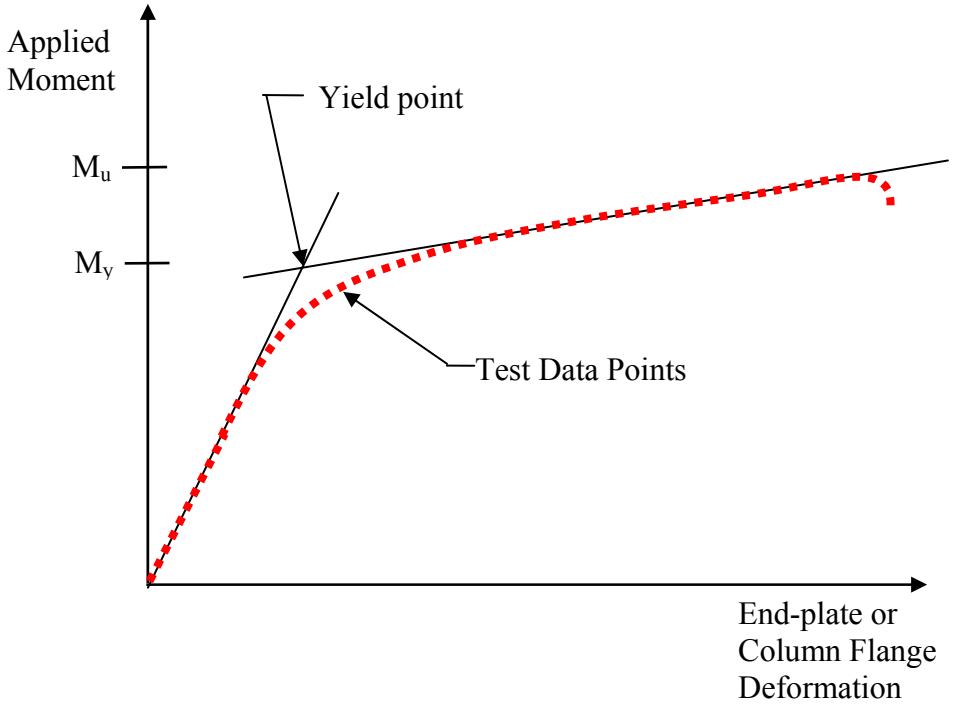

FIGURE 5.1: END-PLATE AND COLUMN FLANGE YIELD MOMENT

In cases where the end-plate and column flange deformation were not measured or reported, it is sometimes possible to determine the yield moment from the load versus beam deflection (or rotation) plots. In these cases, a bi-linear fit of load versus deflection plot will provide the end-plate or column flange yield moment if the initial mode of failure was column flange or end-plate bending. In a number of the older tests evaluated, the test observation notes stated that connection yielding was observed. This statement indicates that the limit state of column flange or end-plate bending was reached. For these tests, the load versus beam deflection plots were used to determine the end-plate or column flange yield moment.

5.2.1.2 Bolt Tension Rupture

The majority of the ninety experimental tests resulted in bolt tension rupture. Bolt tension rupture can occur without prying forces and with prying forces. Tension rupture without prying forces requires the end-plate and column flange to be strong enough to develop the connection bolt strength without the development of significant end-plate or column flange deformations (yielding). As discussed in Chapter 4, this distribution of connection element strengths is known as *strong plate* or *thick plate* behavior. Tension rupture of the connection

bolts with prying occurs when the column flange or end-plate is not strong enough to develop the strength of the connection bolts. This results in the formation of significant end-plate or column flange deformations (yielding) and the development of prying forces in the connection bolts. As discussed in Chapter 4, this distribution of connection element strengths is known as *weak plate* or *thin plate* behavior and is not recommended for the design of end-plate connections subject to cyclic/seismic loads. Weak plate behavior results in an experimental test response that indicates end-plate or column flange failure followed by bolt tension rupture.

5.2.1.3 Beam Flexure

Some of the beam-to-column connection tests were designed with connections strong enough to develop the strength of the connecting beam(s). These tests resulted in the development of a plastic hinge in the connecting beam adjacent to the connection region. For these tests, the maximum applied moment is compared to the expected plastic moment strength of the connected beam, M_{pe}. The expected plastic moment strength was discussed in Chapter 4 and is calculated using Equation 4.1. The value of R_y in Equation 4.1 was taken as unity because the actual yield and tensile strength values were used in the calculations instead of assumed nominal values.

5.2.1.4 Column Flexure and Panel Zone Yielding

None of the tests used in the comparisons presented in this chapter failed in column flexure. A few of the tests noted some column panel zone yielding, but the connection response was not greatly influenced. Consequently, comparisons for these limit states are not presented in this chapter.

5.2.2 Analytical Prediction of Connection Strength

The unified design procedure presented in Chapter 4 was used to predict the strength of ninety end-plate moment connections. The expected connecting beam strength, M_{pe}, the end plate bending strength, M_{pl}, the column flange bending strength, M_{cf}, and the no prying strength of the connection bolts, M_{np} were calculated and are compared to the experimentally observed values. Experimentally measured dimensions and material strengths were used in the calculations. In addition, the nominal connection strength, M_n, was determined and is presented along with the comparisons.

5.3 Experimental and Analytical Comparisons

Comparisons of the experimental and analytical connection component strengths for ninety end-plate moment connection tests are presented herein. Detailed comparisons are presented and discussed for each connection configuration. Additional tables showing the calculated and experimental strengths are included in Appendix C.

Comparisons of the experimental and analytical results are shown in Tables 5.1 through 5.5. The referenced test report or journal paper, the test identification, and the test configuration and loading type are shown in the first three columns. The design ratios for the beam flexural strength, end-plate bending strength, column flange bending strength, and bolt tension rupture strength are shown in the remaining columns. The design ratio for the beam flexural strength is calculated by dividing the expected moment strength of the connected beam, M_{pe}, by the maximum applied moment. The end-plate and column flange design ratios are calculated by dividing the end-plate bending strength, M_{pl}, or column flange bending strength, M_{cf}, (from yield line analysis) by the experimentally observed yield moment, M_y. The bolt design ratio is calculated by dividing the no prying strength of the connection bolts, M_{np}, by the maximum applied moment. Design ratio values less than or equal to one are conservative because the predicted strength is lower than the experimentally observed strength. Conversely, design ratios greater than one are unconservative.

The proposed design methodology presented in Chapter 4 is used to predict the nominal moment strength of the connection, M_n, and to identify the controlling connection limit state (failure mode). The predicted strength of the connection, M_n, is determined using the following rules:

- If $M_{pl} \geq 1.1\ M_{np}$ (*thick plate*) and $M_{cf} \geq 1.1\ M_{np}$ (*thick flange*) then M_n is the minimum of the connected beam strength, M_{pe}, or the no prying bolt strength, M_{np}.

- If $M_{pl} < 1.1\ M_{np}$ (*thin plate*) and $M_{cf} \geq 1.1\ M_{np}$ *(thick flange*) then M_n is the minimum of the connected beam strength, M_{pe}, or the end-plate strength, M_{pl}.

- If $M_{pl} \geq 1.1\ M_{np}$ (*thick plate*) and $M_{cf} < 1.1\ M_{np}$ (*thin flange*) then M_n is the minimum of the connected beam strength, M_{pe}, or the column flange strength, M_{cf}.
- If $M_{pl} < 1.1\ M_{np}$ (*thin plate*) and $M_{cf} < 1.1\ M_{np}$ (*thin flange*) then M_n is the minimum of the connected beam strength, M_{pe}, the end-plate strength, M_{pl}, or the column flange strength, M_{cf}.

The shaded cells indicate the experimentally observed failure modes. Two modes of failure are often observed for an experimental test. This occurs when a yielding limit state such as end-plate or column flange bending is observed and then the test is continued to determine the ultimate strength of the connection test assembly. The bold italic values indicate the controlling failure mode predicted by the proposed design procedure. Cells that contain a dash indicate that the particular value does not apply to the test configuration, or that adequate information was not provided in the test report. The design ratios in the non-shaded cells represent failure modes that were not observed during testing. These values should be greater than one, indicating that the predicted strength for the limit state was not exceeded.

TABLE 5.1: FOUR BOLT EXTENDED UNSTIFFENED COMPARISONS

Connection Type	Reference	Test Identification [1]	Configuration and Loading	Design Ratios [2, 3, 4, 5]			
				M_{pe}/M_u [6]	M_{pl}/M_y	M_{cf}/M_y	M_{np}/M_u
Four Bolt Extended Unstiffened (4E)	Packer & Morris (1977)	4E-3/4-1/2-10	Bm.-Col., Mono.	1.00	***0.98***	1.06	1.26
	Packer & Morris (1977)	4E-3/4-1/2-10	Bm.-Col., Mono.	1.11	1.35	***0.93***	1.40
	Packer & Morris (1977)	4E-3/4-1/2-10	Bm.-Col., Mono.	1.24	3.00	***0.97***	1.57
	Packer & Morris (1977)	4E-3/4-1/2-10	Bm.-Col., Mono.	1.01	2.45	***1.07***	1.28
	Packer & Morris (1977)	4E-3/4-1/2-10	Bm.-Col., Mono.	1.18	3.38	***1.09***	1.49
	Tsai & Popov (1990)	4E-7/8-1 3/8-18	Bm.-Col., Cyclic	1.03	1.94	-	***0.87***
	Tsai & Popov (1990)	4E-1-1 1/4-21	Bm.-Col., Cyclic	***1.02***	1.94	-	1.45
	Ghobarah et al. (1990)	4E-1-1-14	Bm.-Col., Cyclic	1.01	2.39	***0.76***	1.73
	Ghobarah et al. (1990)	4E-1-1-14	Bm.-Col., Cyclic	0.98	2.15	***0.99***	1.67
	Ghobarah et al. (1990)	4E-1-3/4-14	Bm.-Col., Cyclic	1.17	1.14	***1.00***	2.01
	Ghobarah et al. (1992)	4E-1-1.15-14	Bm.-Col., Cyclic	1.06	2.09	***1.03***	1.39
	Ghobarah et al. (1992)	4E-1-1.1-16	Bm.-Col., Cyclic	***0.94***	1.09	1.43	1.16
	Ghobarah et al. (1992)	4E-1-1.1-16	Bm.-Col., Cyclic	***1.07***	1.12	1.55	1.29
	Abel & Murray (1992a)	4E-3/4-5/8-18	Splice, Mono.	-	1.57	-	***1.03***
	Abel & Murray (1992a)	4E-3/4-3/4-18	Splice, Mono.	-	1.89	-	***0.97***
	Abel & Murray (1992a)	4E-1 1/8-7/8-16	Splice, Mono.	-	***1.34***	-	1.52
	Abel & Murray (1992a)	4E-1 1/4-7/8-16	Splice, Mono.	-	***1.05***	-	1.28
	Borgsmiller et al. (1995)	4E-1/2-3/8-16 1/2	Splice, Mono.	-	***1.03***	-	1.04
	Borgsmiller et al. (1995)	4E-1-3/4-64	Splice, Mono.	-	***1.02***	-	1.02
	Meng & Murray (1996)	4E-1-1-18	Bm.-Col., Cyclic	***0.98***	1.24	1.63	1.18
	Meng & Murray (1996)	4E-1-1-18	Bm.-Col., Cyclic	***1.02***	1.30	1.70	1.23
	Meng & Murray (1996)	4E-1.25-1-24	Bm.-Col., Cyclic	0.91	***0.75***	2.92	1.09
	Meng & Murray (1996)	4E-1.25-2.25-24	Bm.-Col., Cyclic	***0.72***	2.76	2.13	1.00
	Ryan & Murray (1999)	4E-7/8-1/2-55	Bm.-Col., Cyclic	-	***0.99***	1.77	1.09
	Adey et al. (1997)	4E-7/8-3/4-14	Bm.-Col., Cyclic	1.03	***0.96***	1.53	1.03
	Adey et al. (1997)	4E-1-1/2-14	Bm.-Col., Cyclic	2.12	***0.65***	3.56	2.48
	Adey et al. (1997)	4E-1-1/2-14	Bm.-Col., Cyclic	2.06	***0.79***	4.60	2.54
	Adey et al. (1997)	4E-11/8-5/8-18	Bm.-Col., Cyclic	1.37	***0.61***	2.22	1.02
	Adey et al. (1997)	4E-1 1/8-5/8-18	Bm.-Col., Cyclic	1.93	***0.91***	4.08	1.54
	Adey et al. (1997)	4E-1 1/4-3/4-18	Bm.-Col., Cyclic	1.64	***1.11***	3.26	2.01
	Adey et al. (1997)	4E-1-5/8-24	Bm.-Col., Cyclic	2.13	***0.92***	2.70	1.09
	Adey et al. (1997)	4E-1-5/8-24	Bm.-Col., Cyclic	2.97	***1.06***	3.77	1.60
	Sumner et al. (2000)	4E-1.25-1.5-24	Bm.-Col., Cyclic	***0.98***	1.51	1.45	1.15
	Sumner et al. (2000)	4E-1.25-1.125-24	Bm.-Col., Cyclic	1.03	***1.09***	1.87	0.97
	Sumner et al. (2000)	4E-1.25-1.375-24	Bm.-Col., Cyclic	***0.79***	1.02	1.77	0.94
	Sumner et al. (2000)	4E-1.25-1.375-24	Bm.-Col., Cyclic	***0.80***	1.03	1.77	0.94

Notes: 1. Test identification: "Conn. type - Bolt dia. - End-plate thickness - Beam depth"
2. Dash "-" indicates that the parameter was not applicable to the test configuration or not available from the test report
3. Shaded cell indicate an observed failure mode
4. ***Bold italic*** values indicate the predicted failure mode using the proposed design procedure
5. Design ratios $\leq$ 1.0 are conservative
6. Mpe = ((Fy + Fu) / 2) Zx

TABLE 5.2: FOUR BOLT EXTENDED STIFFENED COMPARISONS

Connection Type	Reference	Test Identification [1]	Configuration and Loading	Design Ratios [2, 3, 4, 5]			
				M_{pe}/M_u [6]	M_{pl}/M_y	M_{cf}/M_y	M_{np}/M_u
Four Bolt Extended Stiffened (4ES)	Morrison et al. (1985)	4ES-5/8-3/8-16	Splice, Mono.	-	***1.48***	-	1.24
	Morrison et al. (1985)	4ES-3/4-1/2-16	Splice, Mono.	-	***1.36***	-	1.25
	Morrison et al. (1985)	4ES-3/4-7/16-20	Splice, Mono.	-	***1.25***	-	1.10
	Morrison et al. (1985)	4ES-3/4-1/2-20	Splice, Mono.	-	***1.21***	-	1.27
	Morrison et al. (1985)	4ES-1-1/2-24	Splice, Mono.	-	***1.07***	-	1.59
	Morrison et al. (1985)	4ES-1-5/8-24	Splice, Mono.	-	***1.44***	-	1.46
	Tsai & Popov (1990)	4ES-7/8-1 3/8-18	Bm.-Col., Cyclic	***0.98***	2.81	-	1.36
	Ghobarah et al. (1990)	4ES-1-3/4-14	Bm.-Col., Cyclic	***0.96***	1.41	1.23	1.64
	Ghobarah et al. (1990)	4ES-1-3/4-14	Bm.-Col., Cyclic	***0.97***	0.99	1.23	1.64
	Ghobarah et al. (1992)	4ES-1-1.1-16	Bm.-Col., Cyclic	***0.96***	1.25	1.32	1.12
	Adey et al. (1997)	4ES-1 1/4-5/8-18	Bm.-Col., Cyclic	1.29	***0.80***	2.09	1.58
	Adey et al. (1997)	4ES-1 1/4-5/8-18	Bm.-Col., Cyclic	1.23	***0.90***	2.34	1.50
	Adey et al. (1997)	4ES-1 1/4-5/8-24	Bm.-Col., Cyclic	1.64	***1.05***	2.54	1.58
	Ryan & Murray (1999)	4ES-1-1/2-24a	Bm.-Col., Cyclic	-	1.00	***0.92***	1.33
	Ryan & Murray (1999)	4ES-1-1/2-24a	Bm.-Col., Cyclic	-	1.07	***0.96***	1.18
	Ryan & Murray (1999)	4ES-1-1/2-24b	Bm.-Col., Cyclic	-	***1.03***	1.04	1.22

Notes: 1. Test identification: "Conn. type - Bolt dia. - End-plate thickness - Beam depth"
2. Dash "-" indicates that the parameter was not applicable to the test configuration or not available from the test report
3. Shaded cell indicate an observed failure mode
4. ***Bold italic*** values indicate the predicted failure mode using the proposed design procedure
5. Design ratios $\leq$ 1.0 are conservative
6. Mpe = ((Fy + Fu) / 2) Zx

TABLE 5.3: EIGHT BOLT EXTENDED STIFFENED COMPARISONS

Connection Type	Reference	Test Identification [1]	Configuration and Loading	Design Ratios [2, 3, 4, 5]			
				M_{pe}/M_u [6]	M_{pl}/M_y	M_{cf}/M_y	M_{np}/M_u
Eight Bolt Extended Stiffened (8ES)	Ghassemieh (1983)	8ES-0.875-0.75-24	Splice, Mono.	-	***1.05***	-	1.23
	Ghassemieh (1983)	8ES-0.875-1-24	Splice, Mono.	-	1.76	-	***1.12***
	Adey et al. (1997)	8ES-1 1/8-3/4-18	Bm.-Col., Cyclic	***0.93***	1.30	2.18	1.38
	Adey et al. (1997)	8ES-1 1/8-3/4-18	Bm.-Col., Cyclic	***0.87***	1.22	2.05	1.30
	Sumner et al. (2000)	8ES-1.25-1.75-30	Bm.-Col., Cyclic	***1.00***	2.82	3.17	1.64
	Sumner et al. (2000)	8ES-1.25-1-30	Bm.-Col., Cyclic	0.94	***1.05***	3.65	1.23
	Sumner et al. (2000)	8ES-1.25-2.5-36	Bm.-Col., Cyclic	***0.93***	3.91	1.92	0.99
	Sumner et al. (2000)	8ES-1.25-1.25-36	Bm.-Col., Cyclic	1.11	1.58	3.24	***0.94***

Notes: 1. Test identification: "Conn. type - Bolt dia. - End-plate thickness - Beam depth"
2. Dash "-" indicates that the parameter was not applicable to the test configuration or not available from the test report
3. Shaded cell indicate an observed failure mode
4. ***Bold italic*** values indicate the predicted failure mode using the proposed design procedure
5. Design ratios $\leq$ 1.0 are conservative
6. Mpe = ((Fy + Fu) / 2) Zx

TABLE 5.4: EIGHT BOLT EXTENDED, FOUR BOLTS WIDE COMPARISONS

Connection Type	Reference	Test Identification [1]	Configuration and Loading	Design Ratios [2, 3, 4, 5]			
				M_{pe}/M_u [6]	M_{pl}/M_y	M_{cf}/M_y	M_{np}/M_u
Eight Bolt, Unstiffened Four Bolts Wide (8E-4W)	Sumner et al. (2000)	8E-4W-1.25-1.125-30	Bm.-Col., Cyclic	***1.02***	1.17	3.19	1.32
	Sumner et al. (2000)	8E-4W-1.25-1-30	Bm.-Col., Cyclic	1.10	***1.04***	3.66	1.43
	Sumner et al. (2000)	8E-4W-1.25-1.375-36	Bm.-Col., Cyclic	1.10	1.21	2.11	***0.94***
	Sumner et al. (2000)	8E-4W-1.25-1.25-36	Bm.-Col., Cyclic	1.11	***1.11***	2.25	0.95
	Sumner & Murray (2001b)	8E-4W-1-1/2-62	Splice, Mono.	-	***0.96***	-	1.86
	Sumner & Murray (2001b)	8E-4W-3/4-3/4-62	Splice, Mono.	-	1.60	-	***0.88***
	Sumner & Murray (2001b)	8E-4W-3/4-3/4-62	Splice, Mono.	-	1.24	-	***0.92***
8ES-4W	Meng & Murray (1996)	8ES-4W-1.25-1.5-36	Bm.-Col., Cyclic	***0.91***	1.39	1.93	1.02

Notes: 1. Test identification: "Conn. type - Bolt dia. - End-plate thickness - Beam depth"
2. Dash "-" indicates that the parameter was not applicable to the test configuration or not available from the test report
3. Shaded cell indicate an observed failure mode
4. ***Bold italic*** values indicate the predicted failure mode using the proposed design procedure
5. Design ratios $\leq$ 1.0 are conservative
6. Mpe = ((Fy + Fu) / 2) Zx

TABLE 5.5: MULTIPLE ROW EXTENDED COMPARISONS

Connection Type	Reference	Test Identification [1]	Configuration and Loading	Design Ratios [2, 3, 4, 5]			
				M_{pe}/M_u [6]	M_{pl}/M_y	M_{cf}/M_y	M_{np}/M_u
Multiple Row Extended 1/2 Unstiffened (MRE 1/2)	Abel & Murray (1992b)	MRE1/2-3/4-3/4-26	Splice, Mono.	-	1.86	-	***1.29***
	Abel & Murray (1992b)	MRE1/2-3/4-3/8-26	Splice, Mono.	-	***0.73***	-	1.56
	Sumner & Murray (2001a)	MRE1/2-3/4-3/8-30	Splice, Mono.	-	***0.77***	-	1.22
	Sumner & Murray (2001a)	MRE1/2-3/4-3/4-30	Splice, Mono.	-	1.83	-	***0.89***
	Sumner & Murray (2001a)	MRE1/2-3/4-3/4-30	Splice, Mono.	-	1.54	-	***0.94***
	Sumner & Murray (2001a)	MRE1/2-3/4-1/2-30	Splice, Mono.	-	***0.86***	-	1.07
	Sumner & Murray (2001a)	MRE1/2-3/4-3/4-30	Splice, Mono.	-	1.63	-	***0.92***
	Sumner & Murray (2001a)	MRE1/2-3/4-3/4-30	Splice, Mono.	-	1.82	-	***1.03***
Multiple Row Extended 1/3 Unstiffened (MRE 1/3)	Morrison et al. (1986)	MRE1/3-3/4-3/8-30	Splice, Mono.	-	***0.93***	-	1.77
	Morrison et al. (1986)	MRE1/3-1-1/2-30	Splice, Mono.	-	***1.05***	-	2.94
	Morrison et al. (1986)	MRE1/3-7/8-7/16-46	Splice, Mono.	-	***1.07***	-	1.79
	Morrison et al. (1986)	MRE1/3-1 1/8-5/8-46	Splice, Mono.	-	***0.96***	-	2.59
	Morrison et al. (1986)	MRE1/3-1 1/4-5/8-62	Splice, Mono.	-	***0.94***	-	2.57
	Morrison et al. (1986)	MRE1/3-1 1/2-3/4-62	Splice, Mono.	-	***0.97***	-	2.55
	Rodkey & Murray (1993)	MRE1/3-3/4-5/8-33 1/4	Splice, Mono.	-	***1.06***	-	1.13
	Structural Eng. Inc. (1984)	MRE1/3-3/4-1/2-62	Splice, Mono.	-	***1.21***	-	1.67
	Structural Eng. Inc. (1984)	MRE1/3-1-3/4-62	Splice, Mono.	-	***1.48***	-	1.99
	Borgsmiller et al. (1995)	MRE1/3-1-3/4-64	Splice, Mono.	-	***0.94***	-	1.46
	Ryan & Murray (1999)	MRE 1/3-7/8-5/8-55	Bm.-Col., Cyclic	-	***1.04***	1.17	1.21
	Ryan & Murray (1999)	MRE 1/3-7/8-5/8-55	Bm.-Col., Cyclic	-	***1.05***	1.16	1.08
	Ryan & Murray (1999)	MRE 1/3-7/8-1/2-55	Bm.-Col., Cyclic	-	***0.96***	0.99	1.53
MRES 1/3	Structural Eng. Inc. (1984)	MRES1/3-1-3/4-62	Splice, Mono.	-	***1.41***	-	1.48

Notes: 1. Test identification: "Conn. type - Bolt dia. - End-plate thickness - Beam depth"
2. Dash "-" indicates that the parameter was not applicable to the test configuration or not available from the test report
3. Shaded cell indicate an observed failure mode
4. ***Bold italic*** values indicate the predicted failure mode using the proposed design procedure
5. Design ratios $\leq$ 1.0 are conservative
6. Mpe = ((Fy + Fu) / 2) Zx

5.4 Evaluation of Proposed Design Method

5.4.1 Four Bolt Extended Connections

5.4.1.1 Four Bolt Extended Unstiffened

Thirty-six tests of the four bolt extended unstiffened end-plate moment connection were analyzed with the results summarized in Table 5.1. The design ratios for the predicted failure mode (bold italic values) vary from 0.61 to 1.34, and have an average ratio of 0.95. Noteworthy is that only two of the design ratios were greater than 1.10. Although there is some variability in the predicted strength and the values are not always conservative, the proposed design method predictions do correlate well with the experimental results.

5.4.1.2 Four Bolt Extended Stiffened

Sixteen four bolt extended stiffened end-plate moment connection tests were analyzed to determine the predicted to experimentally observed strength design ratios. A summary of the results is shown in Table 5.2. The predicted failure mode design ratios (bold italic values) range from 0.80 to 1.48 with an average value of 1.08. The results of the six tests conducted by Morrison et al. (1985) appear to be inconsistent with the other research studies. All of the tests conducted by Morrison et al. (1985) have unconservative design ratios ranging from 1.07 to 1.48. The remaining ten tests have more conservative controlling design ratios ranging from 0.80 to 1.05 with an average value of 0.95. Noteworthy is that the three tests conducted by Adey et al. (1997) had "relaxed" geometry with outer pitch distances, p_{fo}, equal to 4.0 in. and 5.4 in. instead of the normal 2 in. His tests were designed to maximize the possible energy dissipation of the end-plate. The geometry used for the test connections is not very efficient and would not commonly be used. Except for the tests conducted by Morrison et al. (1985), the proposed design methodology correlates well with the experimental test results.

5.4.2 Eight Bolt Extended Stiffened Connections

Eight tests of the eight bolt extended stiffened end-plate moment connection were analyzed and the results presented in Table 5.3. Good correlation with the experimental results is observed with the predicted failure mode design ratios (bold italic values) ranging from 0.87 to 1.12. The average controlling design ratio is 0.99.

5.4.3 Eight Bolt Extended, Four Bolts Wide Connections

Results from eight tests of the eight bolt extended, four bolts wide connection were analyzed with the results presented in Table 5.4. Seven of the tests utilized the unstiffened configuration and one test was stiffened. The predicted failure mode design ratios (bolt italic values) vary from 0.88 to 1.11 and have an average value of 0.97. Although not all the predictions are conservative, good correlation with the experimental results exists.

5.4.4 Multiple Row Extended Connections

5.4.4.1 Multiple Row Extended 1/2 Connections

Eight tests of the multiple row extended 1/2 end-plate moment connection were analyzed with the results as shown in Table 5.5. The design ratios for the predicted failure mode (bold italic values) vary from 0.73 to 1.29, and have an average ratio of 0.93. The proposed design method predicts the controlling failure mode consistently. Noteworthy is that only one test has a significantly unconservative design ratio of 1.29. The remaining tests have more conservative design ratios ranging from 0.73 to 1.03 with an average value of 0.88. Although there is some variability in the predicted strength, the proposed design method predictions do correlate well with the experimental results.

5.4.4.2 Multiple Row Extended 1/3 Connections

Test results from fourteen tests of the multiple row extended 1/3 end-plate moment connection were analyzed and the results presented in Table 5.5. Thirteen of the tests utilized the unstiffened configuration and one test utilized the stiffened configuration. The predicted failure mode design ratios (bolt italic values) for the unstiffened configuration vary from 0.93 to 1.48 and have an average value of 1.05. The design ratio for the one stiffened configuration test was 1.41. Initial evaluation of the design ratios indicates that the proposed method is slightly unconservative. Further consideration of the values in Table 5.5 shows that the results of the tests conduced by SEI (1984) are inconsistent with the other experimental studies considered in the comparisons. The two unstiffened tests and the one stiffened test have design ratios of 1.21, 1.48, and 1.41 respectively. If the tests conducted by SEI (1984) are not included, the design ratios for the four studies included in the comparisons vary from 0.93 to 1.07 with an average value of 1.0. With the exception of the SEI (1984) results, good correlation between the

experimental results and the proposed design methodology exists for the unstiffened configuration. With the exception of the SEI (1984) test, no experimental tests of the stiffened configuration are available for comparison with the proposed design methodology.

5.4.5 Overall Evaluation

To obtain an overall evaluation of the correlation of the proposed design method predictions with the experimental results, the design ratios of the previously presented test results were combined. The predicted failure mode design ratios (bolt italic values) vary from 0.61 to 1.34 with an average value of 0.96 and a standard deviation of 12.0 percent. To further investigate the proposed method predictions, the ratios for prediction of the beam, end-plate, column flange, and bolts are considered separately. All of the shaded cell design ratio values (observed failure modes in a test) are included in these comparisons, and the tests of the four bolt stiffened connections by Morrison et al. (1985) and the tests of the multiple row extended 1/3 by SEI (1984) have been excluded from the comparisons. The expected beam moment design ratios vary from 0.72 to 1.29 with an average value of 1.00 and a standard deviation of 12.1 percent. The end-plate moment design ratios vary from 0.61 to 1.35 with an average value of 0.99 and a standard deviation of 15.3 percent. The column flange moment design ratios vary from 0.76 to 1.09 with an average value of 0.98 and a standard deviation of 8.7 percent. The no prying bolt strength design ratios vary from 0.87 to 1.29 with an average value of 0.98 and a standard deviation of 10.7 percent. Although there is some variance in the prediction of the controlling strength design ratio, the average values are all conservative. With only a few exceptions, the proposed design method predicts the controlling failure mode correctly. Good correlation with the observed experimental test results is also obtained.

5.5 Summary

The experimental results of ninety extended end-plate moment connection tests have been compared to strength predictions calculated using the proposed design procedure presented in Chapter 4. Comparisons for each connection type and for all of the connections together were presented. Some variability in the predictions was noted, but good correlation with the test results was observed in all cases.

Chapter 6 – FINITE ELEMENT ANALYSIS

6.1 Introduction

Numerous studies have been conducted to investigate the use of finite element analysis to predict the behavior of end-plate moment connections (Krishnamurthy and Grady, 1976; Ahuja et al., 1982; Ghassemieh et al., 1983; Abolmaali et al., 1984; Kukreti et al, 1990; Gebbeken et al., 1994; Bahaari and Sherbourne, 1994, 1996a, 1996b; Choi and Chung, 1996; Bose et al., 1997; Bursi and Jaspart, 1998; Meng, 1996; Ryan, 1999; Sumner et al. 2000; and Mays 2000). Past studies have correlated finite element analysis results and experimental test results using two-dimensional and three-dimensional modeling. It has been concluded that finite element modeling can be used to accurately predict the behavior of end-plate moment connections (Mays, 2000). In this chapter, a brief summary of three directly related finite element studies and the results of a study, conduced as a part of this research, to investigate the column flange bending strength in extended end-plate moment connections are presented.

6.2 Directly Related Studies

Finite element studies presented by Mays (2000), Sumner et al. (2000) and Ryan (1999) were conducted concurrently with the experimental testing phase of this research study. Mays performed extensive modeling of the four bolt unstiffened, eight bolt stiffened, and the eight bolt, four bolts wide unstiffened extended end-plate moment connections. He correlated the finite element results with the experimental values from the SAC Steel Project connection tests conducted as a part of this research (see Section 3.2). Excellent correlation of the end-plate separation from the column flange and the bolt forces was observed. Ryan (1999) modeled the four bolt unstiffened, four bolt stiffened, and the multiple row 1/3 unstiffened extended end-plate moment connections and correlated the results with experimental test results. Excellent correlation between the finite element and experimental test results was observed. The work by Mays (2000) and Ryan (1999) focused on the end-plate and bolt behavior and did not investigate the behavior of the column flange. In their studies, the column flange was modeled as a rigid member.

6.3 Overview of Current Study

To expand on the related work conducted by Mays and Ryan, a finite element study was conducted to investigate the column flange bending strength in moment end-plate connections. Six connection models were analyzed and compared to the strength predictions of the proposed design procedure. The connection models consisted of a cantilever beam section connected to a flexible column flange using an extended end-plate moment connection. A description of the finite element model details and the analytical comparisons are presented herein.

6.4 Finite Element Model

The details of the finite element models used in this study are very closely based on the models presented by Mays (2000) and Sumner et al. (2000). ANSYS, a commercial finite element analysis software package, was used to create and analyze finite element models of six beam-to-column extended end-plate moment connections. Full beam-to-column flange connection models were developed to investigate the column flange bending behavior. Stiffened and unstiffened column flange conditions were modeled for the four bolt extended unstiffened, eight bolt extended stiffened, and the multiple row extended 1/3 end-plate moment connection configurations.

A W30x124 section was used as the connecting beam for each of the models. The connection bolts were one inch diameter, A325 strength bolts. The end-plate, beam, and column flange dimensions used for all of the models are shown in Table 6.1. The end-plate thickness and column flange thickness were selected for each connection configuration to ensure column flange bending failure. The selected plate and flange thicknesses and the corresponding strengths are shown in Table 6.2.

The proposed design procedure was used to design the modeled connections. To isolate the behavior of the column flange, the connecting beam, connection bolts and end-plate were designed stronger than the column flange. The strength of the connection bolts, M_{np}, is approximately twenty-five percent greater than the column flange bending strength, M_{cf}. The end-plate strength, M_{pl}, is approximately twenty-five percent greater than the connection bolts, M_{np}. The separation between strengths of the different components was designed to avoid premature failure of the connection model. Connections designed using the proposed design

procedure would normally have end-plate, M_{pl}, and column flange strengths, M_{cf}, at least ten percent greater than the connection bolt strength, M_{np}. The design of the connection models in this manner results in a connection with a strong beam, strong end-plate, strong bolts, and a flexible column flange.

TABLE 6.1: END-PLATE, BEAM, AND COLUMN FLANGE DIMENSIONS

Component	Dimension*		
End-Plate	b_p =	11.5	in.
	g =	5.5	in.
	p_{fi} =	1.75	in.
	p_{fo} =	1.75	in.
	p_b =	3.0	in.
Beam	Section:	W30x124	
	d =	30.0	in.
	b_f =	10.5	in.
	t_f =	1.0	in.
	t_w =	0.5625	in.
Column	Section:	Built-Up (similar to W14)	
	b_{fc} =	15.5	in.
	c =	4.5	in.
	t_s =	1.0	in.
	p_{so} =	1.75	in.
	p_{si} =	1.75	in.

* Note: See Figures 4.4, 4.6, 4.10, 4.12, 4.13, and 4.16 for illustration of dimensions

Three-dimensional solid finite element models were used to analyze the six end-plate moment connections. Symmetry about the vertical plane through the beam web and flange was used and only half of the structure analyzed. Solid eight-node brick elements (SOLID45) were used to model the beam flanges and web. The end-plate, column flange, and the connection bolts were modeled with solid twenty-node brick elements (SOLID95). Past studies have shown that the use of the twenty node elements required less mesh refinement when compared to using eight-node elements (Mays, 2000). The effects of bolt pretension were not considered in this study. Plasticity effects were included in both element types. The complex interaction of the end-plate and column flange was modeled using contact elements (CONTACT49) at the end-

plate to column flange interface. Constraint equations were used to make the bolt heads continuous with the end-plate and column flange. The beam and end-plate nodes along the plane of symmetry were restrained against lateral translation. The column flange nodes along the plane of symmetry were restrained against all translations. The column flange stiffeners were modeled by restraining the column flange nodes at the stiffener locations against out-of-plane translation. To isolate the behavior of the column flange, only the column flange and a small portion of the column web and flange stiffeners were modeled. Typical connection model meshes are shown in Figure 6.1. The connecting beam, column flange and end-plate are shown.

TABLE 6.2: FINTE ELEMENT MODEL ANALYSIS MATRIX

Connection ID	End-Plate Thickness (in.)	Col. Flange Thickness (in.)	Stiffened Column	Calculated Strengths*		
				M_{np} (k-ft)	M_{pl} (k-ft)	M_{cf} (k-ft)
4E-1-7/8-30	0.875	0.625	No	683	810	402
	0.875	0.5	Yes	683	810	509
8ES-1-1-30	1	0.875	No	1367	1853	1011
	1	0.625	Yes	1367	1853	910
MRE 1/3-1-1 1/8-30	1.125	0.875	No	1208	1701	915
	1.125	0.625	Yes	1208	1701	856

* Note: Strengths calculated using the proposed deisgn procedure.

A tri-linear stress strain relationship was utilized for the structural steel models. The stress-strain relationship utilized for the beam, end-plate, and column flange steel is shown in Figure 6.2. A yield strength, F_y, of 50 ksi and a tensile strength, F_u, of 65 ksi were utilized. The high-strength bolt stress-strain relationship used is shown in Figure 6.3. The bolt yield stress, F_{yb}, was 90 ksi and the tensile strength, F_{ub}, was 100 ksi.

The moment at the connection was induced by applying three vertical loads to beam tip. The vertical loads were increased until the model became unstable due to excessive inelastic behavior of the structure. Nodal displacements of the end-plate and column flange were used to calculate the end-plate and column flange separation. The end-plate and column flange separation was closely monitored to detect the formation of a yield mechanism in the column flange. End-plate and column flange separation values were recorded for each load step and used to generate an applied moment versus end-plate separation response plot.

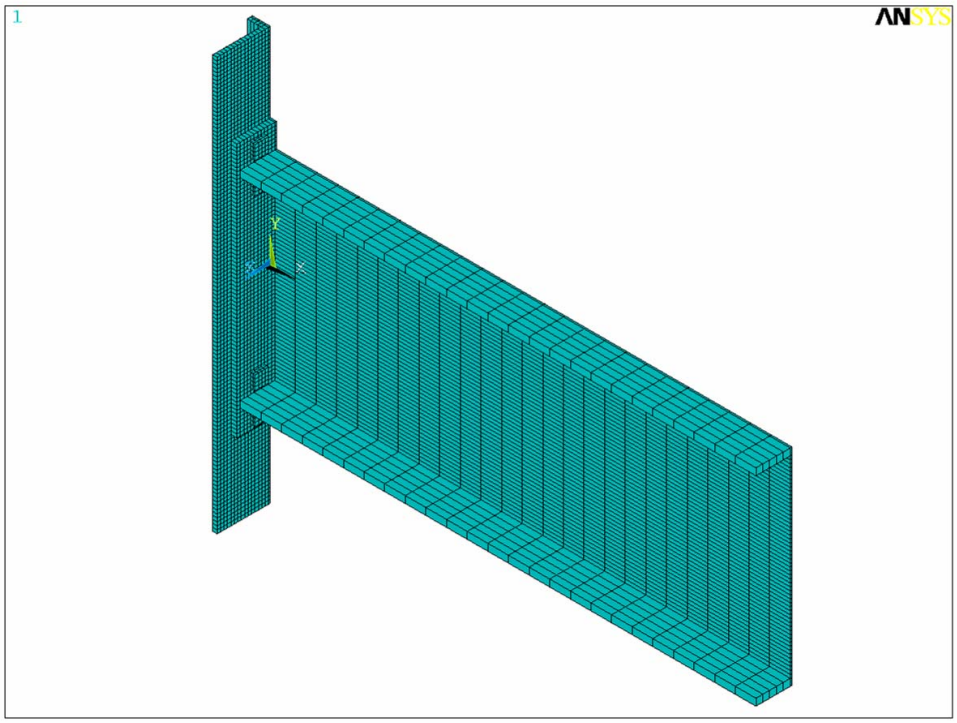

a) Four Bolt Extended Unstiffened Connection with Unstiffened Column Flange

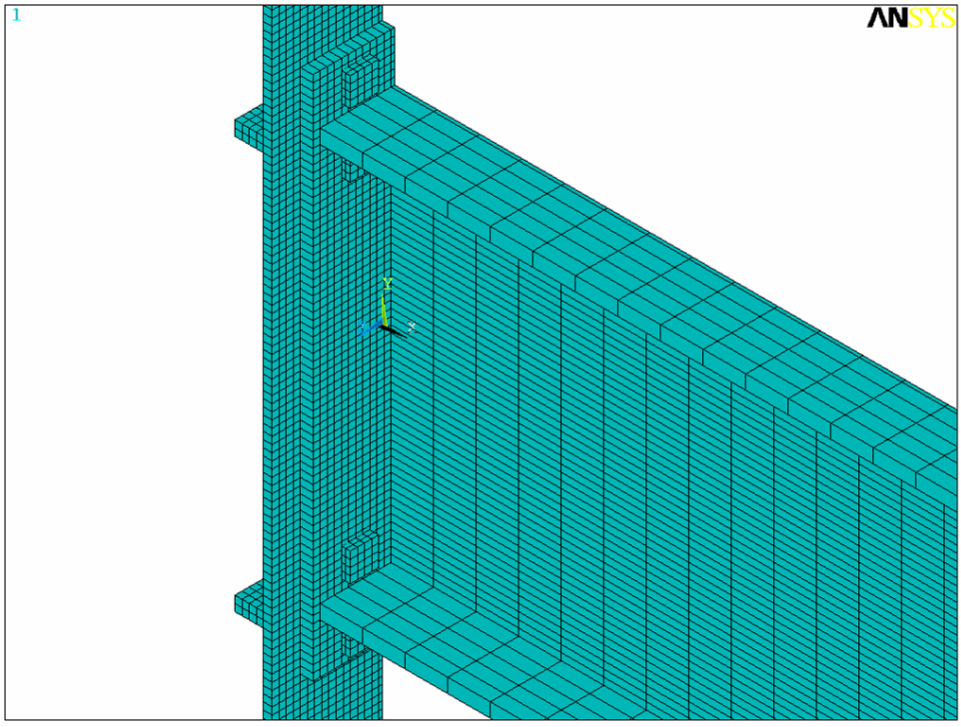

a) Four Bolt Extended Unstiffened Connection with Stiffened Column Flange

FIGURE 6.1: TYPICAL FINITE ELEMENT MESH

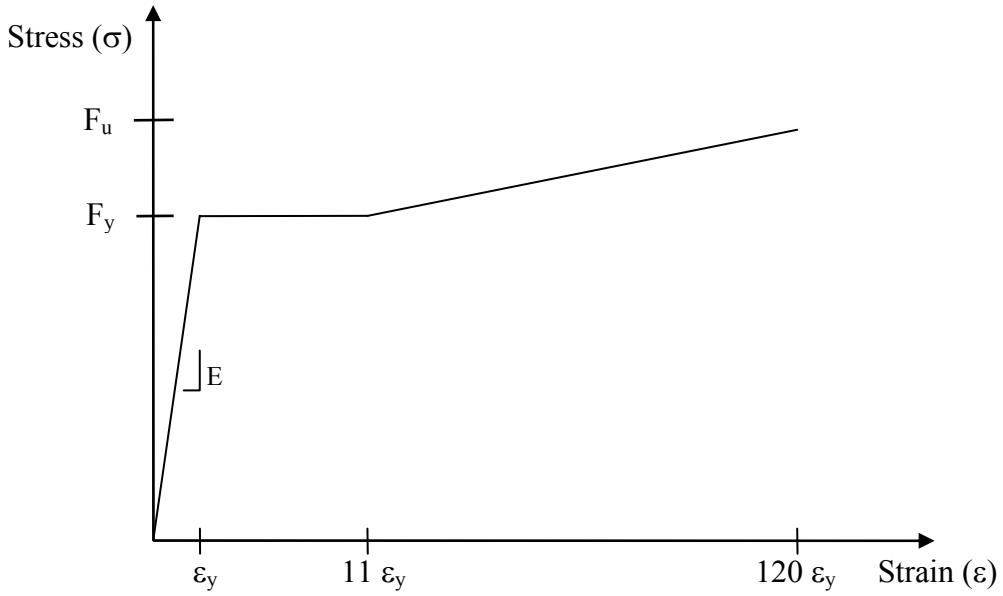

FIGURE 6.2: STRESS-STRAIN RELATIONSHIP FOR BEAM, END-PLATE AND COLUMN MATERIAL

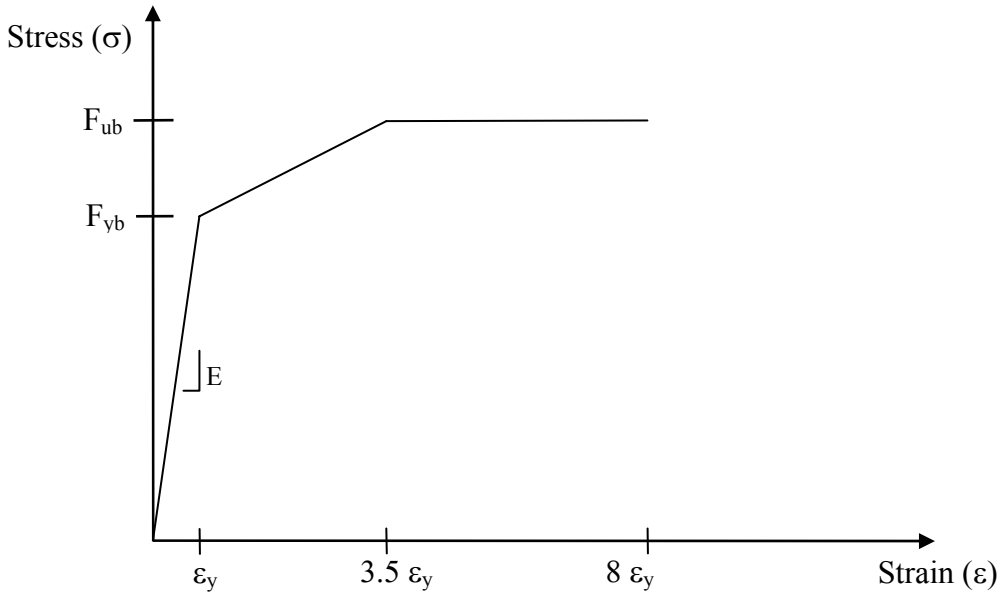

FIGURE 6.3: STRESS-STRAIN RELATIONSHIP FOR HIGH STRENGTH BOLTS

6.5 Comparison of Results

The applied moment versus end-plate and column flange separation response plots were generated from the results of the six models. The column flange yield moment was determined from the response plots. The procedure for determining the yield moment was the same previously discussed in Chapters 3 and 5. As an example of the finite element results, the response plots for unstiffened and stiffened column flange models of the four bolt connections are shown in Figures 6.4 and 6.5 respectively. The response of the unstiffened column flange is similar to elastic-plastic behavior, with little additional strength after reaching the yield moment. In contrast, the stiffened column flange response exhibits additional strength above the yield moment. This difference in response was observed for each of the connection types. The additional strength of the stiffened flange is most likely due to membrane action, which may be increased by the presence of the flange stiffeners.

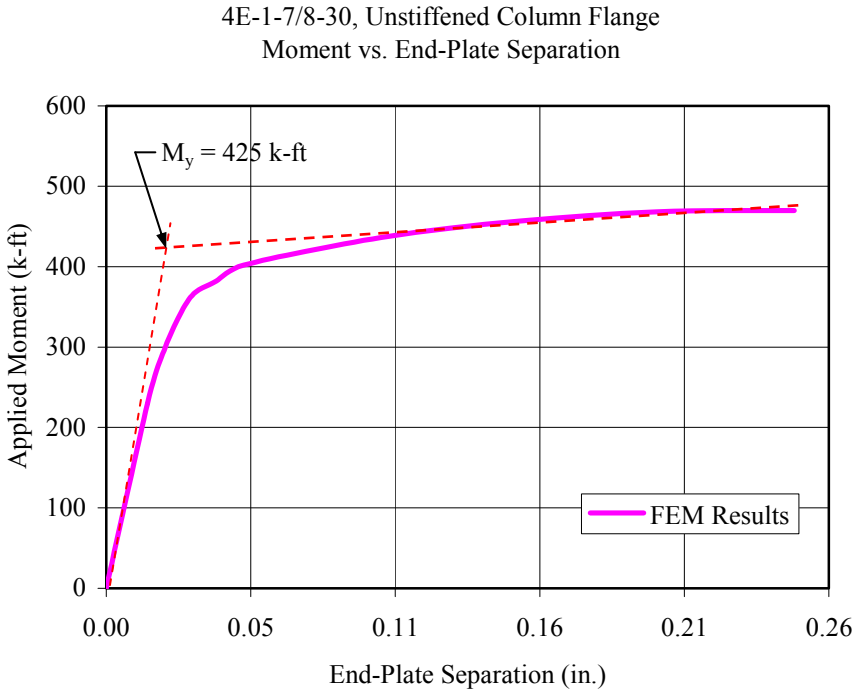

FIGURE 6.4: END-PLATE AND COLUMN FLANGE SEPARATION RESPONSE FOR THE FOUR BOLT CONNECTION, UNSTIFFENED COLUMN FLANGE

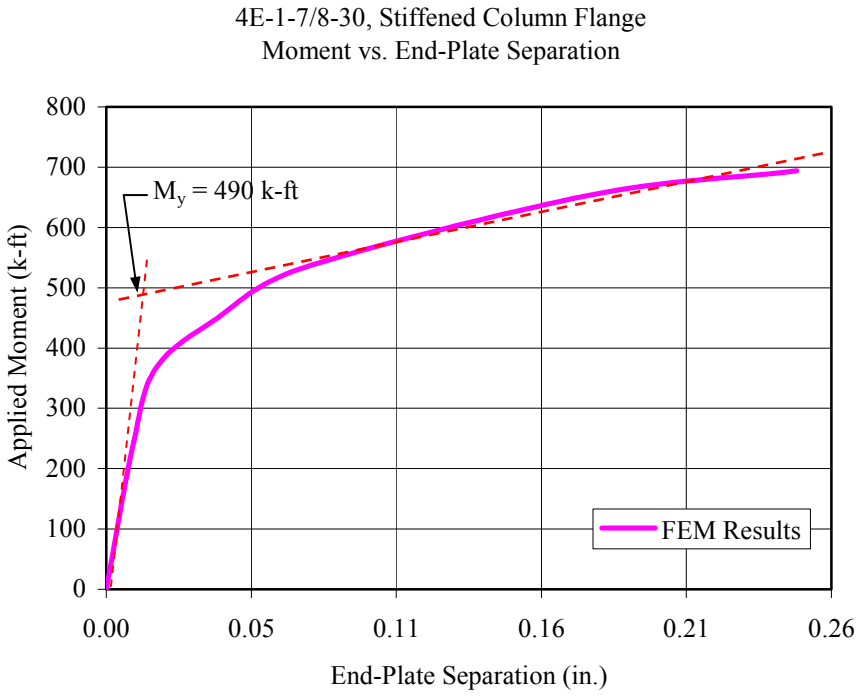

FIGURE 6.5: END-PLATE AND COLUMN FLANGE SEPARATION RESPONSE FOR THE FOUR BOLT CONNECTION, STIFFENED COLUMN FLANGE

The column flange yield moments for the six connection models are summarized in Table 6.3. The ratios of the predicted column flange bending strength to the yield moments obtained from the finite element modeling are also shown. Excellent correlation of the finite element analysis results to the proposed design method predictions exists. The strength ratios vary from 0.95 to 1.06 with an average value of 1.01 and a standard deviation of 5 percent.

TABLE 6.3: SUMMARY OF FINTE ELEMENT RESULTS

Connection ID	End-Plate Thickness (in.)	Col. Flange Thickness (in.)	Stiffened Column	Calculated M_{cf} (k-ft)	Finite Element M_y (k-ft)	Ratio M_{cf} / M_y
4E-1-7/8-30	0.875	0.625	No	402	425	0.95
	0.875	0.5	Yes	509	490	1.04
8ES-1-1-30	1	0.875	No	1011	965	1.05
	1	0.625	Yes	910	940	0.97
MRE 1/3-1-1 1/8-30	1.125	0.875	No	915	890	1.03
	1.125	0.625	Yes	856	810	1.06

6.6 Summary

Finite element models of six extended end-plate moment connections were created to investigate the column flange bending strength. The models closely followed a study presented by Mays (2000) and Sumner et al. (2000). The column flange bending response was compared to the strength predictions of the proposed design procedure. Excellent correlation of the finite element and design procedure results exists.

Chapter 7 – RECOMMENDED DETAILING AND FABRICATION PRACTICES

7.1 Introduction

One of the most important aspects of connection design that is sometimes overlooked is proper detailing of the connection elements. Proper detailing of an end-plate connection will ensure that the load path and geometric assumptions integrated into the design procedure are properly observed. Another critical aspect of end-plate connection design is the welding procedure used to install the welds that connect the end-plate to the connected beam. As observed in the 1994 Northridge earthquake, inadequate welding procedures and details used in the direct welded beam-to-column connections caused premature failure of the connection. The importance of proper weld detailing of end-plate connections is presented by Meng (1996) and Meng and Murray (1997). They observed premature beam flange fractures in end-plate connections that utilized weld access holes, sometimes called "rat holes", to install the end-plate to beam flange welds. This chapter presents end-plate connection detailing guidelines and welding procedures that are required to satisfy the load path and geometric assumptions integrated into the design procedures presented in Chapter 4.

7.2 Connection Detailing

7.2.1 Bolt Layout Dimensions

Proper selection of the bolt layout dimensions is critical part of end-plate connection design. Smaller bolt spacing will result in connections that are more economical than ones with larger bolt spacing. However, small bolt spacing can cause difficulties with fit-up and bolt tightening during erection. There are three primary dimensions that must be selected when designing end-plate moment connections; the bolt gage (g), bolt pitch to the flange (p_f), and bolt pitch to adjacent bolt row (p_b). The bolt gage and pitch distances are illustrated in Figure 7.1.

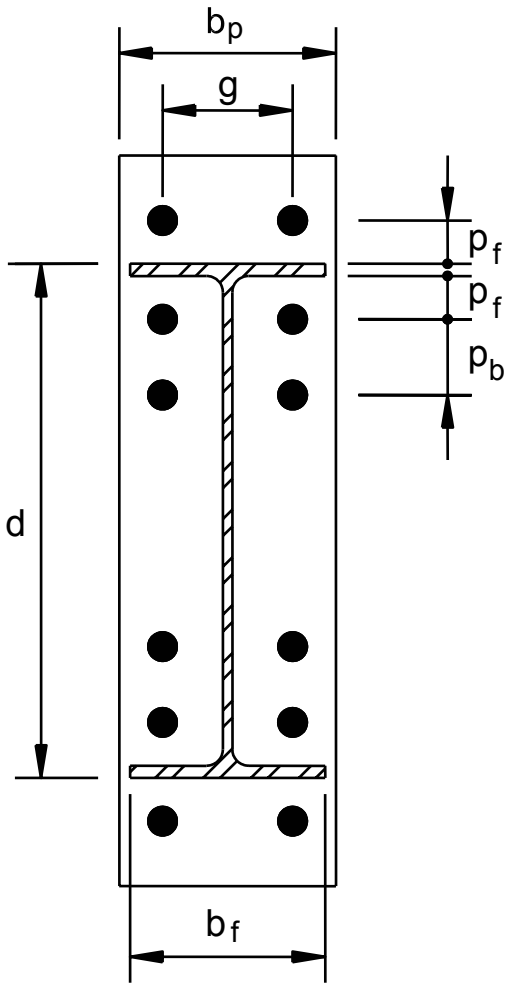

FIGURE 7.1: END-PLATE GEOMETRY (MRE 1/2)

The bolt gage should be selected to allow for adequate clearance to install and tighten the connection bolts. In addition, for beam-to column connections, the gage must be large enough for the bolts to clear the fillets between the column web and flange. The "workable gage" (minimum gage) for a connection to a column flange is tabulated along with the section properties for each hot-rolled shape in Section 1 of the *Manual of Steel Construction* (AISC, 2001). The maximum gage dimension is limited to the width of the connected beam flange. This restriction is to ensure that a favorable load path between the beam flange and the connection bolts is provided.

The pitch to flange and pitch to adjacent bolt row distances should be selected to allow for adequate clearance to install and tighten the connection bolts. The bolt pitch to the flange

distance, p_f, is the distance from the face of the flange to the centerline of the nearer bolt row. The absolute minimum pitch dimension for standard bolts is the bolt diameter plus 1/2 in. for bolts up to 1 in. diameter, and the bolt diameter plus 3/4 in. for larger diameter bolts (Murray, 1990; Murray and Shoemaker, 2002). For tension control bolts, a larger pitch to flange dimension may be required.

The bolt pitch to adjacent bolt row, p_b, is the distance from the centerline of bolt row to the adjacent bolt row. The spacing of the bolt rows should be at least 2/3 times the bolt diameter. However, a distance of 3 times the bolt diameter is preferred (AISC, 1999).

7.2.2 End-Plate Width

The width of the end-plate should be greater than or equal to the connected beam flange width. Typically, the width of the end-plate is selected by adding one inch to the beam flange width and then rounding the width up or down to the closest standard plate width. The additional end-plate width allows additional tolerance during fit-up of the end-plate and an area for welding "runoff" in the fabrication shop. In design calculations, the effective end-plate width should not be taken greater than the connected beam flange plus one inch (Murray, 1990; Murray and Shoemaker, 2002). This provision ensures that the excess end-plate material outside the beam flange width, which may not be effective, is not considered in the end-plate strength calculations.

7.2.3 End-Plate Stiffener

The four extended stiffened end-plate connections (4ES, 8ES, 8ES-4W, MRES 1/3) utilize a gusset plate welded between the connected beam flange and the end-plate to stiffen the extended portion of the end-plate. The stiffening of the end-plate increases the strength and results in a thinner end-plate when compared to an equivalent unstiffened connection. The end-plate stiffener acts like a portion of the beam web to transfer part of the beam flange tension force to the end-plate and then to the connection bolts. To ensure a favorable load path, the detailing of the stiffener geometry is very important.

Analytical and experimental studies have shown that a concentrated stress applied to an unsupported edge of a gusset plate is distributed out from that point towards the supported edge at an angle of approximately thirty degrees as shown in Figure 7.2. This force distribution model

was first presented by Whitmore (1952) and is commonly referred to as the "Whitmore Section". The same force distribution model is applied to the detailing of the end-plate stiffeners. The portion of the flange force that is transferred to the stiffener is assumed to distribute into the stiffener plate at an angle of thirty degrees. Using this model the length of the stiffener along the outside face of the beam flange can be determined using:

$$L_{stiff} = \frac{h_{st}}{tan\,30^{\circ}} \tag{7.1}$$

where h_{st} is the length of the end-plate from the outside face of the beam flange to the end of the end-plate (see Figure 7.3).

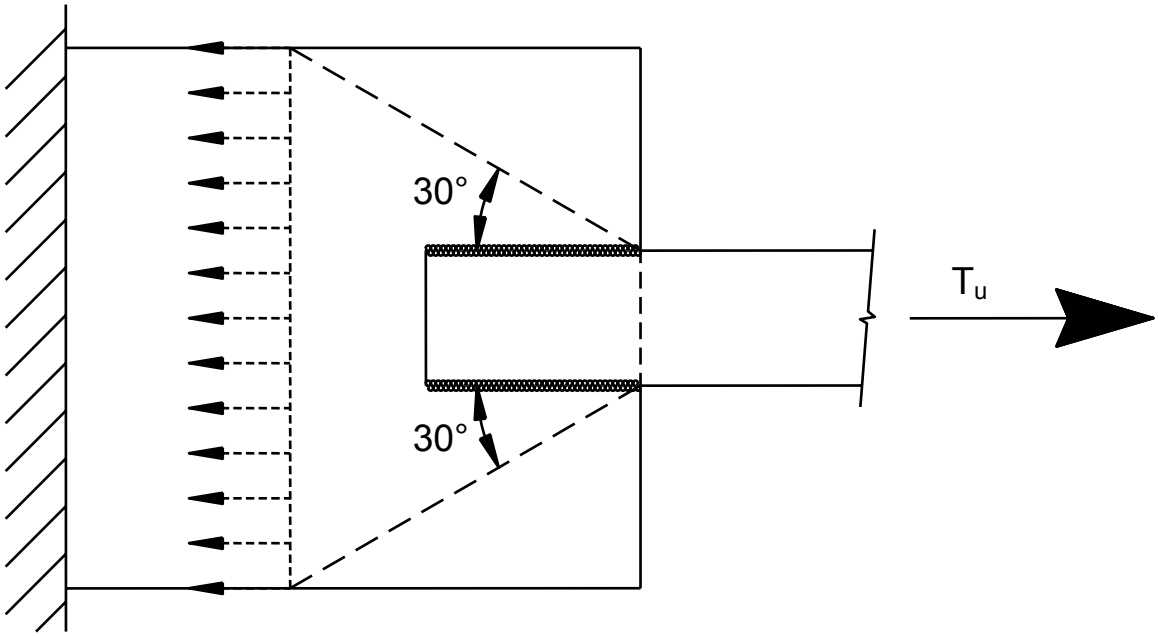

FIGURE 7.2: FORCE DISTRIBUTION INTO A GUSSET PLATE

To facilitate welding of the stiffener, the stiffener plates are terminated at the beam flange and at the end of the end-plate with landings approximately 1 in. long. The landings provide a consistent termination point for the stiffener plate and the welds. Figure 7.3 shows the landings and illustrates the layout of the end-plate stiffener geometry.

The thickness of the stiffener is another critical parameter that can have an affect on the load path. The end-plate stiffener must have adequate strength to transfer a portion of the beam flange force from the beam flange to the bolts on the extended portion of the end-plate. To provide a consistent load path through the end-plate connection, the end-plate stiffener should provide the same strength as the beam web. For a beam and end-plate stiffeners that have the same material strengths, the thickness of the stiffeners should be greater than or equal to the beam web thickness. For a beam and end-plate stiffeners with different material strengths, the thickness of the stiffener should be multiplied by the ratio of the material yield strengths.

7.2.4 Beam Length and Column Depth Tolerance

One of the concerns that arises during the fabrication and erection of structural steel moment frames utilizing end-plate moment connections is the beam length and column depth tolerances. The end-plates are welded to the beam or girder in the fabrication shop and the column flanges are drilled to match the end-plate bolt pattern. This results in a connection with very little adjustment, which can cause considerable difficulties during erection.

According to the *Code of Standard Practice for Steel Buildings and Bridges* (AISC, 2000) the allowable fabrication tolerance for the length of a beam connected on both ends is 1/16 in. for members less than 30 ft. and 1/8 in. for all others. The *Standard Specification for General Requirements for Rolled Structural Steel Bars, Plates, Shapes, and Sheet Piling, ASTM A6* (ASTM, 2001) specifies that the maximum hot-rolled section depth variation and flange out of straightness tolerances are ± 1/8 in. and ± 5/16 in. respectively for sections less than or equal 12 in. in depth (± 1/8 in. and ± 1/4 in. for section depths greater than 12 in.). The cumulative effect of these tolerances can result in many problems with connection fit-up during erection.

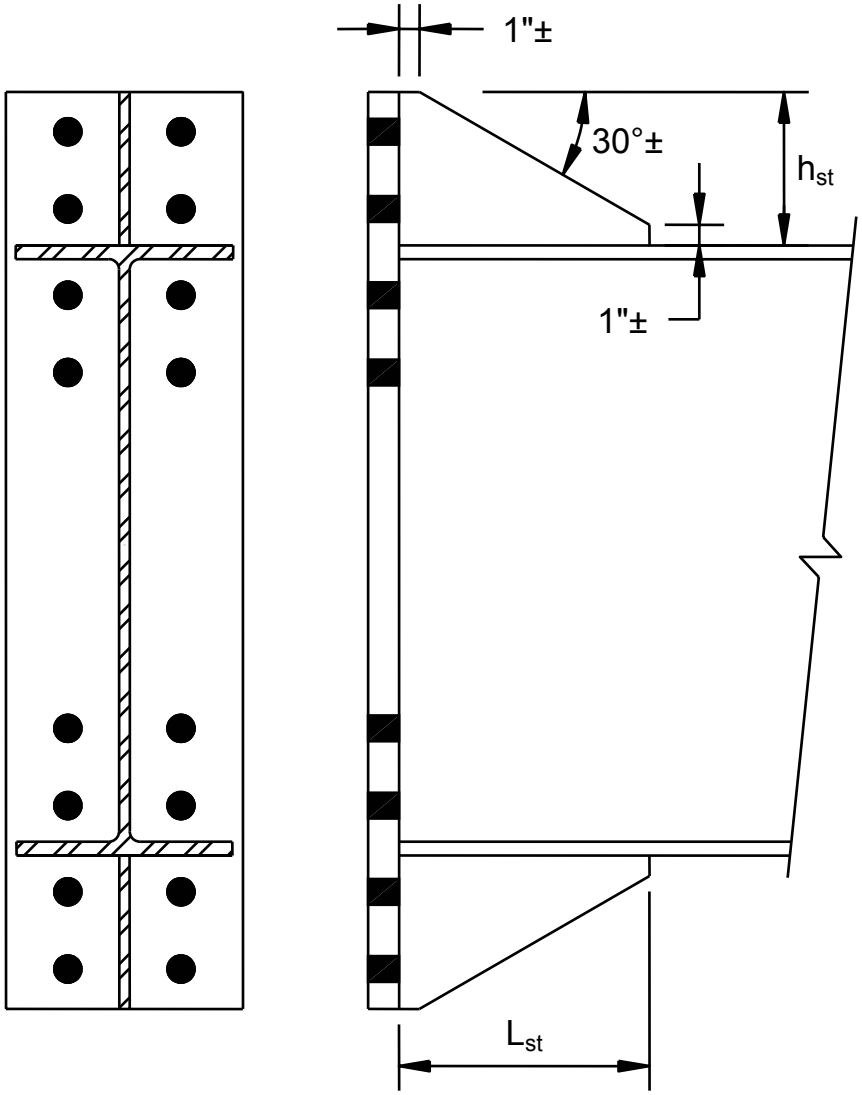

FIGURE 7.3: END-PLATE STIFFENER LAYOUT AND GEOMETRY (8ES)

The solution to the majority of the fit-up problems can be solved by following two simple steps. The beam or girder is detailed and fabricated 3/16 in. short and then any gaps between the end-plate and column flange filled using finger shims. Finger shims are thin steel plates, usually 1/16 in. thick, that are cut to match the connection bolt pattern so that they can be inserted between the column flange and the end-plate. Figure 7.4 illustrates the use of finger shims. Figure 7.5 is a photograph of a set of finger shims used in a four bolt extended end-plate connection. The finger shims can be stacked together to fill gaps larger than 1/16 in. A skewed column flange or end-plate can be corrected by inserting more shims on one side of the

connection than the other. Experimental tests, conducted as a part of this research (Sumner et al. 2000), were performed with finger shims. No adverse consequences or differences in connection behavior were observed.

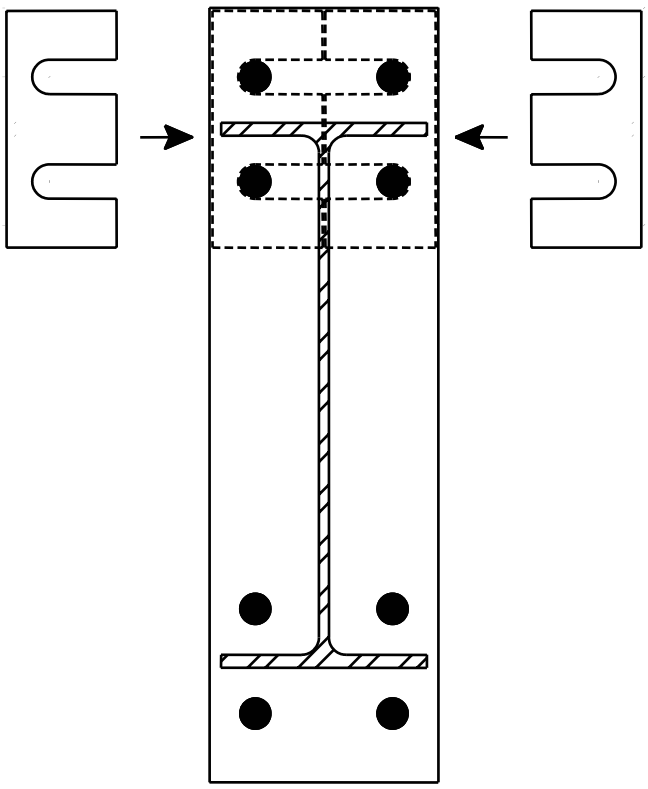

FIGURE 7.4: TYPICAL USE OF FINGER SHIMS

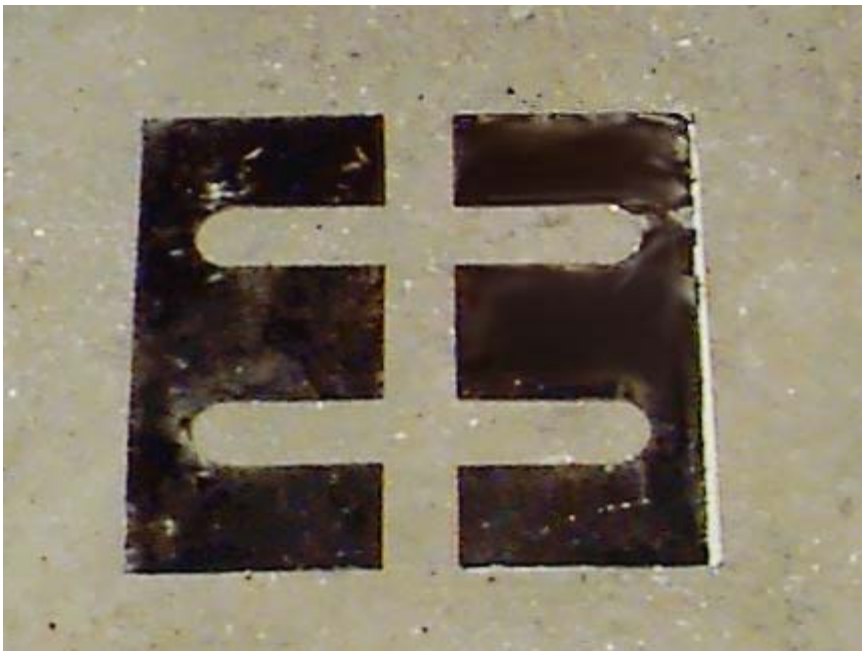

FIGURE 7.5: PHOTOGRAPH OF FINGER SHIMS

7.3 Composite Slab Detailing

The majority of multistory steel building construction today utilizes a concrete floor slab cast onto steel decking supported by steel beams and girders. The beams and girders are connected to the concrete slab using headed shear studs which make the concrete slab partially composite with the supporting steel beam or girder. This composite action greatly increases the strength of the beams and girders. Traditionally, the strength added by the composite slab is not considered in the design of the members of the seismic force resisting moment frames (FEMA 1997). The assumption has been that the composite concrete slab will crack, the concrete will crush around the column, and the strength added by the composite slab will be reduced to an insignificant level before the large inelastic deformations of the beam will occur. This philosophy has been incorporated into the current design criteria for beam-to-column moment connections which consider only the strength of the connected bare steel beams.

As observed in the cyclic end-plate connection test that included a composite slab (4E-1.25-1.375-24, see Chapter 3), it is possible for the composite slab to contribute to the strength of the connected beams during the inelastic load cycles. As a result, two different design philosophies can be considered: one that includes the strength of the slab, and one that does not

include the strength of the slab but includes detailing requirements to ensure the loss of the slab and beam composite action. In keeping with the traditional design assumptions, a design philosophy that does not include the strength of the composite slab will be discussed. Using this philosophy requires special composite slab detailing considerations in the region around the columns.

The goal of the special slab detailing requirements is to eliminate the composite action of the slab and beam in the regions of the beam where plastic hinges are expected to form. To reduce the contribution of the composite slab during the large inelastic load cycles, the slab and shear studs should be detailed as follows:

- Shear studs should not be placed along the top flange of the connecting beams for a distance, from the face of the column, one and a half times the depth of the connecting beam.

- Compressible expansion joint material, at least ½ in. thick, should be installed between the slab and the column face.

- The slab reinforcement in the area within two times the depth of the connecting beam from the face of the column should be minimized.

Even though a second composite slab test utilizing the recommended details was not conducted during the experimental investigation, it is expected that the composite shear connection between the connecting beams and the slab would be lost prior to the large inelastic load cycles. These details should allow the connection assemblies with a composite slab to exhibit a more predictable inelastic response similar to the bare steel connection assemblies.

7.4 Welding Procedures

The welding procedures outlined in this section are designed to provide welded connections between the connected beam and the end-plate that can meet the demands of inelastic cyclic loading. The detailing and fabrication requirements have been developed from

the experience of fabricators across the country and from experimental testing programs conducted at Virginia Tech over the past ten years. All welds specified in the forthcoming procedures should be made in accordance with the American Welding Society (AWS), *Structural Welding Code, AWS D1.1* (AWS, 1998). The welding electrodes used to make the welds specified in the procedures shall conform to the requirements of the *Seismic Provisions for Structural Steel Buildings* (AISC 1997, 1999b, 2000b). The specification requires that the weld filler metal have a minimum Charpy V-Notch (CVN) toughness of 20 ft-lbs at 70 degrees F. The procedures outlined in this chapter have been developed as a part of this research and are already published in the *Recommended Specifications and Quality Assurance Guidelines for Steel Moment-Frame Construction for Seismic Applications, FEMA-353* (FEMA, 2000d).

7.4.1 Beam Web to End-Plate Weld

The beam web to end-plate connection should be made using either fillet welds or complete joint penetration welds. The fillet welds should be sized to develop the full strength of the beam web in tension. If the fillet weld size becomes large, a complete joint penetration weld may be more economical. The beam web to end-plate weld should be installed before beam flange to end-plate welds. This sequence is used to avoid inducing additional stresses in the beam flange to end-plate welds due to shrinkage of the web welds.

7.4.2 Beam Flange to End-Plate Weld

The beam flange to end-plate connection should be made using a complete joint penetration groove weld. The weld should be made such that the root of the weld is on the beam web side of the flange. The flange weld is similar to the AWS prequalified TC-U4b-GF with a full depth 45-degree bevel and a minimal root opening. The root of the weld should be backed by a 5/16 in. fillet weld installed on the web side of the flange. Most important, weld access holes in the beam web should not be used. Once the 5/16 in. backing weld is installed, the root of the groove weld should be backgouged to solid weld metal and the groove weld placed. One exception to this procedure is that in the area of the flange directly above the beam web, backgouging of the root is not required. This exception is necessary because, in the area above the beam web, the backing fillet weld is not present. A summary of the welding procedure is presented in Table 7.1.

TABLE 7.1: SUMMARY OF RECOMMENDED WELDING PROCEDURE

WELDING PROCEDURE
• Prepare the flanges of the beam with a 45 degree, full depth bevel. • Fit up the end-plate and beam with a minimum root opening. • Preheat the specimens as required by AWS specifications. • Prepare the surfaces for welding as required by AWS specifications. • Install the web welds (1). • Install the 5/16 in. backing fillet welds on the beam web side of the beam flanges (2). • Backgouge the root of the bevel to remove any contaminants from the 5/16 in. backer fillet welds (3). • Install the flange groove welds (AWS TC-U4b-GF). • All welding is to be done in the down hand or flat position.
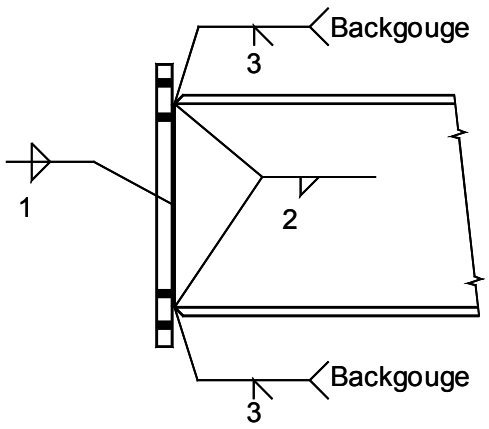

7.4.3 End-Plate Stiffener Welds

The connection of the end-plate stiffener to the outside face of the beam flange and to the face of the end-plate should be made using complete joint penetration groove welds. The complete joint penetration groove welds can be single or double bevel groove welds. A stiffener clip should be provided at the intersection of the beam flange and the end-plate to provide clearance between the stiffener and the beam flange weld.

7.5 Summary

Proper detailing and fabrication practices are two of the most important aspects of connection design. The recommended detailing and fabrication practices for end-plate moment connections subject to cyclic loading have been presented in this chapter.

Chapter 8 – SUMMARY, RECOMMENDATIONS, AND CONCLUSIONS

8.1 Summary

The primary objectives of this research were to determine the suitability of end-plate moment connections for seismic regions, to develop unified end-plate and connection bolt design procedures, to develop column flange bending design procedures, and to compare the strength predictions of the newly developed design method with the available experimental data and limited finite element analysis results. To fulfill these objectives, a research program that included an extensive literature review, experimental testing, finite element analyses, and analytical development of the design models was completed. Five extended end-plate moment connection configurations and three multiple row extended end-plate moment connection configurations were included in this study.

The first stage of the research study was an extensive literature review to identify the state of knowledge and gather the existing experimental test data. The literature review identified the need for further investigation into the possible use of end-plate moment connection in seismic regions and the need for development of unified design procedure.

The second stage of research was the experimental testing of eleven beam-to-column assemblies subjected to cyclic loading and nine beam splice end-plate moment connections subject to monotonic loading. The experimental testing showed that end-plate moment connections can be successfully designed to resist cyclic loading. The monotonic test results were used to validate the end-plate bending and bolt tension rupture limit states for two connection configurations.

The third stage of research was to develop the analytical design models for the unified design procedure. As recommended by FEMA (2000a) and AISC (1997, 1999b, 2000b, 2002), a strong column, strong connection, and weak beam design philosophy is incorporated into the design procedure. The simplified bolt force model developed by Borgsmiller (1995) was utilized to predict the onset of bolt prying forces in the connections. Yield line analysis was used to

predict the end-plate and column flange bending strengths. New yield line models were developed for some of the end-plate configurations and all of the column flange configurations.

The fourth stage of the research study was to compare the available experimental test results with the values predicted by the proposed unified design method. Ninety extended end-plate connection tests were identified and used in the comparisons. Some variability in the strength predictions was observed. The range of predicted-to-experimental design ratios varies from 0.61 to 1.34 with an average value of 0.96 and a standard deviation of 12.0 percent. With only a few exceptions, the proposed design method correctly predicted the controlling limit state. Good correlation with the experimental test results was observed.

The final stage of the research was to use three-dimensional finite element analysis to model a limited number of end-plate-to-column flange connection configurations. The ANSYS finite element code was used to develop and analyze the connection models. Investigation of the column flange bending limit state was the primary focus of the finite element study. Good correlation with the analytical predictions was observed.

Another important portion of the research study was to identify the proper detailing and fabrication practices to accompany the unified design procedure.

8.2 Analysis and Design Recommendations

8.2.1 General

The recommended analysis and design procedures presented herein are based upon the methodology and design models presented in Chapter 4. Tables 8.1 through 8.8 summarize the proposed design models and equations to determine the end-plate bending (M_{pl}) and bolt tension rupture strength (M_{np}) of the eight extended end-plate moment connection configurations (4E, 4ES, 8ES, 8E-4W, 8ES-4W, MRE 1/2, MRE 1/3, MRES 1/3). Tables 8.9 through 8.13 summarize the proposed design models and equations to determine the column flange bending strength (M_{cf}) of the five different column flange configurations. Stiffened and unstiffened cases are included for each column flange configuration. The applicable *Load and Resistance Factor Design* (LRFD) strength reduction factors, ϕ's, are integrated into the summary tables. The

standard LRFD strength reduction factors for flexural yielding ($\phi_b = 0.9$) and bolt tension rupture ($\phi = 0.75$) are utilized.

The end-plate and column flange bending strength equations presented in the summary tables have been modified slightly from the form presented in Chapter 4. The yield strength, F_y, and thickness squared, t_p^2 and t_{cf}^2, terms have been factored out of the yield line solution equations. The remaining terms represent the geometric yield line mechanism expression and are designed as Y_p for the end-plate and Y_c for the column flange.

TABLE 8.1: SUMMARY OF FOUR BOLT EXTENDED UNSTIFFENED END-PLATE DESIGN MODEL

End-Plate Geometry and Yield Line Pattern	Bolt Force Model
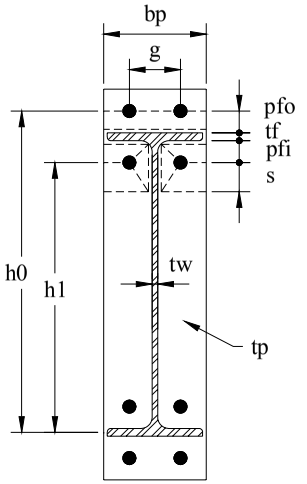	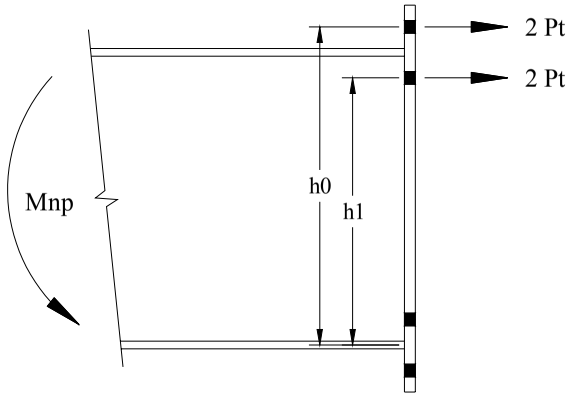

End-Plate	$\phi M_{pl} = \phi_b F_{yp} t_p^2 Y_p$ $Y_p = \frac{b_p}{2}\left[h_1\left(\frac{1}{p_{fi}} + \frac{1}{s}\right) + h_0\left(\frac{1}{p_{fo}}\right) - \frac{1}{2}\right] + \frac{2}{g}\left[h_1\left(p_{fi} + s\right)\right]$ $s = \frac{1}{2}\sqrt{b_p\, g}$ $\quad \phi_b = 0.90$ $\quad$ Note: If $p_{fi} > s$, use $p_{fi} = s$
Bolt Rupture	$\phi M_{np} = \phi\, 2\, P_t \left(h_o + h_1\right)$ $\quad \phi = 0.75$

TABLE 8.2: SUMMARY OF FOUR BOLT EXTENDED STIFFENED END-PLATE DESIGN MODEL

<table>
<tr><th colspan="2">End-Plate Geometry and Yield Line Pattern</th><th>Bolt Force Model</th></tr>
<tr><td>Case 1 ($d_e \leq s$)</td><td>Case 2 ($d_e > s$)</td><td rowspan="2"></td></tr>
<tr><td> 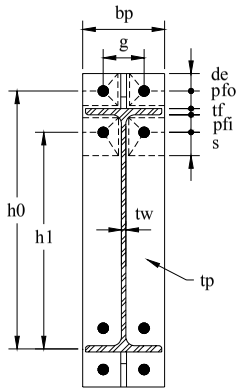
</td><td> 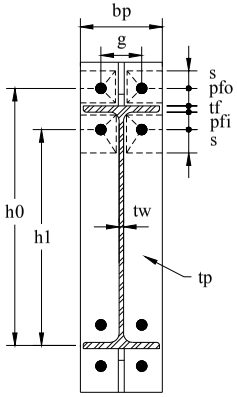
</td></tr>
<tr><td>End-Plate</td><td colspan="2">$\phi M_{pl} = \phi_b F_{yp} t_p^2 Y_p$
Case 1 ($d_e < s$)
$Y_p = \frac{b_p}{2}\left[h_1\left(\frac{1}{p_{fi}}+\frac{1}{s}\right)+h_0\left(\frac{1}{s}+\frac{1}{p_{fo}}\right)\right]+\frac{2}{g}\left[h_1\left(p_{fi}+s\right)+h_0\left(s+p_{fo}\right)\right]$
Case 2 ($d_e > s$)
$Y_{p\backslash} = \frac{b_p}{2}\left[h_1\left(\frac{1}{p_{fi}}+\frac{1}{s}\right)+h_0\left(\frac{1}{p_{fo}}+\frac{1}{2s}\right)\right]+\frac{2}{g}\left[h_1(p_{fi}+s)+h_0(d_e+p_{fo})\right]$
$s = \frac{1}{2}\sqrt{b_p\, g}$ $\phi_b = 0.90$ Note: If $p_{fi} > s$, use $p_{fi} = s$</td></tr>
<tr><td>Bolt Rupture</td><td colspan="2">$\phi M_{np} = \phi\, 2\, P_t\,(h_o + h_1)$ $\phi = 0.75$</td></tr>
</table>

TABLE 8.3: SUMMARY OF EIGHT BOLT EXTENDED STIFFENED END-PLATE DESIGN MODEL

<table>
<tr><th colspan="2">End-Plate Geometry and Yield Line Pattern</th><th>Bolt Force Model</th></tr>
<tr><td>Case 1 ($d_e \leq s$)</td><td>Case 2 ($d_e > s$)</td><td rowspan="2"></td></tr>
<tr><td> 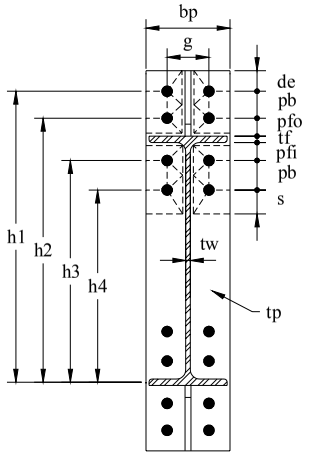
</td><td> 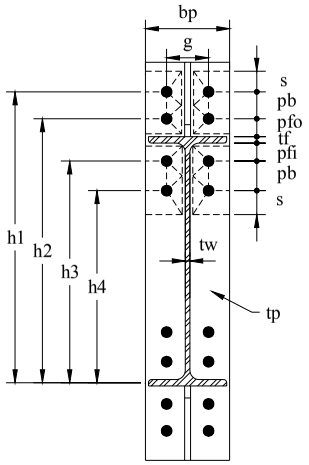
</td></tr>
<tr><td>End-Plate</td><td colspan="2">$\phi M_{pl} = \phi_b F_{yp} t_p^2 Y_p$
Case 1 ($d_e < s$)
$Y_p = \frac{b_p}{2}\left[h_1\left(\frac{1}{2d_e}\right)+h_2\left(\frac{1}{p_{fo}}\right)+h_3\left(\frac{1}{p_{fi}}\right)+h_4\left(\frac{1}{s}\right)\right]+\frac{2}{g}\left[h_1\left(d_e+\frac{p_b}{4}\right)+h_2\left(p_{fo}+\frac{3p_b}{4}\right)+h_3\left(p_{f,i}+\frac{p_b}{4}\right)+h_4\left(s+\frac{3p_b}{4}\right)+p_b^2\right]+g$
Case 2 ($d_e > s$)
$Y_p = \frac{b_p}{2}\left[h_1\left(\frac{1}{s}\right)+h_2\left(\frac{1}{p_{fo}}\right)+h_3\left(\frac{1}{p_{fi}}\right)+h_4\left(\frac{1}{s}\right)\right]+\frac{2}{g}\left[h_1\left(s+\frac{p_b}{4}\right)+h_2\left(p_{fo}+\frac{3p_b}{4}\right)+h_3\left(p_{fi}+\frac{p_b}{4}\right)+h_4\left(s+\frac{3p_b}{4}\right)+p_b^2\right]+g$
$s = \frac{1}{2}\sqrt{b_p\, g}$ $\quad \phi_b = 0.90$ $\quad$ Note: If $p_{fi} > s$, use $p_{fi} = s$</td></tr>
<tr><td>Bolt Rupture</td><td colspan="2">$\phi M_{np} = \phi\, 2\, P_t\,(h_o + h_1 + h_2)$ $\quad \phi = 0.75$</td></tr>
</table>

TABLE 8.4: SUMMARY OF EIGHT BOLT, FOUR BOLTS WIDE, EXTENDED UNSTIFFENED END-PLATE DESIGN MODEL

End-Plate Geometry and Yield Line Pattern	Bolt Force Model
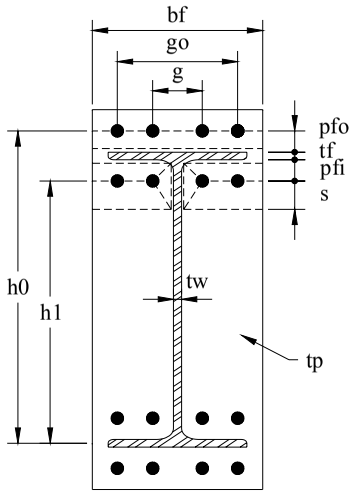	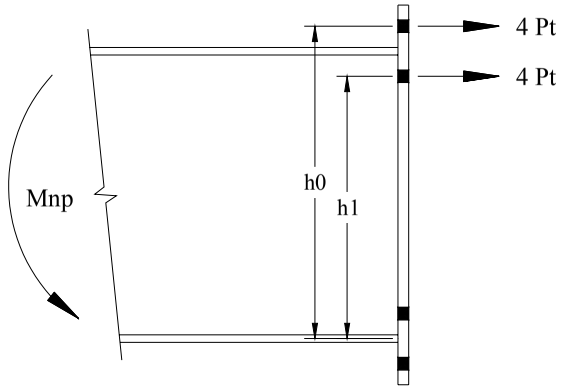

End-Plate	$\phi M_{pl} = \phi_b F_{yp} t_p^2 Y_p$ $Y_p = \frac{b_p}{2}\left[h_1\left(\frac{1}{p_{fi}} + \frac{1}{s}\right) + h_0\left(\frac{1}{p_{fo}}\right) - \frac{1}{2}\right] + \frac{2}{g}\left[h_1\left(p_{fi} + s\right)\right]$ $s = \frac{1}{2}\sqrt{b_p\, g}$ $\quad \phi_b = 0.90$ $\quad$ Note: If $p_{fi} > s$, use $p_{fi} = s$
Bolt Rupture	$\phi M_{np} = \phi\, 4\, P_t \left(h_o + h_1\right)$ $\quad \phi = 0.75$

TABLE 8.5: SUMMARY OF EIGHT BOLT, FOUR BOLTS WIDE, EXTENDED STIFFENED END-PLATE DESIGN MODEL

<table>
<tr><td colspan="2">End-Plate Geometry and Yield Line Pattern</td><td>Bolt Force Model</td></tr>
<tr><td>Case 1 ($d_e \leq s$)</td><td>Case 2 ($d_e > s$)</td><td rowspan="2"></td></tr>
<tr><td> 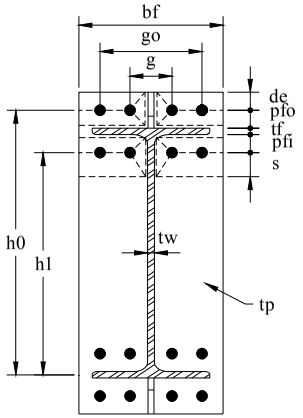
</td><td> 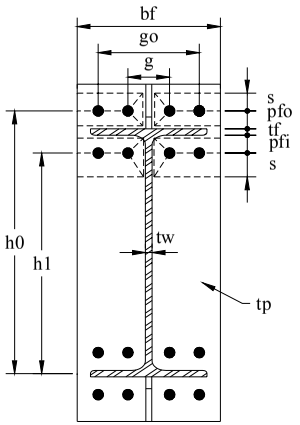
</td></tr>
<tr><td>End-Plate</td><td colspan="2">$\phi M_{pl} = \phi_b F_{yp} t_p^2 Y_p$
Case 1 ($d_e < s$)
$Y_p = \frac{b_p}{2}\left[h_1\left(\frac{1}{p_{fi}}+\frac{1}{s}\right)+h_0\left(\frac{1}{s}+\frac{1}{p_{fo}}\right)\right]+\frac{2}{g}\left[h_1\left(p_{fi}+s\right)+h_0\left(s+p_{fo}\right)\right]$
Case 2 ($d_e > s$)
$Y_p = \frac{b_p}{2}\left[h_1\left(\frac{1}{p_{fi}}+\frac{1}{s}\right)+h_0\left(\frac{1}{p_{fo}}+\frac{1}{2s}\right)\right]+\frac{2}{g}\left[h_1(p_{fi}+s)+h_0(d_e+p_{fo})\right]$
$s = \frac{1}{2}\sqrt{b_p\, g}$ $\phi_b = 0.90$ Note: If $p_{fi} > s$, use $p_{fi} = s$</td></tr>
<tr><td>Bolt Rupture</td><td colspan="2">$\phi M_{np} = \phi 4 P_t \left(h_o + h_1\right)$ $\phi = 0.75$</td></tr>
</table>

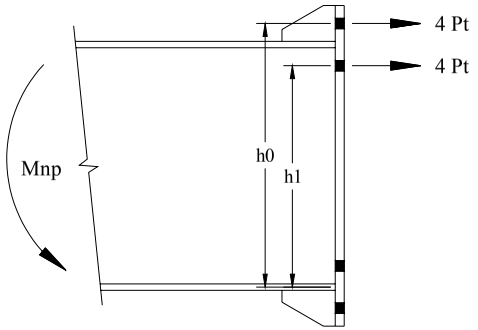

TABLE 8.6: SUMMARY OF MULTIPLE ROW EXTENDED 1/2 UNSTIFFENED END-PLATE DESIGN MODEL

End-Plate Geometry and Yield Line Pattern	Bolt Force Model
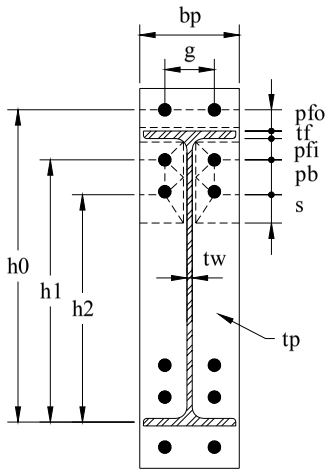	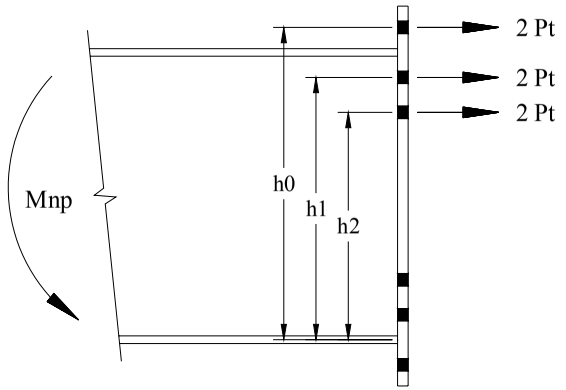

End-Plate	$\phi M_{pl} = \phi_b F_{yp} t_p^2 Y_p$ $Y_p = \frac{b_p}{2}\left[h_1\left(\frac{1}{p_{fi}}\right) + h_2\left(\frac{1}{s}\right) + h_0\left(\frac{1}{p_{fo}}\right) - \frac{1}{2}\right] + \frac{2}{g}\left[h_1\left(p_{fi} + \frac{3p_b}{4}\right) + h_2\left(s + \frac{p_b}{4}\right)\right] + \frac{g}{2}$ $s = \frac{1}{2}\sqrt{b_p\, g}$ $\quad \phi_b = 0.90$ $\quad$ Note: If $p_{fi} > s$, use $p_{fi} = s$
Bolt Rupture	$\phi M_{np} = \phi\, 2\, P_t \left(h_o + h_1 + h_2\right)$ $\quad \phi = 0.75$

TABLE 8.7: SUMMARY OF MULTIPLE ROW EXTENDED 1/3 UNSTIFFENED END-PLATE DESIGN MODEL

End-Plate Geometry and Yield Line Pattern	Bolt Force Model
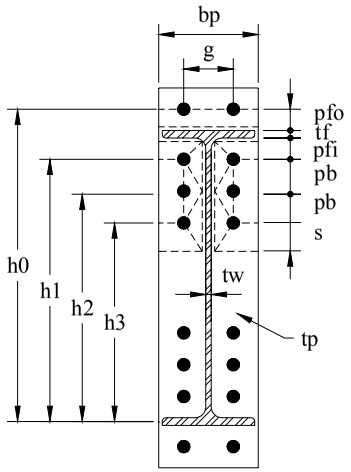	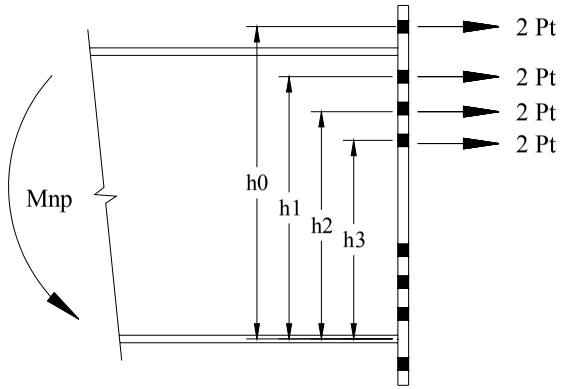

End-Plate	$\phi M_{pl} = \phi_b F_{yp} t_p^2 Y_p$ $Y_p = \frac{b_p}{2}\left[h_1\left(\frac{1}{p_{fi}}\right) + h_3\left(\frac{1}{s}\right) + h_0\left(\frac{1}{p_{fo}}\right) - \frac{1}{2}\right] + \frac{2}{g}\left[h_1\left(p_{fi} + \frac{3p_b}{2}\right) + h_3\left(s + \frac{p_b}{2}\right)\right] + \frac{g}{2}$ $s = \frac{1}{2}\sqrt{b_p\, g}$ $\quad \phi_b = 0.90$ $\quad$ Note: If $p_{fi} > s$, use $p_{fi} = s$
Bolt Rupture	$\phi M_{np} = \phi\, 2\, P_t \left(h_o + h_1 + h_2 + h_3\right)$ $\quad \phi = 0.75$

TABLE 8.8: SUMMARY OF MULTIPLE ROW EXTENDED 1/3 STIFFENED END-PLATE DESIGN MODEL

<table>
<tr><th colspan="2">End-Plate Geometry and Yield Line Pattern</th><th>Bolt Force Model</th></tr>
<tr><td>Case 1 ($d_e \leq s$)</td><td>Case 2 ($d_e > s$)</td><td rowspan="2"></td></tr>
<tr><td> 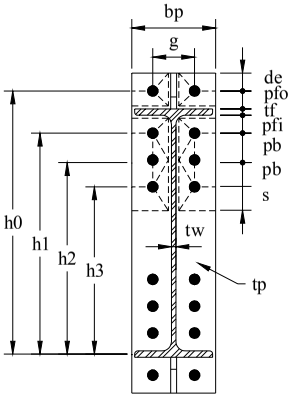
</td><td> 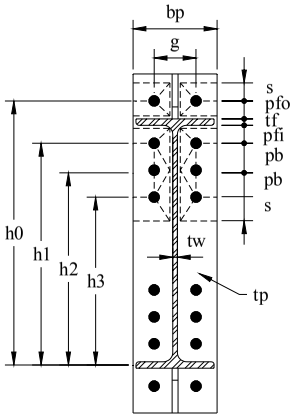
</td></tr>
<tr><td colspan="3"> 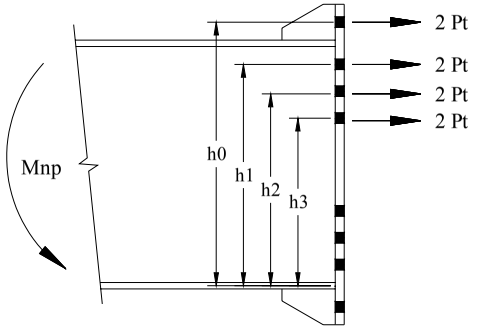
</td></tr>
<tr><td>End-Plate</td><td colspan="2">$\phi M_{pl} = \phi_b F_{yp} t_p^2 Y_p$
Case 1 ($d_e < s$)
$Y_p = \frac{b_p}{2}\left[h_1\left(\frac{1}{p_{fi}}\right) + h_3\left(\frac{1}{s}\right) + h_0\left(\frac{1}{p_{fo}} + \frac{1}{2s}\right)\right] + \frac{2}{g}\left[h_1\left(p_{fi} + \frac{3p_b}{2}\right) + h_3\left(s + \frac{p_b}{2}\right) + h_0\left(d_e + p_{fo}\right)\right] + \frac{g}{2}$
Case 2 ($d_e > s$)
$Y_p = \frac{b_p}{2}\left[h_1\left(\frac{1}{p_{fi}}\right) + h_3\left(\frac{1}{s}\right) + h_0\left(\frac{1}{p_{fo}} + \frac{1}{s}\right)\right] + \frac{2}{g}\left[h_1\left(p_{fi} + \frac{3p_b}{2}\right) + h_3\left(s + \frac{p_b}{2}\right) + h_0\left(s + p_{fo}\right)\right] + \frac{g}{2}$
$s = \frac{1}{2}\sqrt{b_p\, g}$ $\phi_b = 0.90$ Note: If $p_{fi} > s$, use $p_{fi} = s$</td></tr>
<tr><td>Bolt Rupture</td><td colspan="2">$\phi M_{np} = \phi\, 2\, P_t \left(h_o + h_1 + h_2 + h_3\right)$ $\phi = 0.75$</td></tr>
</table>

TABLE 8.9: SUMMARY OF FOUR BOLT EXTENDED COLUMN FLANGE DESIGN MODEL

Unstiffened Column Flange Geometry and Yield Line Pattern	Stiffened Column Flange Geometry and Yield Line Pattern
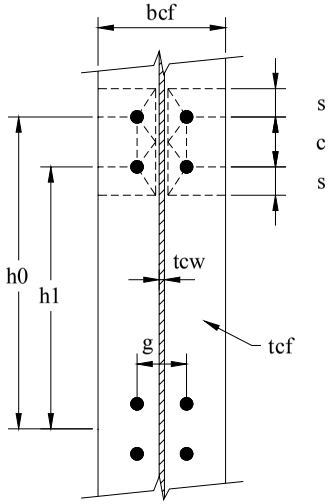	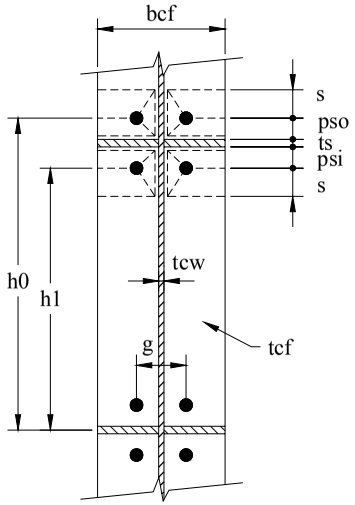

Unstiffened Column Flange

$$\phi M_{cf} = \phi_b F_{yc} t_{cf}^2 Y_c$$

$$Y_c = \frac{b_{cf}}{2}\left[h_1\left(\frac{1}{s}\right) + h_0\left(\frac{1}{s}\right)\right] + \frac{2}{g}\left[h_1\left(s + \frac{3c}{4}\right) + h_0\left(s + \frac{c}{4}\right) + \frac{c^2}{2}\right] + \frac{g}{2}$$

$$s = \frac{1}{2}\sqrt{b_{cf}\, g} \qquad \phi_b = 0.90$$

Stiffened Column Flange

$$\phi M_{cf} = \phi_b F_{yc} t_{cf}^2 Y_c$$

$$Y_c = \frac{b_{cf}}{2}\left[h_1\left(\frac{1}{s} + \frac{1}{p_{si}}\right) + h_0\left(\frac{1}{s} + \frac{1}{p_{so}}\right)\right] + \frac{2}{g}\left[h_1\left(s + p_{si}\right) + h_0\left(s + p_{so}\right)\right]$$

$$s = \frac{1}{2}\sqrt{b_{cf}\, g} \qquad \phi_b = 0.90$$

TABLE 8.10: SUMMARY OF EIGHT BOLT EXTENDED STIFFENED COLUMN FLANGE DESIGN MODEL

Unstiffened Column Flange Geometry and Yield Line Pattern	Stiffened Column Flange Geometry and Yield Line Pattern
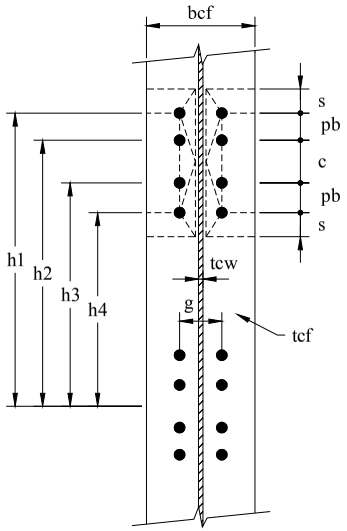	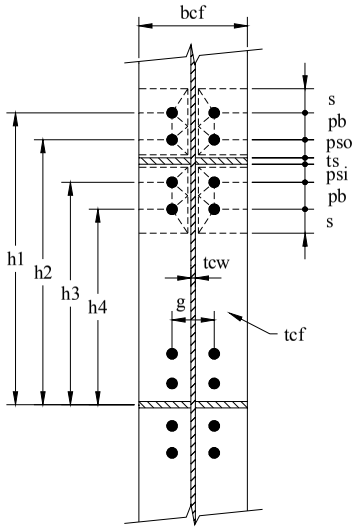

Unstiffened Column Flange	$\phi M_{cf} = \phi_b F_{yc} t_{cf}^2 Y_c$ $Y_c = \frac{b_{cf}}{2}\left[h_1\left(\frac{1}{s}\right)+h_4\left(\frac{1}{s}\right)\right]+\frac{2}{g}\left[h_1\left(p_b+\frac{c}{2}+s\right)+h_2\left(\frac{p_b}{2}+\frac{c}{4}\right)+h_3\left(\frac{p_b}{2}+\frac{c}{2}\right)+h_4(s)\right]+\frac{g}{2}$ $s = \frac{1}{2}\sqrt{b_{cf}\, g}$ $\qquad \phi_b = 0.90$
Stiffened Column Flange	$\phi M_{cf} = \phi_b F_{yc} t_{cf}^2 Y_c$ $Y_c = \frac{b_{cf}}{2}\left[h_1\left(\frac{1}{s}\right)+h_2\left(\frac{1}{p_{so}}\right)+h_3\left(\frac{1}{p_{si}}\right)+h_4\left(\frac{1}{s}\right)\right]+\frac{2}{g}\left[h_1\left(s+\frac{p_b}{4}\right)+h_2\left(p_{so}+\frac{3p_b}{4}\right)+h_3\left(p_{si}+\frac{p_b}{4}\right)+h_4\left(s+\frac{3p_b}{4}\right)+p_b^2\right]+g$ $s = \frac{1}{2}\sqrt{b_{cf}\, g}$ $\qquad \phi_b = 0.90$

TABLE 8.11: SUMMARY OF EIGHT BOLT, FOUR BOLTS WIDE EXTENDED COLUMN FLANGE DESIGN MODEL

Unstiffened Column Flange Geometry and Yield Line Pattern	Stiffened Column Flange Geometry and Yield Line Pattern
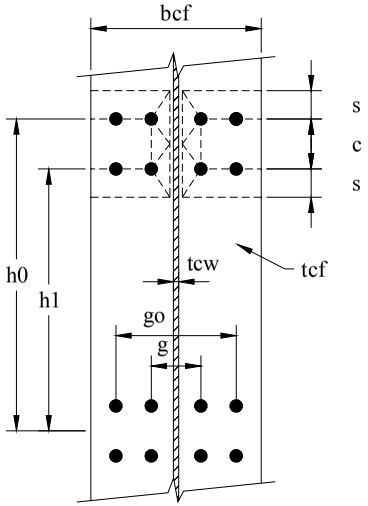	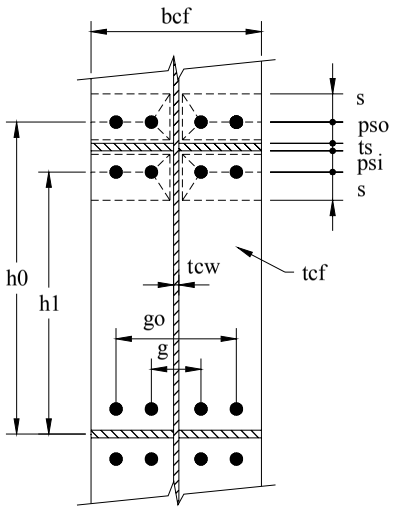

Unstiffened Column Flange	$\phi M_{cf} = \phi_b F_{yc} t_{cf}^2 Y_c$ $Y_c = \frac{b_{cf}}{2}\left[h_1\left(\frac{1}{s}\right)+h_0\left(\frac{1}{s}\right)\right]+\frac{2}{g}\left[h_1\left(s+\frac{3c}{4}\right)+h_0\left(s+\frac{c}{4}\right)+\frac{c^2}{2}\right]+\frac{g}{2}$ $s = \frac{1}{2}\sqrt{b_{cf}\, g}$ $\qquad \phi_b = 0.90$
Stiffened Column Flange	$\phi M_{cf} = \phi_b F_{yc} t_{cf}^2 Y_c$ $Y_c = \frac{b_{cf}}{2}\left[h_1\left(\frac{1}{s}+\frac{1}{p_{si}}\right)+h_0\left(\frac{1}{s}+\frac{1}{p_{so}}\right)\right]+\frac{2}{g}\left[h_1(s+p_{si})+h_0(s+p_{so})\right]$ $s = \frac{1}{2}\sqrt{b_{cf}\, g}$ $\qquad \phi_b = 0.90$

TABLE 8.12: SUMMARY OF MULTIPLE ROW EXTENDED 1/2 COLUMN FLANGE DESIGN MODEL

Unstiffened Column Flange Geometry and Yield Line Pattern	Stiffened Column Flange Geometry and Yield Line Pattern
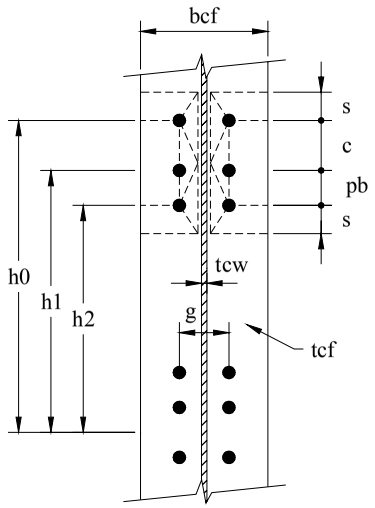	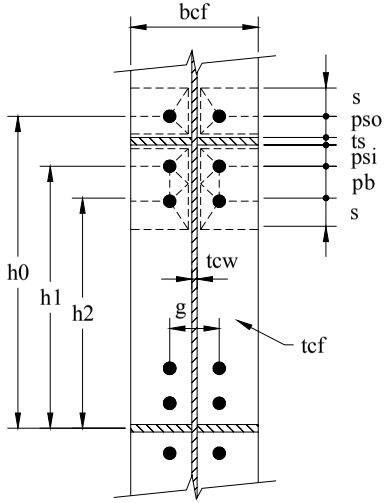

Unstiffened Column Flange	$\phi M_{cf} = \phi_b F_{yc} t_{cf}^2 Y_c$ $Y_c = \frac{b_{cf}}{2}\left[h_0\left(\frac{1}{s}\right)+h_2\left(\frac{1}{s}\right)\right]+\frac{2}{g}\left[h_0(s+c)+h_1(p_b)+h_2(s)\right]+\frac{g}{2}$ $s = \frac{1}{2}\sqrt{b_{cf}\, g}$ $\qquad \phi_b = 0.90$
Stiffened Column Flange	$\phi M_{cf} = \phi_b F_{yc} t_{cf}^2 Y_c$ $Y_c = \frac{b_{cf}}{2}\left[h_1\left(\frac{1}{p_{si}}\right)+h_2\left(\frac{1}{s}\right)+h_0\left(\frac{1}{p_{so}}+\frac{1}{s}\right)\right]+\frac{2}{g}\left[h_1\left(p_{si}+\frac{3p_b}{4}\right)+h_2\left(s+\frac{p_b}{4}\right)+h_0(s+p_{so})\right]+\frac{g}{2}$ $s = \frac{1}{2}\sqrt{b_{cf}\, g}$ $\qquad \phi_b = 0.90$

TABLE 8.13: SUMMARY OF MULTIPLE ROW EXTENDED 1/3 COLUMN FLANGE DESIGN MODEL

Unstiffened Column Flange Geometry and Yield Line Pattern	Stiffened Column Flange Geometry and Yield Line Pattern
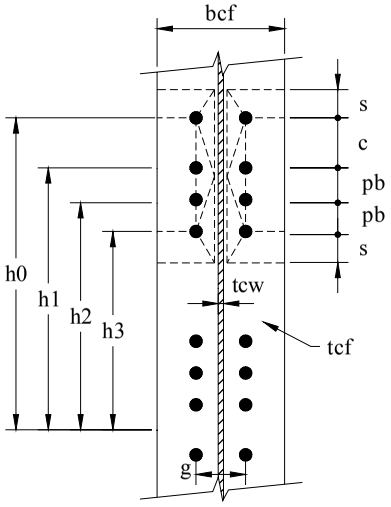	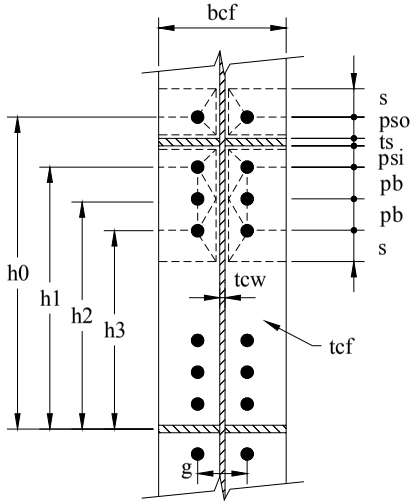

Unstiffened Column Flange	$\phi M_{cf} = \phi_b F_{yc} t_{cf}^2 Y_c$ $Y_c = \frac{b_{cf}}{2}\left[h_0\left(\frac{1}{s}\right)+h_3\left(\frac{1}{s}\right)\right]+\frac{2}{g}\left[h_0\left(\frac{p_b}{2}+c+s\right)+h_1\left(\frac{3p_b}{4}\right)+h_2\left(\frac{3p_b}{4}\right)+h_3(s)\right]+\frac{g}{2}$ $s = \frac{1}{2}\sqrt{b_{cf}\, g}$ $\qquad \phi_b = 0.90$
Stiffened Column Flange	$\phi M_{cf} = \phi_b F_{yc} t_{cf}^2 Y_c$ $Y_c = \frac{b_{cf}}{2}\left[h_1\left(\frac{1}{p_{si}}\right)+h_3\left(\frac{1}{s}\right)+h_0\left(\frac{1}{p_{so}}+\frac{1}{s}\right)\right]+\frac{2}{g}\left[h_1\left(p_{si}+\frac{3p_b}{2}\right)+h_3\left(s+\frac{p_b}{2}\right)+h_0(s+p_{so})\right]+\frac{g}{2}$ $s = \frac{1}{2}\sqrt{b_{cf}\, g}$ $\qquad \phi_b = 0.90$

8.2.2 Design Procedure

To design an end-plate connection using the proposed design provisions, the following procedure is used.

a) Determine the sizes of the connected members (beams and column) and compute the moment at the face of the column, M_{fc}. The ultimate factored moment at the connection, M_u, is then determined by multiplying the moment at the face of the column, M_{fc}, by the appropriate *LRFD* load factor.

$$M_u = (Load\ Factor) \times M_{fc} \tag{8.1}$$

$$M_{fc} = M_{pe} + V_p\left(\frac{d}{2}\right) \qquad for\ unstiffened\ connections \tag{8.2}$$

$$M_{fc} = M_{pe} + V_p\left(L_{st} + t_p\right) \qquad for\ stiffened\ connections \tag{8.3}$$

where:

$$M_{pe} = R_y\left(\frac{F_y + F_u}{2}\right)Z_x \tag{8.4}$$

b) Select one of the eight end-plate moment connection configurations and establish preliminary values for the connection geometry (g, p_{fi}, p_{fo}, p_b, etc.).

c) Set the factored moment at the face of the column, M_u, equal to the no prying bolt strength moment, M_{np}, and solve for the required bolt diameter. This results in the following expression.

$$d_{b\ \text{Req'd}} = \sqrt{\frac{n_b\ M_u}{\pi\ \phi\ F_t\left(\sum h_n\right)}} \tag{8.5}$$

where n_b is the number of bolts per row, $\phi = 0.75$, F_t is the specified *LRFD* bolt tensile strength (90 ksi for A325 bolts and 113 ksi for A490 bolts), and h_n is the distance from the centerline of the beam compression flange to the centerline of the n^{th} tension bolt row.

d) Select a trial bolt diameter and grade and calculate the no prying bolt moment strength, M_{np}, using the appropriate equation from the summary tables (Tables 8.1 to 8.8).

e) Set the end-plate, M_{pl}, and column flange bending, M_{cf}, strengths equal to 1.1 times the no prying bolt moment and solve for the required end-plate and column flange thicknesses. This results in the following expressions.

$$t_{p\ \text{Req'd}} = \sqrt{\frac{1.1\phi M_{np}}{\phi_b F_{yp} Y_p}} \tag{8.6}$$

$$t_{cf\ \text{Req'd}} = \sqrt{\frac{1.1\phi M_{np}}{\phi_b F_{yc} Y_c}} \tag{8.7}$$

where $\phi_b = 0.9$, F_{yp} is the end-plate material yield strength, F_{yc} is the column flange material yield strength, Y_p is the end-plate yield line mechanism parameter, and Y_c is the column flange yield line mechanism parameter.

f) Select an end-plate and column flange thickness greater than the required values.

8.2.3 Analysis Procedure

To analyze an end-plate moment connection and determine the design strength, ϕM_n, the following procedure is used.

a) Calculate the end-plate bending strength, $\phi_b M_{pl}$, column flange bending strength, $\phi_b M_{cf}$, and the no-prying bolt tension rupture strength, ϕM_{np}, using the equations presented in the summary tables (Tables 8.1 through 8.13).

b) Determine the behavior, 'thick' or 'thin', of the end-plate and column flange using the following.

If $M_{pl} \geq 1.1\ M_{np}$ → *Thick plate* If $M_{pl} < 1.1\ M_{np}$ → *Thin plate*

If $M_{cf} \geq 1.1\ M_{np}$ → *Thick flange* If $M_{cf} < 1.1\ M_{np}$ → *Thin flange*

c) If the end-plate and the column flange are exhibiting thick plate behavior, then the connection design strength, ϕM_n, is equal to the no prying bolt strength, ϕM_{np}.

d) If the end-plate and/or the column flange are exhibiting thin plate behavior, then the connection does not comply with the requirements of the proposed design procedure. The connection strength can not be calculated using the procedures outline herein because an additional limit state, bolt rupture with prying, is induced by the thin plate behavior.

e) The adequacy of the analyzed connection can then be determined by comparing the calculated design strength, ϕM_n, to the factored moment at the face of the column M_{fc}. The moment at the face of the column is multiplied by the applicable *LRFD* load factor and calculated using the following.

$$M_{fc} = M_{pe} + V_p\left(\frac{d}{2}\right) \qquad \textit{for unstiffened connections} \qquad (8.8)$$

$$M_{fc} = M_{pe} + V_p\left(L_{st} + t_p\right) \qquad \textit{for stiffened connections} \qquad (8.9)$$

8.3 Conclusions

Based upon the experimental and analytical research conducted as a part of the study, the primary conclusions can be summarized as follows:

- Extended End-plate moment connections can be designed and detailed to be suitable for use in seismic force resisting moment frames. A strong column, strong connection and weak beam philosophy should be utilized to force the connecting beam to provide the required inelastic deformations through formation of a plastic hinge. Experimental testing conducted as a part of this research shows that the four bolt extended unstiffened and the eight bolt extended stiffened end-plate moment connections can provide the

required strength, stiffness and ductility required for use in seismic regions. The six other end-plate connection configuration should also be capable of providing the necessary strength, stiffness, and ductility, but additional experimental testing is recommended;

- The moment used to design the extended end-plate moment connections subject to cyclic loads should be calculated using Equations 4.1 through 4.3. This provides a more conservative estimate of the expected beam strength and accounts for the additional moment generated by the shear at the hinge region. Of the ninety end-plate connection tests analyzed, thirty three of the tests observed beam failure. The predicted to experimentally observed strength ratios, calculated using equations 4.1 through 4.3, varied from 0.72 to 1.29 with an average value of 1.00 and a standard deviation of 12.1 percent;
- The end-plate bending strength model included in the proposed design method produces good correlation with the experimental results. The predicted to experimental strength ratios varied from 0.61 to 1.35 with a mean value of 0.99 with a standard deviation of 15.3 percent. Although there is some scatter in the results, the majority of ratio values were very close to unity;
- The proposed column flange bending design model produces good correlation with the twelve experimental tests available for comparison. The predicted to experimental strength ratios varied from 0.76 to 1.09 with an average value of 0.98. Although the number of experimental tests available for comparison is relatively small, good correlation for the four bolt extended and the multiple row extended 1/3 connections exists;

- The proposed bolt force model correlated well with the sixteen experimental tests available for comparison. The predicted to experimental strength ratios varied from 0.87 to 1.29 with an average value of 0.98 and a standard deviation of 10.7 percent;
- The bolt force model assumption, established by Borgsmiller (1995), that the outermost bolts in the connection will yield and provide enough deformation to allow all of the connection bolts to contribute their full tensile strength (P_t) is valid for all of the connections considered in this study except for the multiple row extended 1/3 (MRE 1/3) unstiffened and stiffened configurations. This conclusion is based primarily upon the results of the 'thick plate' multiple row extended 1/2 connection tests conducted as a part of this study. The MRE 1/3 connections is excluded because of no experimental test results are available for comparison. The MRE 1/3 connections have three rows of bolts inside the flanges of the beam that must be fully developed in tension. This condition is more critical than the MRE 1/2 connections and requires experimental validation;
- The experimental testing showed that ASTM A490 bolts can be successfully used in extended end-plate moment connections subject to cyclic loads. No differences in behavior of ASTM A490 and A325 bolts were observed throughout the research program;
- The effects of a composite slab attached to the top flange of a connecting beam should be considered in the design of beam-to-column end-plate moment connections. This conclusion is based upon the results of the one beam-to-column test with at composite slab in which the strength demand observed on the connection was twenty-seven percent greater than the demand observed in the bare steel specimen test;

- For beam-to-column end-plate connections with a composite slab, the slab and shear studs should be detailed to ensure that the composite shear connection in the area around the column is lost prior to the application of large inelastic load cycles;
- The welding procedure outlined in Chapter 7 is an acceptable procedure for making the end-plate to beam connection. The procedure should be used to fabricate end-plate moment connections that are designed as a part of seismic force resisting moment frames;
- The use of three-dimensional finite element analysis can successfully predict the behavior of end-plate moment connections. The finite element analysis performed as a part of this research program correlated well with the strength predictions produced by the proposed design procedure;
- Based upon the experimental testing, analytical investigation, and finite element modeling results presented herein, it is concluded that the proposed design method does adequately predict the behavior of the eight extended end-plate moment connection configurations and should be used for the design of end-plate moment connections subject to cyclic/seismic forces.

8.4 Future Research Needs

Although there is a great deal of literature available on end-plate moment connections, there are several key areas that are not well covered by the existing literature. A summary of the future research needs is as follows:

- An experimental study is needed to investigate the column flange bending strength for all eight end-plate connection configurations.
- A probabilistic study is needed to determine if the currently utilized LRFD load factors for yielding and rupture are reliable enough to provide the necessary factor of safety.

- Additional cyclic testing is necessary to establish a base of qualifying tests for each connection configuration. Adequate testing has been completed on the four bolt extended unstiffened, but additional testing is necessary for the other seven configurations.
- Additional 'thick plate' tests should be conducted on the eight bolt extended stiffened and the multiple row 1/3 connection configurations to continue validation of the bolt force model.

REFERENCES

AWS (1998). *Structural Welding Code – Steel, AWS D1.1-98*, American Welding Society, Miami.

AISC (2002). *Seismic Provisions for Structural Steel Buildings*, American Institute of Steel Construction, Chicago.

AISC (2001). *Manual of Steel Construction, Load and Resistance Factor Design*, American Institute of Steel Construction, Chicago.

AISC (2000a). *Code of Standard Practice for Steel Buildings and Bridges*, American Institute of Steel Construction, Chicago.

AISC (2000b). *Seismic Provisions for Structural Steel Buildings (1997) Supplement No. 2*, American Institute of Steel Construction, Chicago.

AISC (1999a). *Load and Resistance Factor Design Specification for Structural Steel Buildings*, American Institute of Steel Construction, Chicago.

AISC (1999b). *Seismic Provisions for Structural Steel Buildings (1997) Supplement No. 1*, American Institute of Steel Construction, Chicago.

AISC (1997). *Seismic Provisions for Structural Steel Buildings*, American Institute of Steel Construction, Chicago.

Abel, M.S. and Murray, T.M. (1992a). "Analytical and Experimental Investigation of the Extended Unstiffened Moment End-Plate Connection with Four Bolts at the Beam Tension Flange," *Research Report No. CE/VPI-ST-93/08*, Dept. of Civil Engineering, Virginia Polytechnic Institute and State University, Blacksburg, VA, Revised October 1994.

Abel, M.S. and Murray, T.M. (1992b). "Multiple Row, Extended Unstiffened End-Plate Connection Tests," *Research Report No. CE/VPI-ST-92/04*, Dept. of Civil Engineering, Virginia Polytechnic Institute and State University, Blacksburg, VA,.

Abolmaali, A., Kukreti, A.R. and Murray, T.M. (1984). "Finite Element Analysis of Two Tension Bolt Flush End-Plate Connections," *Research Report No. FSEL/MBMA 84-01*, Fears Structural Engineering Laboratory, School of Civil Engineering and Environmental Science, University of Oklahoma, Norman, Oklahoma.

Adey, B.T., Grondin, G.Y., Cheng, J.J.R. (1997). "Extended End Plate Moment Connections Under Cyclic Loading," *Structural Engineering Report No. 216*, Department of Civil and Environmental Engineering, University of Alberta, Alberta, Canada.

Adey, B.T., Grondin, G.Y., Cheng, J.J.R. (1998). "Extended End Plate Moment Connections Under Cyclic Loading," *Journal of Constructional Steel Research*, Elsevier Applied Science, 46(1-3), Paper No. 133.

Adey, B.T., Grondin, G.Y., Cheng, J.J.R. (2000). "Cyclic Loading of End Plate Moment Connections," *Canadian Journal of Civil Engineering*, National Research Council of Canada, 27(4), 683-701.

Agerskov, H. (1976). "High-Strength Bolted Connections Subject to Prying," *Journal of the Structural Division*, ASCE, 102(1), 161-175.

Agerskov, H. (1977). "Analysis of Bolted Connections Subject to Prying," *Journal of the Structural Division*, ASCE, 103(11), 2145-2163.

Aggarwal, A.K. and Coates, R.C. (1987). "Strength Criteria for Bolted Beam-Column Connections," *Journal of Constructional Steel Research*, Elsevier Applied Science, 7(3), 213-227.

Ahuja, V, Kukreti, A.R. and Murray, T.M. (1982). "Analysis of Stiffened End-Plate Connections Using the Finite Element Method," *Research Report No. FSEL/MBMA 82-01*, Fears Structural Engineering Laboratory, School of Civil Engineering and Environmental Science, University of Oklahoma, Norman, Oklahoma.

Astaneh-Asl, A. (1995) *Seismic Design of Bolted Steel Moment-Resisting Frames,* Steel Tips, Structural Steel Education Council, Moraga, CA, 82 pp.

Bahaari, M.R. and Sherbourne, A.N. (1994). "Computer Modeling of an Extended End-Plate Bolted Connection," *Computers and Structures*, 52, 879-893.

Bahaari, M.R. and Sherbourne, A.N. (1996a). "Structural Behavior of End-Plate Bolted Connections to Stiffened Columns," *Journal of Structural Engineering*, ASCE, 122(8), 926-935.

Bahaari, M.R. and Sherbourne, A.N. (1996b). "3D Simulation of Bolted Connections to Unstiffened Columns - II. Extended Endplate Connections," *Journal of Constructional Steel Research*, Elsevier Applied Science, 40(3), 189-223.

Bahia, C.S., Graham, J. and Martin, L.H. (1981). "Experiments on Rigid Beam to Column Connections Subject to Shear and Bending Forces," *Proceedings of the International Conference: Joints in Structural Steelwork: The Design and Performance of Semi-Rigid and Rigid Joints in Steel and Composite Structures and Their Influence on Structural Behaviour*, Teesside Polytechnic, Middlesbrough, Cleveland, England, April 6-9, 1981, 6.37-6.56.

Bailey, J.R. (1970). "Strength and Rigidity of Bolted Beam to Column Connections," *Conference on Joints in Structures*, University of Sheffield, Sheffield, England, July 8-10, 1970, Paper A4, A401-A429.

Beedle, L.S. and Christopher, R. (1964). "Tests of Steel Moment Connections," *Engineering Journal*, AISC, 1(4), 116-125.

Bond, D.E. and Murray, T.M. (1989). "Analytical and Experimental Investigation of a Flush Moment End-Plate Connection with Six Bolts at the Tension Flange," *Research Report No. CE/VPI-ST-89/10*, Dept. of Civil Engineering, Virginia Polytechnic Institute and State University, Blacksburg, VA.

Boorse, M.R. (1999). "Evaluation of the Inelastic Rotation Capability of Flush End-Plate Moment Connections," M.S. Thesis, Department of Civil Engineering, Virginia Polytechnic Institute and State University, Blacksburg, Virginia.

Borgsmiller, J.T. (1995). "Simplified Method for Design of Moment End-Plate Connections," M.S. Thesis, Department of Civil Engineering, Virginia Polytechnic Institute and State University, Blacksburg, Virginia.

Borgsmiller, J.T., Sumner, E.A. and Murray, T.M. (1995). "Extended Unstiffened Moment End-Plate Connection Tests," *Research Report No. CE/VPI-ST-95/13*, Dept. of Civil Engineering, Virginia Polytechnic Institute and State University, Blacksburg, VA.

Bose, B., Wang, Z.M., and Sarkar, S. (1997). "Finite-Element Analysis of Unstiffened Flush End-Plate Bolted Joints," *Journal of Structural Engineering*, ASCE, 123,1614-1621.

Bursi, O.S. and Jaspart, J.P. (1998). "Basic Issues in the Finite Element Simulation of Extended End Plate Connections," *Computers & Structures*, Pergamon, 69(3), 361-382.

Chasten, C.P., Lu, L.W. and Driscoll, G.C. (1992). "Prying and Shear in End-Plate Connection Design," *Journal of Structural Engineering*, ASCE, 118(5), 1295-1311.

Choi, C.K., Chung, G.T. (1996). "Refined Three-Dimensional Finite Element Model for End-Plate Connection," *Journal of Structural Engineering*, ASCE, 122(11), 1307-1316.

Coons, R. G., (1999) *Seismic Design and Database of End Plate and T-stub Connections*, M.S. Thesis, University of Washington, Seattle, Washington.

Curtis, L.E. and Murray, T.M. (1989). "Column Flange Strength at Moment End-Plate Connections," *Engineering Journal*, AISC, 26(2), 41-50.

Disque, R.O. (1962). "End Plate Connections," *Proceedings of the 1962 AISC National Engineering Conference*, Columbus, OH, April 12-13, 1962, AISC, 30-37.

Douty, R.T. and McGuire, W. (1963). "Research on Bolted Moment Connections – A Progress Report," *Proceedings of the 1963 AISC National Engineering Conference*, Tulsa, OK, April 24-26, 1963, AISC, 48-55.

Douty, R.T. and McGuire, W. (1965). "High Strength Bolted Moment Connections," *Journal of the Structural Division*, ASCE, 91(2), 101-128.

FEMA (1995), *FEMA 267 (SAC 95-02) Interim Guidelines: Evaluation, Repair, Modification and Design of Steel Moment Frames,* Federal Emergency Management Agency, Washington, DC.

FEMA (1996), *FEMA 267A (SAC 96-03) Interim Guidelines Advisory No. 1: Supplement to FEMA 267,* Federal Emergency Management Agency, Washington, DC.

FEMA (1997), FEMA-288 (SAC-95-09), *Background Reports: Metallurgy, Fracture Mechanics, Welding, Moment Connections and Frame Systems Behavior,* Federal Emergency Management Agency, Washington, DC.

FEMA (2000a), FEMA-350, *Recommended Seismic Design Criteria for New Steel Moment Frame Buildings,* Federal Emergency Management Agency, Washington, DC.

FEMA (2000b), FEMA-351, *Recommended Seismic Evaluation and Upgrade Criteria for Welded Moment-Resisting Steel Frame Structures,* Federal Emergency Management Agency, Washington, DC.

FEMA (2000c), FEMA-352, *Recommended Post-Earthquake Evaluation and Repair Criteria for Welded Moment-Resisting Steel Frame Structures,* Federal Emergency Management Agency, Washington, DC.

FEMA (2000d), FEMA-353, *Recommended Specifications and Quality Assurance Guidelines for Steel Moment Frame Construction for Seismic Applications,* Federal Emergency Management Agency, Washington, DC.

Fisher, J.W., and Struik, J.H.A. (1974). *Guide to Design Criteria for Bolted and Riveted Joints*, John Wiley and Sons, New York.

Fleischman, R.B., Chasten, C.P., Lu, L.W. and Driscoll, G.C. (1991). "Top-and-Seat Agnles Connections and End-Plate Connections: Snug vs. Fully Pretensioned Bolts," AISC Engineering Journal, 1st Qtr., 28, 18-28.

Fleischman, R.B., Chasten, C.P., Lu, L.W. and Driscoll, G.C. (1990). "Cyclic Behavior of Large Size Flexible Beam-to-Column Connections," *Proceedings: Fourth U.S. National Conference on Earthquake Engineering*, El Cerrito, CA, EERI, Vol. 2, May 20-24, 1990, 687-696.

Gebbeken, N., Rothert, H. and Binder, B. (1994). "On the Numerical Analysis of Endplate Connections," *Journal of Constructional Steel Research*, Elsevier Applied Science, 30(1), 177-196.

Ghassemieh, M., Kukreti, A.R. and Murray, T.M. (1983). "Inelastic Finite Element Analysis of Stiffened End-Plate Moment Connections," *Research Report No. FSEL/MBMA 83-02*, Fears Structural Engineering Laboratory, School of Civil Engineering and Environmental Science, University of Oklahoma, Norman, Oklahoma.

Ghobarah, A., Korol, R.M. and Osman, A. (1992). "Cyclic Behavior of Extended End-Plate Joints," *Journal of Structural Engineering*, ASCE, 118(5), 1333-1353.

Ghobarah, A., Osman, A. and Korol, R.M. (1990). "Behaviour of Extended End-Plate Connections Under Cyclic Loading," *Engineering Structures*, Elsevier Science, Vol. 12, 15-26.

Graham, J. (1981). "Beam to Column Bolted Connections," *Ph.D. Thesis*, University of Aston in Birmingham, England, 1981.

Graham, J. (1993). "Observations from the Behaviour of Bolted Beam to Unstiffened Column Rigid Connections," *The Structural Engineer*, Institution of Structural Engineers, 71(6), 99-105.

Grundy, P., Thomas, I.R. and Bennetts, I.D. (1980). "Beam-to-Column Moment Connections," *Journal of the Structural Division,* ASCE, 106(1), 313-330.

Hendrick, A. and Murray, T.M. (1983). "Column Web Compression Strength at End-Plate Connections," *Research Report No. FSEL/AISC 83-01*, Fears Structural Engineering Laboratory, School of Civil Engineering and Environmental Science, University of Oklahoma, Norman, OK.

Hendrick, A. and Murray, T.M. (1984). "Column Web Compression Strength at End-Plate Connections," *Engineering Journal*, AISC, 21(3), 161-169.

Hendrick, D.M., Kukreti, A.R. and Murray, T.M. (1984). "Analytical and Experimental Investigation of Stiffened Flush End-Plate Connections with Four Bolts at the Tension Flange," *Research Report No. FSEL/MBMA 84-02*, Fears Structural Engineering Laboratory, School of Civil Engineering and Environmental Science, University of Oklahoma, Norman, OK.

Hendrick, D.M., Kukreti, A.R. and Murray, T.M. (1985). "Unification of Flush End-Plate Design Procedures," *Research Report No. FSEL/MBMA 85-01*, Fears Structural Engineering Laboratory, School of Civil Engineering and Environmental Science, University of Oklahoma, Norman, OK.

Johansen, K. W. (1972). Yield-line Formulae for Slabs, Cement and Concrete Association, London, England.

Johnson, L.G., Cannon, J.C. and Spooner, L.A. (1960). "High Tensile Preloaded Bolted Joints for Development of Full Plastic Moments," *British Welding Journal*, 7, 560-569.

Johnstone, N.D. and Walpole, W.R., (1981). "Bolted End-Plate Beam-to-Column Connections Under Earthquake Type Loading," *Report 81-7*, Department of Civil Engineering, University of Canterbury, Christchurch, New Zealand.

Kato, B. and McGuire, W. (1973). "Analysis of T-Stub Flange-to-Column Connections," *Journal of the Structural Division*, ASCE, 99(5), 865-888.

Kennedy, D.J. and Hafez, M.A. (1984). "A Study of End Plate Connections for Steel Beams," *Canadian Journal of Civil Engineering*, 11(2), 139-149.

Kennedy, N.A., Vinnakota, S. and Sherbourne, A.N. (1981). "The Split-Tee Analogy in Bolted Splices and Beam-Column Connections," *Proceedings of the International Conference: Joints in Structural Steelwork: The Design and Performance of Semi-Rigid and Rigid Joints in Steel and Composite Structures and Their Influence on Structural Behaviour*, Teesside Polytechnic, Middlesbrough, Cleveland, England, April 6-9, 1981, 2.138-2.157.

Kline, D.P., Rojiani, K.B., and Murray, T.M. (1989). "Performance of Snug Tight Bolts in Moment End-Plate Connections," *MBMA Research Report*, Dept. of Civil Engineering, Virginia Polytechnic Institute and State University, Blacksburg, VA, Revised July 1995.

Korol, R.M., Ghobarah, A. and Osman, A. (1990). "Extended End-Plate Connections Under Cyclic Loading: Behaviour and Design," *Journal of Constructional Steel Research*, Elsevier Applied Science, 16(4), 253-279.

Krishnamurthy, N. (1978). "A Fresh Look at Bolted End-Plate Behavior and Design," *Engineering Journal*, AISC, 15(2), 39-49.

Krishnamurthy, N. and Graddy, D.E. (1976). "Correlation Between 2- and 3-Dimensional Finite Element Analysis of Steel Bolted End-Plate Connections," *Computers & Structures*, Pergamon, 6(4-5/6), 381-389.

Kukreti, A.R., Ghassemieh, M. and Murray, T.M. (1990). "Behavior and Design of Large-Capacity Moment End Plates," *Journal of Structural Engineering*, ASCE, 116(3), 809-828.

Leon, R.T. (1995). "Seismic Performance of Bolted and Riveted Connections," *Background Reports: Metallurgy, Fracture Mechanics, Welding, Moment Connections and Frame System Behavior,* Report No SAC-95-09, FEMA-288 / March 1997, Federal Emergency Management Agency, Washington, DC.

Mann, A.P. (1968). "Plastically Designed Endplate Connections," *Ph.D. Thesis*, University of Leeds, England, 1968.

Mann, A.P. and Morris, L.J. (1979). "Limit Design of Extended End-Plate Connections," *Journal of the Structural Division*, ASCE, 105(3), 511-526.

Mays, T. W., (2000). *Application of the Finite Element Method to the Seismic Design and Analysis of Large Moment End-Plate Connections*, Ph.D. Dissertation, Virginia Polytechnic Institute and State University, Blacksburg, Virginia.

Meng, R.L. (1996). "Design of Moment End-Plate Connections for Seismic Loading," Ph.D. Dissertation submitted to Virginia Polytechnic Institute and State University, Virginia Polytechnic Institute and State University, Blacksburg, Virginia, 1996.

Meng, R.L. and Murray, T.M. (1996). *Moment End-Plate Connections for Seismic Loading*, Research Report No. CE/VPI-ST-96/04, submitted to National Science Foundation, Arlington, Virginia, May 1996.

Meng, R.L. and Murray, T.M. (1997). "Seismic Performance of Bolted End-Plate Moment Connections," *Proceedings of the 1997 National Steel Construction Conference, Chicago, Illinois*, AISC, May 7-9, 1997, 30-1 –30-14.

Morris, L.J. (1988). "Design Rules for Connections in the United Kingdom," *Journal of Constructional Steel Research*, Elsevier Applied Science, 10, 375-413.

Morrison, S.J., Astaneh-Asl, A. and Murray, T.M. (1985). "Analytical and Experimental Investigation of the Extended Stiffened Moment End-Plate Connection with Four Bolts at the Beam Tension Flange," *Research Report No. FSEL/MBMA 85-05*, Fears Structural Engineering Laboratory, School of Civil Engineering and Environmental Science, University of Oklahoma, Norman, Oklahoma.

Morrison, S.J., Astaneh-Asl, A. and Murray, T.M. (1986). "Analytical and Experimental Investigation of the Multiple Row Extended Moment End-Plate Connection with Eight Bolts at the Beam Tension Flange," *Research Report No. FSEL/MBMA 86-01*, Fears Structural Engineering Laboratory, School of Civil Engineering and Environmental Science, University of Oklahoma, Norman, Oklahoma.

Murray, T.M. (1988). "Recent Developments for the Design of Moment End-Plate Connections," *Steel Beam-to-Column Building Connections*, W.F. Chen, ed., Elsevier Applied Science, New York, 133-162.

Murray, T. M., (1990). *AISC Design Guide Series 4, Extended End-Plate Moment Connections*, American Institute of Steel Construction, Chicago.

Murray, T.M., Kline, D.P. and Rojiani, K.B. (1992). "Use of Snug-Tightened Bolts in End-Plate Connections," *Connections in Steel Structures II: Behaviour, Strength and Design: Proceedings of the Second International Workshop*, Pittsburgh, PA, April 10-12, 1991, Bjorhovde, Colson, Haaijer and Stark, ed., Pergamon, 1991, 27-34.

Murray, T.M. and Kukreti, A.R. (1985). "Design of 8-Bolt Stiffened End-Plate Moment Connections," *Proceedings of the Third Conference on Steel Developments*, Melbourne, Australia, May 20-22, 1985, AISC, 1985, 74-78.

Murray, T.M. and Kukreti, A.R. (1988). "Design of 8-Bolt Stiffened Moment End Plates," *Engineering Journal*, AISC, Second Quarter, 1988, 45-52.

Murray, T.M. and Shoemaker, W.L. (2002). Steel Design Guide Series 16, *Flush and Extended Multiple-Row Moment End-Plate Connections,* American Institute of Steel Construction, Chicago, IL.

Nair, R.S., Birkemoe, P.C. and Munse, W.H. (1974). "High Strength Bolts Subject to Tension and Prying," *Journal of the Structural Division*, ASCE, 100(2), 351-372.

Newlin, D.E. and Chen, W.E. (1971). "Strength and Stability of Column Webs in Welded Beam-to-Column Connections," *Fritz Engineering Laboratory, Report No. 333.14*, Lehigh University, Bethlehem, Pennsylvania.

Ober, E.R. (1995). "Simplified Design of Moment End-Plate Connections," Master of Science Thesis, Department of Civil Engineering, Virginia Polytechnic Institute and State University, Blacksburg, Virginia, 1995.

Packer, J.A. and Morris, L.J. (1977). "A Limit State Design Method for the Tension Region of Bolted Beam-Column Connections," *The Structural Engineer*, Institution of Structural Engineers, 55(10), 446-458.

Popov, E. and Tsai, K.C. (1989). "Performance of Large Seismic Steel Moment Connections Under Cyclic Loads," *AISC Engineering Journal*, 2nd Qtr., 12, 51-60.

Rodkey, R.W. and Murray, T.M. (1993). "Eight Bolt Extended Unstiffened End-Plate Connection Test," *Research Report No. CE/VPI-ST-93/10*, Dept. of Civil Engineering, Virginia Polytechnic Institute and State University, Blacksburg, VA.

Ryan, J. C. (1999). "Evaluation of the Inelastic Rotation Capability of Extended End-Plate Moment Connections," M.S. Thesis, Department of Civil Engineering, Virginia Polytechnic Institute and State University, Blacksburg, Virginia.

Ryan, J. C., and Murray, T. M. (1999), *Evaluation of the Inelastic Rotation Capability of Extended End-Plate Moment Connections*, Research Report No. CE/VPI-ST-99/13, submitted to Metal Building Manufacturers Association, Cleveland, Ohio and American Institute of Steel Construction, Chicago, Illinois, September 1999.

SAC (1997). *Protocol for Fabrication, Inspection, Testing and Documentation of Beam-Column Connection Tests and Other Experimental Specimens*, Report No. SAC/BD-97/02, SAC Joint Venture.

Sherbourne, A. (1961). "Bolted Beam-to-Column Connections," *The Structural Engineer*, 39, 203-210.

Srouji, R., Kukreti, A.R. and Murray, T.M. (1983a). "Strength of Two Tension Bolt Flush End-Plate Connections," *Research Report No. FSEL/MBMA 83-03*, Fears Structural Engineering Laboratory, School of Civil Engineering and Environmental Science, University of Oklahoma, Norman, Oklahoma.

Srouji, R., Kukreti, A.R. and Murray, T.M. (1983b). "Yield-Line Analysis of End-Plate Connections with Bolt Force Predictions," *Research Report No. FSEL/MBMA 83-05*, Fears Structural Engineering Laboratory, School of Civil Engineering and Environmental Science, University of Oklahoma, Norman, Oklahoma.

Structural Engineers, Inc. (1984). "Multiple Row, Extended End Plate Connections Tests," December, 1984, Norman, OK.

Sumner, E. A., Mays, T. W., and Murray, T. M. (2000), *Cyclic Testing of Bolted Moment End-Plate Connections*, Research Report No. CE/VPI-ST-00/03, SAC Report No. SAC/BD-00/21, submitted to the SAC Joint Venture, May 2000, 327 pages.

Sumner, E. A., and Murray, T. M. (2001a), *Experimental Investigation of the MRE 1/2 End-Plate Moment Connection*, Research Report No. CE/VPI-ST-01/14, submitted to Metal Building Manufacturers Association, Cleveland, Ohio, December 2001, 91 pages.

Sumner, E. A., and Murray, T. M. (2001b), *Experimental Investigation of Four Bolts Wide Extended End-Plate Moment Connections*, Research Report No. CE/VPI-ST-01/15, submitted to Star Building Systems, Inc., Oklahoma City, Oklahoma, December 2001, 114 pages.

Surtees, J.O. and Mann, A.P. (1970). "End Plate Connections in Plastically Designed Structures," *Conference on Joints in Structures*, University of Sheffield, Sheffield, England, July 8-10, 1970, Paper A5, A501-A520.

Tarpy, Jr., T.S and Cardinal, J.W. (1981). "Behavior of Simi-Rigid Beam-to Column End Plate Connections," *Proceedings of the International Conference: Joints in Structural Steelwork: The Design and Performance of Semi-Rigid and Rigid Joints in Steel and Composite Structures and Their Influence on Structural Behaviour*, Teesside Polytechnic, Middlesbrough, Cleveland, England, April 6-9, 1981, 2.3-2.25.

Tsai, K.C. and Popov, E.P. (1990). "Cyclic Behavior of End-Plate Moment Connections," *Journal of Structural Engineering*, ASCE, 116(11), 2917-2930.

Whitmore, R. E., (1952). "Experimental Investigation of Stresses in Gusset Plates," *Bulletin No. 16,* Civil Engineering, The University of Tennessee Engineering Experiment Station, Knoxville, TN.

Witteveen, J., Stark, J.W.B., Bijlaard, F.S.K. and Zoetemeijer, P. (1982). "Welded and Bolted Beam-to Column Connections," *Journal of the Structural Division*, ASCE, 108(2), 433-455.

Zoetemeijer, P. (1974). "A Design Method for the Tension Side of Statically Loaded, Bolted Beam-to-Column Connections," *Heron*, 20(1), Stevin-Laboratory of the Dept. of Civil Engineering of the Technological University, Delft, The Netherlands, ed., 1-59.

Zoetemeijer, P. (1981). "Semi-Rigid Bolted Beam-to-Beam Column Connections with Stiffened Column Flanges and Flush-End Plates," *Proceedings of the International Conference: Joints in Structural Steelwork: The Design and Performance of Semi-Rigid and Rigid Joints in Steel and Composite Structures and Their Influence on Structural Behaviour*, Teesside Polytechnic, Middlesbrough, Cleveland, England, April 6-9, 1981, 2.99-2.118.

APPENDIX A

CYCLIC END-PLATE MOMENT CONNECTION TEST SUMMARY SHEETS

TEST SUMMARY

Test ID: 4E-1.25-1.5-24
Test Date: February 21, 1999

Beam Data	Section: W24x68				
	Steel Grade: ASTM A572 Gr. 50				
	Measured Properties:	d =	23.875	in.	
		t_w =	0.438	in.	
		b_f =	9.156	in.	
		t_f =	0.583	in.	
		Z_x =	177	$in.^3$	(nominal)
		L_{bm} =	169.75	in.	(to CL column)
	Coupon Test	F_y =	53.6	ksi	
		F_u =	70.7	ksi	
	Mill Test Report	F_y =	55.0	ksi	
		F_u =	71.5	ksi	
Column Data	Section: W14x120				
	Steel Grade: ASTM A572 Gr. 50				
	Measured Properties:	d =	14.5	in.	
		t_w =	0.601	in.	
		b_f =	14.75	in.	
		t_f =	0.933	in.	
		L_{col} =	218.625	in.	
	Coupon Test	F_y =	52.0	ksi	
		F_u =	70.6	ksi	
	Mill Test Report	F_y =	53.0	ksi	
		F_u =	71.5	ksi	
Panel Zone Data	Doubler Plate:	t_p =	0.375	in.	
		F_y =	42.1	ksi	
		F_u =	64.95	ksi	
	Continuity Plates:	t_p =	0.63	in.	
		F_y =	36	ksi	(nominal)
		F_u =	58	ksi	(nominal)

TEST SUMMARY (continued)

End-Plate Data	Plate Size: PL 1 1/2" x 10" x 2'-9 1/4"				
	Steel Grade: ASTM A36				
	Measured Properties:	t_p =	1.535	in.	
		b_p =	10	in.	
		L_{pl} =	33.75	in.	
	Top Flange	g =	5.98	in.	
		p_f =	1.71	in.	
		p_t =	2.81	in.	
	Bottom Flange	g =	5.96	in.	
		p_f =	2.093	in.	
		p_t =	2.48	in.	
	Coupon Test	F_y =	38.1	ksi	
		F_u =	68.8	ksi	
	Mill Test Report	F_y =	n/a	ksi	
		F_u =	n/a	ksi	
Bolt Data		d_{bt} =	1.25	in.	
		Grade =	A490		
	Nominal Tensile Strength, Ft =		113	ksi	(AISC J3.6)
		Pt =	138.7	kips	(nominal)
		F_u =	n/a	ksi	(mill test)
Experimental Results	Failure Mode: Flange and web local buckling				
		P_{max} =	68.94	kips	
		M_{max} =	11,703	in.-kips	
		Δ_{max} =	10.27	in.	
		θ_{max} =	0.061	rad.	
		$\theta_{p\,max}$ =	0.044	rad.	
Sustained at least one complete cycle		θ_{max} =	0.052	rad.	
Sustained at least one complete cycle		$\theta_{p\,max}$ =	0.038	rad.	

TEST SUMMARY

Test ID: 4E-1.25-1.125-24
Test Date: March 1, 1999

Beam Data	Section: W24x68				
	Steel Grade: ASTM A572 Gr. 50				
	Measured Properties:	d =	23.875	in.	
		t_w =	0.438	in.	
		b_f =	9.156	in.	
		t_f =	0.583	in.	
		Z_x =	177	$in.^3$	(nominal)
		L_{bm} =	169.75	in.	(to CL column)
	Coupon Test	F_y =	53.6	ksi	
		F_u =	70.7	ksi	
	Mill Test Report	F_y =	55.0	ksi	
		F_u =	71.5	ksi	
Column Data	Section: W14x120				
	Steel Grade: ASTM A572 Gr. 50				
	Measured Properties:	d =	14.5	in.	
		t_w =	0.601	in.	
		b_f =	14.75	in.	
		t_f =	0.933	in.	
		L_{col} =	218.625	in.	
	Coupon Test	F_y =	52.0	ksi	
		F_u =	70.6	ksi	
	Mill Test Report	F_y =	53.0	ksi	
		F_u =	71.5	ksi	
Panel Zone Data	Doubler Plate:	t_p =	0.375	in.	
		F_y =	42.1	ksi	
		F_u =	64.95	ksi	
	Continuity Plates:	t_p =	0.63	in.	
		F_y =	36	ksi	(nominal)
		F_u =	58	ksi	(nominal)

TEST SUMMARY (continued)

End-Plate Data	Plate Size: PL 1 1/8" x 10" x 2'-9 1/4"				
	Steel Grade: ASTM A36				
	Measured Properties:	t_p =	1.148	in.	
		b_p =	10.125	in.	
		L_{pl} =	33.75	in.	
	Top Flange	g =	5.97	in.	
		p_f =	1.88	in.	
		p_t =	2.63	in.	
	Bottom Flange	g =	5.96	in.	
		p_f =	2.09	in.	
		p_t =	1.85	in.	
	Coupon Test	F_y =	37.9	ksi	
		F_u =	63.4	ksi	
	Mill Test Report	F_y =	n/a	ksi	
		F_u =	n/a	ksi	
Bolt Data		d_{bt} =	1.25	in.	
		Grade =	A325		
	Nominal Tensile Strength, Ft =		90	ksi	(AISC J3.6)
		Pt =	110.4	kips	(nominal)
		F_u =	n/a	ksi	(mill test)
Experimental Results	Failure Mode: End-plate yielding and bolt ruputre				
		P_{max} =	65.56	kips	
		M_{max} =	11,128	in.-kips	(at CL column)
		Δ_{max} =	8.54	in.	
		θ_{max} =	0.05	rad.	
		$\theta_{p\,max}$ =	0.031	rad.	
Sustained at least one complete cycle		θ_{max} =	0.04	rad.	
Sustained at least one complete cycle		$\theta_{p\,max}$ =	0.021	rad.	

TEST SUMMARY

Test ID: 4E-1.25-1.375-24 Slab Test
Test Date: February 21, 1999

North Beam Data

Section: W24x68
Steel Grade: ASTM A572 Gr. 50

Measured Properties:	d =	24.813	in.	
	t_w =	0.375	in.	
	b_f =	9.125	in.	
	t_f =	0.581	in.	
	Z_x =	177	$in.^3$	(nominal)
	L_{bm} =	132	in.	(to CL column)
Coupon Test	F_y =	56.5	ksi	
	F_u =	71.7	ksi	
Mill Test Report	F_y =	55.0	ksi	
	F_u =	71.5	ksi	

South Beam Data

Section: W24x68
Steel Grade: ASTM A572 Gr. 50

Measured Properties:	d =	24.813	in.	
	t_w =	0.375	in.	
	b_f =	9.188	in.	
	t_f =	0.575	in.	
	Z_x =	177	$in.^3$	(nominal)
	L_{bm} =	132	in.	(to CL column)
Coupon Test	F_y =	56.5	ksi	
	F_u =	71.7	ksi	
Mill Test Report	F_y =	55.0	ksi	
	F_u =	71.5	ksi	

TEST SUMMARY (continued)

Column Data	Section:	W14x257			
	Steel Grade:	ASTM A36			
	Measured Properties:	d =	16.1875	in.	
		t_w =	1.188	in.	
		b_f =	15.938	in.	
		t_f =	1.875	in.	
		L_{col} =	144	in.	
	Coupon Test	F_y =	n/a	ksi	
		F_u =	n/a	ksi	
	Mill Test Report	F_y =	n/a	ksi	
		F_u =	n/a	ksi	
Panel Zone Data	Doubler Plate:	t_p =	0.375	in.	(nominal)
	Coupon Test	F_y =	46.2	ksi	
		F_u =	69.0	ksi	
	Continuity Plates:	t_p =	-	in.	
		F_y =	-	ksi	
		F_u =	-	ksi	
North End-Plate Data	Plate Size:	PL 1 3/8" x 10" x 2'-9 1/4"			
	Steel Grade:	ASTM A36			
	Measured Properties:	t_p =	1.402	in.	
		b_p =	10	in.	
		L_{pl} =	34.75	in.	
	Top Flange	g =	6.001	in.	
		p_f =	1.97	in.	
		p_t =	2.579	in.	
	Bottom Flange	g =	5.98	in.	
		p_f =	1.99	in.	
		p_t =	2.675	in.	
	Coupon Test	F_y =	38.9	ksi	
		F_u =	64.5	ksi	
	Mill Test Report	F_y =	48.1	ksi	
		F_u =	73.4	ksi	

TEST SUMMARY (continued)

South End-Plate Data

Plate Size: PL 1 3/8" x 10" x 2'-9 1/4"
Steel Grade: ASTM A36

Measured Properties:	t_p =	1.403	in.	
	b_p =	10	in.	
	L_{pl} =	34.75	in.	
Top Flange	g =	6.015	in.	
	p_f =	1.97	in.	
	p_t =	2.6	in.	
Bottom Flange	g =	5.988	in.	
	p_f =	1.997	in.	
	p_t =	2.607	in.	
Coupon Test	F_y =	38.9	ksi	
	F_u =	64.5	ksi	
Mill Test Report	F_y =	48.1	ksi	
	F_u =	73.4	ksi	

Bolt Data

d_{bt} =	1.25	in.	
Grade =	A490		
Nominal Tensile Strength, Ft =	113	ksi	(AISC J3.6)
Pt =	138.7	kips	(nominal)
F_u =	161.1	ksi	(mill test)

Experimental Results

North Beam Failure Mode: Bolt rupture and flange local buckling

P_{max} =	115.6	kips	
M_{max} =	15,255	in.-kips	
θ_{max} =	0.092	rad.	
$\theta_{p\,max}$ =	0.075	rad.	
θ_{max} =	0.05	rad.	*Sustained at least one complete cycle*
$\theta_{p\,max}$ =	0.025	rad.	*Sustained at least one complete cycle*

South Beam Failure Mode: Bolt rupture and flange local buckling

P_{max} =	115.1	kips	
M_{max} =	15,193	in.-kips	
θ_{max} =	0.075	rad.	
$\theta_{p\,max}$ =	0.049	rad.	
θ_{max} =	0.06	rad.	*Sustained at least one complete cycle*
$\theta_{p\,max}$ =	0.035	rad.	*Sustained at least one complete cycle*

TEST SUMMARY

Test ID: 8ES-1.25-1.75-30
Test Date: March 16-18, 1999

Beam Data	Section: W30x99				
	Steel Grade: ASTM A572 Gr. 50				
	Measured Properties:	d =	29.75	in.	
		t_w =	0.5	in.	
		b_f =	10.563	in.	
		t_f =	0.639	in.	
		Z_x =	312	$in.^3$	(nominal)
		L_{bm} =	241.25	in.	(to CL column)
	Coupon Test	F_y =	54.9	ksi	
		F_u =	70.8	ksi	
	Mill Test Report	F_y =	55.5	ksi	
		F_u =	74.0	ksi	
Column Data	Section: W14x193				
	Steel Grade: ASTM A572 Gr. 50				
	Measured Properties:	d =	15.563	in.	
		t_w =	0.899	in.	
		b_f =	15.813	in.	
		t_f =	1.375	in.	
		L_{col} =	266.438	in.	
	Coupon Test	F_y =	55.5	ksi	
		F_u =	74.3	ksi	
	Mill Test Report	F_y =	55.5	ksi	
		F_u =	74.0	ksi	
Panel Zone Data	Doubler Plate:	t_p =	0.375	in.	
		F_y =	41.4	ksi	
		F_u =	63.8	ksi	
	Continuity Plates:	t_p =	0.75	in.	
		F_y =	36	ksi	(nominal)
		F_u =	58	ksi	(nominal)

TEST SUMMARY (continued)

End-Plate Data	Plate Size: PL 1 3/4" x 11 1/2" x 3'-8 1/2"				
	Steel Grade: ASTM A36				
	Measured Properties:	t_p =	1.8	in.	
		b_p =	11.5	in.	
		L_{pl} =	44.625	in.	
	Top Flange	g =	5.487	in.	
		p_f =	1.751	in.	
		p_b =	3.776	in.	
	Bottom Flange	g =	5.488	in.	
		p_f =	1.751	in.	
		p_b =	3.76	in.	
	Coupon Test	F_y =	37.2	ksi	
		F_u =	63.4	ksi	
	Mill Test Report	F_y =	n/a	ksi	
		F_u =	n/a	ksi	
		t_s =	0.499	in.	
		L_{st} =	15.91	in.	
		F_y =	36	ksi	(nominal)
		F_u =	58	ksi	(nominal)
Bolt Data		d_{bt} =	1.25	in.	
		Grade =	A490		
		Nominal Tensile Strength, Ft =	113	ksi	(AISC J3.6)
		Pt =	138.7	kips	(nominal)
		Fu =	154.3	ksi	(mill test)
Experimental Results	Failure Mode: Flange and web local buckling				
		P_{max} =	84.11	kips	
		M_{max} =	20,291	in.-kips	(at CL column)
		Δ_{max} =	12.51	in.	
		θ_{max} =	0.05	rad.	
		$\theta_{p\,max}$ =	0.042	rad.	
Sustained at least one complete cycle		θ_{max} =	0.05	rad.	
Sustained at least one complete cycle		$\theta_{p\,max}$ =	0.036	rad.	

TEST SUMMARY

Test ID: 8ES-1.25-1-30
Test Date: March 26, 1999

Beam Data	Section: W30x99				
	Steel Grade: ASTM A572 Gr. 50				
	Measured Properties:	d =	29.75	in.	
		t_w =	0.5	in.	
		b_f =	10.563	in.	
		t_f =	0.639	in.	
		Z_x =	312	$in.^3$	(nominal)
		L_{bm} =	240.5	in.	(to CL column)
	Coupon Test	F_y =	54.9	ksi	
		F_u =	70.8	ksi	
	Mill Test Report	F_y =	55.5	ksi	
		F_u =	74.0	ksi	
Column Data	Section: W14x193				
	Steel Grade: ASTM A572 Gr. 50				
	Measured Properties:	d =	15.563	in.	
		t_w =	0.899	in.	
		b_f =	15.813	in.	
		t_f =	1.375	in.	
		L_{col} =	266.438	in.	
	Coupon Test	F_y =	55.5	ksi	
		F_u =	74.3	ksi	
	Mill Test Report	F_y =	55.5	ksi	
		F_u =	74.0	ksi	
Panel Zone Data	Doubler Plate:	t_p =	0.375	in.	
		F_y =	41.4	ksi	
		F_u =	63.8	ksi	
	Continuity Plates:	t_p =	0.75	in.	
		F_y =	36	ksi	(nominal)
		F_u =	58	ksi	(nominal)

TEST SUMMARY (continued)

End-Plate Data	Plate Size: PL 1" x 11 1/2" x 3'-8 1/2"				
	Steel Grade: ASTM A36				
	Measured Properties:	t_p =	1.01	in.	
		b_p =	11.5	in.	
		L_{pl} =	44.5	in.	
	Top Flange	g =	5.508	in.	
		p_f =	1.77	in.	
		p_b =	3.77	in.	
	Bottom Flange	g =	5.509	in.	
		p_f =	1.77	in.	
		p_b =	3.78	in.	
	Coupon Test	F_y =	37.8	ksi	
		F_u =	60.8	ksi	
	Mill Test Report	F_y =	n/a	ksi	
		F_u =	n/a	ksi	
		t_s =	0.499	in.	
		L_{st} =	15.938	in.	
		F_y =	36	ksi	(nominal)
		F_u =	58	ksi	(nominal)
Bolt Data		d_{bt} =	1.25	in.	
		Grade =	A325		
		Nominal Tensile Strength, Ft =	113	ksi	(AISC J3.6)
		Pt =	138.7	kips	(nominal)
		Fu =	138.7	ksi	(mill test)
Experimental Results	Failure Mode: Flange and web local buckling				
		P_{max} =	89.72	kips	
		M_{max} =	21,578	in.-kips	(at CL column)
		Δ_{max} =	14.91	in.	
		θ_{max} =	0.06	rad.	
		$\theta_{p\,max}$ =	0.049	rad.	
Sustained at least one complete cycle		θ_{max} =	0.056	rad.	
Sustained at least one complete cycle		$\theta_{p\,max}$ =	0.039	rad.	

TEST SUMMARY

Test ID: 8ES-1.25-2.5-36
Test Date: May 14 & 17, 1999

Beam Data	Section: W36x150				
	Steel Grade: ASTM A572 Gr. 50				
	Measured Properties:	d =	35.813	in.	
		t_w =	0.6875	in.	
		b_f =	12.25	in.	
		t_f =	0.931	in.	
		Z_x =	581	$in.^3$	(nominal)
		L_{bm} =	265.81	in.	(to CL column)
	Coupon Test	F_y =	54.5	ksi	
		F_u =	70.4	ksi	
	Mill Test Report	F_y =	56.5	ksi	
		F_u =	71.5	ksi	
Column Data	Section: W14x257				
	Steel Grade: ASTM A572 Gr. 50				
	Measured Properties:	d =	16.375	in.	
		t_w =	1.19	in.	
		b_f =	16.125	in.	
		t_f =	1.98	in.	
		L_{col} =	266.5	in.	
	Coupon Test	F_y =	51.2	ksi	
		F_u =	68.3	ksi	
	Mill Test Report	F_y =	53.0	ksi	
		F_u =	71.0	ksi	
Panel Zone Data	Doubler Plate:	t_p =	0.75	in.	
		F_y =	36	ksi	(nominal)
		F_u =	58	ksi	(nominal)
	Continuity Plates:	t_p =	-	in.	
		F_y =	-	ksi	(nominal)
		F_u =	-	ksi	(nominal)

TEST SUMMARY (continued)

End-Plate Data	Plate Size: PL 2 1/2" x 13" x 4'-2 1/2"				
	Steel Grade: ASTM A36				
	Measured Properties:	t_p =	2.55	in.	
		b_p =	15	in.	
		L_{pl} =	50.625	in.	
	Top Flange	g =	6.05	in.	
		p_f =	1.925	in.	
		p_b =	3.72	in.	
	Bottom Flange	g =	6.01	in.	
		p_f =	1.906	in.	
		p_b =	3.73	in.	
	Coupon Test	F_y =	38.2	ksi	
		F_u =	72.3	ksi	
	Mill Test Report	F_y =	n/a	ksi	
		F_u =	n/a	ksi	
		t_s =	0.755	in.	
		L_{st} =	13	in.	
		F_y =	36	ksi	(nominal)
		F_u =	58	ksi	(nominal)
Bolt Data		d_{bt} =	1.25	in.	
		Grade =	A490		
		Nominal Tensile Strength, Ft =	113	ksi	(AISC J3.6)
		Pt =	138.7	kips	(nominal)
		Fu =	n/a	ksi	(mill test)
Experimental Results	Failure Mode: Flange and web local buckling				
		P_{max} =	151.27	kips	
		M_{max} =	40,209	in.-kips	(at CL column)
		Δ_{max} =	16.46	in.	
		θ_{max} =	0.06	rad.	
		$\theta_{p\,max}$ =	0.045	rad.	
Sustained at least one complete cycle		θ_{max} =	0.05	rad.	
Sustained at least one complete cycle		$\theta_{p\,max}$ =	0.028	rad.	

TEST SUMMARY

Test ID: 8ES-1.25-1.25-36
Test Date: May 28, 1999

Beam Data	Section: W36x150				
	Steel Grade: ASTM A572 Gr. 50				
	Measured Properties:	d =	35.813	in.	
		t_w =	0.6875	in.	
		b_f =	12.25	in.	
		t_f =	0.931	in.	
		Z_x =	581	$in.^3$	(nominal)
		L_{bm} =	265.81	in.	(to CL column)
	Coupon Test	F_y =	54.5	ksi	
		F_u =	70.4	ksi	
	Mill Test Report	F_y =	56.5	ksi	
		F_u =	71.5	ksi	
Column Data	Section: W14x257				
	Steel Grade: ASTM A572 Gr. 50				
	Measured Properties:	d =	16.375	in.	
		t_w =	1.19	in.	
		b_f =	16.125	in.	
		t_f =	1.98	in.	
		L_{col} =	266.5	in.	
	Coupon Test	F_y =	51.2	ksi	
		F_u =	68.3	ksi	
	Mill Test Report	F_y =	53.0	ksi	
		F_u =	71.0	ksi	
Panel Zone Data	Doubler Plate:	t_p =	0.75	in.	
		F_y =	36	ksi	(nominal)
		F_u =	58	ksi	(nominal)
	Continuity Plates:	t_p =	-	in.	
		F_y =	-	ksi	(nominal)
		F_u =	-	ksi	(nominal)

TEST SUMMARY (continued)

End-Plate Data	Plate Size: PL 1 1/4" x 13" x 4'-2 1/2"				
	Steel Grade: ASTM A36				
	Measured Properties:	t_p =	1.265	in.	
		b_p =	13	in.	
		L_{pl} =	40.44	in.	
	Top Flange	g =	5.98	in.	
		p_f =	1.897	in.	
		p_b =	3.761	in.	
	Bottom Flange	g =	6.05	in.	
		p_f =	1.894	in.	
		p_b =	3.737	in.	
	Coupon Test	F_y =	40.5	ksi	
		F_u =	67.1	ksi	
	Mill Test Report	F_y =	n/a	ksi	
		F_u =	n/a	ksi	
		t_s =	0.763	in.	
		L_{st} =	13	in.	
		F_y =	36	ksi	(nominal)
		F_u =	58	ksi	(nominal)
Bolt Data		d_{bt} =	1.25	in.	
		Grade =	A325		
		Nominal Tensile Strength, Ft =	113	ksi	(AISC J3.6)
		Pt =	138.7	kips	(nominal)
		Fu =	n/a	ksi	(mill test)
Experimental Results	Failure Mode: End-plate yielding and bolt ruputre				
		P_{max} =	126.82	kips	
		M_{max} =	33,710	in.-kips	(at CL column)
		Δ_{max} =	10.99	in.	
		θ_{max} =	0.04	rad.	
		$\theta_{p\ max}$ =	0.019	rad.	
Sustained at least one complete cycle		θ_{max} =	0.03	rad.	
Sustained at least one complete cycle		$\theta_{p\ max}$ =	0.011	rad.	

TEST SUMMARY

Test ID: 4W-1.25-1.125-30
Test Date: June 10, 1999

Beam Data	Section: W30x99				
	Steel Grade: ASTM A572 Gr. 50				
	Measured Properties:	d =	29.688	in.	
		t_w =	0.5	in.	
		b_f =	10.688	in.	
		t_f =	0.659	in.	
		Z_x =	312	$in.^3$	(nominal)
		L_{bm} =	241.25	in.	(to CL column)
	Coupon Test	F_y =	55.9	ksi	
		F_u =	70.8	ksi	
	Mill Test Report	F_y =	57.0	ksi	
		F_u =	73.0	ksi	
Column Data	Section: W14x193				
	Steel Grade: ASTM A572 Gr. 50				
	Measured Properties:	d =	15.563	in.	
		t_w =	0.899	in.	
		b_f =	15.813	in.	
		t_f =	1.375	in.	
		L_{col} =	266.438	in.	
	Coupon Test	F_y =	55.5	ksi	
		F_u =	74.3	ksi	
	Mill Test Report	F_y =	55.5	ksi	
		F_u =	74.0	ksi	
Panel Zone Data	Doubler Plate:	t_p =	0.375	in.	
		F_y =	36	ksi	(nominal)
		F_u =	58	ksi	(nominal)
	Continuity Plates:	t_p =	0.75	in.	
		F_y =	36	ksi	(nominal)
		F_u =	58	ksi	(nominal)

TEST SUMMARY (continued)

End-Plate Data	Plate Size: PL 1 1/8" x 15" x 2'-4 1/4"				
	Steel Grade: ASTM A36				
	Measured Properties:	t_p =	1.14	in.	
		b_p =	15	in.	
		L_{pl} =	37.125	in.	
	Top Flange	g =	4.97	in.	
		g_o =	3.388	in.	
		p_f =	1.744	in.	
	Bottom Flange	g =	4.988	in.	
		g_o =	3.383	in.	
		p_f =	1.808	in.	
	Coupon Test	F_y =	42.0	ksi	
		F_u =	70.3	ksi	
	Mill Test Report	F_y =	43	ksi	
		F_u =	69.7	ksi	
Bolt Data		d_{bt} =	1.25	in.	
		Grade =	A325		
	Nominal Tensile Strength, Ft =		90	ksi	(AISC J3.6)
		Pt =	110.4	kips	(nominal)
		Fu =	n/a	ksi	(mill test)
Experimental Results	Failure Mode: Bolt rupture and end-plate tearing				
		P_{max} =	82.63	kips	
		M_{max} =	19,935	in.-kips	(at CL column)
		Δ_{max} =	12.48	in.	
		θ_{max} =	0.05	rad.	
		$\theta_{p\ max}$ =	0.031	rad.	
Sustained at least one complete cycle		θ_{max} =	0.05	rad.	
Sustained at least one complete cycle		$\theta_{p\ max}$ =	0.029	rad.	

TEST SUMMARY

Test ID: 4W-1.25-1-30
Test Date: June 15, 1999

Beam Data	Section: W30x99				
	Steel Grade: ASTM A572 Gr. 50				
	Measured Properties:	d =	29.688	in.	
		t_w =	0.5	in.	
		b_f =	10.688	in.	
		t_f =	0.659	in.	
		Z_x =	312	$in.^3$	(nominal)
		L_{bm} =	241.25	in.	(to CL column)
	Coupon Test	F_y =	55.9	ksi	
		F_u =	70.8	ksi	
	Mill Test Report	F_y =	57.0	ksi	
		F_u =	73.0	ksi	
Column Data	Section: W14x193				
	Steel Grade: ASTM A572 Gr. 50				
	Measured Properties:	d =	15.563	in.	
		t_w =	0.899	in.	
		b_f =	15.813	in.	
		t_f =	1.375	in.	
		L_{col} =	266.438	in.	
	Coupon Test	F_y =	55.5	ksi	
		F_u =	74.3	ksi	
	Mill Test Report	F_y =	55.5	ksi	
		F_u =	74.0	ksi	
Panel Zone Data	Doubler Plate:	t_p =	0.375	in.	
		F_y =	36	ksi	(nominal)
		F_u =	58	ksi	(nominal)
	Continuity Plates:	t_p =	0.75	in.	
		F_y =	36	ksi	(nominal)
		F_u =	58	ksi	(nominal)

TEST SUMMARY (continued)

End-Plate Data	Plate Size: PL 1" x 15" x 2'-4 1/4"				
	Steel Grade: ASTM A36				
	Measured Properties:	t_p =	1.025	in.	
		b_p =	15	in.	
		L_{pl} =	37.06	in.	
	Top Flange	g =	4.975	in.	
		g_o =	3.385	in.	
		p_f =	1.743	in.	
	Bottom Flange	g =	4.997	in.	
		g_o =	3.382	in.	
		p_f =	1.808	in.	
	Coupon Test	F_y =	40.4	ksi	
		F_u =	59.7	ksi	
	Mill Test Report	F_y =	42.8	ksi	
		F_u =	66.3	ksi	
Bolt Data		d_{bt} =	1.25	in.	
		Grade =	A325		
	Nominal Tensile Strength, Ft =		90	ksi	(AISC J3.6)
		Pt =	110.4	kips	(nominal)
		Fu =	n/a	ksi	(mill test)
Experimental Results	Failure Mode: Bolt rupture and end-plate tearing				
		P_{max} =	76.77	kips	
		M_{max} =	18,521	in.-kips	(at CL column)
		Δ_{max} =	10.05	in.	
		θ_{max} =	0.04	rad.	
		$\theta_{p\ max}$ =	0.021	rad.	
Sustained at least one complete cycle		θ_{max} =	0.04	rad.	
Sustained at least one complete cycle		$\theta_{p\ max}$ =	0.021	rad.	

TEST SUMMARY

Test ID: 4W-1.25-1.375-36
Test Date: June 28, 1999

Beam Data	Section: W36x150				
	Steel Grade: ASTM A572 Gr. 50				
	Measured Properties:	d =	35.875	in.	
		t_w =	0.6875	in.	
		b_f =	12.25	in.	
		t_f =	0.897	in.	
		Z_x =	581	$in.^3$	(nominal)
		L_{bm} =	266.19	in.	(to CL column)
	Coupon Test	F_y =	55.8	ksi	
		F_u =	68.6	ksi	
	Mill Test Report	F_y =	56.5	ksi	
		F_u =	71.5	ksi	
Column Data	Section: W14x257				
	Steel Grade: ASTM A572 Gr. 50				
	Measured Properties:	d =	16.375	in.	
		t_w =	1.19	in.	
		b_f =	16.125	in.	
		t_f =	1.98	in.	
		L_{col} =	266.5	in.	
	Coupon Test	F_y =	51.2	ksi	
		F_u =	68.3	ksi	
	Mill Test Report	F_y =	53.0	ksi	
		F_u =	71.0	ksi	
Panel Zone Data	Doubler Plate:	t_p =	0.75	in.	
		F_y =	36	ksi	(nominal)
		F_u =	58	ksi	(nominal)
	Continuity Plates:	t_p =	1.012	in.	
		F_y =	36	ksi	(nominal)
		F_u =	58	ksi	(nominal)

TEST SUMMARY (continued)

End-Plate Data Plate Size: PL 1 3/8" x 15" x 3'-7"
Steel Grade: ASTM A36

Measured Properties:	t_p =	1.404	in.	
	b_p =	15.063	in.	
	L_{pl} =	43	in.	
Top Flange	g =	4.972	in.	
	g_o =	3.403	in.	
	p_f =	1.764	in.	
Bottom Flange	g =	5.008	in.	
	g_o =	3.398	in.	
	p_f =	1.803	in.	
Coupon Test	F_y =	40.8	ksi	
	F_u =	72.0	ksi	
Mill Test Report	F_y =	45.2	ksi	
	F_u =	67.1	ksi	

Bolt Data

	d_{bt} =	1.25	in.	
	Grade =	A325		
Nominal Tensile Strength,	Ft =	90	ksi	(AISC J3.6)
	Pt =	110.4	kips	(nominal)
	Fu =	n/a	ksi	(mill test)

Experimental Results Failure Mode: Bolt rupture and end-plate tearing

	P_{max} =	126.82	kips	
	M_{max} =	33,758	in.-kips	(at CL column)
	Δ_{max} =	10.98	in.	
	θ_{max} =	0.04	rad.	
	$\theta_{p\,max}$ =	0.019	rad.	
Sustained at least one complete cycle	θ_{max} =	0.04	rad.	
Sustained at least one complete cycle	$\theta_{p\,max}$ =	0.019	rad.	

TEST SUMMARY

Test ID: 4W-1.25-1.25-36
Test Date: June 30, 1999

Beam Data	Section: W36x150				
	Steel Grade: ASTM A572 Gr. 50				
	Measured Properties:	d =	35.875	in.	
		t_w =	0.6875	in.	
		b_f =	12.25	in.	
		t_f =	0.897	in.	
		Z_x =	581	$in.^3$	(nominal)
		L_{bm} =	266.19	in.	(to CL column)
	Coupon Test	F_y =	55.8	ksi	
		F_u =	68.6	ksi	
	Mill Test Report	F_y =	56.5	ksi	
		F_u =	71.5	ksi	
Column Data	Section: W14x257				
	Steel Grade: ASTM A572 Gr. 50				
	Measured Properties:	d =	16.375	in.	
		t_w =	1.19	in.	
		b_f =	16.125	in.	
		t_f =	1.98	in.	
		L_{col} =	266.5	in.	
	Coupon Test	F_y =	51.2	ksi	
		F_u =	68.3	ksi	
	Mill Test Report	F_y =	53.0	ksi	
		F_u =	71.0	ksi	
Panel Zone Data	Doubler Plate:	t_p =	0.75	in.	
		F_y =	36	ksi	(nominal)
		F_u =	58	ksi	(nominal)
	Continuity Plates:	t_p =	1.012	in.	
		F_y =	36	ksi	(nominal)
		F_u =	58	ksi	(nominal)

TEST SUMMARY (continued)

End-Plate Data	Plate Size: PL 1 1/4" x 15" x 3'-7"				
	Steel Grade: ASTM A36				
	Measured Properties:	t_p =	1.404	in.	
		b_p =	15.0625	in.	
		L_{pl} =	43	in.	
	Top Flange	g =	4.972	in.	
		g_o =	3.448	in.	
		p_f =	1.764	in.	
	Bottom Flange	g =	5.008	in.	
		g_o =	3.398	in.	
		p_f =	1.8	in.	
	Coupon Test	F_y =	40.3	ksi	
		F_u =	66.3	ksi	
	Mill Test Report	F_y =	45.2	ksi	
		F_u =	67.2	ksi	
Bolt Data		d_{bt} =	1.25	in.	
		Grade =	A325		
	Nominal Tensile Strength, Ft =		90	ksi	(AISC J3.6)
		Pt =	110.4	kips	(nominal)
		Fu =	n/a	ksi	(mill test)
Experimental Results	Failure Mode: Bolt rupture and end-plate tearing				
		P_{max} =	125.49	kips	
		M_{max} =	33,404	in.-kips	(at CL column)
		Δ_{max} =	10.99	in.	
		θ_{max} =	0.04	rad.	
		$\theta_{p\ max}$ =	0.019	rad.	
Sustained at least one complete cycle		θ_{max} =	0.04	rad.	
Sustained at least one complete cycle		$\theta_{p\ max}$ =	0.019	rad.	

APPENDIX B

MONOTONIC END-PLATE MOMENT CONNECTION TEST SUMMARY SHEETS

TEST SUMMARY

TEST NAME: Test A - MRE 1/2-3/4-3/8-30
TEST DATE: June 4, 2001

CONNECTION DESCRIPTION

TYPE:	Multiple Row Extended 1/2 (MRE 1/2)	
NUMBER OF TENSION BOLTS:	6 (2 outside, 4 inside)	
NUMBER OF COMPRESSION BOLTS:	2	

BEAM DATA

SECTION TYPE:	Built-Up	
DEPTH, h:	30.0	in.
FLANGE WIDTH, b_f:	8.0	in.
FLANGE THICKNESS, t_f:	0.496	in.
WEB THICKNESS, t_w:	0.375	in.
MOMENT OF INERTIA, I:	2500	$in.^4$
NOMINAL YIELD STRESS, F_y:	50	ksi

END-PLATE DATA

END PLATE THICKNESS, t_p:	0.381	in.
END PLATE WIDTH, b_p:	8.0	in.
END PLATE LENGTH, L_p:	33.0	in.
END-PLATE EXTENSION OUTSIDE FLANGE, p_{ext}:	2.56	in.
OUTER PITCH, BOLT TO FLANGE, p_{fo}:	1.29	in.
INNER PITCH, BOLT TO FLANGE, p_{fi}:	1.17	in.
INNER PITCH, BOLT TO BOLT, p_b:	2.24	in.
GAGE, g:	3.00	in.
MEASURED YIELD STRESS, F_{yp}:	62.0	ksi

BOLT DATA

BOLT DIAMETER, d_b:	3/4	in.	
BOLT LENGTH, L_b:	2.0	in.	
BOLT TYPE:	ASTM A325		
BOLT PRETENSION, T_b:	Snug Tight (Average:	14.6	kips/bolt)
NOMINAL BOLT TENSILE STRESS (AISC J3.6), F_t:	90.0	ksi	
NOMINAL BOLT TENSILE STRENGTH, P_t:	39.8	kips	

EXPERIMENTAL RESULTS

MAXIMUM APPLIED MOMENT, M_{max}:	462.1	k-ft
YIELD MOMENT (Based on plate separation), M_y:	330.0	k-ft
FAILURE MODE:	End-Plate Yielding / Bolt Tension Rupture	

PREDICTED STRENGTHS

END-PLATE STRENGTH, M_{PL}:	256.6	k-ft
BOLT TENSION RUPTURE (w/o Prying), M_{NP}:	563.1	k-ft
BOLT TENSION RUPTURE (w/Prying), M_Q:	286.4	k-ft
CONTROLLING STRENGTH, M_n:	256.6	k-ft

TEST SUMMARY

TEST NAME: Test B - MRE 1/2-3/4-3/4-30
TEST DATE: June 5, 2001

CONNECTION DESCRIPTION

TYPE:	Multiple Row Extended 1/2 (MRE 1/2)	
NUMBER OF TENSION BOLTS:	6 (2 outside, 4 inside)	
NUMBER OF COMPRESSION BOLTS:	2	

BEAM DATA

SECTION TYPE:	Built-Up	
DEPTH, h:	30.0	in.
FLANGE WIDTH, b_f:	8.0	in.
FLANGE THICKNESS, t_f:	0.496	in.
WEB THICKNESS, t_w:	0.375	in.
MOMENT OF INERTIA, I:	2500	$in.^4$
NOMINAL YIELD STRESS, F_y:	50	ksi

END-PLATE DATA

END PLATE THICKNESS, t_p:	0.751	in.
END PLATE WIDTH, b_p:	8.0	in.
END PLATE LENGTH, L_p:	33.0	in.
END-PLATE EXTENSION OUTSIDE FLANGE, p_{ext}:	2.56	in.
OUTER PITCH, BOLT TO FLANGE, p_{fo}:	1.25	in.
INNER PITCH, BOLT TO FLANGE, p_{fi}:	1.24	in.
INNER PITCH, BOLT TO BOLT, p_b:	2.24	in.
GAGE, g:	3.02	in.
MEASURED YIELD STRESS, F_{yp}:	62.3	ksi

BOLT DATA

BOLT DIAMETER, d_b:	3/4		in.
BOLT LENGTH, L_b:	2.5		in.
BOLT TYPE:	ASTM A325		
BOLT PRETENSION, T_b:	Snug Tight (Average:	16.1	kips/bolt)
NOMINAL BOLT TENSILE STRESS (AISC J3.6), F_t:	90.0		ksi
NOMINAL BOLT TENSILE STRENGTH, P_t:	39.8		kips

EXPERIMENTAL RESULTS

MAXIMUM APPLIED MOMENT, M_{max}:	633.3	k-ft
YIELD MOMENT (Based on plate separation), M_y:	540.0	k-ft
FAILURE MODE:	Bolt Tension Rupture	

PREDICTED STRENGTHS

END-PLATE STRENGTH, M_{PL}:	994.7	k-ft
BOLT TENSION RUPTURE (w/o Prying), M_{NP}:	561.9	k-ft
BOLT TENSION RUPTURE (w/Prying), M_Q:	335.1	k-ft
CONTROLLING STRENGTH, M_n:	561.9	k-ft

TEST SUMMARY

TEST NAME: Test B1 - MRE 1/2-3/4-3/4-30
TEST DATE: June 6, 2001

CONNECTION DESCRIPTION

TYPE:	Multiple Row Extended 1/2 (MRE 1/2)	
NUMBER OF TENSION BOLTS:	6 (2 outside, 4 inside)	
NUMBER OF COMPRESSION BOLTS:	2	

BEAM DATA

SECTION TYPE:	Built-Up	
DEPTH, h:	30.0	in.
FLANGE WIDTH, b_f:	8.0	in.
FLANGE THICKNESS, t_f:	0.496	in.
WEB THICKNESS, t_w:	0.375	in.
MOMENT OF INERTIA, I:	2500	$in.^4$
NOMINAL YIELD STRESS, F_y:	50	ksi

END-PLATE DATA

END PLATE THICKNESS, t_p:	0.751	in.
END PLATE WIDTH, b_p:	8.0	in.
END PLATE LENGTH, L_p:	33.0	in.
END-PLATE EXTENSION OUTSIDE FLANGE, p_{ext}:	2.56	in.
OUTER PITCH, BOLT TO FLANGE, p_{fo}:	1.25	in.
INNER PITCH, BOLT TO FLANGE, p_{fi}:	1.24	in.
INNER PITCH, BOLT TO BOLT, p_b:	2.24	in.
GAGE, g:	3.02	in.
MEASURED YIELD STRESS, F_{yp}:	62.3	ksi

BOLT DATA

BOLT DIAMETER, d_b:	3/4	in.
BOLT LENGTH, L_b:	2.5	in.
BOLT TYPE:	ASTM A490	
BOLT PRETENSION, T_b:	Snug Tight	kips/bolt)
NOMINAL BOLT TENSILE STRESS (AISC J3.6), F_t:	113.0	ksi
NOMINAL BOLT TENSILE STRENGTH, P_t:	49.9	kips

EXPERIMENTAL RESULTS

MAXIMUM APPLIED MOMENT, M_{max}:	749.9	k-ft
YIELD MOMENT (Based on plate separation), M_y:	640.0	k-ft
FAILURE MODE:	Bolt Tension Rupture	

PREDICTED STRENGTHS

END-PLATE STRENGTH, M_{PL}:	994.7	k-ft
BOLT TENSION RUPTURE (w/o Prying), M_{NP}:	705.5	k-ft
BOLT TENSION RUPTURE (w/Prying), M_Q:	441.9	k-ft
CONTROLLING STRENGTH, M_n:	705.5	k-ft

TEST SUMMARY

TEST NAME: Test C - MRE 1/2-3/4-1/2-30 (Large inner pitch distance)
TEST DATE: June 7, 2001

CONNECTION DESCRIPTION

TYPE:	Multiple Row Extended 1/2 (MRE 1/2)	
NUMBER OF TENSION BOLTS:	6 (2 outside, 4 inside)	
NUMBER OF COMPRESSION BOLTS:	2	

BEAM DATA

SECTION TYPE:	Built-Up	
DEPTH, h:	30.0	in.
FLANGE WIDTH, b_f:	8.0	in.
FLANGE THICKNESS, t_f:	0.497	in.
WEB THICKNESS, t_w:	0.375	in.
MOMENT OF INERTIA, I:	2500	$in.^4$
NOMINAL YIELD STRESS, F_y:	50	ksi

END-PLATE DATA

END PLATE THICKNESS, t_p:	0.498	in.
END PLATE WIDTH, b_p:	8.0	in.
END PLATE LENGTH, L_p:	33.0	in.
END-PLATE EXTENSION OUTSIDE FLANGE, p_{ext}:	2.59	in.
OUTER PITCH, BOLT TO FLANGE, p_{fo}:	1.35	in.
INNER PITCH, BOLT TO FLANGE, p_{fi}:	4.88	in.
INNER PITCH, BOLT TO BOLT, p_b:	2.23	in.
GAGE, g:	3.01	in.
MEASURED YIELD STRESS, F_{yp}:	60.7	ksi

BOLT DATA

BOLT DIAMETER, d_b:	3/4	in.	
BOLT LENGTH, L_b:	2.0	in.	
BOLT TYPE:	ASTM A325		
BOLT PRETENSION, T_b:	Snug Tight (Average:	15.2	kips/bolt)
NOMINAL BOLT TENSILE STRESS (AISC J3.6), F_t:	90.0	ksi	
NOMINAL BOLT TENSILE STRENGTH, P_t:	39.8	kips	

EXPERIMENTAL RESULTS

MAXIMUM APPLIED MOMENT, M_{max}:	482.0	k-ft
YIELD MOMENT (Based on plate separation), M_y:	405.0	k-ft
FAILURE MODE:	End-Plate Yielding / Bolt Tension Rupture	

PREDICTED STRENGTHS

END-PLATE STRENGTH, M_{PL}:	353.0	k-ft
BOLT TENSION RUPTURE (w/o Prying), M_{NP}:	514.4	k-ft
BOLT TENSION RUPTURE (w/Prying), M_Q:	316.2	k-ft
CONTROLLING STRENGTH, M_n:	316.2	k-ft

TEST SUMMARY

TEST NAME: Test D - MRE 1/2-3/4-3/4-30 (Large inner pitch distance)
TEST DATE: June 8, 2001

CONNECTION DESCRIPTION

TYPE:	Multiple Row Extended 1/2 (MRE 1/2)	
NUMBER OF TENSION BOLTS:	6 (2 outside, 4 inside)	
NUMBER OF COMPRESSION BOLTS:	2	

BEAM DATA

SECTION TYPE:	Built-Up	
DEPTH, h:	30.0	in.
FLANGE WIDTH, b_f:	8.0	in.
FLANGE THICKNESS, t_f:	0.498	in.
WEB THICKNESS, t_w:	0.375	in.
MOMENT OF INERTIA, I:	2500	$in.^4$
NOMINAL YIELD STRESS, F_y:	50	ksi

END-PLATE DATA

END PLATE THICKNESS, t_p:	0.751	in.
END PLATE WIDTH, b_p:	8.0	in.
END PLATE LENGTH, L_p:	33.0	in.
END-PLATE EXTENSION OUTSIDE FLANGE, p_{ext}:	2.56	in.
OUTER PITCH, BOLT TO FLANGE, p_{fo}:	1.27	in.
INNER PITCH, BOLT TO FLANGE, p_{fi}:	4.94	in.
INNER PITCH, BOLT TO BOLT, p_b:	2.23	in.
GAGE, g:	3.01	in.
MEASURED YIELD STRESS, F_{yp}:	61.3	ksi

BOLT DATA

BOLT DIAMETER, d_b:	3/4		in.
BOLT LENGTH, L_b:	2.5		in.
BOLT TYPE:	ASTM A325		
BOLT PRETENSION, T_b:	Snug Tight (Average:	17.5	kips/bolt)
NOMINAL BOLT TENSILE STRESS (AISC J3.6), F_t:	90.0		ksi
NOMINAL BOLT TENSILE STRENGTH, P_t:	39.8		kips

EXPERIMENTAL RESULTS

MAXIMUM APPLIED MOMENT, M_{max}:	558.7	k-ft
YIELD MOMENT (Based on plate separation), M_y:	500.0	k-ft
FAILURE MODE:	Bolt Tension Rupture	

PREDICTED STRENGTHS

END-PLATE STRENGTH, M_{PL}:	825.3	k-ft
BOLT TENSION RUPTURE (w/o Prying), M_{NP}:	513.0	k-ft
BOLT TENSION RUPTURE (w/Prying), M_Q:	305.6	k-ft
CONTROLLING STRENGTH, M_n:	513.0	k-ft

TEST SUMMARY

TEST NAME: Test D1 - MRE 1/2-3/4-3/4-30 (Large inner pitch distance)
TEST DATE: June 8, 2001

CONNECTION DESCRIPTION

TYPE:	Multiple Row Extended 1/2 (MRE 1/2)	
NUMBER OF TENSION BOLTS:	6 (2 outside, 4 inside)	
NUMBER OF COMPRESSION BOLTS:	2	

BEAM DATA

SECTION TYPE:	Built-Up	
DEPTH, h:	30.0	in.
FLANGE WIDTH, b_f:	8.0	in.
FLANGE THICKNESS, t_f:	0.498	in.
WEB THICKNESS, t_w:	0.375	in.
MOMENT OF INERTIA, I:	2500	$in.^4$
NOMINAL YIELD STRESS, F_y:	50	ksi

END-PLATE DATA

END PLATE THICKNESS, t_p:	0.751	in.
END PLATE WIDTH, b_p:	8.0	in.
END PLATE LENGTH, L_p:	33.0	in.
END-PLATE EXTENSION OUTSIDE FLANGE, p_{ext}:	2.56	in.
OUTER PITCH, BOLT TO FLANGE, p_{fo}:	1.27	in.
INNER PITCH, BOLT TO FLANGE, p_{fi}:	4.94	in.
INNER PITCH, BOLT TO BOLT, p_b:	2.23	in.
GAGE, g:	3.01	in.
MEASURED YIELD STRESS, F_{yp}:	31.3	ksi

BOLT DATA

BOLT DIAMETER, d_b:	3/4	in.
BOLT LENGTH, L_b:	2.5	in.
BOLT TYPE:	ASTM A490	
BOLT PRETENSION, T_b:	Snug Tight	kips/bolt)
NOMINAL BOLT TENSILE STRESS (AISC J3.6), F_t:	113.0	ksi
NOMINAL BOLT TENSILE STRENGTH, P_t:	49.9	kips

EXPERIMENTAL RESULTS

MAXIMUM APPLIED MOMENT, M_{max}:	622.8	k-ft
YIELD MOMENT (Based on plate separation), M_y:	450.0	k-ft
FAILURE MODE:	Bolt Tension Rupture	

PREDICTED STRENGTHS

END-PLATE STRENGTH, M_{PL}:	825.3	k-ft
BOLT TENSION RUPTURE (w/o Prying), M_{NP}:	644.1	k-ft
BOLT TENSION RUPTURE (w/Prying), M_Q:	400.0	k-ft
CONTROLLING STRENGTH, M_n:	644.1	k-ft

TEST SUMMARY

TEST NAME: Test A: 8E-4W-1-1/2-62
TEST DATE: October 16, 2001

CONNECTION DESCRIPTION

TYPE:	Extended Unstiffened End-Plate, 4 Bolts Wide	
NUMBER OF TENSION BOLTS:	8 (4 outside, 4 inside)	
NUMBER OF COMPRESSION BOLTS:	8	

BEAM DATA

SECTION TYPE:	Built-Up	
DEPTH, h:	61.5	in.
FLANGE WIDTH, b_f:	12.0	in.
FLANGE THICKNESS, t_f:	0.77	in.
NOMINAL WEB THICKNESS, t_w:	0.3750	in.
MOMENT OF INERTIA, I:	23358	$in.^4$
NOMINAL YIELD STRESS, F_y:	50	ksi

END-PLATE DATA

END PLATE THICKNESS, t_p:	0.504	in.
END PLATE WIDTH, b_p:	13.96	in.
END PLATE LENGTH, L_p:	67.73	in.
END-PLATE EXTENSION OUTSIDE FLANGE, p_{ext}:	3.12	in.
OUTER PITCH, BOLT TO FLANGE, p_{fo}:	1.38	in.
INNER PITCH, BOLT TO FLANGE, p_{fi}:	1.35	in.
INNER PITCH, BOLT TO BOLT, p_b:	n/a	in.
INSIDE BOLT GAGE, g:	3.48	in.
OUTSIDE BOLT GAGE, g_o:	3.49	in.
MEASURED YIELD STRESS, F_{yp}:	53.8	ksi

BOLT DATA

NOMINAL BOLT DIAMETER, d_b:	1	in.	
NOMINAL BOLT LENGTH, L_b:	2.5	in.	
BOLT TYPE:	ASTM A325		
BOLT PRETENSION, T_b:	Snug Tight (Average:	11.2	kips/bolt)
NOMINAL BOLT TENSILE STRESS (AISC J3.6), F_t:	90	ksi	
NOMINAL BOLT TENSILE STRENGTH, P_t:	70.7	kips	

EXPERIMENTAL RESULTS

MAXIMUM APPLIED MOMENT, M_{max}:	1539	k-ft
YIELD MOMENT (Based on plate separation), M_y:	1075	k-ft
FAILURE MODE:	End-Plate Yielding, High Bolt Forces	

PREDICTED STRENGTHS

END-PLATE STRENGTH, M_{PL}:	1031	k-ft
BOLT TENSION RUPTURE (w/Prying), M_Q:	1707	k-ft
BOLT TENSION RUPTURE (w/o Prying), M_{NP}:	2863	k-ft
CONTROLLING STRENGTH, M_n:	1031	k-ft

TEST SUMMARY

TEST NAME: Test C: 8E-4W-3/4-3/4-62
TEST DATE: October 23, 2001

CONNECTION DESCRIPTION

TYPE:	Extended Unstiffened End-Plate, 4 Bolts Wide	
NUMBER OF TENSION BOLTS:	8 (4 outside, 4 inside)	
NUMBER OF COMPRESSION BOLTS:	8	

BEAM DATA

SECTION TYPE:	Built-Up	
DEPTH, h:	61.5	in.
FLANGE WIDTH, b_f:	12.0	in.
FLANGE THICKNESS, t_f:	0.776	in.
NOMINAL WEB THICKNESS, t_w:	0.3750	in.
MOMENT OF INERTIA, I:	23358	$in.^4$
NOMINAL YIELD STRESS, F_y:	50	ksi

END-PLATE DATA

END PLATE THICKNESS, t_p:	0.753	in.
END PLATE WIDTH, b_p:	13.85	in.
END PLATE LENGTH, L_p:	67.88	in.
END-PLATE EXTENSION OUTSIDE FLANGE, p_{ext}:	3.25	in.
OUTER PITCH, BOLT TO FLANGE, p_{fo}:	1.46	in.
INNER PITCH, BOLT TO FLANGE, p_{fi}:	1.26	in.
INNER PITCH, BOLT TO BOLT, p_b:	n/a	in.
INSIDE BOLT GAGE, g:	3.50	in.
OUTSIDE BOLT GAGE, g_o:	3.49	in.
MEASURED YIELD STRESS, F_{yp}:	61.1	ksi

BOLT DATA

NOMINAL BOLT DIAMETER, d_b:	0.75	in.	
NOMINAL BOLT LENGTH, L_b:	2.5	in.	
BOLT TYPE:	ASTM A325		
BOLT PRETENSION, T_b:	Snug Tight (Average:	15.2	kips/bolt)
NOMINAL BOLT TENSILE STRESS (AISC J3.6), F_t:	90	ksi	
NOMINAL BOLT TENSILE STRENGTH, P_t:	39.8	kips	

EXPERIMENTAL RESULTS

MAXIMUM APPLIED MOMENT, M_{max}:	1825	k-ft
YIELD MOMENT (Based on plate separation), M_y:	1630	k-ft
FAILURE MODE:	Bolt Tension Rupture	

PREDICTED STRENGTHS

END-PLATE STRENGTH, M_{PL}:	2602	k-ft
BOLT TENSION RUPTURE (w/Prying), M_Q:	1039	k-ft
BOLT TENSION RUPTURE (w/o Prying), M_{NP}:	1612	k-ft
CONTROLLING STRENGTH, M_n:	1612	k-ft

TEST SUMMARY

TEST NAME: Test F: 8E-4W-3/4-3/4-62 (A490)
TEST DATE: November 3, 2001

CONNECTION DESCRIPTION

TYPE:	Extended Unstiffened End-Plate, 4 Bolts Wide	
NUMBER OF TENSION BOLTS:	8 (4 outside, 4 inside)	
NUMBER OF COMPRESSION BOLTS:	8	

BEAM DATA

SECTION TYPE:	Built-Up	
DEPTH, h:	61.5	in.
FLANGE WIDTH, b_f:	12.0	in.
FLANGE THICKNESS, t_f:	0.776	in.
NOMINAL WEB THICKNESS, t_w:	0.3750	in.
MOMENT OF INERTIA, I:	23358	$in.^4$
NOMINAL YIELD STRESS, F_y:	50	ksi

END-PLATE DATA

END PLATE THICKNESS, t_p:	0.753	in.
END PLATE WIDTH, b_p:	13.85	in.
END PLATE LENGTH, L_p:	67.88	in.
END-PLATE EXTENSION OUTSIDE FLANGE, p_{ext}:	3.25	in.
OUTER PITCH, BOLT TO FLANGE, p_{fo}:	1.46	in.
INNER PITCH, BOLT TO FLANGE, p_{fi}:	1.26	in.
INNER PITCH, BOLT TO BOLT, p_b:	n/a	in.
INSIDE BOLT GAGE, g:	3.50	in.
OUTSIDE BOLT GAGE, g_o:	3.49	in.
MEASURED YIELD STRESS, F_{yp}:	61.1	ksi

BOLT DATA

NOMINAL BOLT DIAMETER, d_b:	0.75		in.
NOMINAL BOLT LENGTH, L_b:	2.5		in.
BOLT TYPE:	ASTM A490		
BOLT PRETENSION, T_b:	Snug Tight (Average:	17.7	kips/bolt)
NOMINAL BOLT YIELD STRENGTH, F_{yb}:	113		ksi
NOMINAL BOLT TENSILE STRENGTH, P_{ub}:	49.9		kips

EXPERIMENTAL RESULTS

MAXIMUM APPLIED MOMENT, M_{max}:	2204	k-ft
YIELD MOMENT (Based on plate separation), M_y:	2110	k-ft
FAILURE MODE:	End-Plate Yielding	

PREDICTED STRENGTHS

END-PLATE STRENGTH, M_{PL}:	2602	k-ft
BOLT TENSION RUPTURE (w/Prying), M_Q:	1374	k-ft
BOLT TENSION RUPTURE (w/o Prying), M_{NP}:	2024	k-ft
CONTROLLING STRENGTH, M_n:	2024	k-ft

APPENDIX C

EXPERIMENTAL AND ANALYTICAL COMPARISON DATA

Connection Type	Reference	Test Identification [1]	Configuration and Loading	Calculated Strengths						Experimental		Design Ratios [2, 3, 4, 5]			
				$M_{pe\ Beam}$	M_{pl}	M_{cf}	M_{np}	$1.1M_{np}$	M_n	M_y	M_u	M_{pe}/M_u [6]	M_{pl}/M_y	M_{cf}/M_y	M_{np}/M_u
Four Bolt Extended Unstiffened (4E)	Packer & Morris (1977)	4E-3/4-1/2-10	Bm.-Col., Mono.	72	54	58	91	100	54	55	72	1.00	***0.98***	1.06	1.26
	Packer & Morris (1977)	4E-3/4-1/2-10	Bm.-Col., Mono.	72	54	37	91	100	37	40	65	1.11	1.35	***0.93***	1.40
	Packer & Morris (1977)	4E-3/4-1/2-10	Bm.-Col., Mono.	72	54	17	91	100	17	18	58	1.24	3.00	***0.97***	1.57
	Packer & Morris (1977)	4E-3/4-1/2-10	Bm.-Col., Mono.	72	54	24	91	100	24	22	71	1.01	2.45	***1.07***	1.28
	Packer & Morris (1977)	4E-3/4-1/2-10	Bm.-Col., Mono.	72	54	17	91	100	17	16	61	1.18	3.38	***1.09***	1.49
	Tsai & Popov (1990)	4E-7/8-1 3/8-18	Bm.-Col., Cyclic	370	648	-	313	344	313	334	360	1.03	1.94	-	***0.87***
	Tsai & Popov (1990)	4E-1-1 1/4-21	Bm.-Col., Cyclic	421	632	-	599	659	421	325	412	***1.02***	1.94	-	1.45
	Ghobarah et al. (1990)	4E-1-1-14	Bm.-Col., Cyclic	232	339	108	397	437	108	142	229	1.01	2.39	***0.76***	1.73
	Ghobarah et al. (1990)	4E-1-1-14	Bm.-Col., Cyclic	234	339	156	397	437	156	158	238	0.98	2.15	***0.99***	1.67
	Ghobarah et al. (1990)	4E-1-3/4-14	Bm.-Col., Cyclic	232	191	167	397	437	167	167	198	1.17	1.14	***1.00***	2.01
	Ghobarah et al. (1992)	4E-1-1.15-14	Bm.-Col., Cyclic	305	343	169	402	442	169	164	289	1.06	2.09	***1.03***	1.39
	Ghobarah et al. (1992)	4E-1-1.1-16	Bm.-Col., Cyclic	372	362	474	458	504	362	331	395	***0.94***	1.09	1.43	1.16
	Ghobarah et al. (1992)	4E-1-1.1-16	Bm.-Col., Cyclic	378	362	503	459	505	362	324	355	***1.07***	1.12	1.55	1.29
	Abel & Murray (1992a)	4E-3/4-5/8-18	Splice, Mono.	-	392	-	268	294	268	250	260	-	1.57	-	***1.03***
	Abel & Murray (1992a)	4E-3/4-3/4-18	Splice, Mono.	-	521	-	268	294	268	275	275	-	1.89	-	***0.97***
	Abel & Murray (1992a)	4E-1 1/8-7/8-16	Splice, Mono.	-	308	-	514	565	308	230	338	-	***1.34***	-	1.52
	Abel & Murray (1992a)	4E-1 1/4-7/8-16	Splice, Mono.	-	367	-	646	710	367	350	503	-	***1.05***	-	1.28
	Borgsmiller et al. (1995)	4E-1/2-3/8-16 1/2	Splice, Mono.	-	72	-	89	97	72	70	85	-	***1.03***	-	1.04
	Borgsmiller et al. (1995)	4E-1-3/4-64	Splice, Mono.	-	1382	-	1450	1595	1382	1350	1423	-	***1.02***	-	1.02
	Meng & Murray (1996)	4E-1-1-18	Bm.-Col., Cyclic	337	430	564	407	448	337	346	346	***0.98***	1.24	1.63	1.18
	Meng & Murray (1996)	4E-1-1-18	Bm.-Col., Cyclic	337	430	564	407	448	337	331	331	***1.02***	1.30	1.70	1.23
	Meng & Murray (1996)	4E-1.25-1-24	Bm.-Col., Cyclic	714	585	2293	852	937	585	785	785	0.91	***0.75***	2.92	1.09
	Meng & Murray (1996)	4E-1.25-2.25-24	Bm.-Col., Cyclic	776	2978	2299	1074	1182	776	1079	1079	***0.72***	2.76	2.13	1.00
	Ryan & Murray (1999)	4E-7/8-1/2-55	Bm.-Col., Cyclic	-	617	1108	983	1081	617	625	904	-	***0.99***	1.77	1.09
	Adey et al. (1997)	4E-7/8-3/4-14	Bm.-Col., Cyclic	297	226	361	297	327	226	236	288	1.03	***0.96***	1.53	1.03
	Adey et al. (1997)	4E-1-1/2-14	Bm.-Col., Cyclic	297	86	474	347	381	86	133	140	2.12	***0.65***	3.56	2.48
	Adey et al. (1997)	4E-1-1/2-14	Bm.-Col., Cyclic	297	81	474	366	403	81	103	144	2.06	***0.79***	4.60	2.54
	Adey et al. (1997)	4E-11/8-5/8-18	Bm.-Col., Cyclic	705	207	754	527	580	207	339	516	1.37	***0.61***	2.22	1.02
	Adey et al. (1997)	4E-1 1/8-5/8-18	Bm.-Col., Cyclic	705	172	767	563	619	172	188	365	1.93	***0.91***	4.08	1.54
	Adey et al. (1997)	4E-1 1/4-3/4-18	Bm.-Col., Cyclic	705	263	770	865	952	263	236	431	1.64	***1.11***	3.26	2.01
	Adey et al. (1997)	4E-1-5/8-24	Bm.-Col., Cyclic	1208	352	1033	620	682	352	383	568	2.13	***0.92***	2.70	1.09
	Adey et al. (1997)	4E-1-5/8-24	Bm.-Col., Cyclic	1208	269	958	649	714	269	254	406	2.97	***1.06***	3.77	1.60
	Sumner et al. (2000)	4E-1.25-1.5-24	Bm.-Col., Cyclic	917	1408	1354	1077	1184	917	934	934	***0.98***	1.51	1.45	1.15
	Sumner et al. (2000)	4E-1.25-1.125-24	Bm.-Col., Cyclic	917	769	1327	858	944	769	708	888	1.03	***1.09***	1.87	0.97
	Sumner et al. (2000)	4E-1.25-1.375-24	Bm.-Col., Cyclic	945	1218	2105	1120	1232	945	1192	1192	***0.79***	1.02	1.77	0.94
	Sumner et al. (2000)	4E-1.25-1.375-24	Bm.-Col., Cyclic	945	1220	2105	1120	1232	945	1188	1188	***0.80***	1.03	1.77	0.94

Notes: 1. Test identification: "Conn. type - Bolt dia. - End-plate thickness - Beam depth"
2. Dash "-" indicates that the parameter was not applicable to the test configuration or not available from the test report
3. Shaded cell indicate an observed failure mode
4. ***Bold italic*** values indicate the predicted failure mode using the proposed design procedure
5. Design ratios ≤ 1.0 are conservative
6. Mpe = ((Fy + Fu) / 2) Zx

Connection Type	Reference	Test Identification [1]		Configuration and Loading	Calculated Strengths						Experimental		Design Ratios [2, 3, 4, 5]			
					$M_{pe\ Beam}$	M_{pl}	M_{cf}	M_{np}	$1.1M_{np}$	M_n	M_y	M_u	M_{pe}/M_u [6]	M_{pl}/M_y	M_{cf}/M_y	M_{np}/M_u
Four Bolt Extended Stiffened (4ES)	Morrison et al. (1985)	4ES-5/8-3/8-16		Splice, Mono.	-	118	-	143	157	118	80	115	-	***1.48***	-	1.24
	Morrison et al. (1985)	4ES-3/4-1/2-16		Splice, Mono.	-	177	-	204	224	177	130	163	-	***1.36***	-	1.25
	Morrison et al. (1985)	4ES-3/4-7/16-20		Splice, Mono.	-	225	-	258	284	225	180	235	-	***1.25***	-	1.10
	Morrison et al. (1985)	4ES-3/4-1/2-20		Splice, Mono.	-	182	-	258	284	182	150	203	-	***1.21***	-	1.27
	Morrison et al. (1985)	4ES-1-1/2-24		Splice, Mono.	-	278	-	555	611	278	260	350	-	***1.07***	-	1.59
	Morrison et al. (1985)	4ES-1-5/8-24		Splice, Mono.	-	404	-	552	608	404	280	379	-	***1.44***	-	1.46
	Tsai & Popov (1990)	4ES-7/8-1 3/8-18	#10R	Bm.-Col., Cyclic	370	926	-	514	565	370	330	377	***0.98***	2.81	-	1.36
	Ghobarah et al. (1990)	4ES-1-3/4-14	A-3	Bm.-Col., Cyclic	232	277	243	397	437	232	197	242	***0.96***	1.41	1.23	1.64
	Ghobarah et al. (1990)	4ES-1-3/4-14	A-5	Bm.-Col., Cyclic	234	195	243	397	437	195	197	242	***0.97***	0.99	1.23	1.64
	Ghobarah et al. (1992)	4ES-1-1.1-16	CC-3	Bm.-Col., Cyclic	395	512	543	458	504	395	410	410	***0.96***	1.25	1.32	1.12
	Adey et al. (1997)	4ES-1 1/4-5/8-18	M4	Bm.-Col., Cyclic	705	297	774	865	952	297	370	546	1.29	***0.80***	2.09	1.58
	Adey et al. (1997)	4ES-1 1/4-5/8-18	M6	Bm.-Col., Cyclic	705	291	758	860	946	291	324	572	1.23	***0.90***	2.34	1.50
	Adey et al. (1997)	4ES-1 1/4-5/8-24	B4	Bm.-Col., Cyclic	1208	404	974	1163	1279	404	383	737	1.64	***1.05***	2.54	1.58
	Ryan & Murray (1999)	4ES-1-1/2-24a	Test 1	Bm.-Col., Cyclic	-	356	325	557	612	325	355	420	-	1.00	***0.92***	1.33
	Ryan & Murray (1999)	4ES-1-1/2-24a	Test 2	Bm.-Col., Cyclic	-	363	325	557	613	325	340	474	-	1.07	***0.96***	1.18
	Ryan & Murray (1999)	4ES-1-1/2-24b	Test1	Bm.-Col., Cyclic	-	279	282	557	613	279	270	458	-	***1.03***	1.04	1.22

Notes: 1. Test identification: "Conn. type - Bolt dia. - End-plate thickness - Beam depth"

2. Dash "-" indicates that the parameter was not applicable to the test configuration or not available from the test report
3. Shaded cell indicate an observed failure mode
4. ***Bold italic*** values indicate the predicted failure mode using the proposed design procedure
5. Design ratios ≤ 1.0 are conservative
6. $M_{pe} = ((F_y + F_u) / 2)\ Z_x$

Connection Type	Reference	Test Identification [1]	Configuration and Loading	Calculated Strengths						Experimental		Design Ratios [2, 3, 4, 5]			
				$M_{pe\ Beam}$	M_{pl}	M_{cf}	M_{np}	$1.1M_{np}$	M_n	M_y	M_u	M_{pe}/M_u [6]	M_{pl}/M_y	M_{cf}/M_y	M_{np}/M_u
Eight Bolt Extended Stiffened (8ES)	Ghassemieh (1983)	8ES-0.875-0.75-24	Splice, Mono.	-	714	-	838	922	714	680	680	-	***1.05***	-	1.23
	Ghassemieh (1983)	8ES-0.875-1-24	Splice, Mono.	-	1321	-	839	923	839	750	750	-	1.76	-	***1.12***
	Adey et al. (1997)	8ES-1 1/8-3/4-18	Bm.-Col., Cyclic	705	573	965	1046	1151	573	442	756	***0.93***	1.30	2.18	1.38
	Adey et al. (1997)	8ES-1 1/8-3/4-18	Bm.-Col., Cyclic	705	583	983	1051	1156	583	479	811	***0.87***	1.22	2.05	1.30
	Sumner et al. (2000)	8ES-1.25-1.75-30	Bm.-Col., Cyclic	1634	4623	5185	2691	2960	1634	1637	1637	***1.00***	2.82	3.17	1.64
	Sumner et al. (2000)	8ES-1.25-1-30	Bm.-Col., Cyclic	1634	1478	5159	2144	2358	1478	1412	1740	0.94	***1.05***	3.65	1.23
	Sumner et al. (2000)	8ES-1.25-2.5-36	Bm.-Col., Cyclic	3024	12696	6232	3225	3548	3024	3248	3248	***0.93***	3.91	1.92	0.99
	Sumner et al. (2000)	8ES-1.25-1.25-36	Bm.-Col., Cyclic	3024	3067	6288	2568	2825	2568	1942	2723	1.11	1.58	3.24	***0.94***

Notes: 1. Test identification: "Conn. type - Bolt dia. - End-plate thickness - Beam depth"
2. Dash "-" indicates that the parameter was not applicable to the test configuration or not available from the test report
3. Shaded cell indicate an observed failure mode
4. ***Bold italic*** values indicate the predicted failure mode using the proposed design procedure
5. Design ratios $\leq$ 1.0 are conservative
6. Mpe = ((Fy + Fu) / 2) Zx

Connection Type	Reference	Test Identification [1]	Configuration and Loading	Calculated Strengths						Experimental		Design Ratios [2, 3, 4, 5]			
				$M_{pe\ Beam}$	M_{pl}	M_{cf}	M_{np}	$1.1M_{np}$	M_n	M_y	M_u	M_{pe}/M_u [6]	M_{pl}/M_y	M_{cf}/M_y	M_{np}/M_u
Eight Bolt, Unstiffened Four Bolts Wide (8E-4W)	Sumner et al. (2000)	8E-4W-1.25-1.125-30	Bm.-Col., Cyclic	1647	1660	4521	2137	2351	1647	1416	1613	***1.02***	1.17	3.19	1.32
	Sumner et al. (2000)	8E-4W-1.25-1-30	Bm.-Col., Cyclic	1647	1260	4447	2137	2351	1260	1214	1498	1.10	***1.04***	3.66	1.43
	Sumner et al. (2000)	8E-4W-1.25-1.375-36	Bm.-Col., Cyclic	3012	2926	5112	2576	2834	2576	2427	2731	1.10	1.21	2.11	***0.94***
	Sumner et al. (2000)	8E-4W-1.25-1.25-36	Bm.-Col., Cyclic	3012	2512	5091	2576	2834	2512	2265	2703	1.11	***1.11***	2.25	0.95
	Sumner & Murray (2001b)	8E-4W-1-1/2-62	Splice, Mono.	-	1034	-	2863	3149	1034	1075	1539	-	***0.96***	-	1.86
	Sumner & Murray (2001b)	8E-4W-3/4-3/4-62	Splice, Mono.	-	2610	-	1612	1773	1612	1630	1825	-	1.60	-	***0.88***
	Sumner & Murray (2001b)	8E-4W-3/4-3/4-62	Splice, Mono.	-	2610	-	2024	2227	2024	2110	2204	-	1.24	-	***0.92***
8ES-4W	Meng & Murray (1996)	8ES-4W-1.25-1.5-36	Bm.-Col., Cyclic	2267	3486	4815	2559	2815	2267	2500	2500	***0.91***	1.39	1.93	1.02

Notes: 1. Test identification: "Conn. type - Bolt dia. - End-plate thickness - Beam depth"
2. Dash "-" indicates that the parameter was not applicable to the test configuration or not available from the test report
3. Shaded cell indicate an observed failure mode
4. ***Bold italic*** values indicate the predicted failure mode using the proposed design procedure
5. Design ratios $\leq$ 1.0 are conservative
6. Mpe = ((Fy + Fu) / 2) Zx

Connection Type	Reference	Test Identification [1]	Configuration and Loading	Calculated Strengths						Experimental		Design Ratios [2, 3, 4, 5]			
				$M_{pe\ Beam}$	M_{pl}	M_{cf}	M_{np}	$1.1M_{np}$	M_n	M_y	M_u	M_{pe}/M_u [6]	M_{pl}/M_y	M_{cf}/M_y	M_{np}/M_u
Multiple Row Extended 1/2 Unstiffened (MRE 1/2)	Abel & Murray (1992b)	MRE1/2-3/4-3/4-26	Splice, Mono.	-	687	-	482	530	482	370	372.1	-	1.86	-	***1.29***
	Abel & Murray (1992b)	MRE1/2-3/4-3/8-26	Splice, Mono.	-	153	-	482	530	153	210	309.2	-	***0.73***	-	1.56
	Sumner & Murray (2001a)	MRE1/2-3/4-3/8-30	Splice, Mono.	-	254	-	563	619	254	330	462.1	-	***0.77***	-	1.22
	Sumner & Murray (2001a)	MRE1/2-3/4-3/4-30	Splice, Mono.	-	986	-	562	618	562	540	633.3	-	1.83	-	***0.89***
	Sumner & Murray (2001a)	MRE1/2-3/4-3/4-30	Splice, Mono.	-	986	-	706	776	706	640	749.9	-	1.54	-	***0.94***
	Sumner & Murray (2001a)	MRE1/2-3/4-1/2-30	Splice, Mono.	-	349	-	514	566	349	405	482	-	***0.86***	-	1.07
	Sumner & Murray (2001a)	MRE1/2-3/4-3/4-30	Splice, Mono.	-	817	-	513	564	513	500	558.7	-	1.63	-	***0.92***
	Sumner & Murray (2001a)	MRE1/2-3/4-3/4-30	Splice, Mono.	-	817	-	644	709	644	450	622.8	-	1.82	-	***1.03***
Multiple Row Extended 1/3 Unstiffened (MRE 1/3)	Morrison et al. (1986)	MRE1/3-3/4-3/8-30	Splice, Mono.	-	252	-	718	790	252	270	404.9	-	***0.93***	-	1.77
	Morrison et al. (1986)	MRE1/3-1-1/2-30	Splice, Mono.	-	314	-	1248	1373	314	300	425.1	-	***1.05***	-	2.94
	Morrison et al. (1986)	MRE1/3-7/8-7/16-46	Splice, Mono.	-	558	-	1547	1701	558	520	866.1	-	***1.07***	-	1.79
	Morrison et al. (1986)	MRE1/3-1 1/8-5/8-46	Splice, Mono.	-	940	-	2521	2773	940	975	975.1	-	***0.96***	-	2.59
	Morrison et al. (1986)	MRE1/3-1 1/4-5/8-62	Splice, Mono.	-	1133	-	4197	4616	1133	1200	1635	-	***0.94***	-	2.57
	Morrison et al. (1986)	MRE1/3-1 1/2-3/4-62	Splice, Mono.	-	1546	-	5939	6533	1546	1600	2329.6	-	***0.97***	-	2.55
	Rodkey & Murray (1993)	MRE1/3-3/4-5/8-33 1/4	Splice, Mono.	-	733	-	784	862	733	690	692.5	-	***1.06***	-	1.13
	Structural Eng. Inc. (1984)	MRE1/3-3/4-1/2-62	Splice, Mono.	-	907	-	1547	1702	907	750	929	-	***1.21***	-	1.67
	Structural Eng. Inc. (1984)	MRE1/3-1-3/4-62	Splice, Mono.	-	1852	-	2718	2990	1852	1250	1364	-	***1.48***	-	1.99
	Borgsmiller et al. (1995)	MRE1/3-1-3/4-64	Splice, Mono.	-	1763	-	2733	3006	1763	1870	1870	-	***0.94***	-	1.46
	Ryan & Murray (1999)	MRE 1/3-7/8-5/8-55	Bm.-Col., Cyclic	-	1140	1287	1849	2034	1140	1100	1523	-	***1.04***	1.17	1.21
	Ryan & Murray (1999)	MRE 1/3-7/8-5/8-55	Bm.-Col., Cyclic	-	1170	1287	1849	2034	1170	1110	1720	-	***1.05***	1.16	1.08
	Ryan & Murray (1999)	MRE 1/3-7/8-1/2-55	Bm.-Col., Cyclic	-	775	803	1864	2050	775	810	1220	-	***0.96***	0.99	1.53
MRES 1/3	Structural Eng. Inc. (1984)	MRES1/3-1-3/4-62	Splice, Mono.	-	2261	-	2718	2990	2261	1600	1834	-	***1.41***	-	1.48

Notes: 1. Test identification: "Conn. type - Bolt dia. - End-plate thickness - Beam depth"

2. Dash "-" indicates that the parameter was not applicable to the test configuration or not available from the test report
3. Shaded cell indicate an observed failure mode
4. ***Bold italic*** values indicate the predicted failure mode using the proposed design procedure
5. Design ratios $\leq$ 1.0 are conservative
6. Mpe = ((Fy + Fu) / 2) Zx

VITA

Emmett A. Sumner, III was born on June 7, 1970 in Greensboro, North Carolina. In May 1993, he received a Bachelor of Science Degree in Civil Engineering from the University of North Carolina at Charlotte. In May 1995, he received a Master of Science in Civil Engineering from Virginia Polytechnic Institute and State University. He then worked as a design engineer in Columbia, South Carolina. In 1998 he returned to Virginia Polytechnic Institute and State University to pursue a doctoral degree in Civil Engineering. Currently, he is a faculty member at North Carolina State University in Raleigh, North Carolina.

_____
Emmett A. Sumner, III